EMERGING CELLULAR STRESS SENSORS IN NEUROLOGICAL DISORDERS: CLOSING IN ON THE NUCLEOLUS AND THE PRIMARY CILIUM

EDITED BY: Rosanna Parlato and Kerry Lee Tucker

PUBLISHED IN: Frontiers in Cellular Neuroscience

frontiers Research Topics

ISSN 1664-8714
ISBN 978-2-88963-711-9
DOI 10.3389/978-2-88963-711-9

About Frontiers

Frontiers is more than just an open-access publisher of scholarly articles: it is a pioneering approach to the world of academia, radically improving the way scholarly research is managed. The grand vision of Frontiers is a world where all people have an equal opportunity to seek, share and generate knowledge. Frontiers provides immediate and permanent online open access to all its publications, but this alone is not enough to realize our grand goals.

Frontiers Journal Series

The Frontiers Journal Series is a multi-tier and interdisciplinary set of open-access, online journals, promising a paradigm shift from the current review, selection and dissemination processes in academic publishing. All Frontiers journals are driven by researchers for researchers; therefore, they constitute a service to the scholarly community. At the same time, the Frontiers Journal Series operates on a revolutionary invention, the tiered publishing system, initially addressing specific communities of scholars, and gradually climbing up to broader public understanding, thus serving the interests of the lay society, too.

Dedication to Quality

Each Frontiers article is a landmark of the highest quality, thanks to genuinely collaborative interactions between authors and review editors, who include some of the world's best academicians. Research must be certified by peers before entering a stream of knowledge that may eventually reach the public - and shape society; therefore, Frontiers only applies the most rigorous and unbiased reviews.
Frontiers revolutionizes research publishing by freely delivering the most outstanding research, evaluated with no bias from both the academic and social point of view. By applying the most advanced information technologies, Frontiers is catapulting scholarly publishing into a new generation.

What are Frontiers Research Topics?

Frontiers Research Topics are very popular trademarks of the Frontiers Journals Series: they are collections of at least ten articles, all centered on a particular subject. With their unique mix of varied contributions from Original Research to Review Articles, Frontiers Research Topics unify the most influential researchers, the latest key findings and historical advances in a hot research area! Find out more on how to host your own Frontiers Research Topic or contribute to one as an author by contacting the Frontiers Editorial Office: researchtopics@frontiersin.org

EMERGING CELLULAR STRESS SENSORS IN NEUROLOGICAL DISORDERS: CLOSING IN ON THE NUCLEOLUS AND THE PRIMARY CILIUM

Topic Editors:
Rosanna Parlato, University of Ulm, Germany
Kerry Lee Tucker, University of New England, United States

Citation: Parlato, R., Tucker, K. L., eds. (2020). Emerging Cellular Stress Sensors in Neurological Disorders: Closing in on the Nucleolus and the Primary Cilium. Lausanne: Frontiers Media SA. doi: 10.3389/978-2-88963-711-9

Table of Contents

frontiers in Cellular Neuroscience

EDITORIAL
published: 20 March 2020
doi: 10.3389/fncel.2020.00064

Editorial: Emerging Cellular Stress Sensors in Neurological Disorders: Closing in on the Nucleolus and the Primary Cilium

Rosanna Parlato[1,2]* *and Kerry L. Tucker*[3]*

[1] Institute of Applied Physiology, University of Ulm, Ulm, Germany, [2] Institute of Anatomy and Cell Biology, Department of Medical Cell Biology, University of Heidelberg, Heidelberg, Germany, [3] Department of Biomedical Sciences, Center for Excellence in the Neurosciences, College of Osteopathic Medicine, University of New England, Biddeford, ME, United States

Keywords: primary cilia, nucleolus, autophagy, cellular stress, cell homeostasis

Editorial on the Research Topic

Emerging Cellular Stress Sensors in Neurological Disorders: Closing in on the Nucleolus and the Primary Cilium

OPEN ACCESS

Edited by:
Thomas Fath,
Macquarie University, Australia

Reviewed by:
Surya Nauli,
University of California, Irvine, United States

***Correspondence:**
Rosanna Parlato
rosanna.parlato@uni-ulm.de
Kerry L. Tucker
ktucker2@une.edu

Specialty section:
This article was submitted to Cellular Neuropathology, a section of the journal Frontiers in Cellular Neuroscience

Received: *28 January 2020*
Accepted: *04 March 2020*
Published: *20 March 2020*

Citation:
Parlato R and Tucker KL (2020) Editorial: Emerging Cellular Stress Sensors in Neurological Disorders: Closing in on the Nucleolus and the Primary Cilium. Front. Cell. Neurosci. 14:64. doi: 10.3389/fncel.2020.00064

The primary cilium and the nucleolus represent signaling hubs that regulate cell homeostasis and stress responses. Primary cilia have long been considered vestigial organelles but are now viewed as sensory antennae that transduce extracellular signals, including mechano- and chemo-transduction. The nucleolus is traditionally viewed as the site where ribosomal RNA synthesis and ribosome biogenesis occurs, which is now considered both a sensor and a mediator of the cellular stress response. Both organelles transduce developmental and homeostatic pathways, including Wnt signaling, mechanistic target of rapamycin (mTOR) and autophagy. Both organelles adjust their structure and function in response to changes not only in the extracellular environment but also in the intracellular milieu. Interestingly, neither are typical membrane-bound organelles, and they both adapt their structure in a dynamic fashion, suggesting a crucial role in cell homeostasis. These conceptual similarities, along with the newly discovered impact of deficits in primary ciliary and nucleolar function on neuronal homeostasis, raised the idea of the first collection of reviews and original articles addressing primary cilium- and nucleolus-dependent mechanisms in normal neuronal function and neurological disorders.

The Research Article by Monaco et al. describes a novel method to differentially isolate primary cilia from motile cilia by flow cytometry. Differently from motile cilia, primary cilia express type III adenylyl cyclase (AC3), a primary cilium-localized, cAMP-generating enzyme, and prominin, a glycoprotein typical of neural stem cells. Intriguingly, different populations of primary cilia characterized by the expression of specific receptors in an age-dependent fashion are identified here, validating this method for the investigation of primary cilia-dependent signaling pathways in health and disease conditions.

A second Research Article by Zhou et al. focuses on AC3 for its fascinating genetic association in human studies with autistic spectrum and major depressive disorders. The authors use mouse knockout models of the AC3 gene to look at differences in expression of phosphorylated protein isoforms in the brains of control and AC3-knockout mice. Interestingly, the authors also distributed their data sets by sex, and came up with hundreds of sex-specific phosphoprotein expression patterns, one third of which have shown association with autism.

The mini-review by Sarkisian and Semple-Rowland looks at connections between primary cilia and glioma. Gliomas are tumors arising from glial cell populations in the brain and spinal cord, comprising the majority of malignant brain tumors. The authors focus upon the most aggressive tumor type, the glioblastoma, and examine correlations and causative experiments that have been recorded and performed, respectively, to test whether primary cilia influence tumor development and progression. The data are decidedly mixed and do not seem to deliver a consistent answer whether tumor cells are ciliated, and conversely, the tumor identity of ciliated cells identified in biopsies. This uncertainty is mirrored by functional experiments, showing that either the presence or the absence of primary cilia on tumor precursor cells can promote tumor progression. In a second mini-review, the authors Park et al. make an excellent summary of the multiple, diverse, essential functions that primary cilia have in the formation of the brain, including patterning, layering, and neuronal migration within the forebrain, expansion of precursor pools in the cerebellum, and more subtle effects observed in learning and memory. They touch upon the best-investigated pathways, including Hedgehog, Wnt, mTOR, and they even discuss autophagy in this context.

In the Brief Research Report by Mustafa et al. we present the initial characterization of a mutant mouse lacking primary cilia in dopaminoceptive neurons. These models will be useful to investigate the impact of primary cilia in diseases affecting the dopamine system, such as Huntington's disease (HD). We show that either altered structure or loss of primary cilia is associated with increased mTOR activity in a progressive mouse model of HD. In addition loss of primary cilia results in bigger mutant Huntingtin nuclear inclusions, suggesting a more advanced pathological stage. Future studies should address the disease phenotype at later stages. A second Brief Research Report by Lucarelli et al. looks at the distribution of primary cilia in a murine model of the neurodegenerative Niemann-Pick C1 (NPC1) disease. NPC1 is characterized by biochemical changes in lipid and cholesterol metabolism resulting in dopamine imbalances and corresponding locomotor defects. In their mouse model, the authors observe a decrease in dopamine transporter expression, and also an increase in the number of primary cilia, in the dorsal striatum. In line with this concept, both reports strongly suggest that primary cilia are involved in homeostatic responses to changes in striatal dopamine. Future studies should address the impact of primary cilia of mTOR dysregulation and autophagy in neurodegeneration.

On the other side, the excellent Review by Pfister provides an outstanding overview of the regulation of autophagy by the second stress sensor organelle object of this Research Topic, the nucleolus. The author discusses recent findings on the crosstalk between mTOR signaling and nucleolar activity, and how autophagy represents a response to nucleolar stress in numerous human diseases. She provides an unprecedented outline of nucleolar proteins functioning in autophagy regulation. A second exciting Review by Latonen provides a comprehensive overview of the most recent functions discovered for the nucleolus in neuronal homeostasis. The author identifies the nucleolus as a central hub of cellular proteostasis and focuses on its important new role in cell homeostasis, affected by changing its material properties. The role of nucleolar aggresomes is discussed as a potential mechanism of nuclear aggregate accumulation common to many neurodegenerative diseases, such as HD and amyotrophic lateral sclerosis. This Review also presents the emerging role of long non-coding RNA in ribosomal RNA transcription and stress response.

Although there is no current evidence that primary cilia and nucleoli are interdependent, this Research Topic poses the provocative thought that the structure and function of these two key stress sensors and mediators might be connected. This collection promises to inspire original ideas and innovative studies, to provide a deeper understanding of physiological processes and disease mechanisms, and to identify new strategies for the maintenance of neuronal health and disease treatment.

AUTHOR CONTRIBUTIONS

RP and KT drafted the manuscript.

Conflict of Interest: The authors declare that the research was conducted in the absence of any commercial or financial relationships that could be construed as a potential conflict of interest.

frontiers in Cellular Neuroscience

ORIGINAL RESEARCH
published: 14 January 2019
doi: 10.3389/fncel.2018.00519

A Flow Cytometry-Based Approach for the Isolation and Characterization of Neural Stem Cell Primary Cilia

*Sara Monaco†, Katja Baur†, Andrea Hellwig, Gabriele Hölzl-Wenig, Claudia Mandl and Francesca Ciccolini**

Interdisciplinary Center for Neurosciences (IZN), Department of Neurobiology, University of Heidelberg, Heidelberg, Germany

In the adult mammalian brain, the apical surface of the subependymal zone (SEZ) is covered by many motile ependymal cilia and a few primary cilia originating from rare intermingled neural stem cells (NSCs). In NSCs the primary cilia are key for the transduction of essential extracellular signals such as Sonic hedgehog (SHH) and platelet-derived growth factor (PDGF). Despite their importance, the analysis of NSC primary cilia is greatly hampered by the fact that they are overwhelmingly outnumbered by the motile cilia. We here take advantage of flow cytometry to purify the two cilia types and allow their molecular characterization. Primary cilia were identified based on immunoreactivity to the marker adenylate cyclase type III (AC3) and differential levels of prominin-1 whereas motile cilia displayed immunoreactivity only to the latter. Consistent with the morphological differences between the two classes of cilia, enrichment of motile cilia positively correlated with size. Moreover, we observed age-dependent variations in the abundance of the two groups of ciliary organelles reflecting the changes associated with their development. The two cilia groups also differed with respect to the expression of signaling molecules, since PDGF receptor (PDGFR)α, smoothened (Smo) and CXC chemokine receptor (CXCR)4 were only detected in isolated primary but not motile cilia. Thus, our novel method of cilia isolation and characterization by flow cytometry has the potential to be extended to the study of cilia from different tissues and organs, providing a powerful tool for the investigation of primary cilia in physiological and pathological conditions.

Keywords: primary cilium, ependymal cilium, subependymal zone, Sonic hedgehog, platelet-derived growth factor

OPEN ACCESS

Edited by:
Kerry Lee Tucker, University of New England, United States

Reviewed by:
Xuanmao Chen, University of New Hampshire, United States
Matthew Sarkisian, University of Florida, United States

***Correspondence:**
Francesca Ciccolini
ciccolini@nbio.uni-heidelberg.de

†These authors have contributed equally to this work

Received: *28 September 2018*
Accepted: *12 December 2018*
Published: *14 January 2019*

Citation:
Monaco S, Baur K, Hellwig A, Hölzl-Wenig G, Mandl C and Ciccolini F (2019) A Flow Cytometry-Based Approach for the Isolation and Characterization of Neural Stem Cell Primary Cilia. Front. Cell. Neurosci. 12:519. doi: 10.3389/fncel.2018.00519

INTRODUCTION

Primary cilia have an emerging function in the transduction of developmental and homeostatic pathways and their dysfunction is associated with a number of human diseases, collectively referred to as ciliopathies (Berbari et al., 2009; Tobin and Beales, 2009). Primary cilia are present throughout the brain and they are involved in several functions including neurogenesis, migration, autophagy and development (Guemez-Gamboa et al., 2014). The adult subependymal zone (SEZ) is the largest germinal niche in the adult brain, where neural stem cells (NSCs) mainly generate new interneurons for the olfactory bulb throughout adulthood. The apical side of the SEZ is lined with a myriad of motile cilia stemming from ependymal cells and a few primary cilia protruding from NSCs. The two cell types form a characteristic pinwheel structure at the apical SEZ surface in which ependymal cells encircle a NSC (Mirzadeh et al., 2008).

Like adult NSCs, ependymal cells are generated from radial glia precursors perinatally and continue to develop during the first weeks after birth (Merkle et al., 2004; Spassky et al., 2005). As a consequence, primary cilia extending from radial glia represent the prevailing cilia type before birth. Both ependymal cells and NSCs undergo changes during postnatal aging. In particular, pinwheel structures become rarer in aged mice (Shook et al., 2012) likely due to NSCs losing the apical attachment (Obernier et al., 2018). Ageing also affects the ependymal layer with loss of ependymal cells into the ventricular space (Del Bigio, 2010). Primary and motile cilia are defined by striking morphological differences. The primary cilia axoneme, which is 1–9 μm long (Dummer et al., 2016) and 0.2–0.3 μm wide, is constituted at its core by a ring of nine microtubule pairs (9 × 2 + 0). In contrast, the generally longer motile cilia, whose length is extremely variable in different tissues (Lee, 2013), have a 9 × 2 + 2 core structure with the ring of external microtubule doublets connected by inner and outer dynein arms and an additional central pair of microtubule singlets. Despite being structurally and functionally different both primary and motile cilia express prominin-1, a glycoprotein commonly used to isolate stem and progenitor cells from the developing and adult nervous system, which is selectively localized in membrane protrusions (Weigmann et al., 1997), including cilia (Pfenninger et al., 2007; Coskun et al., 2008). However, whereas prominin-1 expression is a constant feature of ependymal motile cilia, a subset of primary cilia in the SEZ lacks the expression of the glycoprotein at the cell membrane (Codega et al., 2014; Khatri et al., 2014). Modification of the tubulin residues such as acetylation and glycosylation, which increase the stability of the microtubule and the length of the axoneme, are found in both types of cilia. However, the type 3 adenylate cyclase (AC3) localizes to primary cilia only and it is considered to be a marker of primary cilia in all regions of the mouse brain (Bishop et al., 2007).

The beating of ependymal motile cilia contributes to the movement of the cerebrospinal fluid (CSF) in the ventricular system of the brain representing an essential component of a protecting barrier whose integrity is important to maintain the size of the ventricles (Shook et al., 2014) as well as to create concentration gradients for the guidance of migrating neurons (Sawamoto et al., 2006). Underscoring the importance of the ependymal ciliary function, several neurological conditions (Ikeda et al., 2005; King, 2006; Suzuki et al., 2009) such as hydrocephalus (Lee, 2013; Jiménez et al., 2014) and schizophrenia (Palha et al., 2012) have been associated to impaired circulation of the CSF. The flow of the CSF is also disrupted in Huntington's disease, which leads to an increase in the length of ependymal cilia (Keryer et al., 2011). In contrast, primary cilia in radial glia have been associated to the regulation of cell cycle progression (Tong et al., 2014; Izawa et al., 2015). This function reflects the fact that the mother centriole in the basal body of the primary cilia is needed for the mitotic spindle formation. Furthermore, the organelle is essential to transduce signals involved in the regulation of progenitor proliferation such as Sonic hedgehog (SHH) and platelet-derived growth factor (PDGF) signaling (Youn and Han, 2018). Although genes coding for ciliary function are specifically enriched in NSCs and cilia depletion affects NSC quiescence in the SEZ (Beckervordersandforth et al., 2010), not all quiescent NSCs in this region display a primary cilium (Khatri et al., 2014). Moreover ablation of primary cilia affects proliferation only in NSCs of the ventral SEZ (Khatri et al., 2014; Tong et al., 2014). Thus, the function of primary cilia in NSCs is still unclear.

The direct analysis of the expression of signaling molecules in primary cilia would significantly contribute to elucidate their function. Here we describe an innovative flow cytometry-based method to isolate motile and primary cilia from the SEZ and provide evidence for its suitability to analyze the molecular composition of cilia both at the population as well as at the single cilia level.

MATERIALS AND METHODS

Analysis and Purification of Cilia From the SEZ by Flow Cytometry

Deciliation and Immunostaining

All animal experiments were approved by the Regierungspräsidium Karlsruhe and the local authorities of Heidelberg University. Adult mice were killed by CO_2 inhalation followed by cervical dislocation whereas E18 embryos were sacrificed by decapitation. The brain was removed from the skull and the SEZ was dissected in ice-cold dissection medium (150 μM sucrose, 125 μM NaCl, 3.5 mM KCl, 1.2 mM NaH_2PO4, 2.4 mM $CaCl_2$, 1.3 mM $MgCl_2$, 2 mM HEPES, 6.65 mM D-(+) glucose; Khatri et al., 2014). The dissected tissue was put in sort medium (NS-A basal medium and L15 medium (1:1), 2% B27 supplement, 1% fetal calf serum (FCS), 0.6% D-(+) glucose, 10 ng/ml huFGF-2, 0.001% DNase) containing APC-conjugated anti-prominin-1 antibody (Becton Dickinson, BD) for 30 min at 4°C and then washed at room temperature with sort medium to eliminate the excess of antibody. Deciliation was performed by combining the two most common methods for cilia detachment: mechanical shear and calcium shock (Mitchell et al., 2009). Briefly, the tissue was incubated in sort medium containing 10 mM $CaCl_2$ and subjected to mechanical agitation on a rotatory shaker (200 rpm) at 4°C. After 20 min, the medium, containing cilia, was centrifuged for 1 min at 2,000 rpm at 4°C to remove cellular debris. The supernatant was collected and immunostained with anti-AC3 antibodies (Santa Cruz) and Alexa Fluor 488-conjugated secondary antibodies for 30 min at 4°C.

Fluorescence Activated Cell Sorting

Cilia preparations were sorted on a FACSAria II cytometer (BD) at single event precision. Sorting gates were set based on florescence levels of samples stained with secondary antibodies only or samples which were not incubated with any antibodies (autofluorescence).

To standardize Forward (FSC) and Side (SSC) scatter values we used as reference beads of known size, i.e., 3 μm (Rainbow Fluorescent Particles, BD) and 6 μm (Accudrop beads, BD). Sorted ciliary particles that based on the reference beads had a size smaller than 3 μm, between 3 μm and 6 μm or greater than 6

μm were separately collected and analyzed. Hereafter they will be referred to as 2 μm (<3 μm), 5 μm (3–5 μm) and 8 μm (≥6 μm) particles.

Characterization of the Cilia Types (Primary vs. Motile)

For each size group, double staining with anti-AC3-Alexa 488 and prominin-APC antibodies was analyzed and four gates were set: $AC3^+/Prom^-$ ($AC3^+$), $AC3^+/Prom^+$ (double positive, DP), $AC3^-/Prom^+$ ($Prom^+$), $AC3^-/Prom^-$ (double negative, DN).

Functional Characterization

For each size group immunostaining was used for detecting one of the following antigens: Smoothened, PDGFRα or CXC chemokine receptor (CXCR)4. For PDGFRα and CXCR4 staining, the dissected tissue was incubated in sort medium containing anti-prominin-APC (Miltenyi Biotec) and anti-PDGFRα or CXCR4 antibodies conjugated with PE (Invitrogen) for 30 min and washed with sort medium before proceeding to deciliation and staining with anti-AC3 antibody (Invitrogen) manually conjugated with Dylight 488 (Abcam, cat# ab201799). For Smoothened analysis, the tissue fragments were incubated with or without SAG (Cayman Chemical, cat# 11914, 200 nM) in NS-A medium (Euroclone/Biozol) containing 2 mM L-glutamine (Gibco), 100 U/ml penicillin/streptomycin (Gibco), 2% B27 supplement (Invitrogen), 10 ng/ml huFGF-2 (Peprotech) overnight at 37°C. The samples were labeled with anti-Smoothened antibodies (Novus Biologicals) and anti-rabbit-APC secondary antibodies for 30 min. The samples were then washed, deciliated and the supernatant was subjected to AC3 staining as described above.

Western Blot

For western blot analysis, a specific number of particles was sorted into PBS containing proteinase inhibitor and after ultracentrifugation at 4°C at 27,000× *g* for 40 min resuspended in RIPA buffer. The samples were subjected to standard immunoblot analysis with mouse anti-acetylated tubulin antibody (Sigma-Aldrich). Immunoreactivity was quantified using ImageJ and the results were normalized by the number of particles collected in each sample.

Whole Mount Immunostaining

Whole mount dissection was performed as previously described (Mirzadeh et al., 2008). The dissected tissue was fixed in 3% formaldehyde/4% sucrose (dissolved in PBS) for 2 h, permeabilized with 0.5% NP-40 for 10 min, incubated in 100 mM glycine to inactivate residual aldehyde groups, and blocked in 5% FCS for 1.5 h. The samples were then incubated with primary antibodies against acetylated tubulin (Sigma Aldrich) and either β-catenin (Santa Cruz), AC3 (Invitrogen) or prominin-1 (kind gift from Denis Corbeil, Technical University of Dresden) in 0.1% NP-40 over night at 4°C. After washing, the samples were incubated with secondary antibodies and DAPI for nuclear counterstain for 2 h and analyzed using a C2 Plus confocal microscope with NIS software (Nikon) or a TCS SP8 confocal microscope with LAS X software (Leica).

Antibodies

A list of all primary antibodies used, source, catalog/lot number and concentration is provided in **Supplementary Table S1**.

Electron Microscopy

Scanning electro microscopy (SEM) was performed as previously described (Khatri et al., 2014). Briefly, the samples were fixed with 2% glutaraldehyde in 0.1 M sodium phosphate buffer. After washing and postfixation with 2% osmium tetroxide/1.5% potassium ferrocyanide for 1 h, they were washed and dehydrated with an ascending series of ethanol and pure acetone before critical point drying. The samples were then sputter-coated with an 80% gold, 20% palladium alloy and examined with a ULTRA 55 field-emission scanning electron microscope (ZEISS).

Statistical Analysis

Statistical significance tests (ANOVA with Tukey's *post hoc* test or Student's *t*-test) of at least three independent experiments were calculated using GraphPad Prism and OriginPro 2016. Data represent means ± SEM. *P*-values are indicated in the figures as follows: $^*p < 0.05$, $^{**}p < 0.01$, $^{***}p < 0.001$, $^{****}p < 0.0001$.

RESULTS

A Flow Cytometry-Based Method for Isolation of Primary Cilia From the SEZ

As schematically illustrated in **Figure 1**, we took advantage of flow cytometry to set up a novel approach to identify and isolate primary cilia from the murine SEZ. We performed this method with samples obtained from the SEZ of adult mice, in which motile ependymal cilia are much more abundant than primary cilia, and the corresponding germinal area dissected from embryos at embryonic day (E) 18, when primary cilia represent the vast majority of the cilia. Such age-dependent differences in cilia type proportion are readily visible upon immunostaining of the apical side of the germinal area at the two ages with antibodies directed against acetylated tubulin, which is expressed in both types of cilia (**Supplementary Table S2**; **Figure 2A**). Critical steps of the procedures are the deciliation, i.e., the detachment of cilia from the cell body, the identification and the separate collection of the two cilia types. To promote deciliation we used the traditional method of mechanical shearing in the presence of a high calcium ion concentration (Hastie et al., 1986; Mitchell et al., 2009; Ishikawa and Marshall, 2013). Comparing SEM images of the apical surface of the lateral ventricle wall of E18 (**Figure 2B**) and adult mice (**Figure 2C**), after deciliation or no treatment (Control), showed that the treatment was effective in removing primary but not motile cilia. In untreated embryonic tissue, primary cilia were readily visible (**Figures 2Ba,a′**, highlighted in green) whereas, after deciliation, they were largely absent (quantification in **Supplementary Figure S1A**). Sometimes a remaining stump could be detected (**Figures 2Bb,b′**, highlighted in green). This suggests that deciliation also gives rise to fragments of different sizes, as previously reported (Mitchell et al., 2009). In contrast, many tufts of ependymal cilia were still present after deciliation, (**Figure 2C**) although their number

was significantly reduced (quantification in **Supplementary Figure S1B**). In order to distinguish motile from primary cilia we have taken advantage of differential expression of prominin-1 (Prom) and AC3 in the two cilia types. As summarized in **Supplementary Table S2**, whereas prominin-1 in the adult tissue is expressed more strongly in ependymal cells, AC3 has only been detected in primary cilia (Bishop et al., 2007). Consistent with this, immunostaining of AC3 in whole mount preparations of the SEZ of mice of different ages revealed AC3 expression in primary but not motile cilia and that the immunostaining decreased with age (**Figure 3A**). On the contrary, prominin-1 expression was detected in both cilia groups (**Figure 3B**). However, whereas in motile cilia prominin-1 was expressed at consistently high levels (**Figure 3B**, white arrow), primary cilia displayed high variability in expression levels, ranging from very high (**Figure 3B**, red arrow) to undetectable (**Figure 3B**, green arrow). To address variability in cilia length, ranging between 1 μm and 9 μm (Dummer et al., 2016), we have used beads of known size to set the forward (FSC) and side light scatter (SSC) parameters (**Figures 1A,B**) and monitor changes in particle size during sorting. Although for bigger particles, like for example cells, the first parameter reflects cell size whereas the second indicates complexity (granularity), for smaller particles the measurement of both parameters provides a better detection of changes in size. Independent of size, we detected four types of particles: primary cilia particles immunopositive for either AC3 only ($AC3^+$) or double immunopositive (DP) for both AC3 and Prom, motile cilia particles immunopositive for Prom only ($Prom^+$) and double immunonegative fragments (DN; **Figure 1C**). To further investigate their nature, the four populations of particles were separately collected by FACS, concentrated by ultracentrifugation and then analyzed by

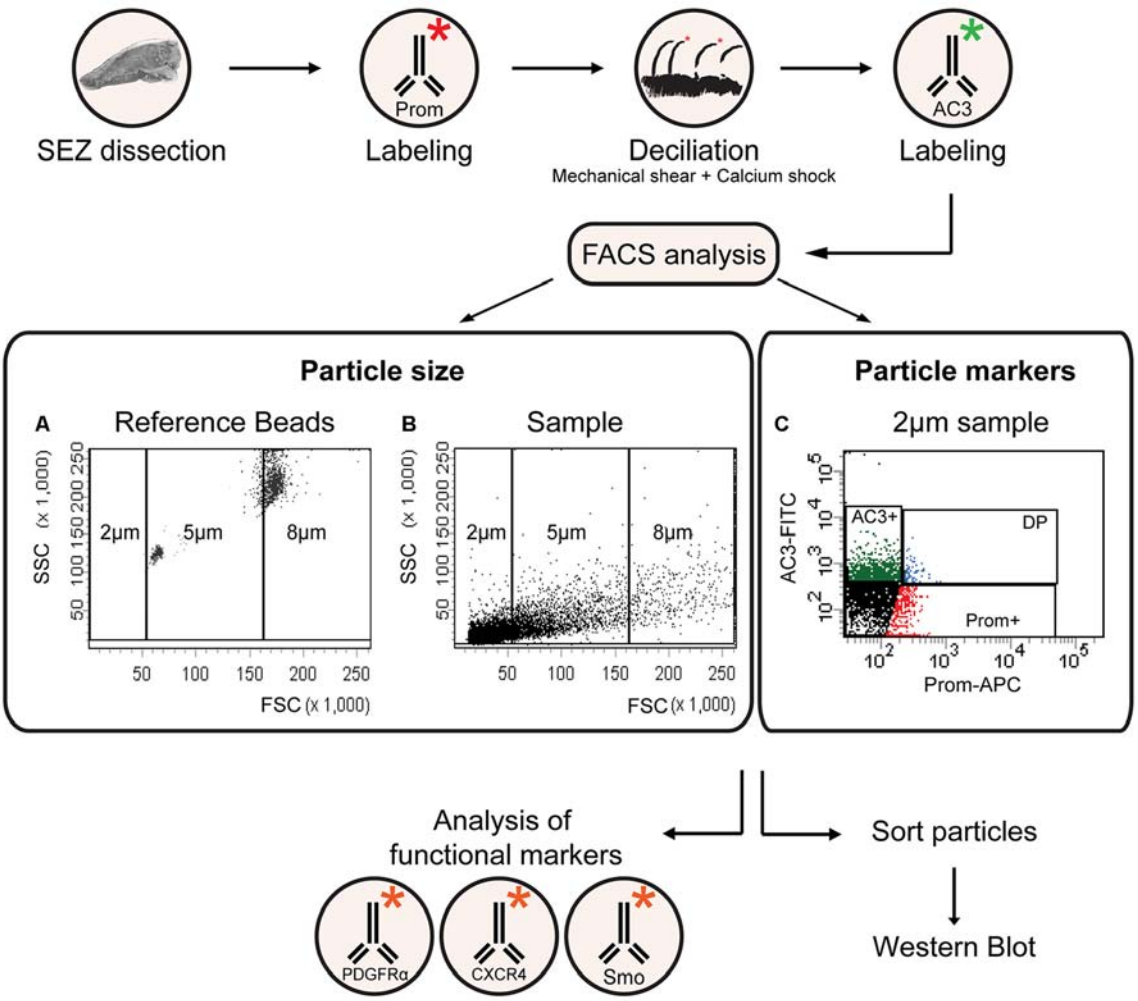

FIGURE 1 | A flow cytometric approach for the isolation and characterization of primary and motile cilia. Flowchart of the experimental procedure for cilia identification and characterization according to size and marker expression. The * symbol represents a conjugated fluorophore. **(A,B)** FACS plots showing the distribution of reference beads and a sample of cilia according to forward (FSC) and side (SSC) scatter. **(C)** Representative FACS plot illustrating the distribution of 2 μm particles upon immunostaining with antibodies directed against adenylate cyclase type iii (AC3; AC3-FITC) and prominin-1 (Prom-APC). The gates indicate AC3 positive (AC3+), Prominin positive (Prom+) and double positive (DP) particles.

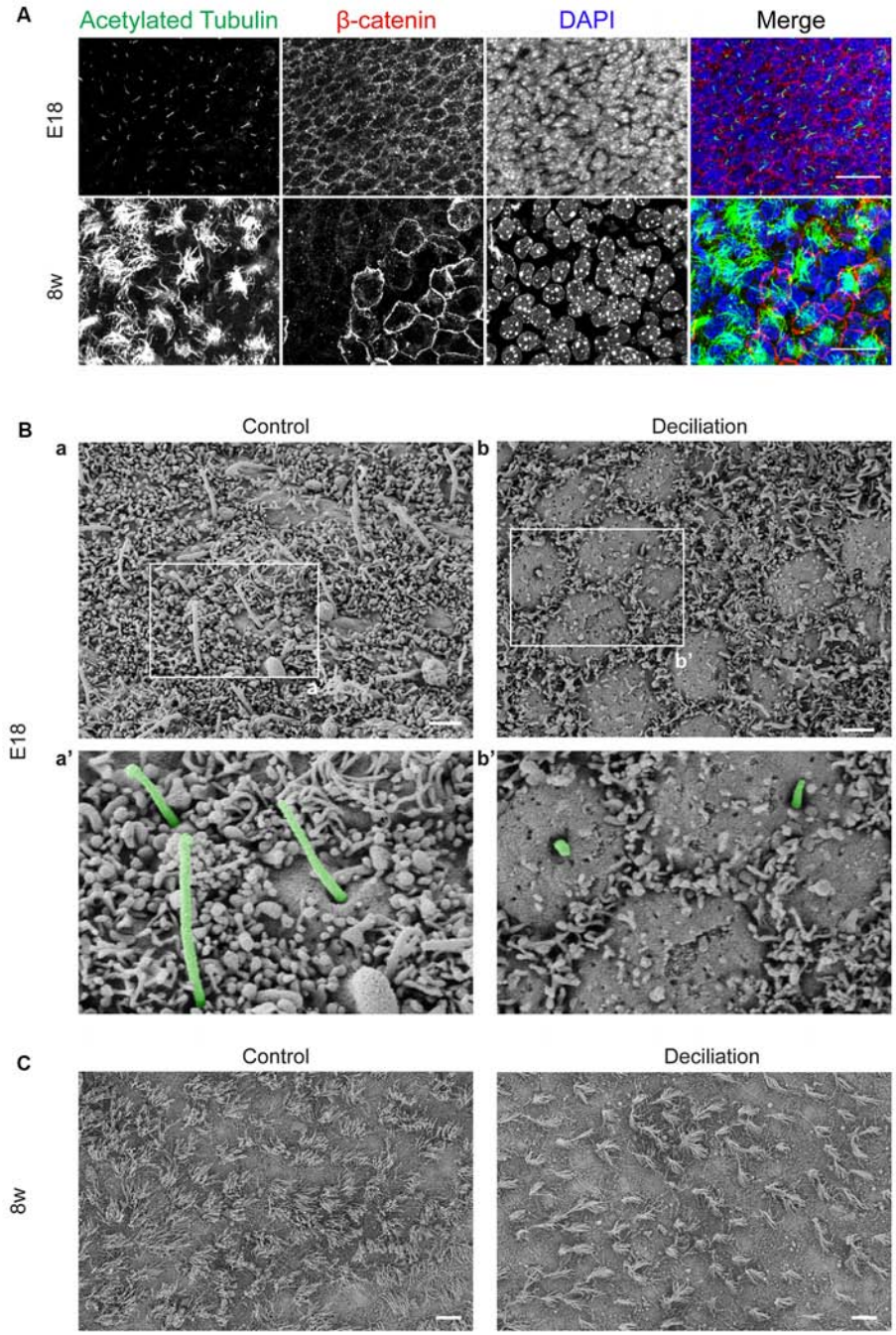

FIGURE 2 | Primary and motile cilia on the apical side of the subependymal zone (SEZ). **(A)** Confocal images showing a representative example of the apical side of the SEZ in whole mount preparations immunostained for acetylated tubulin (green) and β-catenin (red). Nuclei were visualized by DAPI staining (blue). Scale bars: 20 μm. **(B)** Scanning electron microscope (SEM) images of the apical surface of the lateral ventricular wall in whole mount preparations from E18 mice before (Control) and after deciliation. Higher magnification views of panels **(a,b)** are shown in **(a',b')**, respectively. Primary cilia are highlighted in green. After the treatment many of the primary cilia are detached and only short stumps are left on the cell surface **(b')**. Scale bars: 2 μm. **(C)** SEM images of the apical surface of the SEZ in whole mount preparations of 8 week-old mice (8w). Scale bars: 10 μm.

western blot to investigate the expression of acetylated tubulin (**Figure 4**). Particles were first sorted based on differences in size only (**Figure 4A**). After normalization according to the number of sorted particles, quantitative analysis of the western blots showed that although acetylated tubulin was present in all sorted populations, its amount increased with particle size (**Figure 4B**). This corroborates that the sorted material indeed contains cilia. We next sorted the particles based on differential

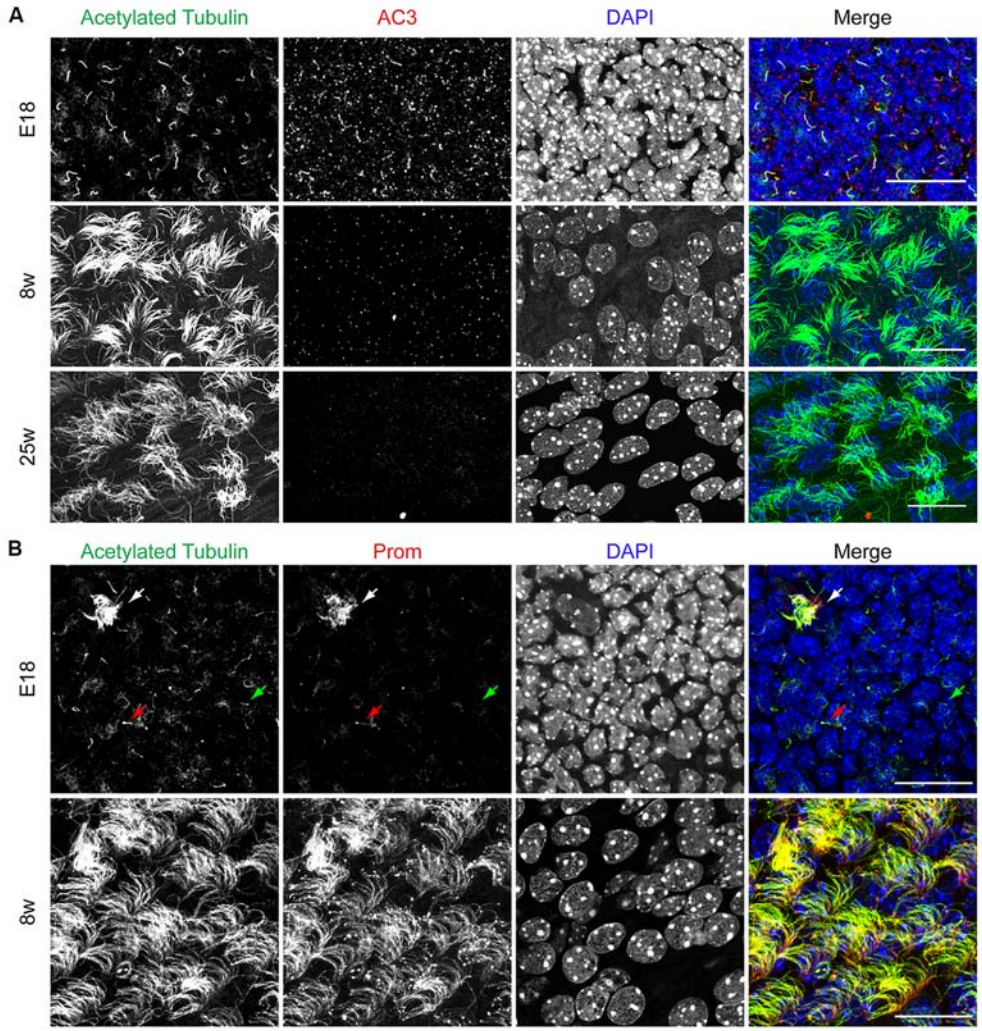

FIGURE 3 | AC3 and prominin-1 expression on the apical side of the SEZ. **(A)** Representative confocal images illustrating the apical side of the SEZ upon immunostaining with acetylated tubulin (green) and AC3 (red). Nuclei were visualized by DAPI. Scale bar: 20 μm. **(B)** Confocal images of whole mount preparations immunostained for acetylated tubulin (green) and prominin-1 (Prom, red). Nuclei were visualized by DAPI. White arrow indicates motile cilia, red arrow indicates $Prom^+$ primary cilia and green arrow indicates $Prom^-$ primary cilia. Scale bars: 20 μm.

staining. We collected the same number of particles (200,000) for DN, $AC3^+$ and $Prom^+$ particles but only 50,000 of the less abundant DP particles (**Figure 4C**). Densitometric analysis after normalization for the number of particles revealed that $AC3^+$, DP and $Prom^+$ populations similarly contain at least double the amount of acetylated tubulin than DN particles (**Figure 4D**). This indicates that the three groups of immunopositive particles indeed contain cilia material whereas the DN particles include contaminating material and a few ciliary fragments.

Flow Cytometric Analysis of Cilia Markers AC3 and Prominin-1 Allows Identification of Primary and Motile Cilia

To further validate our method for the identification of primary and motile cilia by flow cytometry, we took advantage of the fact that before birth motile cilia are very rare whereas primary cilia in the SEZ decrease with aging (**Figure 2A**). Therefore, we next used flow cytometry to investigate the abundance of the three cilia-enriched fractions defined by the differential antigen expression and subdivided according to size in preparations obtained either from E18 embryos or 8 week or 25 week-old mice (**Figure 5**). As illustrated by representative FACS plots (**Figure 5A**), at each age and for each size we measured the same number of total particles. At all ages examined collected cilia consisted mostly of 2 μm particles followed in decreasing order of abundance by 5 μm and 8 μm particles (**Supplementary Figure S2**). This is probably due to the fragmentation of the cilia during the process of deciliation (illustrated in **Figure 2Bb′**). Quantitative analysis of the number of immunopositive particles in each size-defined population highlighted that the abundance of $AC3^+$ (**Figure 5B**) and DP (**Figure 5C**) particles greatly declined with age. However,

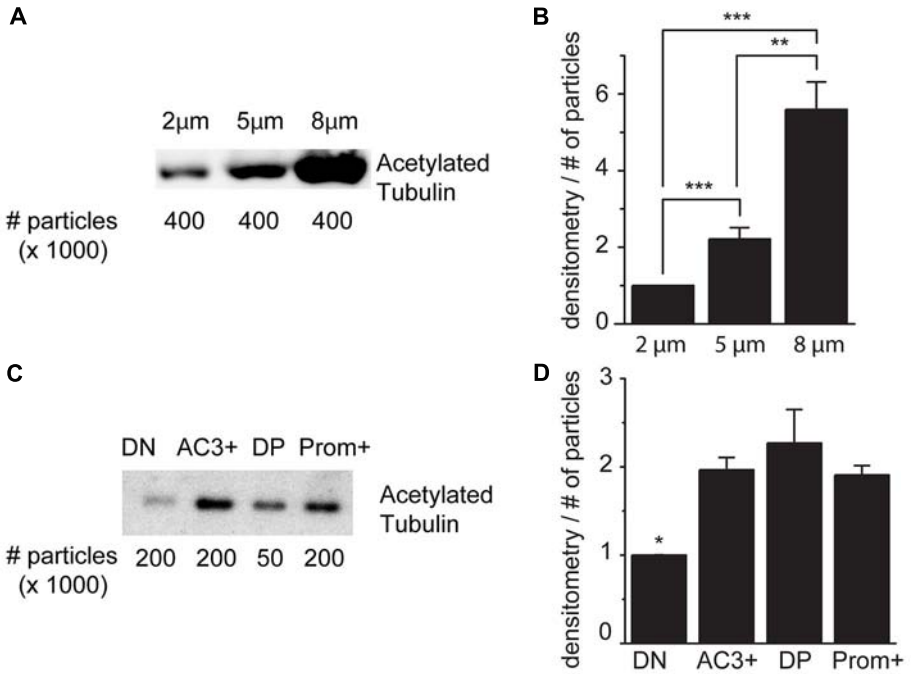

FIGURE 4 | Acetylated tubulin expression in sorted cilia. **(A)** Representative immunoblot analysis of acetylated tubulin in samples of sorted particles of different sizes from adult mice. **(B)** Densitometric analysis of four independent experiments. **(C)** Immunoblot analysis of acetylated tubulin in samples sorted according to the expression of AC3 and prominin-1: double negative (DN), $AC3^+$ only ($AC3^+$), double positive (DP), prominin-1 only ($Prom^+$). **(D)** Densitometric analysis of three independent experiments normalized for the number of particles. Values represent the fold increase relative to the fist sample. Error bars represent SEM. Statistically significant differences are indicated with asterisks (*$p < 0.05$, **$p < 0.01$, ***$p < 0.001$).

whereas the number of $AC3^+$ particles progressively declined with age, the number of DP particles did not vary significantly between samples obtained from E18 embryo and 8-week-old mice, but abruptly decreased thereafter. Moreover, whereas at all ages $AC3^+$ particles were similarly distributed across the various size groups (**Figure 5B**), DP cilia were mostly found in the 8 µm subpopulation. These observations suggest that the $AC3^+$ and DP particles represent distinct types of primary cilia, which is consistent with the variability of prominin-1 expression observed in primary cilia by immunostaining (see **Figure 3B**). In contrast to primary cilia, the fraction of $Prom^+$ particles increased with age, reaching its maximum level in preparations of 25-week-old mice (**Figure 5D**). Moreover, in samples obtained from adult but not E18 mice this group was particularly enriched in the 8 µm fraction, consistent with the fact that motile cilia reach full length after birth and are generally longer than primary cilia.

Taken together, these results show that the number of $AC3^+$ particles is highest in the embryonic preparations and progressively decreases in samples obtained from older mice in contrast to $Prom^+$ particles, which increase with age (**Figure 5E**). Since apical primary cilia in the SEZ are present on NSCs, the observed age-dependent decline in primary cilia particles is consistent with previous findings showing that the neurogenic capacity of the SEZ declines with age due to a progressive decrease in NSCs (Maslov et al., 2004; Luo et al., 2006; Bouab et al., 2011; Capilla-Gonzalez et al., 2014).

Analysis of PDGFRα and CXCR4 Expression in Sorted Particles

To further confirm the identity of the sorted particles as primary or motile cilia, we next investigated the expression of signaling molecules which have been found in primary cilia, such as PDGFRα and CXCR4 (**Supplementary Table S2**; Schneider et al., 2005; Busillo and Benovic, 2007; Christensen et al., 2017; Schmid et al., 2018). To this end we obtained cilia preparations from the tissue of E18, 8 week and 25 week-old mice and analyzed particles of each given size either for PDGFRα (**Figures 6A,B**) or CXCR4 (**Figures 6C,D**) immunoreactivity. This analysis revealed that, independent of the size of the particles, the expression of both receptors drastically decreased after birth and continued to decrease with age in the case of PDGFRα. In contrast, CXCR4 was hardly detectable in cilia obtained from adult mice and no significant difference was observed between the two age groups (**Figures 6A–D**). However, independent of the age there was a positive correlation between the size and the relative expression of both antigens, which may indicate discontinuous expression of the two receptors along the cilia, leading to absent immunoreactivity in some of the fragments. We next investigated similar cilia preparations after triple immunostaining with antibodies specific for prominin-1 and AC3 and either PDGFRα or CXCR4 (**Figures 6E,F**). This analysis revealed that in every sub-population of size and age, almost all the particles displaying PDGFRα (**Figure 6E**) or CXCR4 (**Figure 6F**) immunoreactivity

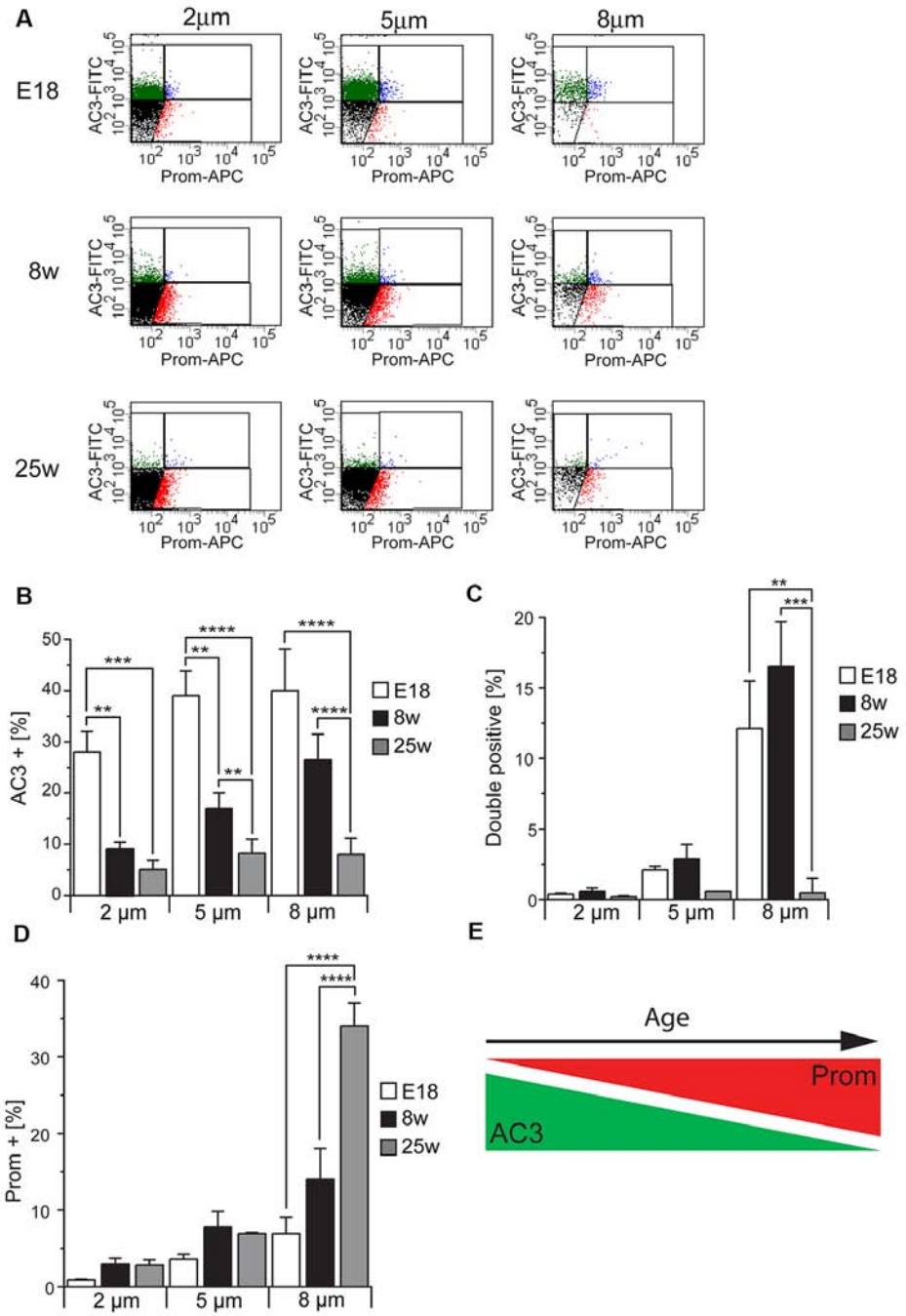

FIGURE 5 | Cilia characterization according to the expression of AC3 and prominin-1 in different mouse ages. **(A)** Representative FACS plots illustrating the distribution of particles of different sizes according to AC3 and prominin-1 (Prom) staining in E18 embryos, 8 week-old (8w) and 25 week-old (25w) mice. **(B–D)** Quantification of AC3$^+$, DP and Prom$^+$ particles in at least three independent experiments. Values represent the average percentage of particles in each population. Error bars represent SEM. Statistically significant differences are indicated with asterisks (**$p < 0.01$, ***$p < 0.001$, ****$p < 0.0005$). **(E)** Schematic representing the relative expression of AC3 and Prom across ages.

had also a marker profile of primary cilia, i.e., AC3$^+$ and DP and not of Prom$^+$ motile cilia. Indeed, depending on size and age, this fraction represented between 0% and 0.7% of the labeled particles. Moreover, although at every age analyzed the majority of the cilia immunoreactive for either receptor were AC3$^+$, with increasing age the abundance of PDGFRα$^+$ and CXCR4$^+$ cilia displaying a DP profile significantly increased, suggesting that not only the number but also the type of primary cilia expressing either receptor changes with age.

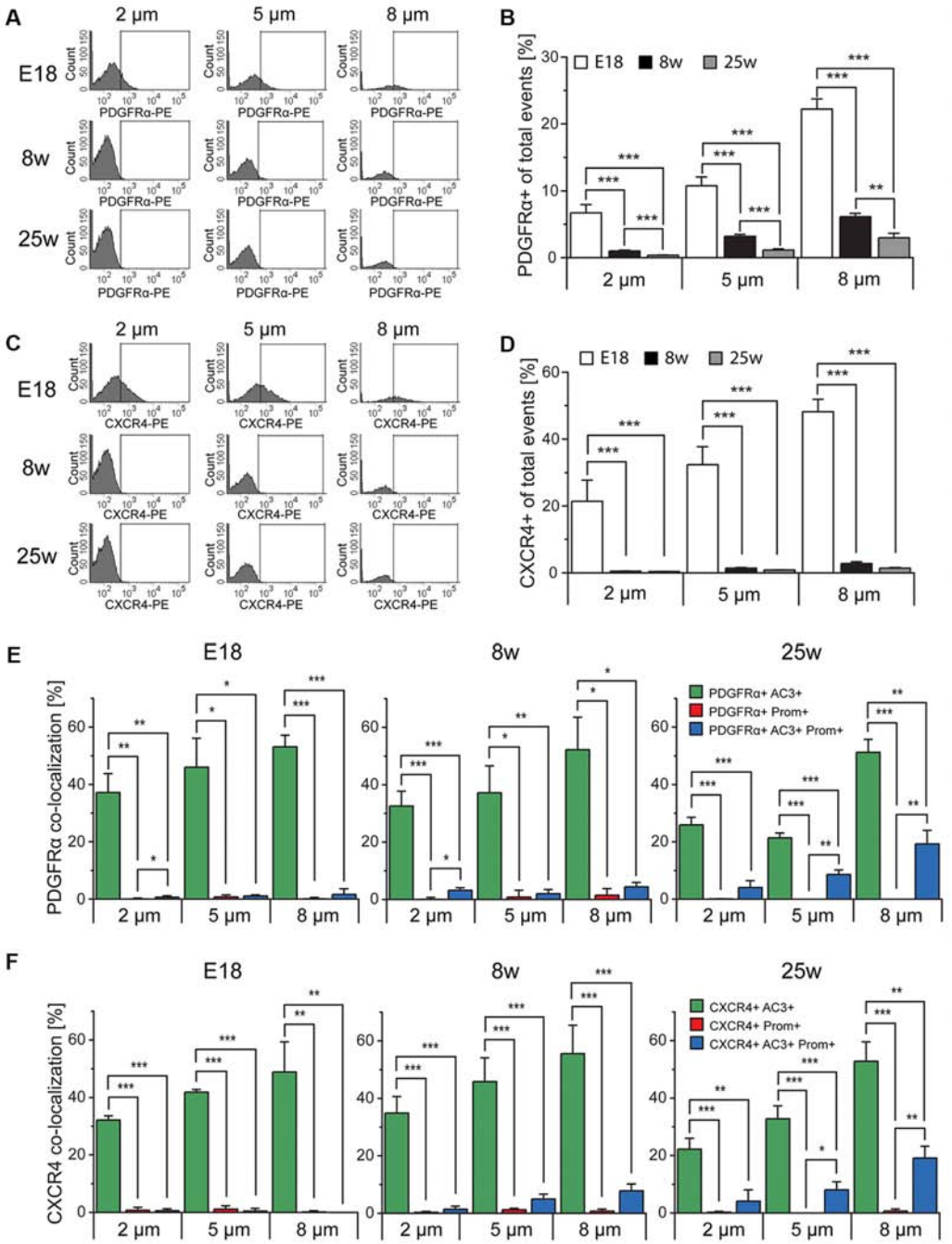

FIGURE 6 | Platelet-derived growth factor receptor α (PDGFRα) and CXC chemokine receptor 4 (CXCR4) expression in primary cilia. **(A,C)** FACS histograms depicting PDGFRα and CXCR4 total expression in particles of different size in E18 embryos (E18), 8 week-old (8w)- and 25 week-old (25w) mice. The gates include PDGFRα-PE or CXCR4-PE positive particles. **(B,D)** Quantification of the average percentage of PDGFRα$^+$ and CXCR4$^+$ particles in at least three independent experiments. **(E,F)** Quantitative analysis of the co-localization of PDGFRα and CXCR4 with AC3 (green bars), prominin-1 (Prom; red bars) and both AC3 and Prom (blue bars), as percentage of PDGFRα$^+$ or CXCR4$^+$ total particles. Values represent the average percentage of particles in each population. Error bars represent SEM. Statistically significant differences are indicated with asterisk (*$p < 0.05$, **$p < 0.01$, ***$p < 0.001$).

Analysis of Smoothened Expression in Sorted Particles

Another protein known to be associated with primary cilia is Smoothened (Smo; **Supplementary Table S2**) which, upon binding of SHH to Patched1, translocates to the primary cilium (Corbit et al., 2005; Eggenschwiler and Anderson, 2007; Rohatgi et al., 2007; Wilson et al., 2009). To activate SHH signaling, we incubated E18 tissue fragments in medium containing

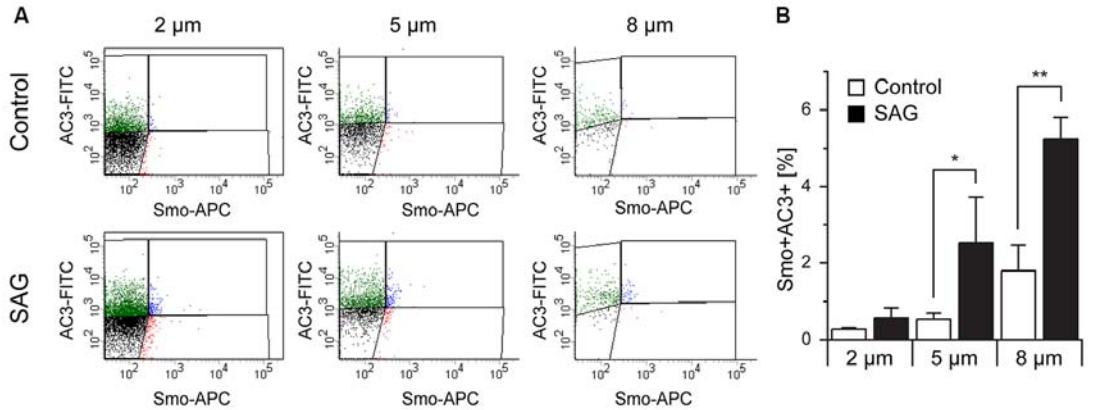

FIGURE 7 | Co-localization of Smoothened and AC3 in primary cilia. **(A)** Representative dot plots of untreated (Control) and SAG-treated samples (SAG) from E18 embryos immunostained for AC3-FITC and Smoothened-APC (Smo-APC). **(B)** Quantification of the percentage of Smo^+AC3^+ particles. Bar graphs show mean ± SEM, *p*-values are calculated with Student's *t*-test. Statistically significant differences are indicated with asterisks (*$p < 0.05$, **$p < 0.01$).

smoothened agonist SAG (Bijlsma et al., 2012; Fan et al., 2014; Lewis and Krieg, 2014; Milenkovic et al., 2015) and analyzed the effect of the treatment on Smo expression in primary cilia (**Figure 7A**). Quantitative analysis of AC3 and Smo co-expression showed that, independent of the particles size, exposure to SAG increased the expression of Smo within the population of $AC3^+$ primary cilia, especially in the subpopulation of bigger (8 µm) particles (**Figure 7B**). This observation is consistent with the notion that activation of Smo leads to its translocation to the primary cilium and it further confirms the identity of the $AC3^+$ particles as primary cilia.

DISCUSSION

Primary cilia have recently come to the forefront of the scientific interest after the discovery that a wide range of human diseases, collectively referred to as ciliopathies, are caused by defective functions of these organelles (Waters and Beales, 2011). For cilia purification and characterization, we took advantage of flow cytometry, which unlike the traditional approach of purification in sucrose density gradient (Raychowdhury et al., 2005; Mitchell et al., 2009) allows combining high throughput characteristics with highly sensitive analysis of multiple parameters in single particles of interest. Because of the analytical power of flow cytometry we were able to distinguish primary from motile cilia and investigate variability within these cilia types. For the differential identification of cilia we exploited the fact that in the brain AC3 is abundantly expressed in primary cilia, but not in motile cilia of the ependymal layer (Bishop et al., 2007). A possible exception may be represented by the cilia lining the 3rd ventricle, which express AC3 (Chen et al., 2016) however it was not investigated whether these organelles are motile cilia or primary cilia derived from tanycytes (Jarvis and Andrew, 1988; Mirzadeh et al., 2017). Consistent with the notion that it is present in primary but not motile cilia, we showed here that AC3 readily stains the primary cilia of embryonic radial glia but not the motile cilia in the adult SEZ. We here found that the majority of primary cilia do not express prominin-1, which is in keeping with previous observations in the adult SEZ (Codega et al., 2014; Khatri et al., 2014). Although prominin-1 was found widely expressed in embryonic radial glia, the expression was often associated with the apical membrane and not only with primary cilia (Dubreuil et al., 2007). Besides marker expression, several lines of evidence support our conclusion that the approach allows to discriminate primary vs. motile cilia. First, we found that the abundance of the two groups varies during aging reflecting the known changes in the presence of apical progenitors (Maslov et al., 2004) and ependymal cells (Capilla-Gonzalez et al., 2014). Second, the expression of the investigated signaling molecules was only observed in the group of primary cilia particles. In neural precursors several receptor-dependent pathways require a functioning primary cilium (Guemez-Gamboa et al., 2014). Despite the mechanism being still unclear, it is well established that SHH stimulation leads to increased presence of Smoothened in the primary cilium (Corbit et al., 2005; Rohatgi et al., 2007). Our data that PDGFRα localizes to primary cilia is also consistent with previous observations showing that neural precursors depend on primary cilia for transduction of PDGFRα signaling (Carter et al., 2012) and indicate that, like in fibroblasts (Schneider et al., 2005), also in neural precursors PDGFRα localizes to the primary cilium. Both CXCR4 and CXCR7 have been shown to localize to the cilia of developing interneurons (Wang et al., 2011). In the postnatal brain CXCR4 has been shown to be present also in neural progenitors of the SEZ (Tran et al., 2007). Moreover CXCR4-mediated signaling affects homing, (Kokovay et al., 2012), proliferation (Wu et al., 2009) and migration (Imitola et al., 2004; Carbajal et al., 2010) of neural precursors in culture and *in vivo*. Since the expression of CXCR4 has been shown throughout the ependymal layer of the SEZ (Stumm et al., 2002) our data suggest that the receptor does not localize to the motile cilia. We also found that the expression of all signaling molecules analyzed was particularly pronounced in AC3 single

positive but not DP primary cilia. This may reflect the different nature of the two ciliary particles. Indeed, the nature of the population expressing PDGFRα in the adult SEZ is still a matter of debate (Jackson et al., 2006; Chojnacki et al., 2011) and it is known that NSCs more differentiated precursors, but not ependymal cells respond to SHH in the adult SEZ (Ahn and Joyner, 2005). The fact that the expression of both PDGFRα and CXCR4 declines with age especially in AC3 single positive particles further supports the hypothesis of two distinct groups of primary cilia. However, further analysis would be necessary to conclusively address this issue.

Further evidence that we could distinguish between motile and primary cilia is the fact that the deciliation method used here allowed us to enrich for the latter organelle type. An increase in the intracellular concentration of calcium was first used for the detachment of flagella from lower eukaryotes (Watson and Hopkins, 1962; Gibbons, 1965; Hansma and Kung, 1975; Adoutte et al., 1980). In these studies exposure to high calcium ion concentration, often in the presence of detergents, was used to elicit the lysis of the membranous fraction and the detachment of the flagella at the level of the transition zone. Intracellular calcium elevations were shown to trigger shedding of flagella in protists by a mechanism that involves microtubule severing activity and contraction of the fibers in the transition zone, which may also lead to membrane fission (Quarmby and Hartzell, 1994; Sanders and Salisbury, 1994; Lohret et al., 1998). Calcium influx leads to deciliation also of olfactory (Anholt et al., 1986) and primary cilia (Overgaard et al., 2009). The relative inefficacy of the approach on the detachment of the motile cilia likely reflects the different expression of molecules regulating calcium homeostasis and sensing in motile cilia compared to primary cilia as well as flagella (Satir and Christensen, 2007; Delling et al., 2013; Doerner et al., 2015; Inaba, 2015; Lishko and Kirichok, 2015). The method triggers membrane fusion after deciliation, thereby minimizing contamination from cellular material (Satir et al., 1976). Nevertheless, contaminating cellular material including mitochondria was often observed in classical preparations. In addition, osmotic lysis of the membrane leading to the separation of the skeletal axoneme from the ciliary membrane was often observed. In contrast, the particles we purify in the present study likely contain both cilium components as for their purification we used antibodies binding to integral or peripheral proteins of the ciliary membrane and by western blot analysis we observed an enrichment in acetylated tubulin, which is found in the axoneme. However, the fact that we observed acetylated tubulin not associated with ciliary membrane proteins, i.e., in the DN particles, may indicate the presence of ciliary axoneme structures dissociated from the membrane.

Thus, our novel flow cytometry-based approach for the isolation of primary cilia is a new tool for the investigation of these organelles whose function is still poorly understood.

AUTHOR CONTRIBUTIONS

SM and KB: data collection and analysis, manuscript writing. AH: data collection, manuscript editing. GH-W and CM: data collection. FC: conception and design and overall data interpretation, manuscript writing.

FUNDING

SM and KB were funded by a Deutsche Forschungsgemeinschaft (DFG) grant (CI 43/11-1). We acknowledge financial support by DFG also within the funding program "Open Access Publishing," by the Baden-Württemberg Ministry for Science, Research and the Arts and by the University of Heidelberg.

ACKNOWLEDGMENTS

We would like to thank the Electron Microscopy Core Facility (EMCF) of the University of Heidelberg and especially Sebastian Wurzbacher for his support in the preparation of the samples. Confocal images in **Figure 2** were taken at the Nikon Imaging Center at the University of Heidelberg.

SUPPLEMENTARY MATERIAL

The Supplementary Material for this article can be found online at: https://www.frontiersin.org/articles/10.3389/fncel.2018.00519/full#supplementary-material

FIGURE S1 | Quantification of primary and motile cilia on SEM images. **(A)** Quantification of the number of primary cilia in four SEM fields of SEZ whole mounts of E18 mice before (control) and after deciliation. **(B)** Quantification of the number of tufts of motile cilia in three SEM fields of SEZ whole mounts of 8 week-old mice (8w) before and after deciliation. Bar graphs show mean ± SEM, *p*-values are calculated with Student's *t*-test. (*$p < 0.05$, ***$p < 0.001$).

FIGURE S2 | Sorting of particles according to size. Quantification of the relative abundance of sorted particles of different sizes in embryo (E18) 8 (8w) and 25 (25w) week-old mice from three independent experiments. Values represent the average percentage of particles in each population.

TABLE S1 | List of antibodies used in this study.

TABLE S2 | List of markers used in this study to identify and characterize primary and motile cilia.

REFERENCES

Adoutte, A., Ramanathan, R., Lewis, R. M., Dute, R. R., Ling, K. Y., Kung, C., et al. (1980). Biochemical studies of the excitable membrane of Paramecium tetraurelia. III. Proteins of cilia and ciliary membranes. *J. Cell Biol.* 84, 717–738. doi: 10.1083/jcb.84.3.717

Ahn, S., and Joyner, A. L. (2005). *In vivo* analysis of quiescent adult neural stem cells responding to Sonic hedgehog. *Nature* 437, 894–897. doi: 10.1038/nature03994

Anholt, R. R., Aebi, U., and Snyder, S. H. (1986). A partially purified preparation of isolated chemosensory cilia from the olfactory epithelium of the bullfrog, Rana catesbeiana. *J. Neurosci.* 6, 1962–1969. doi: 10.1523/jneurosci.06-07-01962.1986

Beckervordersandforth, R., Tripathi, P., Ninkovic, J., Bayam, E., Lepier, A., Stempfhuber, B., et al. (2010). *In vivo* fate mapping and expression analysis reveals molecular hallmarks of prospectively isolated adult neural stem cells. *Cell Stem Cell* 7, 744–758. doi: 10.1016/j.stem.2010.11.017

Berbari, N. F., O'Connor, A. K., Haycraft, C. J., and Yoder, B. K. (2009). The primary cilium as a complex signaling center. *Curr. Biol.* 19, R526–R535. doi: 10.1016/j.cub.2009.05.025

Bijlsma, M. F., Damhofer, H., and Roelink, H. (2012). Hedgehog-stimulated chemotaxis is mediated by smoothened located outside the primary cilium. *Sci. Signal.* 5:ra60. doi: 10.1126/scisignal.2002798

Bishop, G. A., Berbari, N. F., Lewis, J., and Mykytyn, K. (2007). Type III adenylyl cyclase localizes to primary cilia throughout the adult mouse brain. *J. Comp. Neurol.* 505, 562–571. doi: 10.1002/cne.21510

Bouab, M., Paliouras, G. N., Aumont, A., Forest-Berard, K., and Fernandes, K. J. (2011). Aging of the subventricular zone neural stem cell niche: evidence for quiescence-associated changes between early and mid-adulthood. *Neuroscience* 173, 135–149. doi: 10.1016/j.neuroscience.2010.11.032

Busillo, J. M., and Benovic, J. L. (2007). Regulation of CXCR4 signaling. *Biochim. Biophys. Acta* 1768, 952–963. doi: 10.1016/j.bbamem.2006.11.002

Capilla-Gonzalez, V., Cebrian-Silla, A., Guerrero-Cazares, H., Garcia-Verdugo, J. M., and Quinones-Hinojosa, A. (2014). Age-related changes in astrocytic and ependymal cells of the subventricular zone. *Glia* 62, 790–803. doi: 10.1002/glia.22642

Carbajal, K. S., Schaumburg, C., Strieter, R., Kane, J., and Lane, T. E. (2010). Migration of engrafted neural stem cells is mediated by CXCL12 signaling through CXCR4 in a viral model of multiple sclerosis. *Proc. Natl. Acad. Sci. U S A* 107, 11068–11073. doi: 10.1073/pnas.1006375107

Carter, C. S., Vogel, T. W., Zhang, Q., Seo, S., Swiderski, R. E., Moninger, T. O., et al. (2012). Abnormal development of $NG2^+PDGFR\text{-}\alpha^+$ neural progenitor cells leads to neonatal hydrocephalus in a ciliopathy mouse model. *Nat. Med.* 18, 1797–1804. doi: 10.1038/nm.2996

Chen, X., Luo, J., Leng, Y., Yang, Y., Zweifel, L. S., Palmiter, R. D., et al. (2016). Ablation of type III adenylyl cyclase in mice causes reduced neuronal activity, altered sleep pattern and depression-like phenotypes. *Biol. Psychiatry* 80, 836–848. doi: 10.1016/j.biopsych.2015.12.012

Chojnacki, A., Mak, G., and Weiss, S. (2011). PDGFRα expression distinguishes GFAP-expressing neural stem cells from PDGF-responsive neural precursors in the adult periventricular area. *J. Neurosci.* 31, 9503–9512. doi: 10.1523/JNEUROSCI.1531-11.2011

Christensen, S. T., Morthorst, S. K., Mogensen, J. B., and Pedersen, L. B. (2017). Primary cilia and coordination of receptor tyrosine kinase (RTK) and transforming growth factor β (TGF-β) signaling. *Cold Spring Harb. Perspect. Biol.* 9:a028167. doi: 10.1101/cshperspect.a028167

Codega, P., Silva-Vargas, V., Paul, A., Maldonado-Soto, A. R., Deleo, A. M., Pastrana, E., et al. (2014). Prospective identification and purification of quiescent adult neural stem cells from their *in vivo* niche. *Neuron* 82, 545–559. doi: 10.1016/j.neuron.2014.02.039

Corbit, K. C., Aanstad, P., Singla, V., Norman, A. R., Stainier, D. Y., and Reiter, J. F. (2005). Vertebrate Smoothened functions at the primary cilium. *Nature* 437, 1018–1021. doi: 10.1038/nature04117

Coskun, V., Wu, H., Blanchi, B., Tsao, S., Kim, K., Zhao, J., et al. (2008). $CD133^+$ neural stem cells in the ependyma of mammalian postnatal forebrain. *Proc. Natl. Acad. Sci. U S A* 105, 1026–1031. doi: 10.1073/pnas.0710000105

Del Bigio, M. R. (2010). Ependymal cells: biology and pathology. *Acta Neuropathol.* 119, 55–73. doi: 10.1007/s00401-009-0624-y

Delling, M., DeCaen, P. G., Doerner, J. F., Febvay, S., and Clapham, D. E. (2013). Primary cilia are specialized calcium signalling organelles. *Nature* 504, 311–314. doi: 10.1038/nature12833

Doerner, J. F., Delling, M., and Clapham, D. E. (2015). Ion channels and calcium signaling in motile cilia. *Elife* 4:e11066. doi: 10.7554/eLife.11066

Dubreuil, V., Marzesco, A. M., Corbeil, D., Huttner, W. B., and Wilsch-Bräuninger, M. (2007). Midbody and primary cilium of neural progenitors release extracellular membrane particles enriched in the stem cell marker prominin-1. *J. Cell Biol.* 176, 483–495. doi: 10.1083/jcb.200608137

Dummer, A., Poelma, C., DeRuiter, M. C., Goumans, M. J., and Hierck, B. P. (2016). Measuring the primary cilium length: improved method for unbiased high-throughput analysis. *Cilia* 5:7. doi: 10.1186/s13630-016-0028-2

Eggenschwiler, J. T., and Anderson, K. V. (2007). Cilia and developmental signaling. *Annu. Rev. Cell Dev. Biol.* 23, 345–373. doi: 10.1146/annurev.cellbio.23.090506.123249

Fan, C. W., Chen, B., Franco, I., Lu, J., Shi, H., Wei, S., et al. (2014). The Hedgehog pathway effector smoothened exhibits signaling competency in the absence of ciliary accumulation. *Chem. Biol.* 21, 1680–1689. doi: 10.1016/j.chembiol.2014.10.013

Gibbons, I. R. (1965). Chemical dissection of cilia. *Arch. Biol.* 76, 317–352.

Guemez-Gamboa, A., Coufal, N. G., and Gleeson, J. G. (2014). Primary cilia in the developing and mature brain. *Neuron* 82, 511–521. doi: 10.1016/j.neuron.2014.04.024

Hansma, H. G., and Kung, C. (1975). Studies of the cell surface of Paramecium. Ciliary membrane proteins and immobilization antigens. *Biochem. J.* 152, 523–528. doi: 10.1042/bj1520523

Hastie, A. T., Dicker, D. T., Hingley, S. T., Kueppers, F., Higgins, M. L., and Weinbaum, G. (1986). Isolation of cilia from porcine tracheal epithelium and extraction of dynein arms. *Cell Motil. Cytoskeleton* 6, 25–34. doi: 10.1002/cm.970060105

Ikeda, T., Ikeda, K., Enomoto, M., Park, M. K., Hirono, M., and Kamiya, R. (2005). The mouse ortholog of EFHC1 implicated in juvenile myoclonic epilepsy is an axonemal protein widely conserved among organisms with motile cilia and flagella. *FEBS Lett.* 579, 819–822. doi: 10.1016/j.febslet.2004.12.070

Imitola, J., Raddassi, K., Park, K. I., Mueller, F. J., Nieto, M., Teng, Y. D., et al. (2004). Directed migration of neural stem cells to sites of CNS injury by the stromal cell-derived factor 1α/CXC chemokine receptor 4 pathway. *Proc. Natl. Acad. Sci. U S A* 101, 18117–18122. doi: 10.1073/pnas.0408258102

Inaba, K. (2015). Calcium sensors of ciliary outer arm dynein: functions and phylogenetic considerations for eukaryotic evolution. *Cilia* 4:6. doi: 10.1186/s13630-015-0015-z

Ishikawa, H., and Marshall, W. F. (2013). Isolation of mammalian primary cilia. *Methods Enzymol.* 525, 311–325. doi: 10.1016/B978-0-12-397944-5.00015-8

Izawa, I., Goto, H., Kasahara, K., and Inagaki, M. (2015). Current topics of functional links between primary cilia and cell cycle. *Cilia* 4:12. doi: 10.1186/s13630-015-0021-1

Jackson, E. L., Garcia-Verdugo, J. M., Gil-Perotin, S., Roy, M., Quinones-Hinojosa, A., VandenBerg, S., et al. (2006). PDGFRα-positive B cells are neural stem cells in the adult SVZ that form glioma-like growths in response to increased PDGF signaling. *Neuron* 51, 187–199. doi: 10.1016/j.neuron.2006.06.012

Jarvis, C. R., and Andrew, R. D. (1988). Correlated electrophysiology and morphology of the ependyma in rat hypothalamus. *J. Neurosci.* 8, 3691–3702. doi: 10.1523/jneurosci.08-10-03691.1988

Jiménez, A. J., Domínguez-Pinos, M. D., Guerra, M. M., Fernández-Llebrez, P., and Pérez-Fígares, J. M. (2014). Structure and function of the ependymal barrier and diseases associated with ependyma disruption. *Tissue Barriers* 2:e28426. doi: 10.4161/tisb.28426

Keryer, G., Pineda, J. R., Liot, G., Kim, J., Dietrich, P., Benstaali, C., et al. (2011). Ciliogenesis is regulated by a huntingtin-HAP1-PCM1 pathway and is altered in Huntington disease. *J. Clin. Invest.* 121, 4372–4382. doi: 10.1172/JCI57552

Khatri, P., Obernier, K., Simeonova, I. K., Hellwig, A., Holzl-Wenig, G., Mandl, C., et al. (2014). Proliferation and cilia dynamics in neural stem cells prospectively isolated from the SEZ. *Sci. Rep.* 4:3803. doi: 10.1038/srep03803

King, S. M. (2006). Axonemal protofilament ribbons, DM10 domains, and the link to juvenile myoclonic epilepsy. *Cell Motil. Cytoskeleton* 63, 245–253. doi: 10.1002/cm.20129

Kokovay, E., Wang, Y., Kusek, G., Wurster, R., Lederman, P., Lowry, N., et al. (2012). VCAM1 is essential to maintain the structure of the SVZ niche and acts as an environmental sensor to regulate SVZ lineage progression. *Cell Stem Cell* 11, 220–230. doi: 10.1016/j.stem.2012.06.016

Lee, L. (2013). Riding the wave of ependymal cilia: genetic susceptibility to hydrocephalus in primary ciliary dyskinesia. *J. Neurosci. Res.* 91, 1117–1132. doi: 10.1002/jnr.23238

Lewis, C., and Krieg, P. A. (2014). Reagents for developmental regulation of Hedgehog signaling. *Methods* 66, 390–397. doi: 10.1016/j.ymeth.2013.08.022

Lishko, P., and Kirichok, Y. (2015). Signaling the differences between cilia. *Elife* 4:e12760. doi: 10.7554/eLife.12760

Lohret, T. A., McNally, F. J., and Quarmby, L. M. (1998). A role for katanin-mediated axonemal severing during Chlamydomonas deflagellation. *Mol. Biol. Cell* 9, 1195–1207. doi: 10.1091/mbc.9.5.1195

Luo, J., Daniels, S. B., Lennington, J. B., Notti, R. Q., and Conover, J. C. (2006). The aging neurogenic subventricular zone. *Aging Cell* 5, 139–152. doi: 10.1111/j.1474-9726.2006.00197.x

Maslov, A. Y., Barone, T. A., Plunkett, R. J., and Pruitt, S. C. (2004). Neural stem cell detection, characterization and age-related changes in the subventricular zone of mice. *J. Neurosci.* 24, 1726–1733. doi: 10.1523/JNEUROSCI.4608-03.2004

Merkle, F. T., Tramontin, A. D., Garcia-Verdugo, J. M., and Alvarez-Buylla, A. (2004). Radial glia give rise to adult neural stem cells in the subventricular zone. *Proc. Natl. Acad. Sci. U S A* 101, 17528–17532. doi: 10.1073/pnas.0407893101

Milenkovic, L., Weiss, L. E., Yoon, J., Roth, T. L., Su, Y. S., Sahl, S. J., et al. (2015). Single-molecule imaging of Hedgehog pathway protein Smoothened in primary cilia reveals binding events regulated by Patched1. *Proc. Natl. Acad. Sci. U S A* 112, 8320–8325. doi: 10.1073/pnas.1510094112

Mirzadeh, Z., Merkle, F. T., Soriano-Navarro, M., Garcia-Verdugo, J. M., and Alvarez-Buylla, A. (2008). Neural stem cells confer unique pinwheel architecture to the ventricular surface in neurogenic regions of the adult brain. *Cell Stem Cell* 3, 265–278. doi: 10.1016/j.stem.2008.07.004

Mirzadeh, Z., Kusne, Y., Duran-Moreno, M., Cabrales, E., Gil-Perotin, S., Ortiz, C., et al. (2017). Bi- and uniciliated ependymal cells define continuous floor-plate-derived tanycytic territories. *Nat. Commun.* 8:13759. doi: 10.1038/ncomms13759

Mitchell, K. A., Szabo, G., and Otero Ade, S. (2009). Methods for the isolation of sensory and primary cilia—an overview. *Methods Cell Biol.* 94, 87–101. doi: 10.1016/S0091-679X(08)94004-8

Obernier, K., Cebrian-Silla, A., Thomson, M., Parraguez, J. I., Anderson, R., Guinto, C., et al. (2018). Adult neurogenesis is sustained by symmetric self-renewal and differentiation. *Cell Stem Cell* 22, 221.e8–234.e8. doi: 10.1016/j.stem.2018.01.003

Overgaard, C. E., Sanzone, K. M., Spiczka, K. S., Sheff, D. R., Sandra, A., and Yeaman, C. (2009). Deciliation is associated with dramatic remodeling of epithelial cell junctions and surface domains. *Mol. Biol. Cell* 20, 102–113. doi: 10.1091/mbc.E08-07-0741

Palha, J. A., Santos, N. C., Marques, F., Sousa, J., Bessa, J., Miguelote, R., et al. (2012). Do genes and environment meet to regulate cerebrospinal fluid dynamics? Relevance for schizophrenia. *Front. Cell. Neurosci.* 6:31. doi: 10.3389/fncel.2012.00031

Pfenninger, C. V., Roschupkina, T., Hertwig, F., Kottwitz, D., Englund, E., Bengzon, J., et al. (2007). CD133 is not present on neurogenic astrocytes in the adult subventricular zone, but on embryonic neural stem cells, ependymal cells, and glioblastoma cells. *Cancer Res.* 67, 5727–5736. doi: 10.1158/0008-5472.can-07-0183

Quarmby, L. M., and Hartzell, H. C. (1994). Two distinct, calcium-mediated, signal transduction pathways can trigger deflagellation in Chlamydomonas reinhardtii. *J. Cell Biol.* 124, 807–815. doi: 10.1083/jcb.124.5.807

Raychowdhury, M. K., McLaughlin, M., Ramos, A. J., Montalbetti, N., Bouley, R., Ausiello, D. A., et al. (2005). Characterization of single channel currents from primary cilia of renal epithelial cells. *J. Biol. Chem.* 280, 34718–34722. doi: 10.1074/jbc.m507793200

Rohatgi, R., Milenkovic, L., and Scott, M. P. (2007). Patched1 regulates hedgehog signaling at the primary cilium. *Science* 317, 372–376. doi: 10.1126/science.1139740

Sanders, M. A., and Salisbury, J. L. (1994). Centrin plays an essential role in microtubule severing during flagellar excision in Chlamydomonas reinhardtii. *J. Cell Biol.* 124, 795–805. doi: 10.1083/jcb.124.5.795

Satir, P., and Christensen, S. T. (2007). Overview of structure and function of mammalian cilia. *Annu. Rev. Physiol.* 69, 377–400. doi: 10.1146/annurev.physiol.69.040705.141236

Satir, B., Sale, W. S., and Satir, P. (1976). Membrane renewal after dibucaine deciliation of Tetrahymena. Freeze-fracture technique, cilia, membrane structure. *Exp. Cell Res.* 97, 83–91. doi: 10.1016/0014-4827(76)90657-1

Sawamoto, K., Wichterle, H., Gonzalez-Perez, O., Cholfin, J. A., Yamada, M., Spassky, N., et al. (2006). New neurons follow the flow of cerebrospinal fluid in the adult brain. *Science* 311, 629–632. doi: 10.1126/science.1119133

Schmid, F. M., Schou, K. B., Vilhelm, M. J., Holm, M. S., Breslin, L., Farinelli, P., et al. (2018). IFT20 modulates ciliary PDGFRα signaling by regulating the stability of Cbl E3 ubiquitin ligases. *J. Cell Biol.* 217, 151–161. doi: 10.1083/jcb.201611050

Schneider, L., Clement, C. A., Teilmann, S. C., Pazour, G. J., Hoffmann, E. K., Satir, P., et al. (2005). PDGFRαα signaling is regulated through the primary cilium in fibroblasts. *Curr. Biol.* 15, 1861–1866. doi: 10.1016/j.cub.2005.09.012

Shook, B. A., Lennington, J. B., Acabchuk, R. L., Halling, M., Sun, Y., Peters, J., et al. (2014). Ventriculomegaly associated with ependymal gliosis and declines in barrier integrity in the aging human and mouse brain. *Aging Cell* 13, 340–350. doi: 10.1111/acel.12184

Shook, B. A., Manz, D. H., Peters, J. J., Kang, S., and Conover, J. C. (2012). Spatiotemporal changes to the subventricular zone stem cell pool through aging. *J. Neurosci.* 32, 6947–6956. doi: 10.1523/JNEUROSCI.5987-11.2012

Spassky, N., Merkle, F. T., Flames, N., Tramontin, A. D., García-Verdugo, J. M., and Alvarez-Buylla, A. (2005). Adult ependymal cells are postmitotic and are derived from radial glial cells during embryogenesis. *J. Neurosci.* 25, 10–18. doi: 10.1523/JNEUROSCI.1108-04.2005

Stumm, R. K., Rummel, J., Junker, V., Culmsee, C., Pfeiffer, M., Krieglstein, J., et al. (2002). A dual role for the SDF-1/CXCR4 chemokine receptor system in adult brain: isoform-selective regulation of SDF-1 expression modulates CXCR4-dependent neuronal plasticity and cerebral leukocyte recruitment after focal ischemia. *J. Neurosci.* 22, 5865–5878. doi: 10.1523/JNEUROSCI.22-14-05865.2002

Suzuki, T., Miyamoto, H., Nakahari, T., Inoue, I., Suemoto, T., Jiang, B., et al. (2009). Efhc1 deficiency causes spontaneous myoclonus and increased seizure susceptibility. *Hum. Mol. Genet.* 18, 1099–1109. doi: 10.1093/hmg/ddp006

Tobin, J. L., and Beales, P. L. (2009). The nonmotile ciliopathies. *Genet. Med.* 11, 386–402. doi: 10.1097/GIM.0b013e3181a02882

Tong, C. K., Han, Y. G., Shah, J. K., Obernier, K., Guinto, C. D., and Alvarez-Buylla, A. (2014). Primary cilia are required in a unique subpopulation of neural progenitors. *Proc. Natl. Acad. Sci. U S A* 111, 12438–12443. doi: 10.1073/pnas.1321425111

Tran, P. B., Banisadr, G., Ren, D., Chenn, A., and Miller, R. J. (2007). Chemokine receptor expression by neural progenitor cells in neurogenic regions of mouse brain. *J. Comp. Neurol.* 500, 1007–1033. doi: 10.1002/cne.21229

Wang, Y., Li, G., Stanco, A., Long, J. E., Crawford, D., Potter, G. B., et al. (2011). CXCR4 and CXCR7 have distinct functions in regulating interneuron migration. *Neuron* 69, 61–76. doi: 10.1016/j.neuron.2010.12.005

Waters, A. M., and Beales, P. L. (2011). Ciliopathies: an expanding disease spectrum. *Pediatr. Nephrol.* 26, 1039–1056. doi: 10.1007/s00467-010-1731-7

Watson, M. R., and Hopkins, J. M. (1962). Isolated cilia from Tetrahymena pyriformis. *Exp. Cell Res.* 28, 280–295. doi: 10.1016/0014-4827(62)90284-7

Weigmann, A., Corbeil, D., Hellwig, A., and Huttner, W. B. (1997). Prominin, a novel microvilli-specific polytopic membrane protein of the apical surface of epithelial cells, is targeted to plasmalemmal protrusions of non-epithelial cells. *Proc. Natl. Acad. Sci. U S A* 94, 12425–12430. doi: 10.1073/pnas.94.23.12425

Wilson, C. W., Chen, M. H., and Chuang, P. T. (2009). Smoothened adopts multiple active and inactive conformations capable of trafficking to the primary cilium. *PLoS One* 4:e5182. doi: 10.1371/journal.pone.0005182

Wu, Y., Peng, H., Cui, M., Whitney, N. P., Huang, Y., and Zheng, J. C. (2009). CXCL12 increases human neural progenitor cell proliferation through Akt-1/FOXO3a signaling pathway. *J. Neurochem.* 109, 1157–1167. doi: 10.1111/j.1471-4159.2009.06043.x

Youn, Y. H., and Han, Y. G. (2018). Primary cilia in brain development and diseases. *Am. J. Pathol.* 188, 11–22. doi: 10.1016/j.ajpath.2017.08.031

Conflict of Interest Statement: The authors declare that the research was conducted in the absence of any commercial or financial relationships that could be construed as a potential conflict of interest.

frontiers in Cellular Neuroscience

ORIGINAL RESEARCH
published: 13 February 2019
doi: 10.3389/fncel.2019.00034

Comparative Phosphoproteomic Profiling of Type III Adenylyl Cyclase Knockout and Control, Male, and Female Mice

*Yuxin Zhou[1], Liyan Qiu[1], Ashley Sterpka[1], Haiying Wang[2], Feixia Chu[1] and Xuanmao Chen[1]**

[1] Department of Molecular, Cellular and Biomedical Sciences, University of New Hampshire, Durham, NH, United States,
[2] Department of Statistics, University of Connecticut, Storrs, CT, United States

Type III adenylyl cyclase (AC3, *ADCY3*) is predominantly enriched in neuronal primary cilia throughout the central nervous system (CNS). Genome-wide association studies in humans have associated *ADCY3* with major depressive disorder and autistic spectrum disorder, both of which exhibit sexual dimorphism. To date, it is unclear how AC3 affects protein phosphorylation and signal networks in central neurons, and what causes the sexual dimorphism of autism. We employed a mass spectrometry (MS)-based phosphoproteomic approach to quantitatively profile differences in phosphorylation between inducible AC3 knockout (KO) and wild type (WT), male and female mice. In total, we identified 4,655 phosphopeptides from 1,756 proteins, among which 565 phosphopeptides from 322 proteins were repetitively detected in all samples. Over 46% phosphopeptides were identified in at least three out of eight biological replicas. Comparison of AC3 KO and WT datasets revealed that phosphopeptides with motifs matching proline-directed kinases' recognition sites had a lower abundance in the KO dataset than in WTs. We detected 14 phosphopeptides restricted to WT dataset (i.e., *Rabl6*, *Spast and Ppp1r14a*) and 35 exclusively in KOs (i.e., *Sptan1, Arhgap20, Arhgap44, and Pde1b*). Moreover, 95 phosphopeptides (out of 90 proteins) were identified only in female dataset and 26 only in males. Label-free MS spectrum quantification using Skyline further identified phosphopeptides that had higher abundance in each sample group. In total, 204 proteins had sex-biased phosphorylation and 167 of them had increased expression in females relative to males. Interestingly, among the 204 gender-biased phosphoproteins, 31% were found to be associated with autism, including *Dlg1, Dlgap2, Syn1, Syngap1, Ctnna1, Ctnnd1*, *Ctnnd2, Pkp4, and Arvcf*. Therefore, this study also provides the first phosphoproteomics evidence suggesting that gender-biased post-translational phosphorylation may be implicated in the sexual dimorphism of autism.

Keywords: Type III adenylyl cyclase (AC3), primary cilia, major depressive disorder (MDD), autistic spectrum disorder (ASD), phosphoproteomics, delta catenin, sexual dimorphism of autism, gender-biased phosphorylation

OPEN ACCESS

Edited by:
Rosanna Parlato,
University of Ulm, Germany

Reviewed by:
Victor Faundez,
Emory University, United States
Francesca Ciccolini,
Universität Heidelberg, Germany

***Correspondence:**
Xuanmao Chen
Xuanmao.Chen@unh.edu

Received: *30 October 2018*
Accepted: *23 January 2019*
Published: *13 February 2019*

Citation:
Zhou Y, Qiu L, Sterpka A, Wang H, Chu F and Chen X (2019) Comparative Phosphoproteomic Profiling of Type III Adenylyl Cyclase Knockout and Control, Male, and Female Mice. Front. Cell. Neurosci. 13:34. doi: 10.3389/fncel.2019.00034

INTRODUCTION

Primary cilia are tiny microtubule-based, membrane-ensheathed signaling devices present in most mammalian cells (Singla and Reiter, 2006). They depend on a special intraflagellar transport system for trafficking select cargo into and out of the cilium (Rosenbaum and Witman, 2002). Primary cilia are present in virtually every neuron in the brain, although they do not harbor synaptic junctions. Thus far, no ionotropic $GABA_A$ receptor or glutamate receptors have been identified in neuronal cilia (Qiu et al., 2016; Sterpka and Chen, 2018). Although their physiological function is not well-understood (Louvi and Grove, 2011), defects in neuronal primary cilia lead to obesity, psychiatric diseases, intellectual disability, and neurodevelopmental disorders in humans (Fliegauf et al., 2007). Additionally, neuronal primary cilia have abundant expression of G-protein coupled receptors (GPCRs), such as type 3 somatostatin receptor (Wang et al., 2009; Einstein et al., 2010), type 6 serotonin receptor (Brodsky et al., 2017), and melanin-concentrating hormone receptor 1 (Green et al., 2012). This suggests that neuronal primary cilia depend on metabotropic signal pathways, rather than electrical input from synapses, to modulate neuronal activity. Most, if not all, ciliary GPCRs (Schou et al., 2015) are found to be either $G\alpha_s$- or $G\alpha_i$-protein coupled receptors (Qiu et al., 2016; Sterpka and Chen, 2018), which rely on heterotrimeric G-proteins, adenylyl cyclases, and cyclic adenosine monophosphate (cAMP) to send signals to the soma of neurons (Qiu et al., 2016; Sterpka and Chen, 2018).

AC3 represents a key enzyme mediating the cAMP signaling pathway in neuronal cilia (Bishop et al., 2007; Qiu et al., 2016) and is highly expressed in olfactory sensory cilia and in neuronal primary cilia throughout the central nervous system (CNS). It is known that AC3 in olfactory sensory neurons is essential for olfactory signal transduction in the main olfactory epithelium, and loss of AC3 leads to anosmia (loss of smell) (Wong et al., 2000). In the CNS, the physiological function of AC3 is yet to be established, but multiple lines of genetic evidence have associated AC3 with major depressive disorder (MDD) (Wray et al., 2012), obesity (Nordman et al., 2008; Stergiakouli et al., 2014), and autism spectrum disorders (ASD) (Skafidas et al., 2014; Yuen et al., 2017) in humans. Moreover, our previous studies have demonstrated that AC3 ablation in mice leads to pleiotropic phenotypes, including olfactory deficit (Wong et al., 2000; Chen et al., 2012), social interaction deficit (Chen et al., 2016), and depression-like behaviors (Chen et al., 2016). However, thus far it is unknown how AC3 or cAMP generated in neuronal primary cilia regulates signal transduction of central neurons.

Post-translational modifications (PTM) regulate signaling pathway and cellular processes, mediating intracellular communication and neuronal function. Protein phosphorylation is a major type of PTM, which can cause allosteric structure changes of proteins, activation, or inhibition of enzymes, alterations in protein's subcellular localization, and protein-protein interactions (Johnson, 2009). The major downstream effector protein of cAMP in cells is protein kinase A (PKA), whose activation leads to the phosphorylation of various proteins to propagate the cAMP signaling. We hypothesized that cAMP generated by AC3 locally in neuronal primary cilia can trigger a series of phosphorylation events, thereby modulating the structure and function of many downstream proteins and consequently affecting neuronal function. Therefore, identification of protein phosphorylation affected by AC3 will help delineate AC3-signaling network in CNS neurons. To systematically identify phosphorylation that is modulated by AC3, we employed a mass spectrometry-based quantitative phosphoproteomic approach, a powerful method to elucidate many signal pathways including the cAMP signaling pathway (Gunaratne et al., 2010; Roux and Thibault, 2013; Humphrey et al., 2015), to conduct a comparative phosphoproteomic profiling analysis. In this study, using a high-performance liquid chromatography-tandem mass spectrometry technology (HPLC-MS/MS), we identified thousands of peptides from prefrontal cortical tissues, some of which are differentially phosphorylated in AC3 wild type (WT) and knockout (KO) samples.

To date, although phosphoproteomic profiling analyses have identified a high throughput of phosphorylation sites (p-sites) in a variety of tissues, mouse strains, and different brain regions (Huttlin et al., 2010), virtually no studies have specifically compared phosphoproteomic differences between male and female samples. However, many neurodevelopmental disorders or psychiatric diseases such as MDD, attention deficit and hyperactivity disorder (ADHD) and ASD show a profound sex-bias (Halladay et al., 2015). For example, females have a higher risk of MDD than males (Labaka et al., 2018), whereas ASD affects more males than females with a male to female ratio of 4:1 (Kogan et al., 2009). It is unclear what causes the sexual dimorphism of these diseases. To evaluate the possibility that gender may differentially impact protein phosphorylation in the frontal cortex, we specifically compared phosphoproteomic datasets of two genders. This effort led to identification of over 200 proteins, whose phosphorylation were sex-biased. More female-biased phosphopeptides were identified than male-biased. Surprisingly, a high percentage of these targets (31%) are autism-associated proteins/genes, which include *Dlg1*, *Dlgap2*, *Syn1, SynGap1, Ctnna1,* and four delta catenin proteins (*Ctnnd1*, *Ctnnd2, Pkp4, and Arvcf*) (Yuan and Arikkath, 2017). Hence, this study provides the first phosphoproteomic evidence suggesting that gender-biased protein phosphorylation may contribute to the sexual dimorphism of autism.

MATERIALS AND METHODS

Supplemental Information provides additional Methods and Materials including Mice, Immunofluorescence Staining and Confocal Imaging, Western blot methods and detailed statistical methods.

Tissue Preparation, Protein Extraction, and Phosphopeptide Enrichment

Prefrontal cortex tissues were isolated from 18 to 20 week old mice after euthanization, flash-frozen in liquid nitrogen, and stored in −80°C until analysis. Samples were then homogenized

and lysed by grinding on ice in tissue lysis buffer (50 mM Tris-HCl, pH 8.0, 150 mM KCl, 1% TritonX-100, 0.5 mM PMSF, 0.5 mM EDTA) containing proteinase inhibitor cocktail (Cat. No. 04693159001, Roche, Germany) and phosphatase inhibitor cocktail (Cat. No. 04906837001, Roche, Germany). Lysates were cleared twice by centrifugation at 14K RPM for 20 min at 4°C. Protein centration was measured with Qubit fluorometer and ∼3 mg of brain lysate from each sample was loaded in 12–20% gradient SDS-PAGE. In-gel digestion with reduction (final concentration 10 mM dithiothreitol, 56°C, 1 h) and alkylation (final concentration 55 mM iodoacetamide, 45 min in dark) were carried out at 37°C for 4 h. Phosphopeptides were enriched by MOAC (Titansphere^{TM} Phos-TiO Kit; GL Sciences Inc., Tokyo, Japan). Briefly, 500 μl of Speed Vac enriched trypsin digested peptides (1 mg/ml) were mixed with 1,000 μl binding solution (25% lactose acid, 60% acetonitrile, 0.3% trifluoroacetic), loaded onto Phos-TiO tip with 3 mg titanium dioxide (TiO_2) resin. The resin was washed with 80% acetonitrile and 0.4% trifluoroacetic and eluted with 50 μl 5% ammonium hydroxide followed by 50 μl 5% pyrrolidine. Enriched phosphopeptides were concentrated via Speed Vac for pyrrolidine removal and mass spectrometric analysis.

Mass Spectrometry and Database Searching

HPLC-MS/MS data was acquired on a LTQ Orbitrap Elite mass spectrometer (Thermo Fisher, CA) coupled to a NanoAccuity UPLC (Waters, MA) in Whitehead MS Facility at MIT (Boston, MA). Peptides were separated by a C18 column at 250 nL/min flow rate and 90-min gradient program. LC-MS data were acquired in an information-dependent acquisition mode, cycling between a MS scan (m/z 395–1,800, resolution 240,000) acquired in the Orbitrap, followed by 10 low-energy CID analysis in the linear ion trap. The centroided peak lists of the CID spectra were generated by PAVA (Guan and Burlingame, 2010) and searched against SwissProt.2017.11.01 *Mus Musculus* protein database, using Batch-Tag, a program module in Protein Prospector version 5.21.2 (University of California, San Francisco). A precursor mass tolerance of 20 ppm and a fragment mass tolerance of 0.6 Da were used for protein database search with S/T/Y phosphorylation included in variable modifications. Protein hits are reported with a Protein Prospector protein score ≥22, protein discriminant score ≥0.0 and a peptide expectation value ≤0.01 (Chalkley et al., 2005). With similar parameters, false discovery rate (FDR) of all samples was <1.5% when searched against the SwissProt random concatenated database. A threshold of SILP score > 6 was imposed for false phosphorylation site assignment <5%.

Label-Free Quantification

Label-free quantification was performed using Skyline ver 4.1.0.18169 via MS1 full-scan filtering with the library generated by ProteinProspector (Cut-off score = 0.95; Precursor charge = 2, 3, 4, 5; Max Miss Cleavages = 1) and the SwissProt Mus Musculus protein FASTA file (Schilling et al., 2012). MS results of three fractions from each sample were combined into one project. Peak areas of identified peptides were generated from Skyline and normalized to the protein concentration of lysate samples. Phosphopeptides with different phosphorylation states, such as mono-phosphorylation and di-phosphorylation, were considered as different entries for quantitation. Identical phosphopeptides from different gel fractions of a same sample were combined for quantitation. Since methionine oxidation can be introduced during sample handling, phosphopeptides with different methionine oxidation states were combined for quantitation. Phosphopeptides with identical sequence in homologous proteins were included in the calculation of protein phosphorylation level for homologous proteins.

Bioinformatics Analysis

The phosphoprotein lists generated from ProteinProspector were analyzed by AmiGO 2 (Mi et al., 2017) for pathway/network enrichment. The kinase substrate motif search was performed by web-based Motif-X v1.2 10.05.06 (motif-x.med.harvard.edu/motif-x.html) and analyzed basing on the Human Protein Reference Database (www.hprd.org) (Keshava Prasad et al., 2009; Chou and Schwartz, 2011). Phosphopeptides with site assignment confidence level higher than 95% were aligned in Motif-X. The motif widths were adjusted to 6 amino acids from each side of the phosphorylation site. The occurrences were set as 5 and significances were set as 0.000004, which led to a maximal number of motifs and $p < 0.001$. Protein-protein interaction network analysis was performed by the Cytoscape-based Search Tool for the Retrieval of Interacting Genes/Proteins (STRING, string-db.org) (Szklarczyk et al., 2015). All the proteins with phosphorylation that revealed differences between AC3 KO and WT, or between female and male were searched in PubMed and AutDB (Autism Gene Database, updated in Sept. 2018) (Basu et al., 2009), an autism candidate gene database, to explore possible association between the disease and phosphoproteome.

Data Analysis

Data analysis and figure constructs were performed with Origin Pro and Graphpad Prism 7 software for Student's *t*-test, normality test. Phosphopeptides detected in no <3 KO samples but none in any WT control samples (out of $n = 8$ pair) were considered statistically significantly enriched in AC3 KO sample group (determined by Two Population Proportions Comparison). For phosphopeptides that were detected in both genotypes or genders, label-free quantitation of was used to identify statistically significant ($p < 0.05$) differences in phosphorylation between KO and WT, or female and male. Phospho-peptides with $\ln \frac{peak\ area\ of\ KO\#}{average\ peak\ area\ of\ all} \leq 0$ showed lower phosphorylation levels of the target peptide site in AC3 KO samples than in WT samples. Conversely, $\ln \frac{peak\ area\ of\ KO\#}{average\ peak\ area\ of\ all} \geq 0$ showed higher phosphorylation levels of the target phosphopeptide site in AC3 KO samples than in WT samples. For label-free quantification between two genders, phosphopeptides detected in 3 of 8 gender pairs covered both of two genders were analyzed. Phosphopeptides with $\ln \frac{peak\ area\ of\ F\#}{average\ peak\ area\ of\ all} \leq 0$ and $-\ln \frac{peak\ area\ of\ M\#}{average\ peak\ area\ of\ all} \leq 0$ had lower phosphorylation levels in female samples than in male samples. In vice versa,

$\ln \frac{peak\ area\ of\ F\#}{average\ peak\ area\ of\ all} \geq 0$ and $-\ln \frac{peak\ area\ of\ M\#}{average\ peak\ area\ of\ all} \geq 0$ means phosphorylation levels of target phosphopeptide site in female samples were higher than that in males. All peptides spectra presented in the figure and table were reviewed and verified manually. If not otherwise indicated in the figure legends, statistical analysis was a paired student *t*-test with a two-tailed distribution. n.s. not significant, $^{*}p < 0.05$, $^{**}p < 0.01$, $^{***}p < 0.001$. Data were considered as statistically significant if $p < 0.05$. Data in the graph were presented as mean ± standard error of the mean.

Two Population Proportions Comparison

We used "Two Population Proportions" for comparison to set the "3 out of the $n = 8$ samples" cut-off to determine "a phosphopeptide is enriched in one sample group." Mass spectrometer randomly picks a peptide separated by HPLC to be sequenced and identified. High abundance peptides are detected more frequently. We calculated the *p*-value by comparing two population proportions between two groups as the following. Specifically, we wanted to test the null hypothesis of $p_1 = p_2$ against the research hypothesis of $p_1 \neq p_2$ in the following.

For an individual phosphopeptide, in control group, $\widehat{p_1} = \frac{X_1}{n_1} = \frac{3}{8}$; in AC3 KO group, $\widehat{p_2} = \frac{X_2}{n_2} = \frac{0}{8}$; in the combined group $\hat{p} = \frac{X_1+X_2}{n_1+n_2} = \frac{3}{16}$; We calculated the test statistics value according to the z-score $z = \frac{\widehat{p_1}-\widehat{p_2}}{\sqrt{\hat{p}(1-\hat{p})\left(\frac{1}{n_1}+\frac{1}{n_2}\right)}} = 1.92$, and used the standard normal distribution, N (0,1) to approximate the $p = P\left(\mathrm{N}(0,1) > z\right) = 0.027 < 0.05$. Similarly, if a phosphopeptide was detected in 2 control samples and was not detected in any KO samples, then z-score = 1.52, $p = 0.0655$. If a phosphopeptide was detected in three control samples and detected in 1 KO sample, $Z = 1.62$, $p = 0.0526$. Conclusion: If a phosphopeptide was detected in three or more than three control samples (out of $n = 8$), but in none of 8 KO samples, then the proportion that this phosphopeptide in the Control group was significantly higher than that in the KO group. Similarly, this calculating method was applied to the other three groups (KOs, females, and males).

Statistics to Determine "More Female-Biased Phosphorylation Than Male-Biased"

We used two statistical methods "Two Population Proportions" comparison and "Student *t*-test" to determine if there were "more female-biased phosphorylation than male-biased." Using Two Population Proportions comparison, we calculated a z-score = 9.87, $p < 0.0001$. Conducting an unpaired Student *t*-test yielded a $p = 0.023 < 0.05$. Detailed methods were provided in the **Supplemental Information**.

Statistics to Determine "A High Percentage of the Sex-Biased Phosphoproteins Are From ASD-Associated Genes"

AutDB collects a total of 1,053 ASD gene entries. The human genome is estimated to have 20,000 genes. Thus, the 1,053 ASD genes are estimated to represent 5.2% of all human genes in human genome. We have identified 204 sex-biased phosphorylation, among which 32 proteins (15.6%) were listed in the AutDB as ASD genes. The ASD gene percentage is 32/204 = 15.6%. We used "Two Population Proportions" method to compare two groups and produced a *Z*-score = 6.57 and $p < 0.0001$. Detailed statistical method was provided in the **Supplemental Information**.

Statistics of Cross Comparison of Four Groups

We used Pearson's Chi-square test to carry out a cross comparison of four groups (Female KOs, Females WTs, Male KOs, Male WTs). Detailed method as well as the results of cross comparison of 4 groups were provided in the **Supplemental Information**.

Choosing Appropriate Statistical Method for Data Comparison

Throughout this manuscript, we mostly used two population proportions comparison (3 out of $n = 8$ cut off) as well as Student's *t*-test for data comparison. Rationales were provided in the **Supplemental Information**.

RESULTS

AC3 Is Highly Enriched in Neuronal Primary Cilia, but Not in Astrocyte Cilia or Microglia in the Prefrontal Cortex

Because AC3 is associated with MDD (Wray et al., 2012; Chen et al., 2016) and ASD (Skafidas et al., 2014; Yuen et al., 2017), we chose the prefrontal cortex, a brain region important for social behaviors, personality and emotion, and mood state (Siddiqui et al., 2008), in our phosphoproteomics analysis. First, we tested if AC3 is expressed in the prefrontal cortex and if so, in which cell types it is expressed. Immunofluorescence staining images demonstrate that AC3 is highly expressed in neuronal primary cilia (**Figure 1A**), but not microglia (**Figure 1B**) or astrocytic primary cilia (**Figure 1C**) in the prefrontal cortex. These results are consistent with previous reports (Kasahara et al., 2014; Sipos et al., 2018; Sterpka and Chen, 2018), showing that AC3 is primarily confined to neuronal primary cilia in the brain. These data also suggest that AC3 mostly modulates the function of neurons, but not of astrocytes or microglia.

Given the major target protein of cAMP in cells is PKA, which can phosphorylate numerous downstream proteins, we set out to determine if AC3 affects post-translational phosphorylation in neurons in the prefrontal cortex. To circumvent developmental complications, we utilized AC3 floxed:Ubc-Cre/ERT2 KO mouse strain (Chen et al., 2016) to ablate AC3 temporally in adult mice. Ubc-Cre/ERT2 is a tamoxifen-inducible Cre strain with Cre expression driven by the ubiquitin C promoter (Ruzankina et al., 2007). Administration of tamoxifen to the AC3 floxed:Ubc-Cre/ERT2 mice removed more than 95% AC3's immunostaining signal in the prefrontal cortex (**Figure 1F**), whereas vehicle injection had no effect (**Figure 1G**), demonstrating that AC3

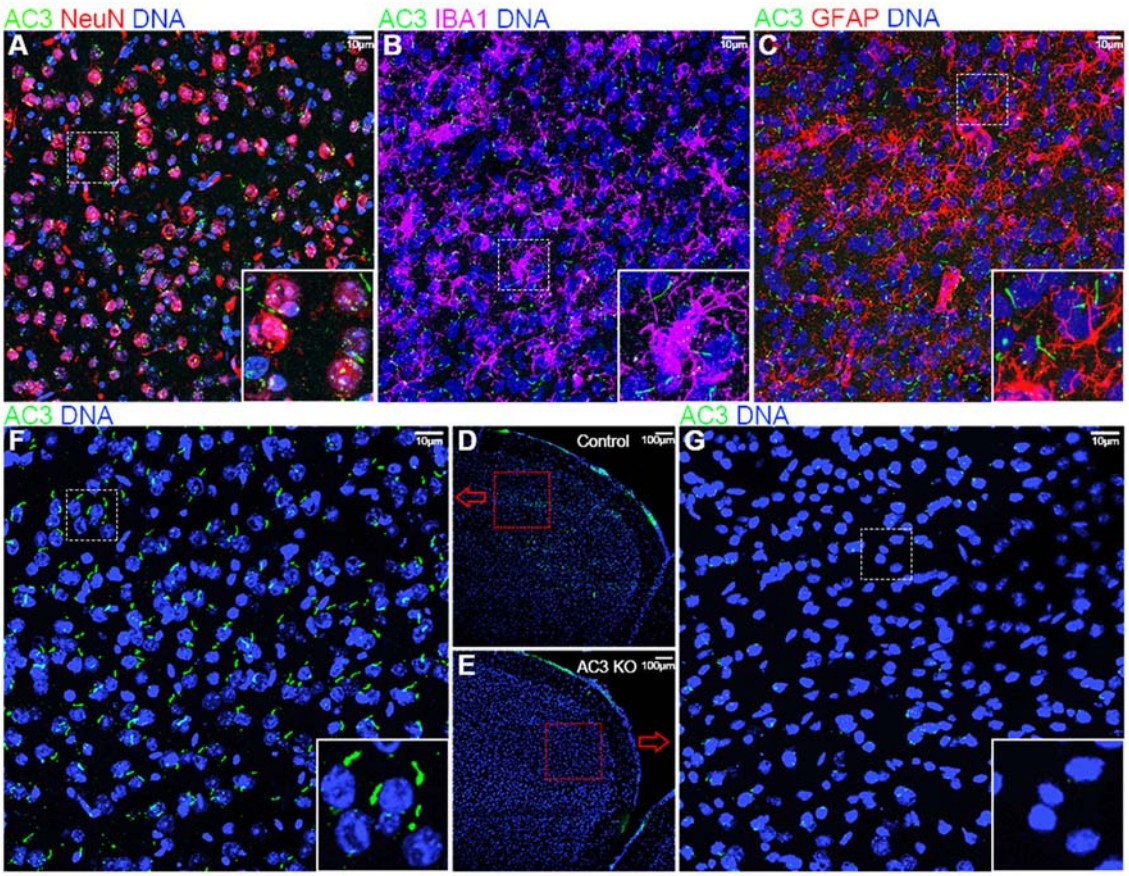

FIGURE 1 | Immunofluorescence staining of AC3 in the mouse prefrontal cortex. AC3 was predominantly enriched in neuronal primary cilia in the prefrontal cortex, but not microglia or astrocyte cilia. **(A)** Co-staining of NeuN (a neuronal marker, red) and AC3 (green) demonstrates that AC3 in primary cilia mostly localize very closely with neuronal soma (red). **(B)** Co-staining of IBA1 (a microglia marker, magenta) with AC3 (green) demonstrates the absence of AC3 in microglia. Note that green staining generally does not overlap with magenta. **(C)** Co-staining of GFAP (an astrocyte marker, red) with AC3 (green) shows that most astrocytes do not have AC3 in cilia. **(D–G)** AC3 was highly expressed neuronal primary cilia in AC3 WT **(D,F)**, but minimally in AC3 inducible KO tissues **(E,G)**. **(F,G)** are enlarged from **(D,E)**, respectively.

was successfully ablated in the adult mouse brain after tamoxifen injection.

Mass Spectrometry-Based Phosphoproteomic Analysis Using AC3 WT and KO, Male and Female Samples

To efficiently identify phosphorylation differences in the prefrontal cortex between AC3 KO and WT mice, we utilized a MS-based phosphoproteomic approach to identify phosphopeptides in large scale. Proteins of the prefrontal cortex (isolated from WT, KO, male, and female mice, respectively) were extracted and digested with trypsin. Resultant phosphopeptides were enriched using TiO_2 enrichment column and then subjected to HPLC-MS/MS analysis and database search for identification using UCSF Protein Prospector (**Figure 2**). Additionally, we determined the relative abundance of (p)Ser, (p)Thr, and (p)Tyr residues in the dataset. On average, ∼94% of detected unique peptides were phosphorylated peptides, indicating that the phosphopeptide TiO_2 enrichment was efficient and successful (**Figure 2**). Among all phosphorylated peptides (total 94%), (p)Ser accounted for 73% of total phospho-peptides, (p)Thr 19%, and (p)Tyr 2% (**Figure 2**), which is consistent with previous phosphoproteomic reporting (Olsen et al., 2006; Huttlin et al., 2010).

In total, 4,655 different phosphopeptides were detected from 1,756 proteins (**Table S1**), among which 2,390 (51.4%) were present at least in three out of the 8 biological replicas in AC3 KO group, 2,244 (48.2%) in AC3 WT group, 2,427 (52.2%) in Female group, 2,158 (46.4%) in Male group (**Table S2**). Five hundred and sixty five phosphorylation sites from 322 proteins were detected out of all 16 samples (**Table S3**). In each sample group (n = 4 for each), 62% of phosphorylated peptides were detected in more than 2 of 4 samples, and 27% of phosphorylated peptides were detected in all 4 samples (**Figure 3A**), demonstrating reproducibility of the phosphoproteomic analysis. Note that the same peptide having two p-sites was counted as two different modifications. Histograms of the average of eight pairs of KO/WT MS1 peak area and 8 pairs of female/male MS1 peak area demonstrate that our datasets largely fell in approximate

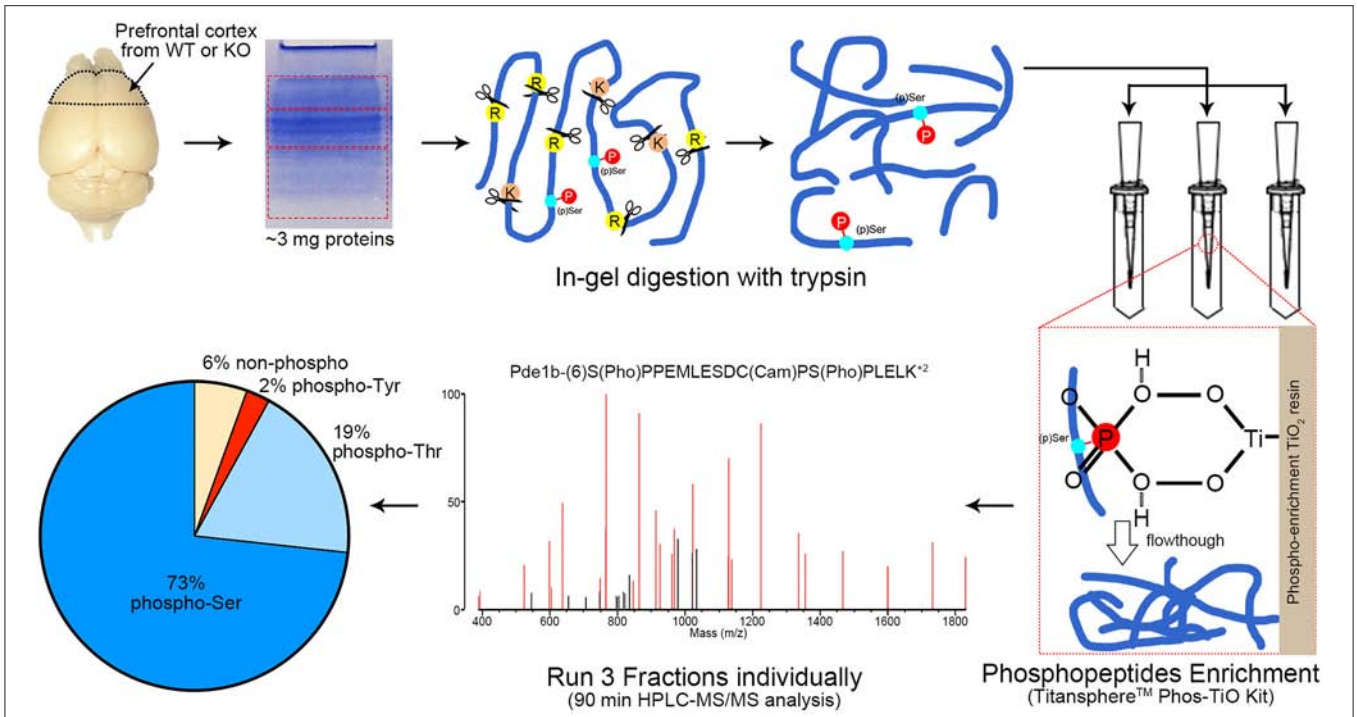

FIGURE 2 | Workflow of phosphoproteomics analysis. Prefrontal cortex tissue homogenizations were separated via SDS-PAGE and cut into 3 fractions with equal protein amount (according to Coomassie blue staining intensity measured by ImageJ). Protein extraction via in-gel digestion with trypsin (1:300 enzyme/substrate) was performed on ~3 mg protein for each sample. Phosphopeptides from each fraction were enriched by Titansphere™ Phos-TiO_2 Kit and analyzed with HPLC-MS/MS for 90 min, respectively. A MS2 spectra of Pde1b (p)Ser7 (p)Ser18 is shown as an example. MS spectra data were analyzed by ProteinProspector (ver. 5.21.2, UCSF, San Francisco, CA) and Skyline (ver. 4.1.0.18169). Among all MS-detected phosphopeptides (94%), 73% are (p)Ser, 19% (p)Thr, and 2% (p)Tyr. $n = 16$, 4 female WTs, 4 female KOs, 4 male WTs, and 4 male KOs.

statistic normal distribution (**Figure 3B**). Our experiments using biological replicas generated a range of 43–62% for peptide-level repeatability and a range of 53–75% for protein-level repeatability, representing a good range for phosphoproteomics analyses (**Figure 3C**). Forty-six to fifty-two percentages of phosphopeptides were present at least in three out of the 8 biological replicas in one sample group. These numbers were consistent with previous report (35–60%) and verified data solidity (Tabb et al., 2010).

For global phosphoproteomic profiling, the average MS1 peak area of KOs relative to WTs (x-axis), and the average MS1 peak area of males relative to females (y-axis) were constructed into a scatter plot (**Figure 3D**). This shows that the phosphorylation levels of most peptides had no general difference between genotypes or between genders, whereas only some modifications exhibit marked differences between AC3 KOs and WTs, or between females and males (**Figure 3D**). To validate our phosphoproteomic data, we also looked into Western blotting as an orthogonal method, but we were limited by the availability of commercial antibodies. We chose three anti-phosphopeptide antibodies (anti-pCaMK2a/b T286/287, anti-pSyn1 S605, anti-pERK1/2 T203/Y205 T183/Y185) for Western blot assays to verified their MS data. The anti-pCaMK2 antibody recognizes both the CaMK2a (p)Thr 286. The Western blot signal shows that CaMK2a (p)Thr 286 had no difference between WT and KO samples, and between male and female samples, which were consistent with their MS1 quantification data (**Figure S1**). Two other antibodies (anti-pSyn1 and anti-pERK1/2) yielded similar results (**Figure S1**).

To determine which classes of proteins were enriched in our MS-based phosphoproteomic analysis, the dataset of all phosphopeptides was subjected to Gene Ontology (GO) enrichment analysis (Mi et al., 2017). The GO analysis demonstrated that synaptic vehicle exocytosis proteins, gluconeogenesis, synaptic membrane protein, SNARE complex, tubulin, kinases, and SNAP receptor activity were highly enriched in our dataset, while G protein-coupled receptors, protease inhibitors, extracellular space proteins, ligand-gated ion channels, proteins mediating immune responses, and phagocytosis, cell recognition proteins, transferase, and nuclease activity were under-represented (**Figure S2**).

Motifs Matching Proline-Directed Kinases' Substrate Motifs Had Decreased Abundance AC3 KO Samples

cAMP regulates many kinases' activity including PKA and ERK1/2 (Waltereit and Weller, 2003; Sassone-Corsi, 2012). To classify MS-identified phosphopeptides into different motif categories and to determine if AC3 ablation affects the overall

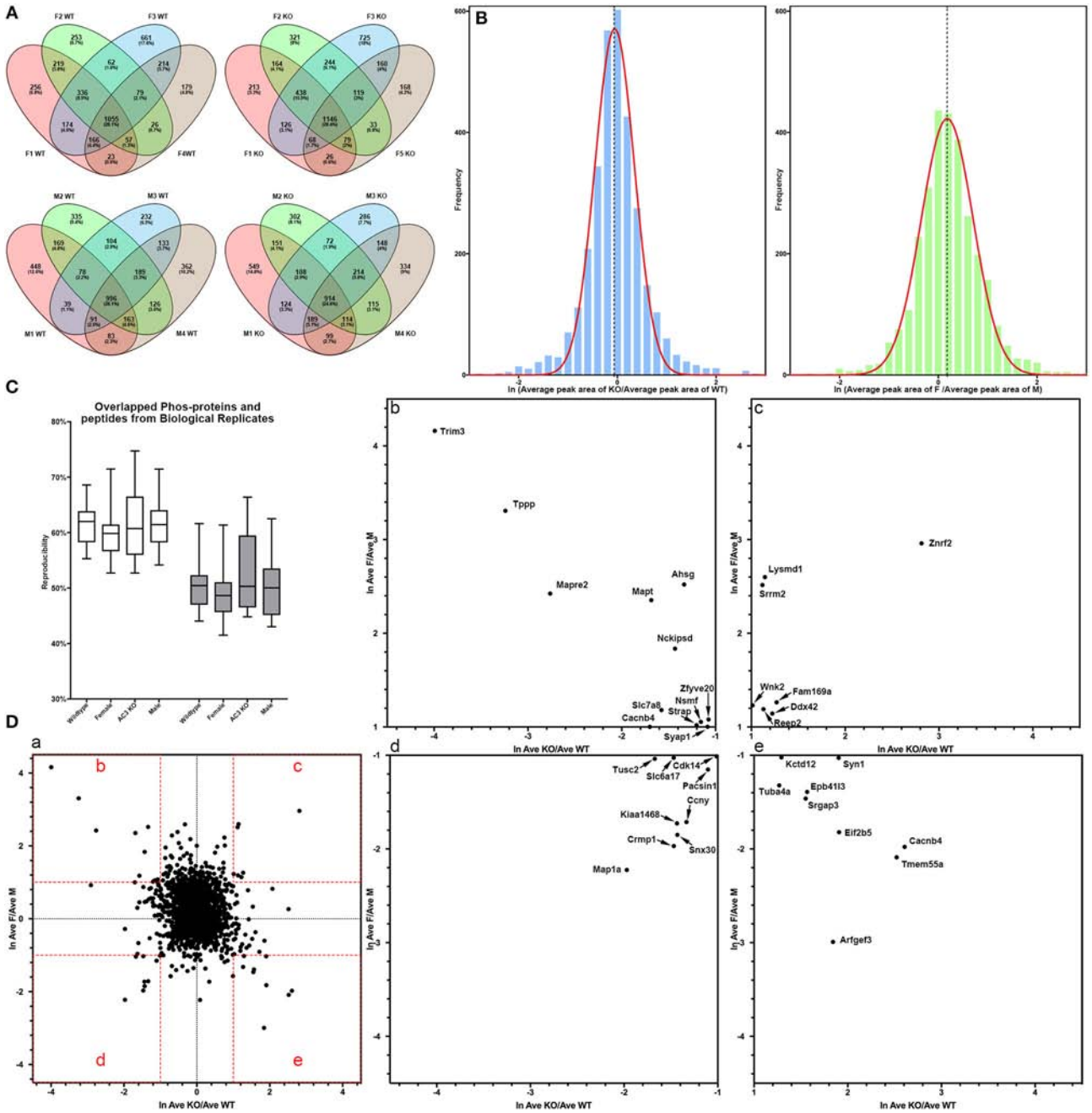

FIGURE 3 | Data quality of phosphoproteomic analysis. **(A)** Venn-diagram of phosphorylated peptides detected from 4 groups (female KO, female WT, male KO, male WT). In each group, around 62% of phosphorylated peptides were detected in more than 2 of 4 samples, and around 27% of phosphorylated peptides were detected in all 4 samples. **(B)** Histogram of relative phosphopeptide abundance of KOs compared to WTs (left), and females compared to males (Autism Genome Project et al., 2007). The histogram indicates that the dataset fits into a normal distribution. The X-axis denotes average ratio of phosphopeptide intensity in AC3 KO relative to WT (left), or females relative to males (Autism Genome Project et al., 2007). **(C)** Peptide and protein repeatability. The 28 random pairs of our biological replicates (8 per groups) showed a range for peptide-level repeatability as 43–62% and a range for protein-level repeatability as 53–75%. **(D)** Scatter plot of phosphopeptide abundance of KOs relative to WTs, and of females relative to males. (**D-**a) The X-axis denotes average ratio of phosphopeptide intensity of AC3 KOs relative to WTs. The Y-axis denotes average ratio of phosphopeptide intensity of females relative to males. (b–e) Zoom-in plot of (a) for phosphopeptides that are highly enriched in female WTs (b); female KOs (c); male WTs (d); and male KOs (e). Cut-off lines ln (KO/WT) or ln (female/male) were set to 1, meaning over 2.7-fold increase in phosphopeptide MS1 spectra intensity. The majority of p-sites exhibit similar expression levels, whereas some p-sites have different phosphorylation levels among AC3 KOs and WTs, or males and females.

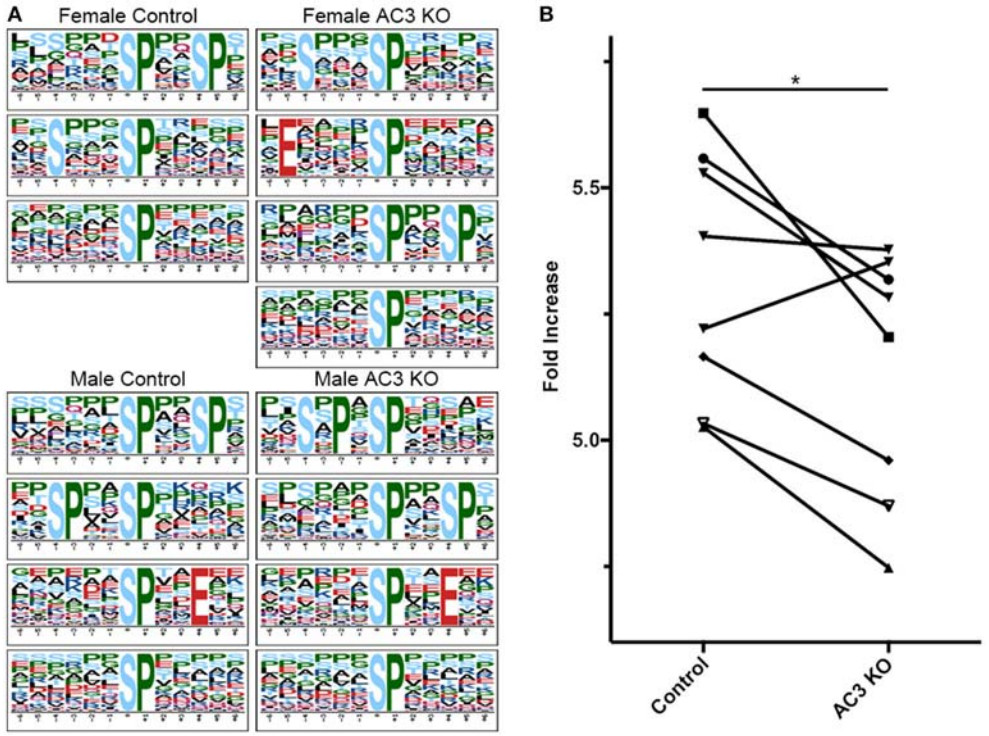

FIGURE 4 | Proline-directed kinase recognized peptide abundance is decreased in AC3 KOs compared to WTs. The sequence logos for (p)Ser with a proline residue at the +1 position for 4 different sample groups. **(A,B)** comparison of proline-detected specific motifs in enrichment fold between AC3 KOs and WTs ($n = 8$ pairs, 4 male pairs and 4 female pairs, $^*P < 0.05$).

activity of certain group of kinases, we used Motif-X (see **Figure S3** for detailed method workflow) to determine the abundance of phospho-motifs in our samples, which infers corresponding kinases' activity (Pinna and Ruzzene, 1996). Motif-X is a software tool to extract overrepresented motifs from all phosphopeptide sequences of a dataset (Chou and Schwartz, 2011). Out of the four sample groups, we found that proline-directed kinase's substrate motifs were the most common motifs in our samples (37% of all p-sites in AC3 KOs and 38% of all p-sites in WTs), largely in line with previous report (Huttlin et al., 2010). The motif [...(p)S-P...] was highly enriched in all four groups of samples (**Figure 4A**). Moreover, we compared the Motif-X sequence logos with Mouse International Protein Index (IPI) database and found that motifs ([Sxxx(pS)P], [Exxxx(pS)P], [(pS)xxSP], [SxPx(pS)P], [(pS)PxxE], [(pS)P]) were enriched in AC3 KO mice, while motifs ([Sxxx(pS)P], [(pS)xxSP], [(pS)P], [SPxx(pS)P], [(pS)PxxE]) were more abundantly present in AC3 WT mice (**Figure 4A**). Notably, the enriched proline-directed kinase-recognized motifs in our dataset matched to the kinase substrate motifs of GSK-3, CDK5, ERK1, ERK2, and mitogen-activated protein kinase-activated protein kinase 3 (Mapkapk3) reported on the Human Protein Reference Database (http://hprd.org/serine_motifs). We discovered that the motifs matching proline-detected kinases' recognition sites had significantly higher abundance in AC3 WT than in AC3 KO mice (**Figure 4B**), and the difference was gender unspecific. These data suggest that ablation of AC3 decreases the overall activity of proline-directed kinases in the prefrontal cortex.

Differential Expression of Phosphopeptides in AC3 KO and WT Mice

To identify phosphopeptides that were differently expressed in AC3 KO and WT mice, we compared AC3 KO and WT datasets. Phosphopeptides that were expressed differently ($p < 0.05$ by Two Populations Proportions comparison) in AC3 WT and KOs were pooled in **Tables 1**, **2**. **Table 1** lists 14 phosphopeptides (from 14 proteins/genes such as *Map2* and *Spast*) that were identified only in AC3 WT dataset. **Table 2** contains 35 phosphorylation sites (out of 35 genes including *Arhgap20, Arhgap44*, *Dlgap2*, *Pde1b, and Sptan1*) that were exclusively detected in AC3 KO dataset. In addition to the presence-or-absence detection, phosphopeptides' mass spectra in a dataset also exhibit variant abundance in different samples, reflecting the phosphopeptides expression levels in tissues. To determine if there are quantitative spectra differences between AC3 WT and KO mice, we used Skyline software (Schilling et al., 2012) to conduct label-free quantification. The Skyline-guided quantification was based on the MS1 peptide level. After completion of the MS1 qualification, we used differentially expressed peptides in WTs and KOs to construct a heat map. Comparison of WT data with KO data led to identification of 20 phosphopeptides

TABLE 1 | Phosphopeptides exclusively detected in AC3 WT dataset.

Gene	Protein name	Detection times (WT)	Peptide	References for ASD or related disorders
Acaca*	Acetyl-CoA carboxylase 1	3	monophos-(18)FIIGSVSEDNSEDEISNLVK	Girirajan et al., 2013
Map1a*	Microtubule-associated protein 1A	4	monophos-(2586)AKPASPARR	Myers et al., 2011
Map2	Microtubule-associated protein 2	3	monophos-(1004)ELITTKDTSPEK	Mukaetova-Ladinska et al., 2004
Spast	Spastin	3	diphos-(89)SSGTAPAPASPSPPEPGPGGEAESVR	Talkowski et al., 2012
Ahsg	Alpha-2-HS-glycoprotein	3	monophos-(301)HAFSPVASVESASGETLHSPK	#N/A
Bloc1s3	Biogenesis of lysosome-related organelles complex 1 subunit 3	3	diphos-(51)VAGEAAETDSEPEPEPTVVPVDLPPLVVQR	#N/A
Ctps1	CTP synthase 1	3	diphos-(570)SGSSSPDSEITELKFPSISQD	#N/A
Kcnip3	Calsenilin	3	diphos-(49)WILSSAAPQGSDSSDSELELSTVR	#N/A
Ppp1r14a	Protein phosphatase 1 regulatory subunit 14A	4	monophos-(19)ARGPGGSPSGLQK	#N/A
Rabl6	Rab-like protein 6	4	monophos-(477)NISLSSEEEAEGLAGHPR	#N/A
Sap30l	Histone deacetylase complex subunit SAP30L	3	diphos-(89)KASDDGGDSPEHDADIPEVDLFQLQVNTLR	#N/A
Slc6a20b	Sodium- and chloride-dependent transporter XTRP3B	3	monophos-(0)MESPSAHAVSLPEDEELQPWGGAGGPGQHPGRPRSTECAHPGVVEK	#N/A
Ube2v1	Ubiquitin-conjugating enzyme E2 variant 1	3	monophos-(135)LPQPPEGQCYSN	#N/A
Znf281	Zinc finger protein 281	3	monophos-(0)MKIGSGFLSGGGGPSSSGGSGSGGSSGSASGGSGGGR	#N/A

*Phosphopeptides listed in the table were detected in no <3 times in AC3 WT dataset (n = 8), but never detected in any AC3 KO dataset (n = 8). Proteins on top of the table were annotated in the AutDB (or per PubMed literature, labeled with *) to be associated with ASD or neurodevelopmental disorders. The number in brackets indicates the position of amino acid just before the peptide.*

(from 19 proteins/genes), which had significantly different phosphorylation levels ($p < 0.05$ by unpaired Student's *t*-test) between AC3 WT and KO dataset (**Figure 5A**). Six of them had higher expression in AC3 KOs (**Figure 5A**, Top), whereas 14 of them (from 13 proteins/genes) were more abundantly expressed in WTs (**Figure 5A**, Bottom). The overall phosphorylation levels of all phosphopeptides and the 20 differentially expressed phosphopeptides have no significant difference between AC3 WT and KO datasets (**Figure 5B**). **Figure 5C** shows that three representative phosphopeptides (identified from *Cntnap2*, *Atp2b2*, and *Ctnnd2*) exhibited significant different MS1 peak area between WT and KO dataset.

In total, we identified 65 proteins either with phosphopeptides exclusively present in AC3 WTs or KOs (as listed in **Tables 1**, **2**) or with phosphopeptide abundance having significant differences in WTs or KOs (as shown in **Figure 5A**). Since *ADCY3* is associated with MDD (Wray et al., 2012; Chen et al., 2016) and ASD (Skafidas et al., 2014; Yuen et al., 2017), we asked if AC3 affects phosphorylation of other autism-associated proteins. While MDD does not have a candidate gene databank thus far, ASD does have several databases, among which AutDB provides rich resources on ASD candidate genes (http://autism.mindspec.org/autdb/search) (Basu et al., 2009). We used these 65 proteins to search against AutDB as well as PubMed and found that 9 out of 65 were annotated in AutDB and other 7 were annotated in PubMed to be associated with ASD, which include phosphopeptides from *Dlgap2*, *Map2*, *Ank2*, *Ctnnb2*, *Cntnap2*, *Sptan1*, and *Spast* (**Tables 1**, **2** and **Figure 5A**). To explore if *Adcy3* ablation affects ciliary protein phosphorylation, we compared AC3 WT and KO datasets with Ciliome Database, a comprehensive ciliary proteome database maintained by the Leroux lab (http://www.sfu.ca/$\sim$leroux/ciliome_database.htm). Nine of the sixty five of proteins (14%) were listed in the Ciliome Database. Five of them (*Fam126a*, *Ggct*, *Pde1b*, *Ctnnd2,* and *Gapvd1)* were highly phosphorylated, whereas 4 (*Rabl6*, *Eif3b*, *Klc2,* and *Numbl*) exhibited lower phosphorylation in AC3 KOs. We did not find many hits (only 14%) that match with proteins that are listed in the Ciliome Database. We reasoned that our TiO_2 enrichment method harvested phosphopeptides from whole tissue lysate of prefrontal cortex (mostly cytosol), and primary cilia or the basal body only contributed to a little portion of the peptide pool. Still, there are several interesting targets such as *Pde1b* (Li et al., 2004), *Rabl6* (Blacque et al., 2005), *Klc2* (Li et al., 2004), and *Numbl* (Ramamurthy et al., 2014) that have been reported to be involved in ciliary biology.

To determine if some protein interaction network may be associated with the phosphoproteins differentially expressed in AC3 KOs and WTs, the 65 proteins were mapped onto the mouse Search Tool for the Retrieval of Interacting Genes/Proteins (STRING) database (string-db.org) of known

TABLE 2 | Phosphopeptides exclusively detected in AC3 KO dataset.

Gene	Protein name	Detection times (KO)	Peptide	References for ASD or related disorders
Dlgap2	Disks large-associated protein 2	3	monophos-(717)CSSIGVQDSEFPDHQPYPR	Girirajan et al., 2013
Hepacam	Hepatocyte cell adhesion molecule	5	monophos-(316)DKDSSEPDENPATEPR	Myers et al., 2011
Lsm14a*	Protein LSM14 homolog A	3	monophos-(214)RSPVPARPLPPTSQK	Mukaetova-Ladinska et al., 2004
Map1a*	Microtubule-associated protein 1A	3	monophos-(457)KFSKPDLKPFTPEVR	Talkowski et al., 2012
Map2	Microtubule-associated protein 2	4	monophos-(1634)SGILVPSEK	Girirajan et al., 2013
Myh11*	Myosin-11	4	monophos-(1946)VIENTDGSEEEMDAR	Myers et al., 2011
Nav1*	Neuron navigator 1	3	monophos-(374)LELVESLDSDEVDLK	Mukaetova-Ladinska et al., 2004
Sptan1*	Spectrin alpha chain, non-erythrocytic 1	4	diphos-(1181)DEADSKTASPWK	Talkowski et al., 2012
Strip2*	Striatin-interacting proteins 2	3	monophos-(361)QDSLDIYNER	Girirajan et al., 2013
Agk	Acylglycerol kinase, mitochondrial	3	monophos-(281)LASFWAQPQDASSR	#N/A
Arfgap2	ADP-ribosylation factor GTPase-activating protein 2	4	monophos-(428)AISSDMFFGR	#N/A
Arhgap20	Rho GTPase-activating protein 20	3	diphos-(795)SKPVPISVASYSHGSSQDHPRK	#N/A
Arhgap44	Rho GTPase-activating protein 44	3	monophos-(604)GSPGSIQGTPCPGTQLGPQPAASPSQLPADQSPHTLR	#N/A
C2cd2l	C2 domain-containing protein 2-like	3	monophos-(413)NLGTPTSSTPRPSITPTK	#N/A
Cdk14	Cyclin-dependent kinase 14	3	monophos-(92)VHSENNACINFK	#N/A
Clip2	CAP-Gly domain-containing linker protein 2	3	monophos-(914)VLLLEANRHSPGPER	#N/A
Cops5	COP9 signalosome complex subunit 5	3	monophos-(282)GSFMLGLETHDR	#N/A
Cox4i1	Cytochrome c oxidase subunit 4 isoform 1, mitochondrial	3	monophos-(42)DYPLPDVAHVTMLSASQK	#N/A
F11r	Junctional adhesion molecule A	3	diphos-(278)VIYSQPSTRSEGEFK	#N/A
Fam126a	Hyccin	3	monophos-(452)SFEQVSGAPVPR	#N/A
Ggct	Gamma-glutamylcyclotransferase	3	monophos-(169)GKISDEMEDIIK	#N/A
Itm2c	Integral membrane protein 2C	3	monophos-(20)AAASGPASASAPAAEILLTPAR	#N/A
Kcnb2	Potassium voltage-gated channel subfamily B member 2	3	monophos-(460)SMELIDVAVEK	#N/A
Kctd8	BTB/POZ domain-containing protein KCTD8	3	monophos-(410)RNSELFQSLISK	#N/A
Lysmd2	LysM and putative peptidoglycan-binding domain-containing protein 2	3	monophos-(28)SRSTSEPEEAELSLSLAR	#N/A
Mdh2	Malate dehydrogenase, mitochondrial	4	monophos-(241)AGAGSATLSMAYAGAR	#N/A
Nwd1	NACHT and WD repeat domain-containing protein 1	3	monophos-(935)LWSLLSGQEKVTILDGGSQNPTEPQSWDLHVDER	#N/A
Pde1b	Calcium/calmodulin-dependent 3',5'-cyclic nucleotide phosphodiesterase 1B	4	diphos-(6)SPPEMLESDCPSPLELK	#N/A
Pgam1	Phosphoglycerate mutase 1	3	monophos-(117)SYDVPPPPMEPDHPFYSNISK	#N/A
Pja1	E3 ubiquitin-protein ligase Praja-1	3	monophos-(226)VFFDTDDDDDVPHSTSR	#N/A
Serbp1	Plasminogen activator inhibitor 1 RNA-binding protein	3	monophos-(240)QISYNCSDLDQSNVTEETPEGEEHPVADTENKENEVEEVK	#N/A
Srcin1	SRC kinase signaling inhibitor 1	3	diphos-(1124)AVSEVVRPASTPPIMASAIKDEDDEER	#N/A
Stac2	SH3 and cysteine-rich domain-containing protein 2	3	monophos-(45)SKSVENFFLR	#N/A
Tjp2	Tight junction protein ZO-2	3	monophos-(965)DASPPPAFKPEPPK	#N/A
Tyro3	Tyrosine-protein kinase receptor TYRO3	3	monophos-(799)AEQPTESGSPEVHCGER	#N/A

*Phosphopeptides listed in the table were detected in no <3 times in KO dataset (n = 8), but never detected in any AC3 WT dataset (n = 8). Proteins on top of the table were annotated in the AutDB (or per PubMed literature, labeled with *) to be associated with ASD or neurodevelopmental disorders. The number in brackets indicates the position of amino acid just before the peptide.*

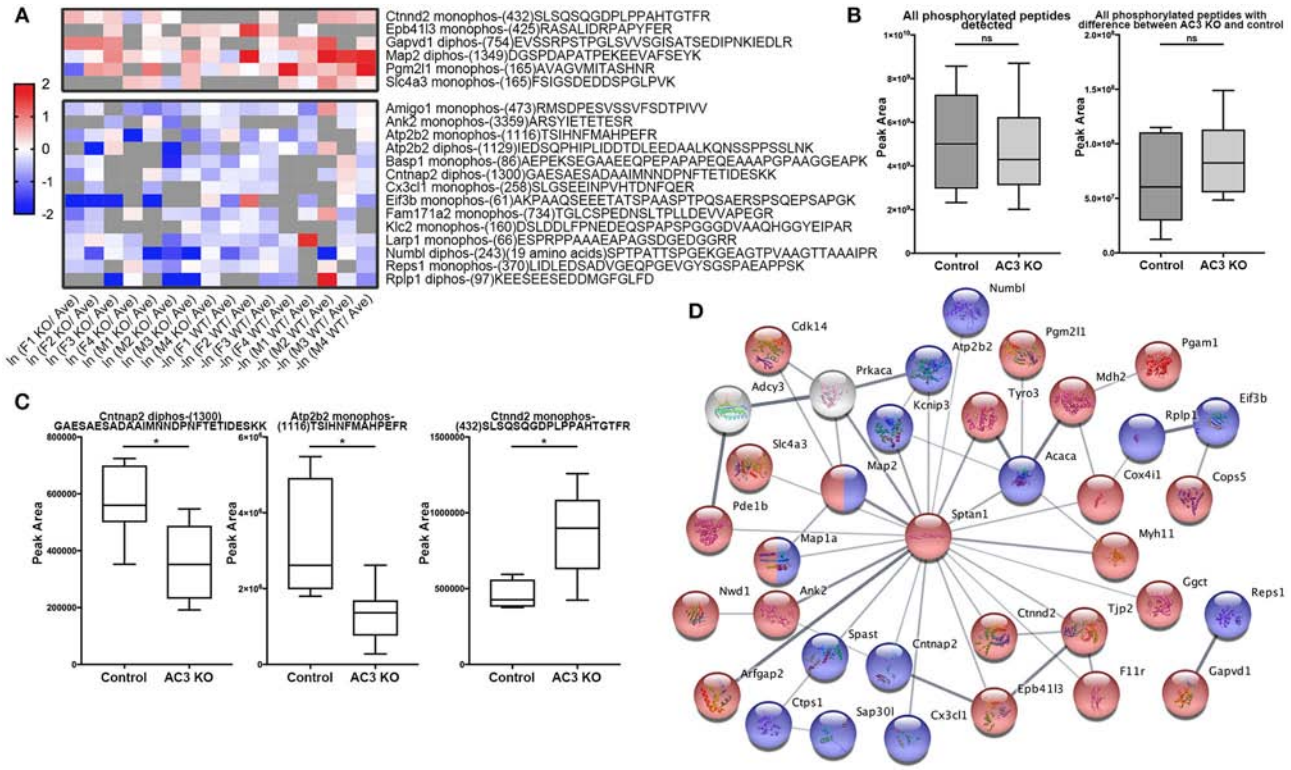

FIGURE 5 | Comparison of phosphopeptide abundance in AC3 KO and WT datasets and their protein interaction. **(A)** Heat map of phosphopeptides that show significant differences in AC3 KOs or WTs. X-axis denotes ln (peak area of individual peptide from KO data/average peak area of all data) for AC3 knockout dataset, or -ln (peak area of individual peptide from WT data/average peak area of all data) for AC3 WT dataset. Peak area differences of phosphopeptides in KO and WT datasets with $p < 0.05$ (unpaired Student's *t*-test) was used to construct the heat map. **(B)** The sum peak areas of all identified phosphopeptides in AC3 WTs ($n = 8$) and AC3 KOs ($n = 8$) have no difference (left). The sum peak areas of 20 phosphopeptides (shown in **A**) in AC3 controls and AC3 KOs have no significant difference (unpaired Student's *t*-test). **(C)** Three representative plots phosphopeptides from *Cntnap2*, *Atp2b2*, and *Ctnnd2* of label-free quantification of phosphorylation levels in WTs and KOs. **(D)** Protein-protein interaction STRING analysis using phosphoproteins differentially expressed in AC3 KOs and WTs. AC3 and PKA were manually included. Phosphoproteins with increased phosphorylated levels in KOs were highlighted in red, or in WTs highlighted in blue. Proteins marked in half red/blue had both increased and decreased p-sites on different positions in both WTs and KOs. Interaction score confidence = 0.400.

protein interactions (**Figure 5D**). STRING is a Cytoscape-based protein-protein interaction network analysis software, which maps and predicts protein-protein interaction (Szklarczyk et al., 2015). AC3 (*Adcy3*) as well as PKA (*Prkaca*) were added into the STRING database manually to examine whether these 65 proteins also have direct or indirect interaction with each other. We found 34 of 65 proteins had direct or indirect interaction with each other (**Figure 5D**). Thirteen out of the thirty-four had decreased expression level in AC3 KOs, whereas 19 of them had increased expression in AC3 KOs. Two of them (*Map1a* and *Map2*) had both up-regulated and down-regulated phosphopeptides (**Figure 5D**). Notably, the protein interaction map centered around *Sptan1* (encoding α-II Spectrin). In the protein-protein interaction network, 45% of connectivity are established between *Sptan1* with other genes, removing *Sptan1* would dramatically change the network (**Figure S4**). *Sptan1* has a bi-phosphorylation site (S1186|T1188|S1190) detected in 4 AC3 KO samples, but in none of 8 WTs (see **Table 2**). *Sptan1* is a principal membrane skeleton component and provides a spectrin-actin cytoskeleton interface to integrate signals (Machnicka et al., 2012, 2014). *Sptan1* plays a critical role in neurodevelopment and mutations of *Sptan1* leads to encephalopathy, intellectual disability and ASD (Syrbe et al., 2017). Note that AC3 is associated with ASD (Skafidas et al., 2014; Yuen et al., 2017) and primary cilia regulate neurodevelopment (Valente et al., 2014).

Differential Expression of Phosphopeptides in Male and Female Samples

Males and females differ greatly in cognition, behaviors, and disease susceptibility (Zagni et al., 2016). Remarkably, many psychiatric diseases, such as ADHD, MDD, and ASD, exhibit a sexual dimorphism (Zagni et al., 2016). But to date it is unclear what causes the sexual dimorphism of these disorders. We hypothesized that post-translational phosphorylation may correlate with the sexual dimorphism of ASD. To determine if there are any gender-biased phosphorylations in our samples, we compared female and male datasets. All phosphopeptides exclusively enriched ($p < 0.05$ by Two Populations Proportions comparison) in males or females are listed in **Tables 3**, **4**. In total, 95 phosphorylated peptides (out of 90 proteins such

TABLE 3 | Phosphopeptides exclusively detected in female dataset.

Gene	Protein name	Detection times (in females)	Peptide	References for ASD or related disorders
Apc	Adenomatous polyposis coli protein	4	monophos-(1434)SKTPPPPPQTVQAK	Girirajan et al., 2013
Atp1a1	Sodium/potassium-transporting ATPase subunit alpha-1	6	monophos-(707)QGAIVAVTGDGVNDSPALKK	Schlingmann et al., 2018
Atp1a3	Sodium/potassium-transporting ATPase subunit alpha-3	6 6	monophos-(466)VAEIPFNSTNK monophos-(697)QGAIVAVTGDGVNDSPALKK	Myers et al., 2011 Mukaetova-Ladinska et al., 2004
Bin1	Myc box-dependent-interacting protein 1	3	monophos-(312)VNHEPEPASGASPGATIPK	Talkowski et al., 2012
Cnksr2	Connector enhancer of kinase suppressor of ras 2	3	monophos-(502)SNSPAHYSLLPSLQMDALR	Girirajan et al., 2013
Dlgap2	Disks large-associated protein 2	3	diphos-(1032)AASFRQNSATER	Myers et al., 2011
Jph3*	Junctophilin-3	5	monophos-(417)EFSPSFQHR	Mukaetova-Ladinska et al., 2004
Lrrc7	Leucine-rich repeat-containing protein 7	3	monophos-(1342)SREQQPYEGNINK	Talkowski et al., 2012
Magi2*	Membrane-associated guanylate kinase, WW and PDZ domain-containing protein 2	4	monophos-(1004)IIPQEELNSPTSAPSSEK	Girirajan et al., 2013
Map1b*	Microtubule-associated protein 1B	4	monophos-(1194)DYNASASTISPPSSMEEDKFSK	Myers et al., 2011
Map2	Microtubule-associated protein 2	3	monophos-(1004)ELITTKDTSPEK	Mukaetova-Ladinska et al., 2004
Map6*	Microtubule-associated protein 6	3	monophos-(293)SEGHEEKPLPPAQSQTQEGGPAAGK	Talkowski et al., 2012
Nav1*	Neuron navigator 1	3	monophos-(374)LELVESLDSDEVDLK	Girirajan et al., 2013
Neo1	Neogenin	3	monophos-(1200)LELKPIDKSPDPNPVMTDTPIPR	Myers et al., 2011
Plcd3*	1-phosphatidylinositol 4,5-bisphosphate phosphodiesterase delta-3	3	monophos-(489)ILSDREEEEEEEEEAEEALEAAEQR	Mukaetova-Ladinska et al., 2004
Prex1	Phosphatidylinositol 3,4,5-trisphosphate-dependent Rac exchanger 1 protein	3	monophos-(1178)SNSSYLGSDEMGSGDELPCDMR	Talkowski et al., 2012
Psmd4*	26S proteasome non-ATPase regulatory subunit 4	4	monophos-(237)AAAASAAEAGIATPGTEDSDDALLK	Girirajan et al., 2013
Ptpn1*	Tyrosine-protein phosphatase non-receptor type 1	4	monophos-(325)ELFSSHQWVSEETCGDEDSLAR	Myers et al., 2011
Slc12a6*	Solute carrier family 12 member 6	3	monophos-(21)IDDIPGLSDTSPDLSSR	Mukaetova-Ladinska et al., 2004
Smarcc1*	SWI/SNF complex subunit SMARCC1	3	diphos-(323)RKPSPSPPPPTATESR	Talkowski et al., 2012
Sorbs1*	Sorbin and SH3 domain-containing protein 1	6	monophos-(49)GTPSSSPVSPQESPKHESK	Girirajan et al., 2013
Spast	Spastin	3	diphos-(89)SSGTAPAPASPSPPEPGPGGEAESVR	Myers et al., 2011
Spry2*	Protein sprouty homolog 2	3	monophos-(108)SISTVSSGSR	Mukaetova-Ladinska et al., 2004
Srgap2*	SLIT-ROBO Rho GTPase-activating protein 2	5 3	monophos-(496)KQDSSQAIPLVVESCIR monophos-(692)GGSMEDYCDSTHGETTSAEDSTQDVTAEHHTSDDECEPIEAIAK	Talkowski et al., 2012 Girirajan et al., 2013
Srpk1*	SRSF protein kinase 1	4 4	monophos-(31)GSAPHSESDIPEQEEEILGSDDDEQEDPNDYCK monophos-(285)MQEIEEMEKESGPGQK	Myers et al., 2011 Mukaetova-Ladinska et al., 2004
Strip1*	Striatin-interacting protein 1	3	monophos-(56)KDSEGYSESPDLEFEYADTDK	Talkowski et al., 2012
Trio	Triple functional domain protein	3	monophos-(2274)NFLNALTSPIEYQR	Girirajan et al., 2013
Aagab	Alpha- and gamma-adaptin-binding protein p34	4	monophos-(196)VASAESCHSEQQEPSPTAER	#N/A
Aak1	AP2-associated protein kinase 1	4	monophos-(678)TSQQNVSNASEGSTWNPFDDDNFSK	#N/A

(Continued)

TABLE 3 | Continued

Gene	Protein name	Detection times (in females)	Peptide	References for ASD or related disorders
Acot11	Acyl-coenzyme A thioesterase 11	3	monophos-(24)SISHPESGDPPTMAEGEGYR	#N/A
Akap12	A-kinase anchor protein 12	4	diphos-(260)EKEPTKPLESPTSPVSNETTSSFK	#N/A
Amer2	APC membrane recruitment protein 2	4	monophos-(551)DSDSGDALCDLYVEPEASPATLPATEDPPCLSR	#N/A
Arfgef3	Brefeldin A-inhibited guanine nucleotide-exchange protein 3	3	monophos-(2050)GPDSPLLQRPQHLIDQGQMR	#N/A
Arhgef12	Rho guanine nucleotide exchange factor 12	3	monophos-(326)SEGVQDAEPQSLVGSPSTR	#N/A
Atg4c	Cysteine protease ATG4C	5	monophos-(424)DFDFTSTAASEEDLFSEDERK	#N/A
Atp1a2	Sodium/potassium-transporting ATPase subunit alpha-2	6	monophos-(474)VAEIPFNSTNK	#N/A
		6	monophos-(704)QGAIVAVTGDGVNDSPALKK	
Bsn	Protein bassoon	3	monophos-(1038)SHGPLLPTIEDSSEEEELREEEELLR	#N/A
Camkv	CaM kinase-like vesicle-associated protein	4	monophos-(395)SATPATDGSATPATDGSVTPATDGSITPATDGSVTPATDR	#N/A
Cir1	Corepressor interacting with RBPJ 1	3	monophos-(188)NLTANDPSQDYVASDCEEDPEVEFLK	#N/A
Cmtm4	CKLF-like MARVEL transmembrane domain-containing protein 4	4	monophos-(191)TESRDVDSRPEIQR	#N/A
Cpsf7	Cleavage and polyadenylation specificity factor subunit 7	3	monophos-(192)DSSDSADGRATPSENLVPSSAR	#N/A
Csnk1a1	Casein kinase I isoform alpha	3	monophos-(304)AAQQAASSSGQGQQAQTPTGK	#N/A
Dos	Protein Dos	3	monophos-(613)RGDSVDCPPEGR	#N/A
Epb41l1	Band 4.1-like protein 1	5	diphos-(465)SEAEEGEVRTPTK	#N/A
Epb41l3	Band 4.1-like protein 3	4	monophos-(48)QQPALEQFPEAAAHSTPVKR	#N/A
Evl	Ena/VASP-like protein	4	monophos-(232)VQRPEDASGGSSPSGTSK	#N/A
Farp1	FERM, RhoGEF and pleckstrin domain-containing protein 1	3	monophos-(387)QSPQSASLTFGEGTESPGGQSCQQAK	#N/A
Gpalpp1	GPALPP motifs-containing protein 1	3	monophos-(127)GREDPGQVSSFFNSEEAESGEDEDIVGPMPAK	#N/A
Hid1	Protein HID1	3	diphos-(583)TPEPLSRTGSQEGTSMEGSRPAAPAEPGTLK	#N/A
Hook3	Protein Hook homolog 3	4	monophos-(226)LNQSDSIEDPNSPAGR	#N/A
Hspa4	Heat shock 70 kDa protein 4	5	monophos-(521)MQVDQEEPHTEEQQQQPQTPAENKAESEEMETSQAGSK	#N/A
Ipo5	Importin-5	3	monophos-(814)RQDEDYDEQVEESLQDEDDNDVYILTK	#N/A
Kctd16	BTB/POZ domain-containing protein KCTD16	4	monophos-(282)WSSSHCDCCCK	#N/A
Lrrc47	Leucine-rich repeat-containing protein 47	3	monophos-(507)STSENKEEDMLSGTEADAGCGLSDPNLTLSSGK	#N/A
Lrsam1	E3 ubiquitin-protein ligase LRSAM1	6	monophos-(206)ESGLDYYPPSQYLLPVLEQDGAENTQDSPDGPASR	#N/A
Mvb12b	Multivesicular body subunit 12B	3	monophos-(194)NHDSSQPTTPSQSSASSTPAPNLPR	#N/A
Nckipsd	NCK-interacting protein with SH3 domain	5	monophos-(257)APSPEPPTEEVAAETNSTPDDLEAQDALSPETTEEK	#N/A
Ndel1	Nuclear distribution protein nudE-like 1	5	monophos-(223)GTENSFPSPK	#N/A
Nsf	Vesicle-fusing ATPase	3	monophos-(202)ENRQSIINPDWNFEK	#N/A
Nufip2	Nuclear fragile X mental retardation-interacting protein 2	4	monophos-(614)DYEIENQNPLASPTNTLLGSAK	#N/A
Ogfrl1	Opioid growth factor receptor-like protein 1	3	monophos-(372)EPGEEADKPSPEPGSGDPKPR	#N/A
Oxr1	Oxidation resistance protein 1	3	diphos-(358)QEKSSDASSESVQTVSQMEVQSLTATSEAANVPDR	#N/A

(Continued)

TABLE 3 | Continued

Gene	Protein name	Detection times (in females)	Peptide	References for ASD or related disorders
Pacsin1	Protein kinase C and casein kinase substrate in neurons protein 1	4	monophos-(388)ALYDYDGQEQDELSFK	#N/A
Pacsin3	Protein kinase C and casein kinase II substrate protein 3	6	monophos-(332)DGTAPPPQSPSSPGSGQDEDWSDEESPRK	#N/A
PAGR1	PAXIP1-associated glutamate-rich protein 1	3	monophos-(222)DLFSLDSEGPSPTSPPLR	#N/A
Pds5b	Sister chromatid cohesion protein PDS5 homolog B	3	monophos-(1353)AESPETSAVESTQSTPQK	#N/A
Pitpnc1	Cytoplasmic phosphatidylinositol transfer protein 1	3	diphos-(112)YEDNKGSNDSIFDSEAK	#N/A
Pnmal1	PNMA-like protein 1	3	monophos-(319)SALPAADSPGNLEDSDQDGGPENPAK	#N/A
Ppp1r7	Protein phosphatase 1 regulatory subunit 7	3	diphos-(20)RVESEESGDEEGK	#N/A
Prkce	Protein kinase C epsilon type	4	monophos-(343)SKSAPTSPCDQELK	#N/A
Psen1	Presenilin-1	3	monophos-(344)DSHLGPHRSTPESR	#N/A
Ptrf	Polymerase I and transcript release factor	4	diphos-(175)ESEALPEKEGDELGEGER PEDDTAAIELSSDEAVEVEEVIEESR	#N/A
Rad23a	UV excision repair protein RAD23 homolog A	4	diphos-(119)EDKSPSEESTTTTSPESISGSVPSSGSSGR	#N/A
Rap1gap2	Rap1 GTPase-activating protein 2	3	monophos-(8)KQELANSSDVTLPDRPLSPPLTAPPTMK	#N/A
Rasgrf2	Ras-specific guanine nucleotide-releasing factor 2	3	monophos-(722)KFSSPPPLAVSR	#N/A
Rps6kc1	Ribosomal protein S6 kinase delta-1	5	monophos-(646)ESEAQDSVSRGSDDSVPVISFK	#N/A
Rragc	Ras-related GTP-binding protein C	3	monophos-(83)MSPNETLFLESTNK	#N/A
Rtn1	Reticulon-1	5	diphos-(303)QDLCLKPSPDTVPTVTVSEPEDDSPGSVTPPSSG TEPSAAESQGK	#N/A
Serbp1	Plasminogen activator inhibitor 1 RNA-binding protein	3	monophos-(240)QISYNCSDLDQSNVTEETPEGEEHPVAD TENKENEVEEVK	#N/A
Snx16	Sorting nexin-16	3	monophos-(91)EAEEQHPEAVNWEDRPSTPTILGYEVMEER	#N/A
Ssbp3	Single-stranded DNA-binding protein 3	5	monophos-(345)NSPNNISGISNPPGTPR	#N/A
Stambpl1	AMSH-like protease	4	monophos-(232)SDGSNFANYSPPVNR	#N/A
Synpo	Synaptopodin	5	monophos-(760)VASLSPAR	#N/A
Tacc1	Transforming acidic coiled-coil-containing protein 1	3	monophos-(549)APVSVACGGESPLDGICLSEADK	#N/A
Tmf1	TATA element modulatory factor	4	monophos-(333)SVSEINSDDELPGK	#N/A
Tmpo	Lamina-associated polypeptide 2, isoforms beta/delta/epsilon/gamma	3	monophos-(60)GPPDFSSDEEREPTPVLGSGASVGR	#N/A
Trappc10	Trafficking protein particle complex subunit 10	4	monophos-(704)RQESGSSLEPPSGLALEDGAHVLR	#N/A
Trim28	Transcription intermediary factor 1-beta	3	monophos-(435)QGSGSSQPMEVQEGYGFGSDDPYSSAEPHVSGMK	#N/A
		4	diphos-(591)LASPSGSTSSGLEVVAPEVTSAPVSGPGILDDSATICR	
Tyro3	Tyrosine-protein kinase receptor TYRO3	3	monophos-(799)AEQPTESGSPEVHCGER	#N/A
Zfyve20	Rabenosyn-5	6	monophos-(206)DSLSTHTSPSQSPNSVHGSR	#N/A

*Phosphopeptides listed in the table were detected in no <3 times in female dataset (n = 8), but never detected in any male dataset (n = 8). Proteins on top of the table were annotated in the AutDB (or per PubMed literature, labeled with *) to be associated with ASD or neurodevelopmental disorders. The number in brackets indicates the position of amino acid just before the peptide.*

as *Atp1a3*, *Srgap2,* and *Dlgap2*) were detected only in female samples, whereas 26 phosphopeptides (out of 26 proteins such as *Ctnnd1*, *Ctnnd2, Efnb3, and Caskin1*) were only found in male samples. Among these p-sites, one striking example is catenin δ-2 (p)Ser7, which was highly enriched in males. This site has been reported in male mice on UniPort database (Huttlin et al., 2010;

TABLE 4 | Phosphopeptides exclusively detected in male dataset.

Gene	Protein name	Detection times (in Males)	Peptide	References for ASD or related disorders
Abi1*	Abl interactor 1	3	monophos-(173)TNPPTQKPPSPPVSGR	Girirajan et al., 2013
Apc	Adenomatous polyposis coli protein	3	diphos-(1856)NDSLSSLDFDDDDVDLSR	Myers et al., 2011
Caskin1*	Caskin-1	3	monophos-(727)SQEYLLDEGMAPGTPPK	Mukaetova-Ladinska et al., 2004
Cspg5*	Chondroitin sulfate proteoglycan 5	3	monophos-(529)LKEEESFNIQNSMSPK	Talkowski et al., 2012
Ctnnd1*	Catenin delta-1	3	monophos-(344)GSLASLDSLRK	Girirajan et al., 2013
Ctnnd2	Catenin delta-2	6	monophos-(4)KQSGAAPFGAMPVPDQPPSASEK	Myers et al., 2011
Efnb3*	Ephrin-B3	3	monophos-(271)GGSLGLGGGGGMGPR	Mukaetova-Ladinska et al., 2004
Irf2bpl	Interferon regulatory factor 2-binding protein-like	3	diphos-(633)RNSSSPVSPASVPGQR	Talkowski et al., 2012
Map1b*	Microtubule-associated protein 1B	3	diphos-(1290)SVSPGVTQAVVEEHCASPEEK	Girirajan et al., 2013
Srgap2*	SLIT-ROBO Rho GTPase-activating protein 2	3	diphos-(981)TSPVVAPTSEPSSPLHTQLLKDPEPAFQR	Myers et al., 2011
Tbc1d5	TBC1 domain family member 5	3	monophos-(543)SESMPVQLNK	Mukaetova-Ladinska et al., 2004
Atat1	Alpha-tubulin N-acetyltransferase 1	3	diphos-(269)SSSLGNSPDRGPLRPFVPEQELLR	#N/A
Camsap1	Calmodulin-regulated spectrin-associated protein 1	4	diphos-(546)TDVSPPSPQMPR	#N/A
Cryab	Alpha-crystallin B chain	4	monophos-(56)APSWIDTGLSEMR	#N/A
Fam103a1	RNMT-activating mini protein	3	monophos-(31)RPPESPPIVEEWNSR	#N/A
Fam134a	Protein FAM134A	3	diphos-(293)TALALAITDSELSDEEASILESGGFSVSR	#N/A
Kbtbd11	Kelch repeat and BTB domain-containing protein 11	4	monophos-(60)ASAAEGSEASPPSLR	#N/A
Kiaa1467	Uncharacterized protein KIAA1467	6	monophos-(15)SPDLGEYDPLTQADSDESEDDLVLNLQQK	#N/A
Map4	Microtubule-associated protein 4	5	monophos-(514)DMSPSAETEAPLAK	#N/A
Mbp	Myelin basic protein	3	monophos-(145)YLATASTMDHAR	#N/A
Mrpl23	39S ribosomal protein L23, mitochondrial	5	monophos-(117)SPEPLEEELPQQR	#N/A
Phactr1	Phosphatase and actin regulator 1	4	diphos-(326)LESSEQRVPCSTSYHSSGLHSSDGITK	#N/A
Rbm5	RNA-binding protein 5	4	monophos-(614)GLVAAYSGDSDNEEELVER	#N/A
Sik3	Serine/threonine-protein kinase SIK3	3	monophos-(490)RASDGGANIQLHAQQLLK	#N/A
Slc6a17	Sodium-dependent neutral amino acid transporter SLC6A17	3	diphos-(679)VPSEAPSPMPTHR	#N/A
Sptbn1	Spectrin beta chain, non-erythrocytic 1	3	monophos-(2122)GDQVSQNGLPAEQGSPR	#N/A

*Phosphopeptides listed in the table were detected in no <3 times in male dataset (n = 8), but never detected in any female dataset (n = 8). Proteins on top of the table were annotated in the AutDB (or per PubMed literature, labeled with *) to be associated with ASD or neurodevelopmental disorders. The number in brackets indicates the position of amino acid just before the peptide.*

UniProt Consortium, 2018). This p-site was detected in six out of eight male samples (3 KOs and 3 controls), but in none of the eight female samples, indicating that catenin δ-2 (p)Ser7 is a male-specific phosphorylate site. Notably, mutations in catenin δ-2 cause autism in female-enriched multiplex autism families (Turner et al., 2015)

Similarly, to compare phosphorylation level differences between females and males, Skyline-based label-free quantification was also performed on female and male datasets. We further found 96 phosphopeptides (out of 88 proteins) having increased phosphorylation levels in females relative to males, whereas only 11 peptides had significantly decreased phosphorylation levels in females (**Figures 6A,B**). Strikingly, 31 proteins (with 34 peptides) out of 88 (∼35%) are associated with ASD, either annotated in the AutDB (Basu et al., 2009) or per PubMed reporting. Thirty-six of phosphopeptides out of the 33 proteins are presented in **Figure 6B**. Note that the overall phosphorylation levels had no differences between male and female samples, while the sum MS1 peak area of the 107 differentially expressed phosphopeptides were much higher in females than in males (**Figure 6C**). Phosphopeptide abundance of four representatives, *Rims1, Pacs1, Syngap1,* and *Ctnnd2* (both associated with ASD) are shown in **Figure 6D**. These data suggest that more proteins in females are highly phosphorylated

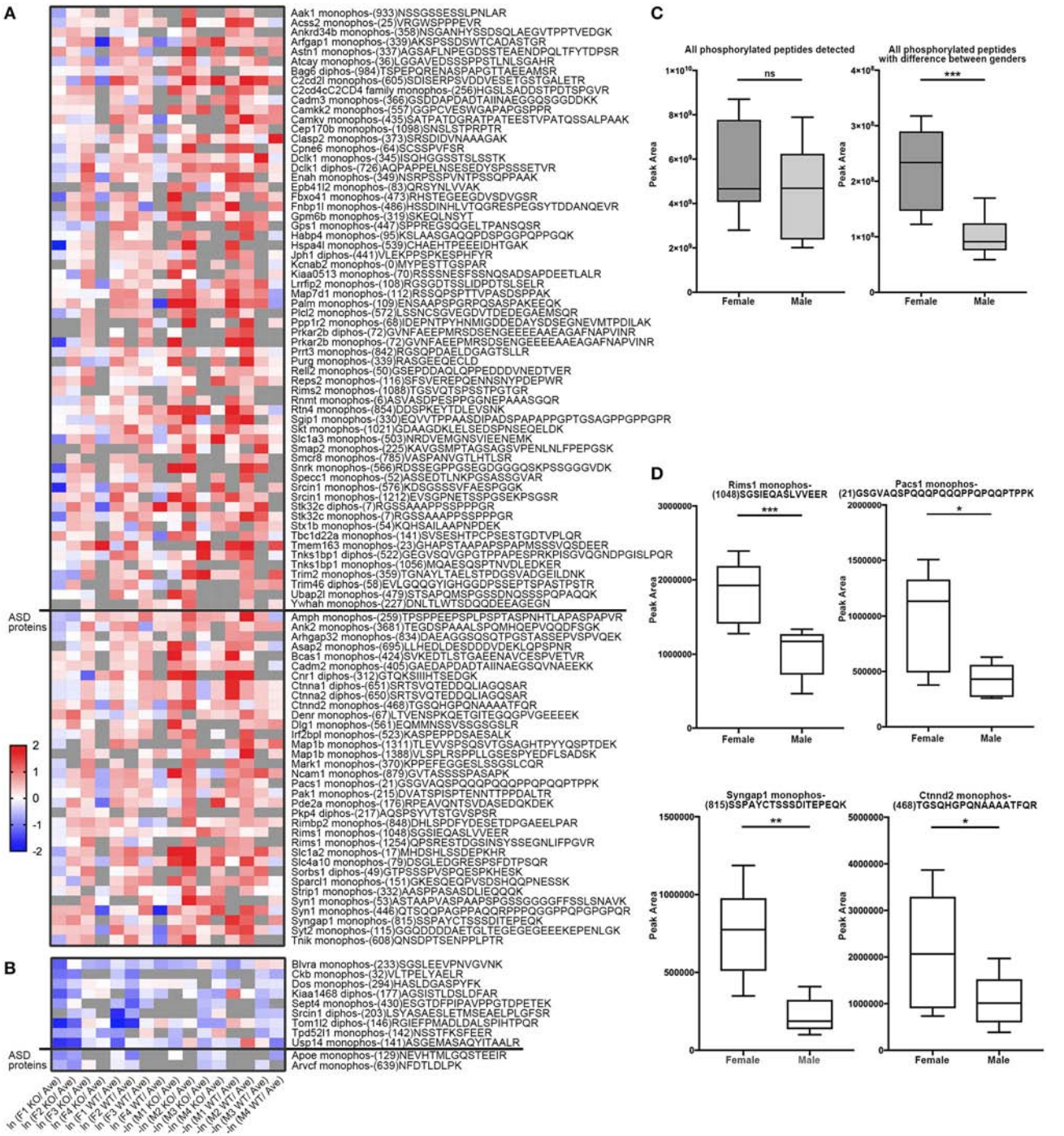

FIGURE 6 | Comparison of phosphopeptide abundance in female and male datasets. **(A)** Heat map of 96 peptides (out of 88 proteins) having increased phosphorylation levels in females relative to males. Phosphopeptides with peak area of MS1 differed in males and females ($p < 0.05$, Student's *t*-test, unpaired) were included into the heatmap. 34 phosphopeptides from 31 Autism-related proteins were on the bottom whereas other 57 proteins were on the top. X-axis donates ln (peak area of individual peptide from female data/average peak area of all data) for female dataset, or –ln (peak area of individual peptide from male data/average peak area of all data) for male dataset. **(B)** Heat map of 11 peptides out of 11 proteins having increased phosphorylation levels in males relative to females. 2 phosphopeptides from 2 Autism-related proteins were on the bottom whereas other nine proteins were on the top. **(C)** The sum spectrum peak areas of all phosphopeptides have no difference in females ($n = 8$) and males ($n = 8$) (left). The sum spectrum peak areas of 107 phosphopeptides out of 99 proteins (as listed in **A,B**) were much higher in females than in males ($p < 0.01$, by unpaired Student's *t*-test). **(D)** Representative plots of four phosphopeptides (from *Rims1, Pacs1, Syngap1,* and *Ctnnd2)* of MS1-based quantification of phosphorylation levels in females compared to males.

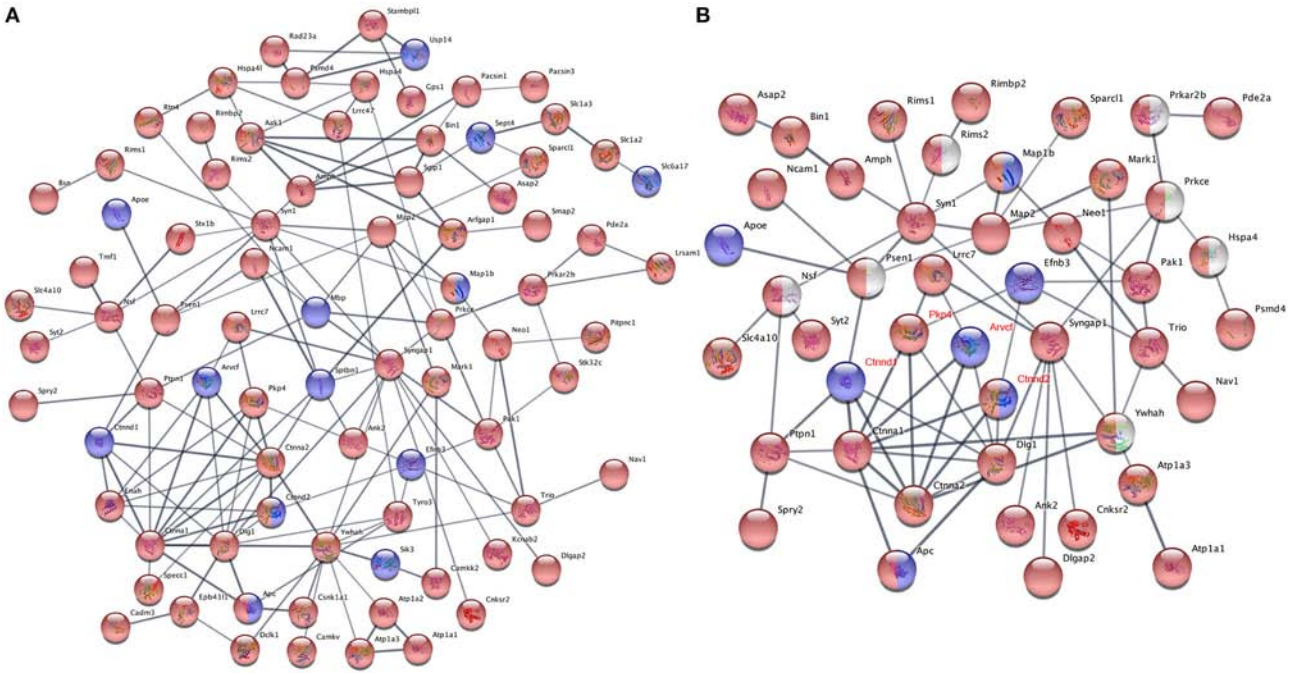

FIGURE 7 | Protein-protein interaction analysis using phosphoproteins differentially expressed in females and males. **(A)** Proteins with phosphorylation differences between female and male dataset, which had presence-or-absence detection differences (listed in **Tables 3**, **4**) or were identified in quantificational analysis (listed in **Figures 6A,B**), were mapped onto the mouse STRING database of protein-protein interactions. One hundred and ten of two hundred and four mapped proteins had interactions with each other, 82 of them were connected in a tight network, whereas other 28 proteins having interaction with a few proteins are not shown. The rest had no interaction with others. **(B)** STRING protein-protein interaction analysis of 63 ASD proteins with different phosphorylation levels in females and males. Thirty-eight of sixty-three proteins were connected in a tight interactions network with each other. Interaction score confidence = 0.400. For **(A,B)**, proteins with increased phosphorylation levels in females were highlighted in red and in males marked in blue. Proteins in red/blue had both increased and decreased p-sites on different positions in females and males. Proteins in white were manually added into the interaction map. The gene names of delta catenin family were written in red.

in the frontal cortex than in males, with a high percentage of them being autism-associated proteins.

It is common that one protein activity can up- or down-regulate the activity of its interacting proteins in shared signal transduction pathways (von Mering et al., 2003). To assess if these ASD-related proteins interact with each other, 204 proteins with different phosphorylation levels in males or females (as listed **Tables 3**, **4** and **Figures 6A,B**) were mapped onto the mouse STRING database to examine protein-protein interaction. **Figure 7A** depicts that 82 out of 204 proteins were connected in a tight network, 69 proteins of the 82 had higher phosphorylation in females, three of them (e.g., *Ctnnd2*) had different phosphorylated peptides with increased phosphorylated levels in both females and males. Further, 63 proteins out of the 204 (∼31%) with different phosphorylation levels in females or males were clearly associated with ASD. Thirty-two out of the sixty three of proteins were autism candidate entries in the AutDB, whereas the other 31 were reported in PubMed. It is noteworthy that all delta catenin proteins (*Ctnnd1, Ctnnd2, Pkp4,* and *Arvcf,* with names marked in red **Figure 7B**) exhibit gender-biased modifications. Furthermore, 50 out of the 63 ASD proteins had increased phosphorylation levels in female samples, whereas only eight proteins increased in male and five proteins had different phosphorylated peptides increased in both genders. STRING analysis further demonstrated that 38 of these 63 ASD proteins showed strong protein-protein interactions with each other (**Figure 7B**). These data demonstrate that 204 proteins had sex-biased phosphorylation and 31% of them were ASD-related genes which showed strong protein-protein interactions, suggesting that autism-related proteins may be highly regulated by post-translational phosphorylation in the female brain.

DISCUSSION

Malfunctions of primary cilia cause a broad spectrum of diseases in humans, particularly developmental disorders. AC3 is highly enriched in neuronal primary cilia, and not well-expressed in mature astrocyte cilia or microglia in the frontal cortex (**Figure 1**). AC3 is genetically associated with many human diseases including obesity (Nordman et al., 2008; Stergiakouli et al., 2014), ASD (Skafidas et al., 2014; Yuen et al., 2017), and MDD (Wray et al., 2012). It is unknown how AC3 regulates signaling network in central neurons. Besides activating the CNG channel in olfactory sensory neurons, AC3 (or cAMP) in olfactory cilia also sends signals to the cytosol of olfactory sensory neurons (DeMaria and Ngai, 2010) and regulates gene transcription (Serizawa et al., 2003). Given PKA is the major downstream protein of cAMP in most tissues, we postulated

that identification of protein phosphorylation modulated by AC3 could help delineate AC3-regulated signaling network in central neurons.

We utilized a high-efficiency method to conduct comparative phosphoproteomics analyses combining TiO_2 phosphopeptide enrichment with HPLC-MS/MS analysis. This approach allows for large-scale identification of phosphopeptides. In our assay, more than 1,500 phosphorylated peptides and 30,000 spectra were detected from each sample (**Figure 3**). We analyzed 16 samples and in total 4655 phosphopeptides were identified from 1756 proteins. We have manually verified all mass spectra presented in **Figures 5**–**7** and **Tables 1**–**4**. This work provided a list of phosphoproteins that help elucidate the function of AC3 in the brain and unravel gender-biased protein phosphorylation. Intriguingly, we identified more gender-biased modifications than those of genotype-biased, suggesting that gender difference is much bigger than genotype differences in the frontal cortex in the phosphoproteomic assay.

To compare phosphorylation levels in proteins that are involved in cAMP signaling pathway, phosphopeptides identified from G-proteins, adenylyl cyclases, PKA, phosphodiesterases (PDE), phosphatases, as well as their regulating proteins were summarized in **Table S4**. It shows that phosphatases (such as *Ppp1r1b*) were highly phosphorylated, while G-protein α-subunits were not. cAMP-dependent protein kinases' catalytic subunits were less phosphorylated than their regulatory subunits (**Table S4**). Phosphorylation of two adenylyl cyclases (*Adcy5* and *Adcy9*) have been detected and apparently that *Adcy9* is highly phosphorylated in the frontal cortex. Among differentially expressed phosphopeptides between WTs and KOs, one interesting hit was *Pde1b* (p)Ser18. *Pde1b* is a calcium/calmodulin-dependent phosphodiesterase that breaks down both cAMP and cGMP (Sharma et al., 2006). *Pde1b* (p)Ser18 was detected in 4 of 8 AC3 KO mice (one female and three male animals), but in none of the control mice (**Table 2**), suggesting that *Pde1b* may function downstream of AC3. Additionally, *Ppp1r14A* (p)Ser19 (protein phosphatase 1 regulatory subunit 14A), which was detected in 4 of 8 WT mice (2 female and 2 male animals), but in none of 8 KO mice (**Table 1**). *Ppp1r14A* is a C-kinase phosphorylation-dependent inhibitor protein of phosphatase, implicated in cerebellar long-term synaptic plasticity (Eto et al., 2002). In contrast, *Ppp1r1b*, which is a cAMP/PKA-dependent phosphoprotein and regulates the activity of phosphatase-1, had at least four sites identified (Ser42|45|46, Ser97, Ser130, Thr182|192) in the dataset. However, we did not detect significant differences in phosphorylation levels in these four sites between WT and KO datasets (**Table S4**). Additionally, both Rho GTPase-activating protein 20 (*Arhgap20*) and Rho GTPase-activating protein 44 (*Arhgap44*) have p-sites that were exclusively detected in KO dataset (**Table 2**), suggesting these RhoGaps may be regulated by AC3 in the frontal cortex.

Male and female brains differ in many aspects including connectivity (Ingalhalikar et al., 2014), disease susceptibility (Zagni et al., 2016), and gene expression (Trabzuni et al., 2013). Numerous studies have attempted to use different approaches including next-generation sequencing technology to decipher the differences between male and female brains (Trabzuni et al., 2013; Werling et al., 2016; Gershoni and Pietrokovski, 2017). However, current research apparently has overlooked posttranslational modification differences in male and female brains, and phosphoproteomics databanks (UnitProt and Phosphosites) thus far have not collected any data specifically from female brain samples. This study filled this gap and we have conducted systematic phosphoproteomic profiling using prefrontal cortical samples of both genders. Consequently, we have identified 95 phosphopeptides only present in female samples, and 26 phosphopeptides restricted to male samples (**Tables 3**, **4**). Label-free mass spectrometric quantification further revealed that 96 phosphopeptides have higher phosphorylation levels in females, while 11 phosphopeptides are more abundantly expressed in males. We found that phosphorylation of many autism-associated proteins, including but not limited to *Dlg1*, *Dlgap2*, *Syn1*, *SynGap1*, and *Srgap2* (**Figures 6**, **7** and **Tables 3**, **4**), are gender-biased, occurring more in females than in males. As shown in **Figure 6B** and **Tables 3**, **4**, 63 out of 204 phosphopeptides (∼31%) are from autism-associated proteins. Some proteins/genes are not listed in the AutDB, but they directly interact with autism proteins or were found to be associated with autism per literature in PubMed. For example, *Caskin1* Ser 728 was only identified in males (**Table 4**). Caskin-1 interacts with neurexins, which bind to neuroligins in the synapses. Both neurexins and neuroligins are strongly associated with autisms (Südhof, 2017). *Caskin1* itself is implicated in autism (Daimon et al., 2015).

Among all differentially modified proteins in genders, one protein family is of particular interest. That is the delta catenin family, which contains ARVCF (encoded by *Arvcf*), catenin δ-1 (*Ctnnd1*), catenin δ-2 (*Ctnnd2*), and plakophilin-4 (*Pkp4*) (Yuan and Arikkath, 2017). All the delta catenin proteins are expressed in the central nervous system and regulate neural development, and they are strongly implicated in neurodevelopmental disorders (Turner et al., 2015; Yuan and Arikkath, 2017). Remarkably, the activity of delta catenin family is highly regulated by post-translational modifications such as ubiquitination and phosphorylation to modulate protein-protein interaction with cadherin, membrane localization, and protein stability (Yuan and Arikkath, 2017). Of note, this family has two regions flanking the ARM domain that are highly enriched with phosphorylation sites (Yuan and Arikkath, 2017). Interestingly, all four delta catenin proteins: ARVCF (Suzuki et al., 2009), catenin δ-1 (Hussman et al., 2011), catenin δ-2 (Turner et al., 2015), and plakophilin-4 (Hussman et al., 2011) are implicated in ASD or neurodevelopmental disorders. Relevant to the sexual dimorphism of autism, mutations of catenin δ-2 has been found to cause severe autism in female-enriched multiplex autism families (Turner et al., 2015). Loss-of-function of catenin δ-2 causes severe developmental phenotypes in animal model. Our MS analysis revealed that catenin δ-2 Ser 7 was restricted to males. Moreover, catenin δ-2 Thr 469 (another p-site) have increased phosphorylation in females relative to males. We have also detected p-sites of the delta catenin family which are also differentially modified in males or females: catenin δ-1 Ser 346 was only detected in males (**Table 4**);

ARVCF Thr 643 has decreased phosphorylation in females; *PKP4* Ser 220 had higher expression in females (**Figure 6**). Together, these data suggest that the delta catenin family may participate in the regulation of gender-biased posttranslational phosphorylations, consequently affecting neuronal development in the prefrontal cortex. This interpretation is further supported by STRING analysis, showing that these four proteins are connected in a String interaction map with gender-biased phosphorylation (**Figure 7B**).

In summary, this comparative phosphoproteomic profiling has generated several interesting findings: (1) AC3 ablation leads to decreased activity of proline-directed kinases in the frontal cortex; (2) There is a gender-biased phosphorylation in 204 proteins, 31% of which are associated with ASD; (3) Four delta catenin family members, all associated with autism, contain gender-biased phosphorylation sites. Hence, although future work is warranted, this study provides useful phosphoproteomic clues to elucidate the function of AC3 in the CNS. It also presents the first proteomic evidence suggesting that sex-biased post-translational phosphorylation is implicated in the sexual dimorphism of autism.

DATA DEPOSITION

Proteome raw and complete datasets (4 groups: AC3 controls, KOs, males and females, 16 mice) have been submitted to ProteomeXchange via the PRIDE-EBI database (PXD012259).

ETHICS STATEMENT

All animal-related procedures were approved and conducted in accordance with the guidelines of the Institutional Animal Care and Use Committee of the University of New Hampshire.

AUTHOR CONTRIBUTIONS

YZ and XC designed experiments. YZ conducted phosphoproteomic assays, immunostaining, and data analysis. LQ maintained mouse colony and provided support for phosphoproteomic assay. AS contributed to immunostaining. FC provided expertise in phosphoproteomic experiments and data analysis. HW provided expertise in statistical methods. YZ and XC interpreted data and wrote the paper.

FUNDING

This study was supported by National Institutes of Health Grants MH105746, AG054729, and COBRE GM113131-7006 to XC; HD093783 to FC. A Cole Neuroscience and Behavioral Faculty Research Award to XC; and UNH Summer TA Research Fellowships to YZ and AS.

SUPPLEMENTARY MATERIAL

The Supplementary Material for this article can be found online at: https://www.frontiersin.org/articles/10.3389/fncel.2019.00034/full#supplementary-material

REFERENCES

Autism Genome Project, C., Szatmari, P., Paterson, A. D., Zwaigenbaum, L., Roberts, W., Brian, J., et al. (2007). Mapping autism risk loci using genetic linkage and chromosomal rearrangements. *Nat. Genet.* 39, 319–328. doi: 10.1038/ng1985

Basu, S. N., Kollu, R., and Banerjee-Basu, S. (2009). AutDB: a gene reference resoursce for autism research. *Nucleic Acids Res.* 37, D832–D836. doi: 10.1093/nar/gkn835

Bishop, G. A., Berbari, N. F., Lewis, J., and Mykytyn, K. (2007). Type III adenylyl cyclase localizes to primary cilia throughout the adult mouse brain. *J. Comp. Neurol.* 505, 562–571. doi: 10.1002/cne.21510

Blacque, O. E., Perens, E. A., Boroevich, K. A., Inglis, P. N., Li, C., Warner, A., et al. (2005). Functional genomics of the cilium, a sensory organelle. *Curr. Biol.* 15, 935–941. doi: 10.1016/j.cub.2005.04.059

Brodsky, M., Lesiak, A. J., Croicu, A., Cohenca, N., Sullivan, J. M., and Neumaier, J. F. (2017). 5-HT6 receptor blockade regulates primary cilia morphology in striatal neurons. *Brain Res.* 1660, 10–19. doi: 10.1016/j.brainres.2017.01.010

Chalkley, R. J., Baker, P. R., Huang, L., Hansen, K. C., Allen, N. P., Rexach, M., et al. (2005). Comprehensive analysis of a multidimensional liquid chromatography mass spectrometry dataset acquired on a quadrupole selecting, quadrupole collision cell, time-of-flight mass spectrometer: II. New developments in Protein Prospector allow for reliable and comprehensive automatic analysis of large datasets. *Mol. Cell Proteomics* 4, 1194–1204. doi: 10.1074/mcp.D500002-MCP200

Chen, X., Luo, J., Leng, Y., Yang, Y., Zweifel, L. S., Palmiter, R. D., et al. (2016). Ablation of Type III adenylyl cyclase in mice causes reduced neuronal activity, altered sleep pattern, and depression-like phenotypes. *Biol. Psychiatry* 80, 836–848. doi: 10.1016/j.biopsych.2015.12.012

Chen, X., Xia, Z., and Storm, D. R. (2012). Stimulation of electro-olfactogram responses in the main olfactory epithelia by airflow depends on the type 3 adenylyl cyclase. *J. Neurosci.* 32, 15769–15778. doi: 10.1523/JNEUROSCI.2180-12.2012

Chou, M. F., and Schwartz, D. (2011). Biological sequence motif discovery using motif-x. *Curr. Protoc. Bioinformatics* 13, 15–24. doi: 10.1002/0471250953.bi1315s35

Daimon, C. M., Jasien, J. M., Wood, W. H., Zhang, Y., Becker, K. G., Silverman, J. L., et al. (2015). Hippocampal transcriptomic and proteomic alterations in the BTBR mouse model of autism spectrum disorder. *Front. Physiol.* 6:324. doi: 10.3389/fphys.2015.00324

DeMaria, S., and Ngai, J. (2010). The cell biology of smell. *J. Cell Biol.* 191, 443–452. doi: 10.1083/jcb.201008163

Einstein, E. B., Patterson, C. A., Hon, B. J., Regan, K. A., Reddi, J., Melnikoff, D. E., et al. (2010). Somatostatin signaling in neuronal cilia is critical for object recognition memory. *J. Neurosci.* 30, 4306–4314. doi: 10.1523/JNEUROSCI.5295-09.2010

Eto, M., Bock, R., Brautigan, D. L., and Linden, D. J. (2002). Cerebellar long-term synaptic depression requires PKC-mediated activation of CPI-17, a myosin/moesin phosphatase inhibitor. *Neuron* 36, 1145–1158. doi: 10.1016/S0896-6273(02)01107-8

Fliegauf, M., Benzing, T., and Omran, H. (2007). When cilia go bad: cilia defects and ciliopathies. *Nat. Rev. Mol. Cell Biol.* 8, 880–893. doi: 10.1038/nrm2278

Gershoni, M., and Pietrokovski, S. (2017). The landscape of sex-differential transcriptome and its consequent selection in human adults. *BMC Biol.* 15:7. doi: 10.1186/s12915-017-0352-z

Girirajan, S., Dennis, M. Y., Baker, C., Malig, M., Coe, B. P., Campbell, C. D., et al. (2013). Refinement and discovery of new hotspots of copy-number variation associated with autism spectrum disorder. *Am. J. Hum. Genet.* 92, 221–237. doi: 10.1016/j.ajhg.2012.12.016

Green, J. A., Gu, C., and Mykytyn, K. (2012). Heteromerization of ciliary G protein-coupled receptors in the mouse brain. *PLoS ONE* 7:e46304. doi: 10.1371/journal.pone.0046304

Guan, S., and Burlingame, A. L. (2010). Data processing algorithms for analysis of high resolution MSMS spectra of peptides with complex patterns of posttranslational modifications. *Mol. Cell Proteomics.* 9, 804–810. doi: 10.1074/mcp.M900431-MCP200

Gunaratne, R., Braucht, D. W., Rinschen, M. M., Chou, C. L., Hoffert, J. D., Pisitkun, T., et al. (2010). Quantitative phosphoproteomic analysis reveals cAMP/vasopressin-dependent signaling pathways in native renal thick ascending limb cells. *Proc. Natl. Acad. Sci. U.S.A.* 107, 15653–15658. doi: 10.1073/pnas.1007424107

Halladay, A. K., Bishop, S., Constantino, J. N., Daniels, A. M., Koenig, K., Palmer, K., et al. (2015). Sex and gender differences in autism spectrum disorder: summarizing evidence gaps and identifying emerging areas of priority. *Mol. Autism* 6:36. doi: 10.1186/s13229-015-0019-y

Humphrey, S. J., Azimifar, S. B., and Mann, M. (2015). High-throughput phosphoproteomics reveals *in vivo* insulin signaling dynamics. *Nat. Biotechnol.* 33, 990–995. doi: 10.1038/nbt.3327

Hussman, J. P., Chung, R. H., Griswold, A. J., Jaworski, J. M., Salyakina, D., Ma, D., et al. (2011). A noise-reduction GWAS analysis implicates altered regulation of neurite outgrowth and guidance in autism. *Mol. Autism* 2:1. doi: 10.1186/2040-2392-2-1

Huttlin, E. L., Jedrychowski, M. P., Elias, J. E., Goswami, T., Rad, R., Beausoleil, S. A., et al. (2010). A tissue-specific atlas of mouse protein phosphorylation and expression. *Cell* 143, 1174–1189. doi: 10.1016/j.cell.2010.12.001

Ingalhalikar, M., Smith, A., Parker, D., Satterthwaite, T. D., Elliott, M. A., Ruparel, K., et al. (2014). Sex differences in the structural connectome of the human brain. *Proc. Natl. Acad. Sci. U.S.A.* 111, 823–828. doi: 10.1073/pnas.1316909110

Johnson, L. N. (2009). The regulation of protein phosphorylation. *Biochem. Soc. Trans.* 37(Pt 4), 627–641. doi: 10.1042/BST0370627

Kasahara, K., Miyoshi, K., Murakami, S., Miyazaki, I., and Asanuma, M. (2014). Visualization of astrocytic primary cilia in the mouse brain by immunofluorescent analysis using the cilia marker Arl13b. *Acta Med. Okayama* 68, 317–322. doi: 10.18926/AMO/53020

Keshava Prasad, T. S., Goel, R., Kandasamy, K., Keerthikumar, S., Kumar, S., Mathivanan, S., et al. (2009). Human protein reference database—2009 update. *Nucleic Acids Res.* 37, D767–D772. doi: 10.1093/nar/gkn892

Kogan, M. D., Blumberg, S. J., Schieve, L. A., Boyle, C. A., Perrin, J. M., Ghandour, R. M., et al. (2009). Prevalence of parent-reported diagnosis of autism spectrum disorder among children in the US, 2007. *Pediatrics* 124, 1395–1403. doi: 10.1542/peds.2009-1522

Labaka, A., Goñi-Balentziaga, O., Lebeña, A., and Perez-Tejada, J. (2018). Biological sex differences in depression: a systematic review. *Biol. Res. Nurs.* 20, 383–392. doi: 10.1177/1099800418776082

Li, J. B., Gerdes, J. M., Haycraft, C. J., Fan, Y., Teslovich, T. M., May-Simera, H., et al. (2004). Comparative genomics identifies a flagellar and basal body proteome that includes the BBS5 human disease gene. *Cell* 117, 541–552. doi: 10.1016/S0092-8674(04)00450-7

Louvi, A., and Grove, E. A. (2011). Cilia in the CNS: the quiet organelle claims center stage. *Neuron* 69, 1046–1060. doi: 10.1016/j.neuron.2011.03.002

Machnicka, B., Czogalla, A., Hryniewicz-Jankowska, A., Bogusławska, D. M., Grochowalska, R., Heger, E., et al. (2014). Spectrins: a structural platform for stabilization and activation of membrane channels, receptors and transporters. *Biochim. Biophys. Acta* 1838, 620–634. doi: 10.1016/j.bbamem.2013.05.002

Machnicka, B., Grochowalska, R., Boguslawska, D. M., Sikorski, A. F., and Lecomte, M. C. (2012). Spectrin-based skeleton as an actor in cell signaling. *Cell. Mol. Life Sci.* 69, 191–201. doi: 10.1007/s00018-011-0804-5

Mi, H., Huang, X., Muruganujan, A., Tang, H., Mills, C., Kang, D., et al. (2017). PANTHER version 11: expanded annotation data from gene ontology and reactome pathways, and data analysis tool enhancements. *Nucleic Acids Res.* 45, D183–D189. doi: 10.1093/nar/gkw1138

Mukaetova-Ladinska, E. B., Arnold, H., Jaros, E., Perry, R., and Perry, E. (2004). Depletion of MAP2 expression and laminar cytoarchitectonic changes in dorsolateral prefrontal cortex in adult autistic individuals. *Neuropathol. Appl. Neurobiol.* 30, 615–623. doi: 10.1111/j.1365-2990.2004.00574.x

Myers, R. A., Casals, F., Gauthier, J., Hamdan, F. F., Keebler, J., Boyko, A. R., et al. (2011). A population genetic approach to mapping neurological disorder genes using deep resequencing. *PLoS Genet.* 7:e1001318. doi: 10.1371/journal.pgen.1001318

Nordman, S., Abulaiti, A., Hilding, A., Långberg, E. C., Humphreys, K., Ostenson, C. G., et al. (2008). Genetic variation of the adenylyl cyclase 3 (AC3) locus and its influence on type 2 diabetes and obesity susceptibility in Swedish men. *Int. J. Obes.* 32, 407–412. doi: 10.1038/sj.ijo.0803742

Olsen, J. V., Blagoev, B., Gnad, F., Macek, B., Kumar, C., Mortensen, P., et al. (2006). Global, *in vivo*, and site-specific phosphorylation dynamics in signaling networks. *Cell* 127, 635–648. doi: 10.1016/j.cell.2006.09.026

Pinna, L. A., and Ruzzene, M. (1996). How do protein kinases recognize their substrates? *Biochim. Biophys. Acta* 1314, 191–225.

Qiu, L., LeBel, R. P., Storm, D. R., and Chen, X. (2016). Type 3 adenylyl cyclase: a key enzyme mediating the cAMP signaling in neuronal cilia. *Int. J. Physiol. Pathophysiol. Pharmacol.* 8, 95–108.

Ramamurthy, V., Jolicoeur, C., Koutroumbas, D., Muhlhans, J., Le, Y. Z., Hauswirth, W. W., et al. (2014). Numb regulates the polarized delivery of cyclic nucleotide-gated ion channels in rod photoreceptor cilia. *J. Neurosci.* 34, 13976–13987. doi: 10.1523/JNEUROSCI.1938-14.2014

Rosenbaum, J. L., and Witman, G. B. (2002). Intraflagellar transport. *Nat. Rev. Mol. Cell Biol.* 3, 813–825. doi: 10.1038/nrm952

Roux, P. P., and Thibault, P. (2013). The coming of age of phosphoproteomics–from large data sets to inference of protein functions. *Mol. Cell. Proteomics* 12, 3453–3464. doi: 10.1074/mcp.R113.032862

Ruzankina, Y., Pinzon-Guzman, C., Asare, A., Ong, T., Pontano, L., Cotsarelis, G., et al. (2007). Deletion of the developmentally essential gene ATR in adult mice leads to age-related phenotypes and stem cell loss. *Cell Stem Cell* 1, 113–126. doi: 10.1016/j.stem.2007.03.002

Sassone-Corsi, P. (2012). The cyclic AMP pathway. *Cold Spring Harb. Perspect. Biol.* 4:a011148. doi: 10.1101/cshperspect.a011148

Schilling, B., Rardin, M. J., MacLean, B. X., Zawadzka, A. M., Frewen, B. E., Cusack, M. P., et al. (2012). Platform-independent and label-free quantitation of proteomic data using MS1 extracted ion chromatograms in skyline: application to protein acetylation and phosphorylation. *Mol. Cell. Proteomics* 11, 202–214. doi: 10.1074/mcp.M112.017707

Schlingmann, K. P., Bandulik, S., Mammen, C., Tarailo-Graovac, M., Holm, R., Baumann, M., et al. (2018). Germline de novo mutations in ATP1A1 cause renal hypomagnesemia, refractory seizures, and intellectual disability. *Am. J. Hum. Genet.* 103, 808–816. doi: 10.1016/j.ajhg.2018.10.004

Schou, K. B., Pedersen, L. B., and Christensen, S. T. (2015). Ins and outs of GPCR signaling in primary cilia. *EMBO Rep.* 16, 1099–1113. doi: 10.15252/embr.201540530

Serizawa, S., Miyamichi, K., Nakatani, H., Suzuki, M., Saito, M., Yoshihara, Y., et al. (2003). Negative feedback regulation ensures the one receptor-one olfactory neuron rule in mouse. *Science* 302, 2088–2094. doi: 10.1126/science.1089122

Sharma, R. K., Das, S. B., Lakshmikuttyamma, A., Selvakumar, P., and Shrivastav, A. (2006). Regulation of calmodulin-stimulated cyclic nucleotide phosphodiesterase (PDE1): review. *Int. J. Mol. Med.* 18, 95–105. doi: 10.3892/ijmm.18.1.95

Siddiqui, S. V., Chatterjee, U., Kumar, D., Siddiqui, A., and Goyal, N. (2008). Neuropsychology of prefrontal cortex. *Indian J. Psychiatry* 50, 202–208. doi: 10.4103/0019-5545.43634

Singla, V., and Reiter, J. F. (2006). The primary cilium as the cell's antenna: signaling at a sensory organelle. *Science* 313, 629–633. doi: 10.1126/science.1124534

Sipos, É., Komoly, S., and Acs, P. (2018). quantitative comparison of primary cilia marker expression and length in the mouse brain. *J. Mol. Neurosci.* 64, 397–409. doi: 10.1007/s12031-018-1036-z

Skafidas, E., Testa, R., Zantomio, D., Chana, G., Everall, I. P., and Pantelis, C. (2014). Predicting the diagnosis of autism spectrum disorder using gene pathway analysis. *Mol. Psychiatry* 19, 504–510. doi: 10.1038/mp.2012.126

Stergiakouli, E., Gaillard, R., Tavare, J. M., Balthasar, N., Loos, R. J., Taal, H. R., et al. (2014). Genome-wide association study of height-adjusted BMI in childhood identifies functional variant in ADCY3. *Obesity* 22, 2252–2259. doi: 10.1002/oby.20840

Sterpka, A., and Chen, X. (2018). Neuronal and astrocytic primary cilia in the mature brain. *Pharmacol. Res.* 137, 114–121. doi: 10.1016/j.phrs.2018.10.002

Südhof, T. C. (2017). Synaptic neurexin complexes: a molecular code for the logic of neural circuits. *Cell* 171, 745–769. doi: 10.1016/j.cell.2017.10.024

Suzuki, G., Harper, K. M., Hiramoto, T., Funke, B., Lee, M., Kang, G., et al. (2009). Over-expression of a human chromosome 22q11.2 segment including TXNRD2, COMT and ARVCF developmentally affects incentive learning and working memory in mice. *Hum. Mol. Genet.* 18, 3914–3925. doi: 10.1093/hmg/ddp334

Syrbe, S., Harms, F. L., Parrini, E., Montomoli, M., Mutze, U., Helbig, K. L., et al. (2017). Delineating SPTAN1 associated phenotypes: from isolated epilepsy to encephalopathy with progressive brain atrophy. *Brain* 140, 2322–2336. doi: 10.1093/brain/awx195

Szklarczyk, D., Franceschini, A., Wyder, S., Forslund, K., Heller, D., Huerta-Cepas, J., et al. (2015). STRING v10: protein-protein interaction networks, integrated over the tree of life. *Nucleic Acids Res.* 43, D447–D452. doi: 10.1093/nar/gku1003

Tabb, D. L., Vega-Montoto, L., Rudnick, P. A., Variyath, A. M., Ham, A. J., Bunk, D. M., et al. (2010). Repeatability and reproducibility in proteomic identifications by liquid chromatography-tandem mass spectrometry. *J. Proteome Res.* 9, 761–776. doi: 10.1021/pr9006365

Talkowski, M. E., Rosenfeld, J. A., Blumenthal, I., Pillalamarri, V., Chiang, C., Heilbut, A., et al. (2012). Sequencing chromosomal abnormalities reveals neurodevelopmental loci that confer risk across diagnostic boundaries. *Cell* 149, 525–537. doi: 10.1016/j.cell.2012.03.028

Trabzuni, D., Ramasamy, A., Imran, S., Walker, R., Smith, C., Weale, M. E., et al. (2013). Widespread sex differences in gene expression and splicing in the adult human brain. *Nat. Commun.* 4:2771. doi: 10.1038/ncomms3771

Turner, T. N., Sharma, K., Oh, E. C., Liu, Y. P., Collins, R. L., Sosa, M. X., et al. (2015). Loss of delta-catenin function in severe autism. *Nature* 520, 51–56. doi: 10.1038/nature14186

UniProt Consortium (2018). UniProt: the universal protein knowledgebase. *Nucleic Acids Res.* 46:2699. doi: 10.1093/nar/gky092

Valente, E. M., Rosti, R. O., Gibbs, E., and Gleeson, J. G. (2014). Primary cilia in neurodevelopmental disorders. *Nat. Rev. Neurol.* 10, 27–36. doi: 10.1038/nrneurol.2013.247

von Mering, C., Huynen, M., Jaeggi, D., Schmidt, S., Bork, P., and Snel, B. (2003). STRING: a database of predicted functional associations between proteins. *Nucleic Acids Res.* 31, 258–261. doi: 10.1093/nar/gkg034

Waltereit, R., and Weller, M. (2003). Signaling from cAMP/PKA to MAPK and synaptic plasticity. *Mol. Neurobiol.* 27, 99–106. doi: 10.1385/MN:27:1:99

Wang, Z., Li, V., Chan, G. C., Phan, T., Nudelman, A. S., Xia, Z., et al. (2009). Adult type 3 adenylyl cyclase-deficient mice are obese. *PLoS ONE* 4:e6979. doi: 10.1371/journal.pone.0006979

Werling, D. M., Parikshak, N. N., and Geschwind, D. H. (2016). Gene expression in human brain implicates sexually dimorphic pathways in autism spectrum disorders. *Nat. Commun.* 7:10717. doi: 10.1038/ncomms10717

Wong, S. T., Trinh, K., Hacker, B., Chan, G. C., Lowe, G., Gaggar, A., et al. (2000). Disruption of the type III adenylyl cyclase gene leads to peripheral and behavioral anosmia in transgenic mice. *Neuron* 27, 487–497. doi: 10.1016/S0896-6273(00)00060-X

Wray, N. R., Pergadia, M. L., Blackwood, D. H., Penninx, B. W., Gordon, S. D., Nyholt, D. R., et al. (2012). Genome-wide association study of major depressive disorder: new results, meta-analysis, and lessons learned. *Mol. Psychiatry* 17, 36–48. doi: 10.1038/mp.2010.109

Yuan, L., and Arikkath, J. (2017). Functional roles of p120ctn family of proteins in central neurons. *Semin. Cell Dev. Biol.* 69, 70–82. doi: 10.1016/j.semcdb.2017.05.027

Yuen, R. K. C., Merico, D., Bookman, M., L Howe, J., Thiruvahindrapuram, B., Patel, R. V., et al. (2017). Whole genome sequencing resource identifies 18 new candidate genes for autism spectrum disorder. *Nat. Neurosci.* 20, 602–611. doi: 10.1038/nn.4524

Zagni, E., Simoni, L., and Colombo, D. (2016). Sex and gender differences in central nervous system-related disorders. *Neurosci J.* 2016:2827090. doi: 10.1155/2016/2827090

Conflict of Interest Statement: The authors declare that the research was conducted in the absence of any commercial or financial relationships that could be construed as a potential conflict of interest.

frontiers in Cellular Neuroscience

MINI REVIEW
published: 20 February 2019
doi: 10.3389/fncel.2019.00055

Emerging Roles of Primary Cilia in Glioma

Matthew R. Sarkisian[1,2]* *and Susan L. Semple-Rowland*[1]

[1] Department of Neuroscience, McKnight Brain Institute, University of Florida College of Medicine, Gainesville, FL, United States, [2] Preston A. Wells, Jr. Center for Brain Tumor Therapy, McKnight Brain Institute, University of Florida College of Medicine, Gainesville, FL, United States

Primary cilia are microtubule-based organelles that are typically present on cells during the G0 or G1-S/G2 phases of the cell cycle. Recent studies of glioblastoma (GBM) biopsies, a brain tumor that is notorious for its aggressive growth and resistance to treatment, show that many cells in the tumor lack cilia. At this point, it remains unclear whether primary cilia promote or suppress glioma tumorigenesis. In this review, we will discuss the different roles that have been proposed for primary cilia in glioma and how cilia may contribute to the resistance of these tumors to current therapies.

Keywords: glioblastoma, cilium, brain cancer, temozolomide, ciliary signaling

INTRODUCTION

Primary cilia are microtubule-based organelles that relay signals to the cell on which they reside and release signals into the cellular microenvironment (Wood and Rosenbaum, 2015; Garcia et al., 2018), but their functions in glioma remain unclear. To our knowledge Schuster (1964) were the first to report the presence of ciliated fibroblasts in a human brain tumor. Despite detecting cilia bearing long axonemes, these investigators concluded that "it is difficult to imagine these cilia fulfilling any useful function, confined and atypical as they are." A few years later, Tani and Ametani (1970) described ciliated cells in human gliomas and concluded that the cilia ". . .might be called vestigial; merely formed because of an inherited tendency of centrioles to form cilia, rather than structures necessarily performing highly specialized functions". The widely held view that these cilia were of little consequence was largely based on the observations that they lacked the central microtubule pair that is a feature of motile cilia. The early 2000s saw renewed interest in mammalian primary cilia and the emergence of a new hypothesis that primary cilia are key signaling cellular organelles that function throughout the body (for review see: Singla and Reiter, 2006; Goetz and Anderson, 2010). With the discovery of new roles for primary cilia in regulating neural stem cell proliferation and migration in embryonic and adult brain regions (e.g., Breunig et al., 2008; Han et al., 2008; Spassky et al., 2008; Han and Alvarez-Buylla, 2010; Baudoin et al., 2012; Higginbotham et al., 2012, 2013; Guo et al., 2015), this hypothesis has triggered new studies designed to understand the function of primary cilia in brain tumors.

Primary cilia are now postulated to be involved in the pathogenesis of various cancers including brain tumors such as medulloblastoma (Han et al., 2009) and choroid plexus tumors (Li et al., 2016); however, the role(s) that these important organelles have in the pathogenesis of glioma, the most common form of brain cancer in adults, are just now beginning to be examined (also see Alvarez-Satta and Matheu, 2018). In this review we focus primarily on the most aggressive form of glioma, glioblastoma (GBM) and discuss the prevalence of ciliated cells in these tumors, the roles that these

OPEN ACCESS

Edited by:
Rosanna Parlato,
University of Ulm, Germany

Reviewed by:
Young-Goo Han,
St. Jude Children's Research Hospital, United States
Sergio Gradilone,
The Hormel Institute, United States

***Correspondence:**
Matthew R. Sarkisian
msarkisian@ufl.edu

Received: *30 November 2018*
Accepted: *04 February 2019*
Published: *20 February 2019*

Citation:
Sarkisian MR and Semple-Rowland SL (2019) Emerging Roles of Primary Cilia in Glioma. Front. Cell. Neurosci. 13:55. doi: 10.3389/fncel.2019.00055

cilia may play in controlling glioma tumorigenesis, and findings that suggest the ciliated state of these cells may affect their susceptibility to standard of care GBM (glioblastoma) therapies.

PREVALENCE OF PRIMARY CILIA IN GLIOMA BIOPSIES AND CELL LINES

A first step toward understanding the functions of primary cilia in tumors is to document the prevalence of these organelles in tumor tissues. For a summary of the status of cilia expression and function in non-glioma cancer subtypes, the reader is referred to a recent review (Eguether and Hahne, 2018). Our group has examined GBM biopsies collected from over 20 patients and have detected primary cilia in all biopsies (Sarkisian et al., 2014). The numbers of ciliated cells in these biopsies ranged from <1 to ∼25% of the population of tumor cells. Cilia were found on cells expressing Ki67, a cellular marker for proliferation, and on cells associated with the vasculature and pseudopalisading necroses, common pathological features of GBM. Closer examination of the cilia using EM analyses revealed the presence of normal appearing primary cilia and of cilia that appeared to have defects affecting the basal body or cilium. A mixture of normal and abnormal cilia in GBM biopsies was also reported by Moser et al. (2014) who examined 7 patient biopsies and reported finding normal cilia in one biopsy and cilia possessing various ultrastructural abnormalities that affected the basal body or axoneme in the remaining 6 biopsies. It is not clear whether these ultrastructural abnormalities affect cilia function. Currently, there are very few methods that allow assessment of cilia function. The best characterized is the sonic hedgehog (SHH) signaling pathway using SHH and subsequently monitor activation of downstream signaling genes (for review see: Goetz and Anderson, 2010). However, it should be noted that primary cilia also host many other signaling pathways including WNT, Notch, Hippo, platelet-derived growth factor (PDGF), insulin-like growth factor (IGF), mechanistic target of rapamycin (mTOR), and multiple G protein-coupled receptors (for review see: Liu et al., 2018; Wheway et al., 2018).

It is important to note that documentation of ciliated cells in human tumor biopsy samples could be significantly affected by the region of the tumor from which the biopsy is obtained, as well as the type of fixative used to preserve the sample and delays in fixation (e.g., Hua and Ferland, 2017). A typical research lab that receives a biopsy may know the general brain region from which the biopsy was obtained and details about the fixation of the tissue. In our experience, immunostaining of many cilia marker proteins in biopsy tissues is significantly improved if the tissues were immediately fixed in 4% paraformaldehyde. Clearly, additional analyses of GBM biopsies will be required to determine the relative frequency of ciliated cells within tumors and to improve the ultrastructural characterization of these cilia.

What cell types are ciliated in GBM tumors? The GBMmicroenvironment can contain multiple cell types that either resemble or derive from glia, microglia, oligodendrocytes, neurons, fibroblasts, and vascular cells (Charles et al., 2012; Rich, 2016). In our analyses of patient-derived xenograft (PDX) tumors, ciliated cells appear to be similarly, distributed in the large core of the tumor and in distal tumor satellite growths (Hoang-Minh L. B. et al., 2016). At this point, the distribution of primary cilia across the various cell types in human GBM *in situ* remains unknown. To determine which cells in GBM tumors are ciliated, it will be necessary to obtain and section larger regions of human brain that contain these tumors and then analyze the sections using combinations of immunohistochemistry, immuno-electron microscopy (EM), and reconstruction of serial sections.

In vitro analyses of tumor cell lines is a second approach used to study the role(s) that cilia might have in regulating tumor cell biology. Moser et al. (2009) performed the first immunocytochemical and quantitative EM analyses of various GBM cell lines (U-87 MG, T98G, U-251 MG, U-373 MG, and U-138 MG) and found that these cells rarely gave rise to cilia, or if the cells were ciliated, the cilia were often ultrastructurally abnormal. These particular GBM cell lines have fallen out of favor with many neurooncology researchers in part because the DNA profiles of the cell lines differ from those of the original tumor cells (Allen et al., 2016). It is unclear how these genetic changes might affect ciliogenesis. In view of this, we have studied ciliogenesis in five different recently derived human and mouse primary GBM cell lines and have found that approximately 5–30% of the cells across these cell lines were ciliated and that the cilia were ultrastructurally normal and stained positively for proteins known to localize to the ciliary axoneme and basal body (e.g., IFT88, ARL13B, SMO, GLI3, ADCY3, gamma and acetylated alpha tubulin, and PCM1; Sarkisian et al., 2014; Hoang-Minh L. et al., 2016; Hoang-Minh et al., 2018).

Can ciliogenesis be induced in GBM cells? Serum withdrawal is one way to induce differentiation and ciliogenesis (Santos and Reiter, 2008); however, we and others have been unable to stimulate ciliogenesis in cultured GBM cells using serum withdrawal (Moser et al., 2009; Sarkisian et al., 2014). These observations suggest that it may not be possible to induce ciliogenesis in glioma cells that if true may explain why many of the commonly used GBM cell lines studied *in vitro* typically lack cilia. Factors that may contribute to the low numbers of ciliated cells present in various cell lines, include structural cilia defects, the rapid turnover of the cultured cells, and heterogeneity of the cells with regard to their ability to generate or retain cilia. GBM growth is aggressive and so it is possible that the rapid turnover of cells within these tumors narrows the window of time during which cilia would be present. Alternatively, it may be that only a small fraction of cells in the tumor are capable of growing cilia. We examined this latter possibility by isolating cell clones from two PDX cell lines that normally display ∼10–25% ciliated cells at any given time and found that most of the clones that we isolated gave rise to ciliated progeny (Hoang-Minh L. B. et al., 2016). This finding indicates that even though ciliation was relatively low, most of the cells in these cell lines were capable of giving rise to ciliated daughter cells.

In summary, the consensus among GBM tumor biopsy and cell line studies indicates that anywhere from ∼<1 up to ∼30% of the cells in glioma biopsies and in these cell lines are ciliated at any given time. Future studies that characterize ciliated glioma

lines should make reference, if possible, to the frequency of ciliated cells in the biopsy from which they were derived. If we are able to associate patient outcomes with the numbers and functions of ciliated cells within GBM tumor biopsies, then it may be possible use this information to better inform patient prognoses and treatments.

CILIA AND GLIOMAGENESIS

Cilia are organelles typically associated with differentiated cells but are also assembled by dividing cells. In dividing cells, cilia are assembled by the mother centriole during G1 and can persist throughout the cell cycle but disappear during mitosis (Ford et al., 2018). Because cilia are intimately involved in cell division, it is possible that mutations that disrupt ciliogenesis could promote tumorigenesis as a result of a loss of cell cycle control (Plotnikova et al., 2008; Basten and Giles, 2013). In this section we will briefly review research data that support diametrically opposed roles for cilia in controlling tumor cell proliferation in glioma.

Recent studies of the lysophosphatidic acid receptor 1 (LPAR1) and cell cycle-related kinase (CCRK) and its substrate, intestinal cell kinase (ICK), suggest that proliferation of normal astrocytes and glioma cells is enhanced in cells that have either lost or have not synthesized primary cilia. The cilia of normal human astrocytes contain elevated levels of the LPAR1 (Loskutov et al., 2018), a receptor whose downstream signaling cascade activates the G-protein, Gα12/ Gαq (Goldsmith et al., 2011). Loskutov et al. (2018) found that proliferation can be induced in immortalized human astrocytes lacking primary cilia by activating LPAR1 signaling, signaling that is normally limited in ciliated cells because Gα12 and Gαq are excluded from the cilium. The increase in proliferation of the deciliated cells was found to be due to redistribution of LPAR1 to the plasma membrane of the cell where it was able to actively signal through association with Gα12/ Gαq. Furthermore, they found that treatments of deciliated astrocytes and of intracranial tumors in a mouse model of GBM with a small molecule inhibitor of LPA signaling significantly reduced proliferation of the astrocytes and growth of the intracranial GBM tumors, respectively. The results of this study support the idea that one function of primary cilia is to limit GBM proliferation, and that loss of tumor cell cilia may lead to the redistribution of LPAR1 to the plasma membrane and lead to cell proliferation as a result of increased LPAR1 signaling.

In addition to LPAR1 signaling, CCRK and its substrate, ICK, have been linked to the regulation of ciliogenesis and proliferation of tumor cells (Tian et al., 2012). Yang et al. (2013) found that knockdown of CCRK in cultured U251 GBM cells increased the numbers of ciliated cells in the cultures from ∼2 to 8% and slowed proliferation of the cells. They also found that depleting CCRK in NIH3T3 fibroblast cells increased levels of ICK at the tips of the cilia and prevented the cells from re-entering the cell cycle. Our group has also found that blocking ciliogenesis in one PDX tumor cell line by expressing a dominant negative form of Kif3a in the cells accelerated proliferation of these cells and their tumorigenic capacity in a PDX model (Hoang-Minh L. B. et al., 2016). Collectively, the results of these studies indicate that deciliation of transformed GBM cells may lead to loss of control of the cell cycle and increased tumor growth.

Interestingly, there is evidence that tumor cells may actively repress ciliogenesis thereby promoting tumor growth. For example, an increase in the levels of the transcription factor EZH2 in melanoma cells, which normally suppresses expression of genes regulating ciliogenesis, can lead to WNT/β-catenin-mediated tumorigenesis (Zingg et al., 2018). Notably, inhibition of EZH2 in GBM with elevated levels of EZH2 has been reported to suppress growth of these tumors (Jin et al., 2017). Thus, future studies should examine how EZH2 affects ciliogenesis in GBM.

There are also studies that suggest that cilia may promote tumor cell proliferation. Cells throughout the brain are ciliated (Fuchs and Schwark, 2004; Bishop et al., 2007; Guemez-Gamboa et al., 2014; Sarkisian and Guadiana, 2015) and it appears that cilia on progenitor cells may activate distinct signaling pathways that regulate cell proliferation. For example, in the hippocampal dentate granule zone of developing and adult brain, the cilia of neuronal progenitor cells mediate SHH signaling thereby promoting neurogenesis (Breunig et al., 2008; Han et al., 2008). Interestingly, a significant number of gliomas also respond to SHH (Dahmane et al., 2001; Bar et al., 2007; Clement et al., 2007; Gruber Filbin et al., 2013; Morgenroth et al., 2014). In a study of a PDX cell line reported to be responsive to SHH, we found that SHH only promoted proliferation of the tumor cells if they were ciliated or were capable of forming cilia, and that proliferation was blocked if ciliogenesis was inhibited using a dominant negative form of KIF3a or if SMO function in cilia was inhibited using cyclopamine (Hoang-Minh L. B. et al., 2016). We also found that CRISPR/Cas9-mediated suppression of PCM1, a protein that localizes to centriolar satellites and is required for ciliogenesis, inhibited the proliferation of two GBM cell lines apparently through enhancement of apoptotic cell death (Hoang-Minh L. et al., 2016).

Glioblastoma cells may also release factors from their cilia that could influence tumorigenesis. Recently, we used piggyBac transgenesis to label GBM cilia with Arl13b:GFP that allowed us to use live imaging to monitor the cilia (Hoang-Minh et al., 2018). We observed that a small fraction of GBM primary cilia released vesicles from their distal tips. We also found that culture media conditioned by ciliated GBM cells enhanced cell proliferation of GBM cells while media conditioned by cultures of GBM cells lacking cilia did not, an observation that suggests cilia themselves may release factors that enhance cell proliferation. The cells that appeared to release ciliary vesicles were $Ki67^{-}$ suggesting that quiescent glioma cells may release factors into the microenvironment that could influence tumor growth. Our findings are noteworthy because they are consistent with recent reports that show primary cilia tip excisions occur in multiple non-cancer cell lines and that these excision events appear to be a mechanism that can drive quiescent cells back into the cell cycle (Nager et al., 2017; Phua et al., 2017; Ford et al., 2018). These observations indicate that examination of the content and the mitogenic activities of glioma-derived primary cilia vesicles may provide insight into mechanisms underlying tumor growth or recurrence.

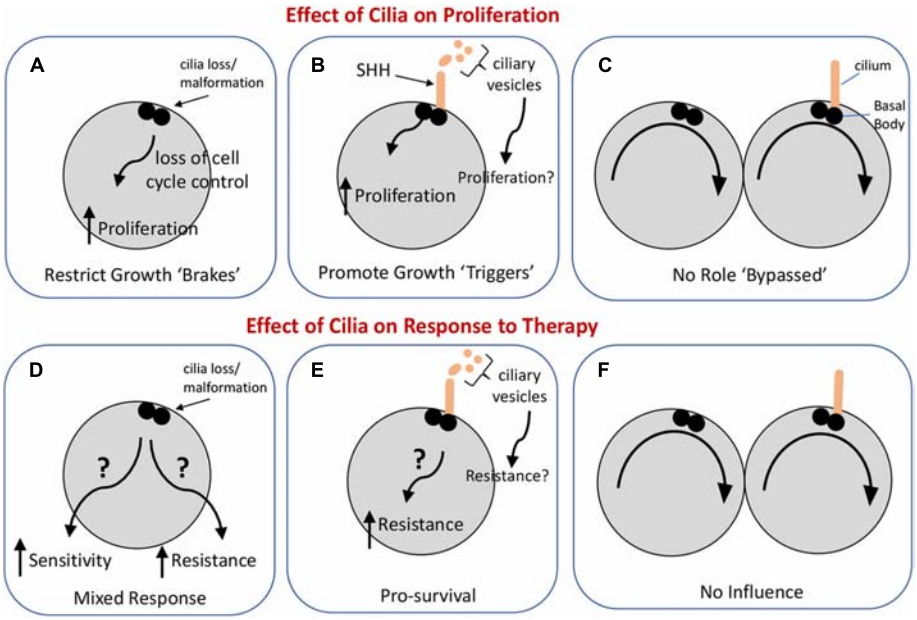

FIGURE 1 | Possible influences of primary cilia on glioma cell proliferation and the response of these cells to standard-of-care therapies. The upper panels illustrate three ways in which cilia could impact glioma cell proliferation. **(A)** Loss or malformation of the cilium could alter signaling pathways in the cell leading to dysregulation of the cell cycle. **(B)** Cilia signaling may actively promote cell proliferation (e.g., in response to SHH) or may, through vesicle release, enhance tumor growth, and proliferation. **(C)** Cilia may not have an impact on cell proliferation. The lower panels illustrate three ways cilia could influence the response of glioma to therapy with the caveat that the type of therapy, e.g., chemotherapy versus irradiation, may shape the cell's response differently. **(D)** Loss or malformation of the cilium could have one of two very different effects: it could increase the sensitivity of the cell to therapy under conditions in which cilia normally support cell survival, or it could increase the resistance of the cell to therapy if cilia-dependent signaling normally activates cell death pathways. **(E)** Cilia signaling could increase cell resistance to therapy by triggering cell survival pathways through either autocrine or paracrine signaling. **(F)** Glioma cells may have evolved so that their response to therapy occurs independently of cilia.

CILIA AND RESISTANCE OF TUMORS TO THERAPY

The standard of care therapies for GBM are surgery, temozolomide (TMZ) chemotherapy, and gamma-irradiation. Very little is known about how the presence or absence of cilia on glioma cells affects the efficacies of these treatments. We found that some ciliated cells express ZEB1, a transcription factor that promotes glioma initiation, invasiveness, and resistance to TMZ chemotherapy (Siebzehnrubl et al., 2013; Sarkisian et al., 2014). Using two PDX cell lines in which we inhibited cilia formation using either CRISPR/Cas9 ablation of either PCM1 or KIF3a, or of both, we found that the loss of either KIF3A or PCM1 in these cells was associated with an increase in the cell's sensitivity to TMZ exposure (Hoang-Minh L. et al., 2016). Depletion of both KIF3A and PCM1 did not increase the sensitivity of the cells to TMZ above that observed in cells in which only one protein was ablated. These results suggest that cilia signaling may contribute to the survival of cells exposed to TMZ chemotherapy. Additional studies will be needed to determine whether this phenomenon is consistently observed in ciliated PDX cell lines and in intracranial models of GBM.

The results of a recent study of multiple types of drug-resistant cancer cell lines (e.g., rhabdoid tumor, non-small cell lung carcinoma, and lung adenocarcinoma) suggest that drug resistance in these cell lines is accompanied by an increase in ciliogenesis and cilia signaling as measured by SHH pathway activation (Jenks et al., 2018). These authors found that increased cilia length was sufficient to confer drug-resistance and that blocking either ciliogenesis or cilia signaling pathways was able to reverse drug-resistance. It would be worthwhile to determine whether these mechanisms are active in GBM cells. It is noteworthy that stimulation of ciliogenesis in cultured U251 GBM cells by knocking out CCRK also promoted the localization of members of the SHH pathway to cilia, an effect that could possibly enhance the signaling capacity of these structures (Yang et al., 2013). Similarly, we reported that Arl13b overexpression promotes SMO localization to GBM cilia in the absence of SHH, and that high levels of ARL13B and SMO expression in the tumors of glioma and gastric tumor patients was positively correlated with shortened post-diagnosis survival in these patients (Shao et al., 2017; Hoang-Minh et al., 2018). Thus, it is possible treatments or conditions that stimulate glioma cell ciliogenesis could induce drug resistance in these cells and lead to tumor recurrence.

SUMMARY AND FUTURE DIRECTIONS

Taken together, the roles or primary cilia in GBM may depend on the relative abundance of ciliated cells in these tumors and the signaling capacities of the cilia. So far, data from existing experiments indicate that glioma cilia may have dual roles,

either restricting or promoting gliomagenesis (**Figure 1**). If we can obtain high quality tumor biopsies, it may be possible to determine the numbers of ciliated cells in specific tumors and what signaling pathways may be active within these tumors. The question is whether this information could be useful in predicting how GBM tumors would respond to therapies employing SHH pathway inhibitors or chemotherapy/radiation. The hypotheses raised in this review require further testing in PDX models. Identification of signaling pathways activated by glioma cell cilia may point to new strategies to slow or inhibit the aggressive growth of these tumors.

AUTHOR CONTRIBUTIONS

MS and SS-R wrote the manuscript.

FUNDING

This work was supported in part by funds from an American Brain Tumor Association Discovery Grant supported by an Family Foundation (MS), and a University of Florida Foundation Fund (SS-R).

REFERENCES

Allen, M., Bjerke, M., Edlund, H., Nelander, S., and Westermark, B. (2016). Origin of the U87MG glioma cell line: good news and bad news. *Sci. Transl. Med.* 8:354re3. doi: 10.1126/scitranslmed.aaf6853

Alvarez-Satta, M., and Matheu, A. (2018). Primary cilium and glioblastoma. *Ther. Adv. Med. Oncol.* 10:1758835918801169. doi: 10.1177/1758835918801169

Bar, E. E., Chaudhry, A., Lin, A., Fan, X., Schreck, K., Matsui, W., et al. (2007). Cyclopamine-mediated hedgehog pathway inhibition depletes stem-like cancer cells in glioblastoma. *Stem Cells* 25, 2524–2533. doi: 10.1634/stemcells.2007-0166

Basten, S. G., and Giles, R. H. (2013). Functional aspects of primary cilia in signaling, cell cycle and tumorigenesis. *Cilia* 2:6. doi: 10.1186/2046-2530-2-6

Baudoin, J. P., Viou, L., Launay, P. S., Luccardini, C., Espeso Gil, S., Kiyasova, V., et al. (2012). Tangentially migrating neurons assemble a primary cilium that promotes their reorientation to the cortical plate. *Neuron* 76, 1108–1122. doi: 10.1016/j.neuron.2012.10.027

Bishop, G. A., Berbari, N. F., Lewis, J., and Mykytyn, K. (2007). Type III adenylyl cyclase localizes to primary cilia throughout the adult mouse brain. *J. Comp. Neurol.* 505, 562–571. doi: 10.1002/cne.21510

Breunig, J. J., Sarkisian, M. R., Arellano, J. I., Morozov, Y. M., Ayoub, A. E., Sojitra, S., et al. (2008). Primary cilia regulate hippocampal neurogenesis by mediating sonic hedgehog signaling. *Proc. Nal. Acad. Sci. U.S.A.* 105, 13127–13132. doi: 10.1073/pnas.0804558105

Charles, N. A., Holland, E. C., Gilbertson, R., Glass, R., and Kettenmann, H. (2012). The brain tumor microenvironment. *Glia* 60, 502–514. doi: 10.1002/glia.21264

Clement, V., Sanchez, P., de Tribolet, N., Radovanovic, I., and Ruiz i Altaba, A. (2007). HEDGEHOG-GLI1 signaling regulates human glioma growth, cancer stem cell self-renewal, and tumorigenicity. *Curr. Biol.* 17, 165–172. doi: 10.1016/j.cub.2006.11.033

Dahmane, N., Sanchez, P., Gitton, Y., Palma, V., Sun, T., Beyna, M., et al. (2001). The Sonic Hedgehog-Gli pathway regulates dorsal brain growth and tumorigenesis. *Development* 128, 5201–5212.

Eguether, T., and Hahne, M. (2018). Mixed signals from the cell's antennae: primary cilia in cancer. *EMBO Rep.* 19:e46589. doi: 10.15252/embr.201846589

Ford, M. J., Yeyati, P. L., Mali, G. R., Keighren, M. A., Waddell, S. H., Mjoseng, H. K., et al. (2018). A cell/cilia cycle biosensor for single-cell kinetics reveals persistence of cilia after G1/S transition is a general property in cells and mice. *Dev. Cell* 47, 509.e5–523.e5. doi: 10.1016/j.devcel.2018.10.027

Fuchs, J. L., and Schwark, H. D. (2004). Neuronal primary cilia: a review. *Cell Biol. Int.* 28, 111–118. doi: 10.1016/j.cellbi.2003.11.008

Garcia, G. III, Raleigh, D. R., and Reiter, J. F. (2018). How the ciliary membrane is organized inside-out to communicate outside-in. *Curr. Biol.* 28, R421–R434. doi: 10.1016/j.cub.2018.03.010

Goetz, S. C., and Anderson, K. V. (2010). The primary cilium: a signalling centre during vertebrate development. *Nat. Rev. Genet.* 11, 331–344. doi: 10.1038/nrg2774

Goldsmith, Z. G., Ha, J. H., Jayaraman, M., and Dhanasekaran, D. N. (2011). Lysophosphatidic acid stimulates the proliferation of ovarian cancer cells via the gep proto-oncogene Galpha(12). *Genes Cancer* 2, 563–575. doi: 10.1177/1947601911419362

Gruber Filbin, M., Dabral, S. K., Pazyra-Murphy, M. F., Ramkissoon, S., Kung, A. L., Pak, E., et al. (2013). Coordinate activation of Shh and PI3K signaling in PTEN-deficient glioblastoma: new therapeutic opportunities. *Nat. Med.* 19, 1518–1523. doi: 10.1038/nm.3328

Guemez-Gamboa, A., Coufal, N. G., and Gleeson, J. G. (2014). Primary cilia in the developing and mature brain. *Neuron* 82, 511–521. doi: 10.1016/j.neuron.2014.04.024

Guo, J., Higginbotham, H., Li, J., Nichols, J., Hirt, J., Ghukasyan, V., et al. (2015). Developmental disruptions underlying brain abnormalities in ciliopathies. *Nat. Commun.* 6:7857. doi: 10.1038/ncomms8857

Han, Y. G., and Alvarez-Buylla, A. (2010). Role of primary cilia in brain development and cancer. *Curr. Opin. Neurobiol.* 20, 58–67. doi: 10.1016/j.conb.2009.12.002

Han, Y. G., Kim, H. J., Dlugosz, A. A., Ellison, D. W., Gilbertson, R. J., and Alvarez-Buylla, A. (2009). Dual and opposing roles of primary cilia in medulloblastoma development. *Nat. Med.* 15, 1062–1065. doi: 10.1038/nm.2020

Han, Y. G., Spassky, N., Romaguera-Ros, M., Garcia-Verdugo, J. M., Aguilar, A., Schneider-Maunoury, S., et al. (2008). Hedgehog signaling and primary cilia are required for the formation of adult neural stem cells. *Nat. Neurosci.* 11, 277–284. doi: 10.1038/nn2059

Higginbotham, H., Eom, T. Y., Mariani, L. E., Bachleda, A., Hirt, J., Gukassyan, V., et al. (2012). Arl13b in primary cilia regulates the migration and placement of interneurons in the developing cerebral cortex. *Dev. Cell* 23, 925–938. doi: 10.1016/j.devcel.2012.09.019

Higginbotham, H., Guo, J., Yokota, Y., Umberger, N. L., Su, C. Y., Li, J., et al. (2013). Arl13b-regulated cilia activities are essential for polarized radial glial scaffold formation. *Nat. Neurosci.* 16, 1000–1007. doi: 10.1038/nn.3451

Hoang-Minh, L. B., Deleyrolle, L. P., Siebzehnrubl, D., Ugartemendia, G., Futch, H., Griffith, B., et al. (2016). Disruption of KIF3A in patient-derived glioblastoma cells: effects on ciliogenesis, hedgehog sensitivity, and tumorigenesis. *Oncotarget* 7, 7029–7043. doi: 10.18632/oncotarget.6854

Hoang-Minh, L., Deleyrolle, L., Nakamura, N., Parker, A., Martuscello, R., Reynolds, B., et al. (2016). PCM1 depletion inhibits glioblastoma cell ciliogenesis and increases cell death and sensitivity to temozolomide. *Transl. Oncol.* 9, 392–402. doi: 10.1016/j.tranon.2016.08.006

Hoang-Minh, L. B., Dutra-Clarke, M., Breunig, J. J., and Sarkisian, M. R. (2018). Glioma cell proliferation is enhanced in the presence of tumor-derived cilia vesicles. *Cilia* 7:6. doi: 10.1186/s13630-018-0060-5

Hua, K., and Ferland, R. J. (2017). Fixation methods can differentially affect ciliary protein immunolabeling. *Cilia* 6:5. doi: 10.1186/s13630-017-0045-9

Jenks, A. D., Vyse, S., Wong, J. P., Kostaras, E., Keller, D., Burgoyne, T., et al. (2018). Primary cilia mediate diverse kinase inhibitor resistance mechanisms in cancer. *Cell Rep.* 23, 3042–3055. doi: 10.1016/j.celrep.2018.05.016

Jin, X., Kim, L. J. Y., Wu, Q., Wallace, L. C., Prager, B. C., Sanvoranart, T., et al. (2017). Targeting glioma stem cells through combined BMI1 and EZH2 inhibition. *Nat. Med.* 23, 1352–1361. doi: 10.1038/nm.4415

Li, L., Grausam, K. B., Wang, J., Lun, M. P., Ohli, J., Lidov, H. G., et al. (2016). Sonic Hedgehog promotes proliferation of Notch-dependent monociliated choroid plexus tumour cells. *Nat. Cell Biol.* 18, 418–430. doi: 10.1038/ncb3327

Liu, H., Kiseleva, A. A., and Golemis, E. A. (2018). Ciliary signalling in cancer. *Nat. Rev. Cancer* 18, 511–524. doi: 10.1038/s41568-018-0023-6

Loskutov, Y. V., Griffin, C. L., Marinak, K. M., Bobko, A., Margaryan, N. V., Geldenhuys, W. J., et al. (2018). LPA signaling is regulated through the primary cilium: a novel target in glioblastoma. *Oncogene* 37, 1457–1471. doi: 10.1038/s41388-017-0049-3

Morgenroth, A., Vogg, A. T., Ermert, K., Zlatopolskiy, B., and Mottaghy, F. M. (2014). Hedgehog signaling sensitizes glioma stem cells to endogenous nano-irradiation. *Oncotarget* 5, 5483–5493. doi: 10.18632/oncotarget.2123

Moser, J. J., Fritzler, M. J., and Rattner, J. B. (2009). Primary ciliogenesis defects are associated with human astrocytoma/glioblastoma cells. *BMC Cancer* 9:448. doi: 10.1186/1471-2407-9-448

Moser, J. J., Fritzler, M. J., and Rattner, J. B. (2014). Ultrastructural characterization of primary cilia in pathologically characterized human glioblastoma multiforme (GBM) tumors. *BMC Clin. Pathol.* 14:40. doi: 10.1186/1472-6890-14-40

Nager, A. R., Goldstein, J. S., Herranz-Perez, V., Portran, D., Ye, F., Garcia-Verdugo, J. M., et al. (2017). An actin network dispatches ciliary GPCRs into extracellular vesicles to modulate signaling. *Cell* 168, 252.e14–263.e14. doi: 10.1016/j.cell.2016.11.036

Phua, S. C., Chiba, S., Suzuki, M., Su, E., Roberson, E. C., Pusapati, G. V., et al. (2017). Dynamic remodeling of membrane composition drives cell cycle through primary cilia excision. *Cell* 168, 264.e15–279.e15. doi: 10.1016/j.cell.2016.12.032

Plotnikova, O. V., Golemis, E. A., and Pugacheva, E. N. (2008). Cell cycle-dependent ciliogenesis and cancer. *Cancer Res.* 68, 2058–2061. doi: 10.1158/0008-5472.CAN-07-5838

Rich, J. N. (2016). Cancer stem cells: understanding tumor hierarchy and heterogeneity. *Medicine* 95(1 Suppl. 1), S2–S7. doi: 10.1097/MD.0000000000004764

Santos, N., and Reiter, J. F. (2008). Building it up and taking it down: the regulation of vertebrate ciliogenesis. *Dev. Dyn.* 237, 1972–1981. doi: 10.1002/dvdy.21540

Sarkisian, M. R., and Guadiana, S. M. (2015). Influences of primary cilia on cortical morphogenesis and neuronal subtype maturation. *Neuroscientist* 21, 136–151. doi: 10.1177/1073858414531074

Sarkisian, M. R., Siebzehnrubl, D., Hoang-Minh, L., Deleyrolle, L., Silver, D. J., Siebzehnrubl, F. A., et al. (2014). Detection of primary cilia in human glioblastoma. *J. Neurooncol.* 117, 15–24. doi: 10.1007/s11060-013-1340-y

Schuster, F. (1964). Ciliated fibroblasts from a a human brain tumor. *Anat. Rec.* 150, 417–422. doi: 10.1002/ar.1091500410

Shao, J., Xu, L., Chen, L., Lu, Q., Xie, X., Shi, W., et al. (2017). Arl13b promotes gastric tumorigenesis by regulating Smo trafficking and activation of the hedgehog signaling pathway. *Cancer Res.* 77, 4000–4013. doi: 10.1158/0008-5472.CAN-16-2461

Siebzehnrubl, F. A., Silver, D. J., Tugertimur, B., Deleyrolle, L. P., Siebzehnrubl, D., Sarkisian, M. R., et al. (2013). The ZEB1 pathway links glioblastoma initiation, invasion and chemoresistance. *EMBO Mol. Med.* 5, 1196–1212. doi: 10.1002/emmm.201302827

Singla, V., and Reiter, J. F. (2006). The primary cilium as the cell's antenna: signaling at a sensory organelle. *Science* 313, 629–633. doi: 10.1126/science.1124534

Spassky, N., Han, Y. G., Aguilar, A., Strehl, L., Besse, L., Laclef, C., et al. (2008). Primary cilia are required for cerebellar development and Shh-dependent expansion of progenitor pool. *Dev. Biol.* 317, 246–259. doi: 10.1016/j.ydbio.2008.02.026

Tani, E., and Ametani, T. (1970). Ciliated human astrocytoma cells. *Acta Neuropathol.* 15, 208–219. doi: 10.1007/BF00686767

Tian, Y., Wan, H., and Tan, G. (2012). Cell cycle-related kinase in carcinogenesis. *Oncol. Lett.* 4, 601–606. doi: 10.3892/ol.2012.828

Wheway, G., Nazlamova, L., and Hancock, J. T. (2018). Signaling through the primary cilium. *Front. Cell Dev. Biol.* 6:8. doi: 10.3389/fcell.2018.00008

Wood, C. R., and Rosenbaum, J. L. (2015). Ciliary ectosomes: transmissions from the cell's antenna. *Trends Cell Biol.* 25, 276–285. doi: 10.1016/j.tcb.2014.12.008

Yang, Y., Roine, N., and Makela, T. P. (2013). CCRK depletion inhibits glioblastoma cell proliferation in a cilium-dependent manner. *EMBO Rep.* 14, 741–747. doi: 10.1038/embor.2013.80

Zingg, D., Debbache, J., Pena-Hernandez, R., Antunes, A. T., Schaefer, S. M., Cheng, P. F., et al. (2018). EZH2-mediated primary cilium deconstruction drives metastatic melanoma formation. *Cancer Cell* 34, 69.e14–84.e14. doi: 10.1016/j.ccell.2018.06.001

Conflict of Interest Statement: The authors declare that the research was conducted in the absence of any commercial or financial relationships that could be construed as a potential conflict of interest.

frontiers in Cellular Neuroscience

REVIEW
published: 26 April 2019
doi: 10.3389/fncel.2019.00151

Phase-to-Phase With Nucleoli – Stress Responses, Protein Aggregation and Novel Roles of RNA

*Leena Latonen**

Institute of Biomedicine, University of Eastern Finland, Kuopio, Finland

Protein- and RNA-containing foci and aggregates are a hallmark of many age- and mutation-related neurodegenerative diseases. This article focuses on the role the nucleolus has as a hub in macromolecule regulation in the mammalian nucleus. The nucleolus has a well-established role in ribosome biogenesis and functions in several types of cellular stress responses. In addition to known reactions to DNA damaging and transcription inhibiting stresses, there is an emerging role of the nucleolus especially in responses to proteotoxic stress such as heat shock and inhibition of proteasome function. The nucleolus serves as an active regulatory site for detention of extranucleolar proteins. This takes place in nucleolar cavities and manifests in protein and RNA collections referred to as intranucleolar bodies (INBs), nucleolar aggresomes or amyloid bodies (A-bodies), depending on stress type, severity of accumulation, and material propensities of the macromolecular collections. These indicate a relevance of nucleolar function and regulation in neurodegeneration-related cellular events, but also provide surprising connections with cancer-related pathways. Yet, the molecular mechanisms governing these processes remain largely undefined. In this article, the nucleolus as the site of protein and RNA accumulation and as a possible protective organelle for nuclear proteins during stress is viewed. In addition, recent evidence of liquid-liquid phase separation (LLPS) and liquid-solid phase transition in the formation of nucleoli and its stress responses, respectively, are discussed, along with the increasingly indicated role and open questions for noncoding RNA species in these events.

Keywords: nucleoli, stress responses, protein aggregation, amyloidosis, proteasome inhibition, non-coding RNA

OPEN ACCESS

Edited by:
Rosanna Parlato,
University of Ulm, Germany

Reviewed by:
Stephen Lee,
University of Miami, United States
Miguel Lafarga,
University of Cantabria-IDIVAL, Spain

***Correspondence:**
Leena Latonen
leena.latonen@uef.fi

Specialty section:
This article was submitted to Cellular Neuropathology, a section of the journal Frontiers in Cellular Neuroscience

Received: *09 January 2019*
Accepted: *08 April 2019*
Published: *26 April 2019*

Citation:
Latonen L (2019) Phase-to-Phase With Nucleoli – Stress Responses, Protein Aggregation and Novel Roles of RNA. Front. Cell. Neurosci. 13:151. doi: 10.3389/fncel.2019.00151

INTRODUCTION

Nucleoli are the site of ribosome biogenesis. They are formed in nuclei around tandem head-to-tail gene repeats of ribosomal DNA (rDNA) in the so called nucleolar organizing regions (NORs). In human cells, NORs are located in the short arms of five acrocentric chromosomes, and their size ranges from 50 kb to >6 Mb (Mangan et al., 2017). The nucleoli are initiated upon and structurally depend on active transcription of rDNA. The nucleoli are dispersed during mitosis as the rDNA transcription is halted. During telophase, the rDNA transcription resumes, and the nucleoli begin to reform as small nucleoli around individual NORs. As the cell cycle progresses, nucleoli fuse, forming larger, mature nucleoli containing multiple NORs (Hernandez-Verdun, 2011; **Figure 1**).

In human cells, the mature nucleoli are associated with perinucleolar heterochromatin (PNH), DNA sequences located distal and proximal to NORs on the acrocentric chromosomal

arms (McStay, 2016), which is likely to contribute to positioning of the nucleoli to the 3D context in the nuclei. Currently, the sequences of the acrocentric arms are missing from human genome drafts. Yet, what is known is that the sequences on the centromeric side of rDNA are heavily segmentally duplicated and likely do not contain NOR regulatory elements (Floutsakou et al., 2013; Mangan et al., 2017). The telomeric sides of NORs contain regions called distal junctions (DJs). Their sequences are shared between the acrocentric chromosomes and dominated by around 100 kb inverted repeats and seem to have a complex chromatin structure (Floutsakou et al., 2013; Mangan et al., 2017). DJ sequences have been suggested to anchor rDNA to the PNH (Mangan et al., 2017). Other anchors for the spatial positioning of the nucleoli are intermediate filament proteins, especially lamins A/C, B1 and B2, that connect the nucleoli to nuclear matrix and contribute to maintaining nucleolar structure and functions (Martin et al., 2009; Louvet et al., 2014; Matsumoto et al., 2016; Buchwalter and Hetzer, 2017; Sen Gupta and Sengupta, 2017).

The nucleoli belong to a group of membraneless organelles (MLOs), and as such, they are dynamic structures with highly mobile constituents that can diffuse in and out to the nucleoplasm. Recently, the role of liquid-liquid phase separation (LLPS) in formation of MLOs has been increasingly recognized (Shin and Brangwynne, 2017; Sawyer et al., 2018). LLPS has a role in the formation and internal organization of the nucleoli to functional substructures (Feric et al., 2016). The current view thus holds that formation of the nucleoli is a combination of both active recruitment of factors and LLPS.

The nucleoli have a tripartite structure (**Figure 1**) with the three substructures functionally separate. The fibrillar centers (FCs) contain non-transcribed rDNA and rDNA chromatin associated factors. The rDNA transcription occurs at the interface between FCs and dense fibrillary component (DFC), in the latter of which occurs the early processing of precursor ribosomal RNA (rRNA). Late processing of rRNA and assembly of ribosome units takes place at the granular component (GC), surrounding the FCs and DFCs. Interestingly, yeast and other lower eukaryotes lack FCs, which may be connected to the closed nuclear division and intactness of the nucleoli through the cell cycle (Thiry and Lafontaine, 2005).

The tripartite nucleolar structure in human cells depends on the active transcription of rDNA, as several studies have shown inhibition of rDNA transcription by RNA polymerase I (RNApolI) disperses the nucleoli (reviewed in Grummt, 2013). The start of rRNA transcription has long been thought to be the initiating event for nucleolar reformation at the end of mitosis. This view was challenged by Dousset et al. (2000), who's work indicate that postmitotic nucleologenesis results from direct recruitment of processing factors and pre-rRNAs to UBF-associated NORs before or at the onset of rDNA transcription. This is followed by fusion of prepackaged prenucleolar bodies into the nucleolus, suggesting that pre-ribosomal ribonucleoproteins synthesized in the previous cell cycle may contribute to nucleolar formation at the end of mitosis (Dousset et al., 2000).

NUCLEOLAR CONTENTS AND LLPS

The nucleolus is packed with protein – protein density in nucleoli is approximately double of that of the nucleoplasm (Handwerger and Gall, 2006). Although very dense, the nucleolus is also very dynamic: many nucleolar proteins are constantly moving between the nucleolus and the nucleoplasm (Leung and Lamond, 2003; Hernandez-Verdun, 2006; Sirri et al., 2008). The proteome of the nucleolus before and after stress is well described (Andersen et al., 2005; Moore et al., 2011). Most nucleolar molecules function in transcription and different maturation steps of rRNA (Andersen et al., 2005). However, there are at least dozens, if not hundreds, of nucleolar proteins with no apparent role in the formation of ribosomes (Andersen et al., 2005). Recently, it has become clear that the nucleolus contributes to biogenesis of multiple ribonucleoprotein particles, and the regulation of cellular events such as mitosis, the cell-cycle, and responses to several types of stress (Boisvert et al., 2007; Boulon et al., 2010; Lindström and Latonen, 2013).

RNA content of the nucleoli is not fully described. The well-recognized components, such as rRNA and snoRNA, are well known for their functions in ribosome production, but other non-coding components are not comprehensively described. In addition to the traditionally viewed roles in processing pre-rRNA and formation of ribosomal particles, nucleolar RNA is increasingly seen to have a role through contributing to nucleolar formation through promoting LLPS (Sawyer et al., 2018). MLOs typically harbor specific RNAs and intrinsically disordered, multivalent hub proteins, both contributing to the LLPS characteristics (Sawyer et al., 2018). It has been shown that the disordered domains in FBL and NPM (key components of DFC and GC, respectively) are required for droplet formation, and that RNA recognition motifs are required for maintaining phase separation (Brangwynne et al., 2011; Mangan et al., 2017). The sequence-encoded features of these proteins influencing their LLPS behavior also lie behind nucleolar compartmentalization, driven by different biophysical properties of the droplets, especially surface tensions (Feric et al., 2016). While specific RNAs themselves may be capable of phase separation as in the case of e.g., extended repetitive RNA motifs in clinical disorders, LLPS for MLOs is viewed to be driven more by RNA-protein interactions than RNAs as such (Sawyer et al., 2018). Long RNA molecules may potentially interact with several other proteins and RNAs simultaneously, favoring and strengthening the interactions between droplet-forming proteins. In addition, RNA-protein ratio and RNA multivalency may also be critical factors for MLO LLPS (reviewed in Sawyer et al., 2018). Interactions between NPM and rRNA promote LLPS in the nucleolar formation and supports the idea of active rDNA transcription spatially and temporally coordinating with critical, intrinsically disordered region (IDR)-containing LLPS drivers (Mitrea et al., 2018; Sawyer et al., 2018). It is likely that, in addition to rRNA, there are other contributing RNA species for LLPS in nucleolar formation yet to be identified. Likely candidates are at least the lncRNAs coded by the DJ regions (Mangan et al., 2017).

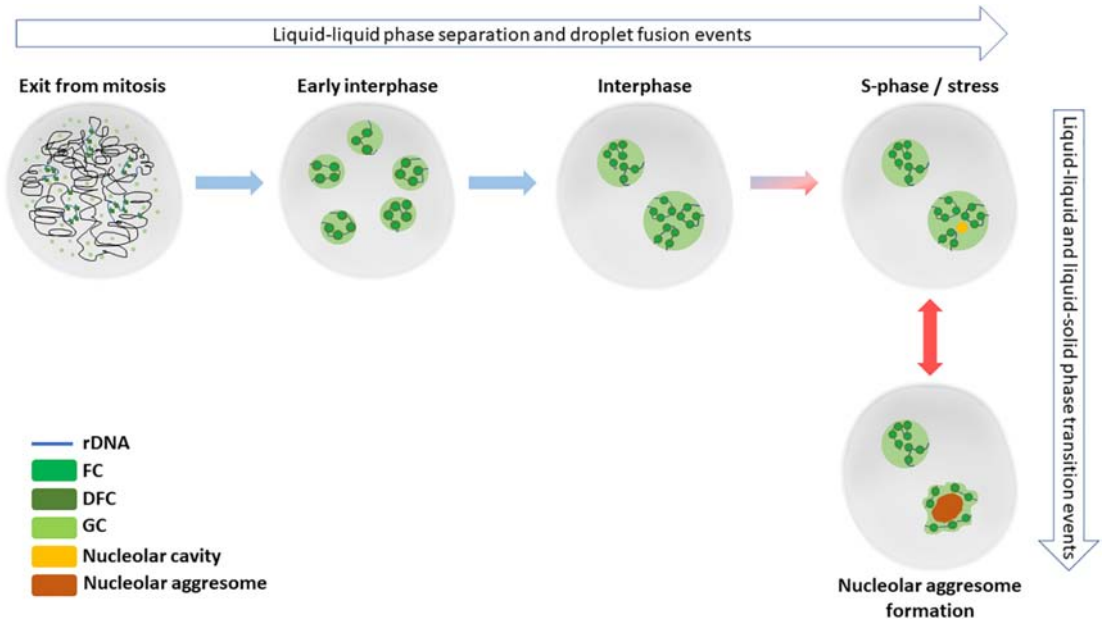

FIGURE 1 | Nucleolar formation and stress responses involve phase separation and transition events. After cell division in late mitosis, nucleoli start to reform by reactivated rRNA transcription and liquid-liquid phase separation events. By early interphase, each individual NOR containing the rDNA repeats are surrounded by a functional nucleolus. Later during the interphase, the small nucleoli fuse to typically form 1–2 mature nucleoli in diploid, non-transformed cells. Nucleolar cavities can be detected in S-phase cells or upon cellular stress, such as DNA damage. When cells are exposed to severe proteotoxic or e.g., heat stress, nucleolar aggressomes and amyloid bodies are formed within one or more nucleoli of a nucleus, involving liquid-solid transition of aggregate contents.

Changes in relative levels of the RNA components, likely to have profounding effects of nucleolar activity as well as organization in terms of LLPS, are not well known. Nucleolar rRNA is so abundant compared to other RNA species in the cell in general that rRNA sequences are often excluded in sequencing assays. The sequence repetitivity and lack of the reference genomes for rDNA areas makes it currently infeasible to align rRNA sequences for most quantitative expression analyses via next generation sequencing approaches. Most importantly, the lack of NORs and adjacent regions from genomic assemblies hampers the expression analyses of these areas and studies for the roles of the ncRNA expressed from these.

NUCLEOLAR ALTERATIONS UPON DNA DAMAGE AND TRANSCRIPTIONAL STRESS

Nucleolar structure changes significantly in response to several types of stress (**Figure 2**). If and when the rRNA production is halted resulting from e.g., double strand break-inducing DNA damage by ionizing radiation (IR) or RNA pol I inhibition by actinomycin D, nucleolar segregation occurs and so called nucleolar caps are formed. Nucleolar caps are bipartite structures containing FCs and DFCs which surround the GC components (Puvion-Dutilleul et al., 1992). A different structural reorganization, the nucleolar necklace, is formed under certain conditions where RNApolI transcription remains active, but rRNA processing is impaired (**Figure 2**). This is evident upon treatment of cells with doxorubicin (DRB), a DNA intercalating agent and inhibitor of DNA topoisomerase II (Louvet et al., 2005).

DNA damage in the form DNA bulges, by e.g., various cytotoxic drugs or UV radiation, cause inhibition of rDNA transcription by RNApolI, resulting in nucleolar disruption. The dispersal of the nucleolus releases proteins to nucleoplasm that normally do not reside in there, a mechanism by which certain stress responses are induced. E.g., p53 nucleolar and ribosomal proteins binds to the MDM2 protein following disruption of ribosome biogenesis. This leads to inhibition of MDM2 E3 ligase activity and thus to p53 activation (reviewed in Lindström and Latonen, 2013). It is interesting that the nucleolar responses to UV and IR differ (Moore et al., 2011). In addition to the different DNA damage types, these insults induce also damage to other macromolecules and partly different cellular responses (Laiho and Latonen, 2003; Goldstein and Kastan, 2015). Currently, it is unclear which other cellular events are involved in dictating the differential nucleolar stress responses upon these stresses (Moore et al., 2011).

It is well established that disruption of the nucleolus triggers a p53-dependent cellular stress response referred to as "nucleolar stress" (Zhang and Lu, 2009; Lindström and Latonen, 2013). This is frequently called also "ribosomal stress," although not all abnormalities in ribosome biogenesis lead to dispersal of the nucleolus. Nucleolar and/or ribosomal stress, mediated to a large extent by interactions of translocated ribosomal and other nucleolar proteins and rRNA, activates signaling pathways leading to cell cycle arrest, apoptosis, differentiation or

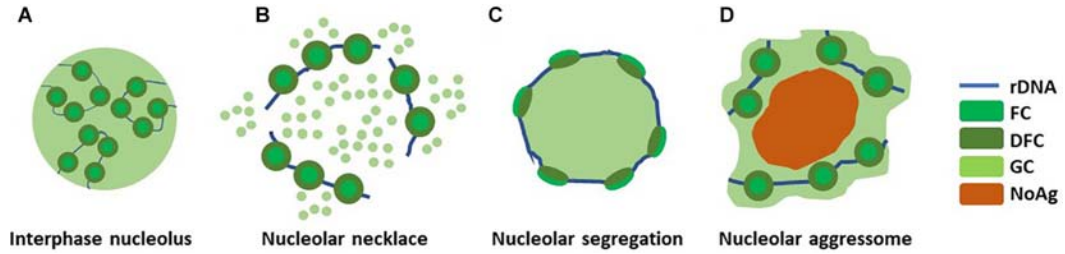

FIGURE 2 | Nucleolar reorganization upon stress. The nucleolus reacts to different types of stress by structural deformations. **(A)** A normal interphase nucleolus under homeostasis shows tripartite structure composed around rDNA. **(B)** Upon DRB treatment, when RNApolI transcription remains active but rRNA processing is impaired, so called nucleolar necklaces are formed. **(C)** Nucleolar segregation, or nucleolar caps, are formed when RNApolI transcription is inactivated, e.g., with Actinomycin D. **(D)** Nucleolar aggresomes are formed within the nucleolus, in the nucleolar detention centers, upon proteotoxic insults such as proteasome inhibition and heat schock. This may or may not involve inhibited RNApolI activity.

senescence, in a cell type and stress severity-dependent manner (reviewed in Lindström and Latonen, 2013).

Translocation to the nucleolus is also a regulatory mechanism under several cellular conditions. Initially, nucleolar sequestration as a concept was introduced by Bachant and Elledge (1999) based on work showing that exit from mitosis in budding yeast is regulated by detention of Cdc14 in the nucleolus (Shou et al., 1999; Visintin et al., 1999). The concept was further supported by the notion that, in mammalian cells, tumor suppressor Arf sequesters Mdm2 in the nucleolus to ensure activation of p53 during oncogene activation and replicative senescence (Weber et al., 1999). Detention in the nucleolus has been described for many proteins especially under different stress conditions. For example, MDM2, which is a ubiquitin ligase for tumor suppressor p53 among others, localizes to the nucleolus also upon transcriptional inhibition by Actinomycin D and possesses lower mobility there (Lohrum et al., 2003; Kurki et al., 2004; Mekhail et al., 2005). MDM2 is also transferred to nucleoli upon DNA damage by PML in an ARF-dependent manner (Bernardi et al., 2004). DNA damage induces translocation of also other proteins to nucleoli. For example, IR restores the disturbed association of telomerase protein with the nucleoli in transformed cells (Wong et al., 2002). Acidosis triggers pH-dependent interaction von Hippel-Lindau tumor suppressor protein (VHL) with rDNA, a phenomenon which is promoted by activation of hypoxia inducible factor HIF (Mekhail et al., 2004a,b, 2006). The authors suggest that this is a way for oxygen-starved cells to maintain energy equilibrium by gauging the environmental H+ concentration to statically retain VHL in nucleoli to restrict ribosomal production (Mekhail et al., 2006).

NUCLEOLAR DETENTION UNDER PROTEIN STRESS – AGGRESOMES, AMYLOIDOGENESIS AND RELEVANCE TO DISEASE

Different from insults directly affecting rRNA transcription and processing, protein stress causes extranucleolar proteins and RNA to be detained in the nucleolus. Initially, certain stress-responsive proteins, such as p53, Mdm2 and PML body proteins, were described to translocate to nucleoli stress-signal-dependently (Klibanov et al., 2001; Mattsson et al., 2001; Xirodimas et al., 2001; Latonen et al., 2003). Later, this phenomenon was described to apply to a number of nuclear UPS client proteins and represent formation a *de novo* stress response organelle (Latonen, 2011; Latonen et al., 2011).

This foci formation takes place in nucleolar cavities, and intranucleolar bodies (INBs) can already be detected in S-phase cells and even after certain types of DNA damage (Abella et al., 2010; Hutten et al., 2011). Upon severe protein stress upon e.g., heat shock, chemical inhibition of proteasome activity, and acidosis, an expanded organelle is formed (Latonen et al., 2011; Audas et al., 2012a, 2016). The intranucleolar stress-responsive macromolecular collections have also been called to occur in so called detention centers, and intranucleolar macromolecular collections showing amyloid properties have been termed amyloid bodies (A-bodies) (Jacob et al., 2013; Audas et al., 2016).

Currently it is not clear how these structures relate to each other, but they share striking similarities: (1) they all form in the nucleoli but are clearly not belonging to normal components of the nucleoli, (2) they involve accumulation of protein which are not normal components of the traditional nucleolar structures, and many of these deposits have been shown to contain at least some of the same proteins, (3) often there is also RNA, which does not belong to normal nucleolar components, accumulating, and (4) formation of many of these structures has been shown to depend on intactness of the nucleoli, with the help experiments utilizing Actinomycin D-mediated nucleolar disruption. Thus, although INBs, nucleolar aggresomes and A-bodies have not been proven to represent same structures, with such striking similarities it seems plausible that they represent a range of sizes and states resulting from same phenomena.

The initial papers describe events occurring upon different cellular stresses (proteasome inhibition, acidosis, heat stress, DNA damage), and certain differences exist in the contents of the organelles. Thus, cellular context- and stress-dependency of RNA and protein recruitment remains to be investigated in future studies. The common denominator seems to be to clear nuclear proteins from the nucleoplasm to regulate cellular activities for the duration of the stress situation, and at least upon

certain insults, the formation of the intranucleolar collections can be transient. For certain proteins, there is evidence for functional impact in the localization to nucleolar aggressomes, such as for TTRAP, which regulates rRNA processing during cellular response to proteasome inhibition (Vilotti et al., 2012). Considering, however, that nucleolar aggresomes can form even as a result of overexpression of exogenous proteins or increased protein synthesis due to a viral infection (reviewed in Latonen, 2011), the role of the nucleolar aggresomes may be, at least at times, to protect the nucleoplasmic environment from excess proteins. In fact, the formation of A-bodies has been suggested as a form of so called protective or functional amyloidosis (Lyons and Anderson, 2016; Woodruff et al., 2018). Amyloid-bodies are solid condensates (Woodruff et al., 2018), and as such, resemble Balbiani-bodies in Xenopus oocytes, forming by amyloid-like assembly of a disordered protein Xvelo (Boke et al., 2016). Proteins in nucleolar aggresomes exhibit decreased mobility (Latonen et al., 2011), while INBs are likely soluble, exhibiting liquid-like spherical appearance (Hutten et al., 2011).

Thus, a plausible, yet speculative, sequence of events (**Figure 2**) in nucleolar aggresome formation involves an initial liquid phase in the nucleolar cavity or detention center (Wang M. et al., 2018). With prolonged accumulation of macromolecules to the structure, the proteins turn immobile (Latonen et al., 2011), liquid-solid phase transition occurs, and may proceed to amyloidogenesis (Audas et al., 2016). RNA seeding is involved in the seeding, at least for the amyloidogenic phase (Audas et al., 2016; Lyons and Anderson, 2016). It is possible that amorphous gel like intermediate states also exist to maturate concentrates of initially liquid state (Woodruff et al., 2018), although this is currently purely speculative. Thus, the exact material properties in each condition, and the mechanisms leading to the possible phase transitions remain to be investigated.

It seems that the composition of the nucleolar aggresomes is somewhat dependent on the stress insult. In general, the proteins are collected to the nucleolar aggresome along with RNA, and most often the aggresomes contain conjugated ubiquitin, SUMO, and heat shock factors (reviewed in Latonen, 2011). Although nucleolar aggresomes bare similarities with cytoplasmic aggresomes especially in the presence of ubiquitin conjugates, heat shock factors and links to hampered protein degradation, they are clearly different structures from cytoplasmic aggresomes (Latonen, 2011). Furthermore, inhibition of lysosomal proteases does not affect nucleolar aggresomes (Latonen et al., 2011; Salmina et al., 2017), indicating that nucleolar aggresome formation is separate from general protein degradation defects. Nucleolar aggresomes can, however, be released to the cytoplasm during mitosis and processed through the autophagocytosis pathway (Salmina et al., 2017). Nucleolar aggresomes can occur in several cell types, their prominence being greatest in normal diploid cells (Latonen et al., 2011). It is possible that the proliferative activity and transformation status of the cells affecting nucleolar activity and organization also affects formation of nucleolar aggresomes.

The roles and identities of the RNA components in nucleolar aggresomes remain to be investigated fully. Non-coding RNA transcribed from rDNA (IGS_{16}RNA, IGS_{22}RNA and IGS_{28}RNA) has been shown to recruit proteins to aggresomes upon hypoxia/acidosis and heat shock (Audas et al., 2012a; Jacob et al., 2012, 2013). Nucleolar aggresomes formed after proteasome inhibition contain polyA-tailed RNA, suggestive of either mRNA, lncRNA or both (Latonen et al., 2011). Due to lack of comprehensive extraction and sequencing studies, the full range of RNA species localized in nucleolar aggresomes is yet to be discovered.

While nucleolar aggresomes formed upon proteasome inhibition or protein overexpression have not yet been shown to be reversible, this has been reported for acidosis and heat shock-induced events (Audas et al., 2016). In addition, certain nucleolar aggresome-inducing stress events seem to inhibit rDNA transcription (Jacob et al., 2013) while others do not (Latonen et al., 2011). Thus, inhibition of rDNA transcription may not be necessary for nucleolar aggresomes to form, but a co-occuring or a following event under certain stress conditions.

Nucleolar Aggresomes and Neurodegeneration

The formation of nucleolar aggresomes in cultured cells resembles – and models – the situation in certain neurodegenerative disorders where proteins and RNA accumulate and aggregate to nuclei of cells, such as Huntington's disease (HD) and spinocerebellar ataxias (SCA). A hallmark of numerous neurodegenerative diseases is ubiquitin, SUMO- and RNA-containing inclusion bodies that link to expression of aggregation-prone mutant forms of disease-related proteins or RNA and to impairment of UPS (Dorval and Fraser, 2007; Lehman, 2009; Huang and Figueiredo-Pereira, 2010). The nuclear inclusions in HD *in vivo* resemble nucleolar aggresomes *in vitro*, although they localize adjacent to the nucleoli and not similarly within the nucleolus (Davies et al., 1997). Upon treatment of sensory ganglion neurons with proteasome inhibitors, and in motor neurons with severe dysfunction of proteostasis in a mouse SMA model, nuclear poly(A) RNA granules are formed frequently adjacent to the nucleolus, but not within it (Palanca et al., 2014; Narcís et al., 2018). These data may indicate differences in the *in vivo* vs. *in vitro* nucleolar state, as in post-replicative cells the nucleoli have adhered to a fully mature form. On the other hand, SUMO1-positive intranucleolar spots lacking nascent RNA and associated with a nucleolar reorganization of fibrillar centers have been found *in vivo* in motor neurons in the spinal muscular atrophy (SMA) (Tapia et al., 2017). Furthermore, nucleolar aggresomes have been shown to occur in *ex vivo* prostate tissue (Latonen et al., 2011) and in human breast and prostate cancer tissue (Audas et al., 2016).

Although the focus on the nucleoli with respect to neurodegeneration has been on effects of diseased mutants on ribosomal production and activity, several neurodegeneration relevant proteins have been shown to localize to nucleoli. A specific form of mutant Htt localizes to the nucleolus in mouse neuronal progenitor cells (Trettel et al., 2000). In addition, artificial β-sheet proteins known to form prefibrillar and fibrillar aggregates have been shown to accumulate

to nucleoli in cultured cells (Woerner et al., 2016). The most compelling *in vitro* evidence for nucleolar aggresome relevance for neurodegenerative disease exists for C9orf72. Expansion of the a GGGGCC hexanucleotide repeat in the first intron of this gene is the most common genetic alteration leading to hereditable amyotrophic lateral sclerosis (ALS). Glycine/arginine and proline/arginine repeats resulting from non-ATG translation of these repeats are recruited to nucleoli and hamper ribosome biogenesis, resulting in cell death (Kwon et al., 2014). Accumulating evidence shows that these dipeptide repeats locate to the GC where they phase-separate with NPM, disrupting nucleolar function (Haeusler et al., 2014; Lee et al., 2016; Lin et al., 2016). These repeats in fact interact with several IDR-containing proteins, many being RNA binding proteins (RBPs) and/or MLO proteins (Lee et al., 2016). While many repeat-expanded proteins accumulate to ribonucleoprotein (RNP) granules (Van Treeck and Parker, 2018), it is not clear what dictates accumulation of C9orf72 repeat peptides to nucleoli. Interestingly, the dipeptide repeats of C9orf72 have been shown to function as polyamines and promote intermolecular RNA-RNA interactions (Van Treeck et al., 2018). Although the functional significance of this in the toxicity of the mutant remains to be shown, it seems likely that these interactions affect the LLPS and/or nucleolar interactions of these peptides.

Nucleolar Aggresomes, Cancer and p53

In general, the nucleolus and interactions with nucleolar proteins and rRNA species is central in regulation of certain tumor suppressor and oncogene activities, the most recognized being p53 and c-myc, respectively (Ruggero and Pandolfi, 2003; Boisvert et al., 2007). As nucleolar aggresomes have been detected in human breast and prostate cancer tissues (Audas et al., 2016), and they can be induced by proteasome inhibition in *ex vivo* prostate tissue (Latonen et al., 2011), nucleolar aggresomes may also be relevant for cancer. Dozens of cancer-related nuclear factors can be targeted to nucleolar aggresomes (Latonen, 2011; Latonen et al., 2011). While some of these have implications in regulation of nucleolar activity and ribosome production, such as c-Myc (reviewed in Lindström and Latonen, 2013), most have no identified function in the nucleoli and are likely regulatory targets of the aggresomes under stress.

p53 was one of the first proteins showed to exhibit stress-responsive nucleolar localization (Klibanov et al., 2001; Xirodimas et al., 2001; Latonen et al., 2003). p53 is a tumor suppressor and the most often mutated gene in human cancers (Muller and Vousden, 2013), and it has several connections to nucleolar-related proteins such as NPM, ARF and MDM2 (Mayer and Grummt, 2005). p53 and p53-derived fragments have been shown to aggregate *in vitro* (Silva et al., 2014), and several p53 mutants have been found as amyloid aggregates in tumor cell lines (Xu et al., 2011) and breast cancer biopsies (Levy et al., 2011). These aggregates inactivate p53 by sequestering the protein, thus blocking its transcriptional activity and pro-apoptotic function (Xu et al., 2011). A cell-penetrating peptide, ReACp53, designed to inhibit p53 amyloid formation, rescues p53 function in cancer cell lines and in organoids derived from high-grade serous ovarian carcinomas (HGSOC) (Soragni et al., 2016).

Tumor suppressor p53 translocates to nucleolus upon treatment of cells by proteasome inhibitors in cultured cells and *ex vivo* tissue (reviewed in Latonen, 2011). In addition, the chemical compounds PRIMA1 and PRIMA-1MET have been reported to induce nucleolar translocation of p53 (Rökaeus et al., 2007; Russo et al., 2010), although contradicting evidence also exists (Rangel et al., 2019). PRIMA1 is a mutant p53 reactivating compound (Bykov et al., 2002) which has been shown to reactivate unfolded p53 mutants to native, functional conformation and, recently, to prevent mutant p53 aggregate accumulation in cancer cells (Rangel et al., 2019). Thus, PRIMA-1 can rescue amyloid state of mutant p53, which has implications for future cancer treatment strategies (Rangel et al., 2019).

Signals Behind Nucleolar Localization of Proteins

Signals in amino acid sequence that target proteins to the nucleolus are referred to as nucleolar localization signals (NoLS). They are arginine/lysine rich and range from seven to approximately 30 aa residues, but they are relatively rare and not a requirement for nucleolar localization. In fact, nucleolar localization of a protein is viewed to most often result from either direct or indirect interaction with nucleolar molecules, either rDNA, its transcripts, or protein components (reviewed in Emmott and Hiscox, 2009).

It is not clear what signals direct the localization and detention of extranucleolar proteins to nucleoli and nucleolar aggregates under stress. These likely depend on molecular interactions and involve changes in phase separation and transition balance due to presence of new molecules, but which specific molecules function in the seeding of the detention remain an open question for several conditions. Recently, using FUS family of proteins as an example it was shown that tyrosine residues in prion-like domains and arginine residues on RNA-binding domains govern the saturation concentration of phase separation (Wang J. et al., 2018). Interestingly, Mekhail et al. (2007) identified a common peptide motif in the proteins detained in the nucleoli during acidosis, including VHL, HSC70, RNF8 and cIAP2. This so called nucleolar detention signal regulated by H^+ ($NoDS^{H+}$) is different from the canonical nucleolar localization signal (NoLS) and is composed of an arginine motif combined to several hydrophobic repeats (Mekhail et al., 2007; Jacob et al., 2012). Up to 9% of all proteins harbor a NoDS, indicating that a substantial amount of the proteome may potentially be regulated in a similar fashion (Jacob et al., 2012). Thus, arginine rich motifs seem as a recurrent event in MLO and nucleolar targeting. The species of ncRNA expressed upon stress signals also have a role in recruiting the proteins to nucleolar aggresomes (discussed below), as specific RNAs, e.g., extended repetitive RNA motifs in clinical disorders, are capable of phase separation (Jain and Vale, 2017; Sawyer et al., 2018).

Post-translational modifications, especially ubiquitin family conjugates, may have a key role in localizing extranucleolar proteins to nucleolar aggresomes. In addition to ubiquitin and

SUMO found in the physiological disease-relevant inclusion bodies (as discussed above), the nucleolar aggresomes have revealed several family members to be relevant for nucleolar aggresomes. The structures contain conjugated ubiquitin, indicating that at least some of the accumulated proteins harbor this modification (Latonen et al., 2011). Especially interesting is the role of SUMO-proteins, which are found in INBs and nucleolar aggresomes (Hutten et al., 2011; Latonen et al., 2011; Souquere et al., 2015). UBC9, the E2 SUMO-conjugating enzyme is also located in INBs, it's depletion reduces INB size, and SUMO-1 mutant unable to conjugate proteins does not localize to INBs, indicating that SUMO conjugation is relevant for INB biology (Brun et al., 2017). Yet another ubiquitin homolog, NEDD8, was recently shown to localize to nucleolar aggresomes formed upon heat shock and proteasome inhibition (Maghames et al., 2018). Similarly to SUMO, this localization was linked to NEDD8 conjugation and even NEDD8/ubiquitin hybrid chain formation (Maghames et al., 2018). Thus it seems that nucleolar localization and aggregation of extranucleolar proteins is regulated by ubiquitin family of protein conjugation, requiring further investigation to understand the exact underlying mechanisms and functional consequences.

EMERGING ROLES OF NON-CODING TRANSCRIPTS IN THE NUCLEOLUS

The nucleolus is packed with non-coding RNA. After the 8S, 18S and 5.8S rRNAs have been transcribed by RNApolI and cleaved from their 47S precursor, they are post-transcriptionally modified through interaction with small nucleolar ribonucleoproteins (snoRNPs) and additional processing factors. For a long time, other rRNA sequences have been neglected as garbage sequences or non-specific degradation products. Recently, it has become clear that many non-coding RNA species in addition to the classical rRNA and snoRNA contribute to nucleolar biology. For example, rDNA is transcribed in antisense orientation to produce RNA contributing to epigenetic silencing of rDNA (Bierhoff et al., 2010).

Perhaps the most interesting resource of ncRNA in the rDNA sequence to be fully explored is the intergenic spacer (IGS). This sequence differs considerably from the rRNA coding sequences and has a high variability in nucleotide composition and length. Mayer et al. (2006) showed that some of these transcripts are required for establishing and maintaining a specific heterochomatic configuration at the promoter of a subset of rDNA arrays via NoRC, a chromatin remodeling complex. The transcripts here are 150–300 nt long and are complementary to the sequences in rDNA promoter (pRNA). During mid-S phase in the cell cycle, these pRNAs increase by 2-fold to repress rRNA synthesis in late replication (Santoro et al., 2010). Interestingly, the pRNA-dependent establishment of heterochromatin condensation of rRNA genes initiates highly condensed chromatin structures outside the nucleolus (Savic et al., 2014). This promotes transcriptional activation of differentiation genes, and is a mechanism shown to be inactivated in pluripotent embryonic stem cells (Savic et al., 2014). Thus, pRNA regulates chromatin plasticity and pluripotency.

Intergenic spacer also produces several stimuli-specific ncRNAs. Stress conditions such as heat shock and acidosis induce transcription of IGS to produce several transcripts shown to be involved in nucleolar aggresome formation, including IGS_{16}RNA, IGS_{22}RNA and IGS_{28}RNA (Audas et al., 2012b; Jacob et al., 2012, 2013). These transcripts are produced from stimuli-specific loci (Audas et al., 2012a). Whether there are more IGS transcripts that are relevant for protein detention in the nucleolus and nucleolar aggresome formation remains to be investigated.

Although most lncRNAs are processed like typical mRNAs to be 5′ capped and 3′ polyadenylated, other lncRNAs are stabilized by alternative mechanisms. One mechanism for this adaptation of snoRNA processing to produce snoRNA-ended lncRNAs (sno-lncRNAs) and 5′ snoRNA-ended and 3′-polyadenylated lncRNAs (SPAs). Some sno-lncRNAs and SPAs have been shown to be involved in the regulation of pre-rRNA transcription and alternative splicing of pre-mRNAs (Xing and Chen, 2018). For example, a box H/ACA small nucleolar RNA (snoRNA)-ended long non-coding RNA (lncRNA) was described to enhance pre-rRNA transcription (SLERT) (Xing et al., 2017). SLERT requires box H/ACA snoRNAs at both ends for its biogenesis and translocation to the nucleolus. SLERT interacts with DEAD-box RNA helicase DDX21 via a 143-nt non-snoRNA sequence, following which DDX21 forms ring-shaped structures surrounding multiple RNApolI complexes and suppresses pre-rRNA transcription (Xing et al., 2017).

In *C. elegans*, there was recently a new class of antisense ribosomal siRNAs (risiRNAs) identified that downregulate pre-rRNA through the nuclear RNAi pathway (Zhou et al., 2017). risiRNAs exhibit sequence characteristics similar to 22G RNA while being complementary to 18S and 26S rRNA. risiRNAs induce translocation of the nuclear Argonaute protein NRDE-3 from the cytoplasm to nucleus and nucleolus, in which the risiRNA/NRDE complex binds to pre-rRNA and silences rRNA expression. Interestingly, exposing *Caenorhabditis elegans* to cold shock or UV radiation, risiRNAs accumulate, turning on the nuclear RNAi-mediated gene silencing pathway (Zhou et al., 2017). Whether similar mechanisms exist in mammalian cells and contribute to nucleolar stress responses remains to be explored.

CONCLUDING REMARKS

It has become clear that, likely due to its phase separating propensities, the nucleolus can serve as a protective site for proteins following several environmental stimuli and stress signals. This detention may lead to formation of nucleolar aggresomes, and targets varying species of RNA and differential pools of proteins dependently on the cellular context and stress signal. What remains to be determined is the general mechanisms

that dictates these responses. The requirements for the phase transition steps are to be studied in detail, and surely more RNA effectors are to be found. Investigation of protein amino acid sequence signals, regulation by conjugation of ubiquitin protein family members, and interactions between RNA-protein and protein-protein domains promoting aggregation and amyloid formation in the nucleolus may enlighten the cellular and molecular routes to target in pathological nuclear aggregation.

AUTHOR CONTRIBUTIONS

The author confirms being the sole contributor of this work and has approved it for publication.

FUNDING

The work was supported by Finnish Academy (Grant No. 317871).

REFERENCES

Abella, N., Brun, S., Calvo, M., Tapia, O., Weber, J. D., Berciano, M. T., et al. (2010). Nucleolar disruption ensures nuclear accumulation of p21 upon DNA damage. *Traffic* 11, 743–755. doi: 10.1111/j.1600-0854.2010.01063.x

Andersen, J. S., Lam, Y. W., Leung, A. K., Ong, S. E., Lyon, C. E., Lamond, A. I., et al. (2005). Nucleolar proteome dynamics. *Nature* 433, 77–83. doi: 10.1038/nature03207

Audas, T. E., Audas, D. E., Jacob, M. D., Ho, J. J., Khacho, M., Wang, M., et al. (2016). Adaptation to stressors by systemic protein amyloidogenesis. *Dev. Cell* 39, 155–168. doi: 10.1016/j.devcel.2016.09.002

Audas, T. E., Jacob, M. D., and Lee, S. (2012a). Immobilization of proteins in the nucleolus by ribosomal intergenic spacer noncoding RNA. *Mol. Cell.* 45, 147–157. doi: 10.1016/j.molcel.2011.12.012

Audas, T. E., Jacob, M. D., and Lee, S. (2012b). The nucleolar detention pathway: a cellular strategy for regulating molecular networks. *Cell Cycle* 11, 2059–2062. doi: 10.4161/cc.20140

Bachant, J. B., and Elledge, S. J. (1999). Mitotic treasures in the nucleolus. *Nature* 398, 757–758. doi: 10.1038/19641

Bernardi, R., Scaglioni, P. P., Bergmann, S., Horn, H. F., Vousden, K. H., and Pandolfi, P. P. (2004). PML regulates p53 stability by sequestering Mdm2 to the nucleolus. *Nat. Cell Biol.* 6, 665–672. doi: 10.1038/ncb1147

Bierhoff, H., Schmitz, K., Maass, F., Ye, J., and Grummt, I. (2010). Noncoding transcripts in sense and antisense orientation regulate the epigenetic state of ribosomal RNA genes. *Cold. Spring Harb. Symp. Quant. Biol.* 75, 357–364. doi: 10.1101/sqb.2010.75.060

Boisvert, F. M., van Koningsbruggen, S., Navascués, J., and Lamond, A. I. (2007). The multifunctional nucleolus. *Nat. Rev. Mol. Cell Biol.* 8, 574–585. doi: 10.1038/nrm2184

Boke, E., Ruer, M., Wühr, M., Coughlin, M., Lemaitre, R., Gygi, S. P., et al. (2016). Amyloid-like self-assembly of a cellular compartment. *Cell* 166, 637–650. doi: 10.1016/j.cell.2016.06.051

Boulon, S., Westman, B. J., Hutten, S., Boisvert, F. M., and Lamond, A. I. (2010). The nucleolus under stress. *Mol. Cell* 40, 216–227. doi: 10.1016/j.molcel.2010.09.024

Brangwynne, C. P., Mitchison, T. J., and Hyman, A. A. (2011). Active liquid-like behavior of nucleoli determines their size and shape in Xenopus laevis oocytes. *Proc. Natl. Acad. Sci. U.S.A.* 108, 4334–4339. doi: 10.1073/pnas.1017150108

Brun, S., Abella, N., Berciano, M. T., Tapia, O., Jaumot, M., Freire, R., et al. (2017). SUMO regulates p21Cip1 intracellular distribution and with p21Cip1 facilitates multiprotein complex formation in the nucleolus upon DNA damage. *PLoS One* 12:e0178925. doi: 10.1371/journal.pone.0178925

Buchwalter, A., and Hetzer, M. W. (2017). Nucleolar expansion and elevated protein translation in premature aging. *Nat. Commun.* 8:328. doi: 10.1038/s41467-017-00322-z

Bykov, V. J. N., Issaeva, N., Shilov, A., Hultcrantz, M., Pugacheva, E., Chumakov, P., et al. (2002). Restoration of the tumor suppressor function to mutant p53 by a low-molecular-weight compound. *Nat. Med.* 8, 282–288. doi: 10.1038/nm0302-282

Davies, S. W., Turmaine, M., Cozens, B. A., DiFiglia, M., Sharp, A. H., Ross, C. A., et al. (1997). Formation of neuronal intranuclear inclusions underlies the neurological dysfunction in mice transgenic for the HD mutation. *Cell* 90, 537–548. doi: 10.1016/s0092-8674(00)80513-9

Dorval, V., and Fraser, P. E. (2007). SUMO on the road to neurodegeneration. *Biochim. Biophys. Acta* 1773, 694–706. doi: 10.1016/j.bbamcr.2007.03.017

Dousset, T., Wang, C., Verheggen, C., Chen, D., Hernandez-Verdun, D., and Huang, S. (2000). Initiation of nucleolar assembly is independent of RNA polymerase I transcription. *Mol. Biol. Cell* 11, 2705–2717. doi: 10.1091/mbc.11.8.2705

Emmott, E., and Hiscox, J. A. (2009). Nucleolar targeting: the hub of the matter. *EMBO Rep.* 10, 231–238. doi: 10.1038/embor.2009.14

Feric, M., Vaidya, N., Harmon, T. S., Mitrea, D. M., Zhu, L., Richardson, T. M., et al. (2016). Coexisting liquid phases underlie nucleolar subcompartments. *Cell* 165, 1686–1697. doi: 10.1016/j.cell.2016.04.047

Floutsakou, I., Agrawal, S., Nguyen, T. T., Seoighe, C., Ganley, A. R., and McStay, B. (2013). The shared genomic architecture of human nucleolar organizer regions. *Genome Res.* 23, 2003–2012. doi: 10.1101/gr.157941.113

Goldstein, M., and Kastan, M. B. (2015). The DNA damage response: implications for tumor responses to radiation and chemotherapy. *Annu. Rev. Med.* 66, 129–143. doi: 10.1146/annurev-med-081313-121208

Grummt, I. (2013). The nucleolus—guardian of cellular homeostasis and genome integrity. *Chromosoma* 122, 487–497. doi: 10.1007/s00412-013-0430-0

Haeusler, A. R., Donnelly, C. J., Periz, G., Simko, E. A., Shaw, P. G., Kim, M. S., et al. (2014). C9orf72 nucleotide repeat structures initiate molecular cascades of disease. *Nature* 507, 195–200. doi: 10.1038/nature13124

Handwerger, K. E., and Gall, J. G. (2006). Subnuclear organelles: new insights into form and function. *Trends Cell Biol.* 16, 19–26. doi: 10.1016/j.tcb.2005.11.005

Hernandez-Verdun, D. (2006). Nucleolus: from structure to dynamics. *Histochem. Cell Biol.* 125, 127–137. doi: 10.1007/s00418-005-0046-4

Hernandez-Verdun, D. (2011). Assembly and disassembly of the nucleolus during the cell cycle. *Nucleus* 2, 189–194. doi: 10.4161/nucl.2.3.16246

Huang, Q., and Figueiredo-Pereira, M. E. (2010). Ubiquitin/proteasome pathway impairment in neurodegeneration: therapeutic implications. *Apoptosis* 15, 1292–1311. doi: 10.1007/s10495-010-0466-z

Hutten, S., Prescott, A., James, J., Riesenberg, S., Boulon, S., Lam, Y. W., et al. (2011). An intranucleolar body associated with rDNA. *Chromosoma* 120, 481–499. doi: 10.1007/s00412-011-0327-8

Jacob, M. D., Audas, T. E., Mullineux, S. T., and Lee, S. (2012). Where no RNA polymerase has gone before: novel functional transcripts derived from the ribosomal intergenic spacer. *Nucleus* 3, 315–319. doi: 10.4161/nucl.20585

Jacob, M. D., Audas, T. E., Uniacke, J., Trinkle-Mulcahy, L., and Lee, S. (2013). Environmental cues induce a long noncoding RNA-dependent remodeling of the nucleolus. *Mol. Biol. Cell* 24, 2943–2953. doi: 10.1091/mbc.E13-04-0223

Jain, A., and Vale, R. D. (2017). RNA phase transitions in repeat expansion disorders. *Nature* 546, 243–247. doi: 10.1038/nature22386

Klibanov, S. A., O'Hagan, H. M., and Ljungman, M. (2001). Accumulation of soluble and nucleolar-associated p53 proteins following cellular stress. *J. Cell Sci.* 114, 1867–1873.

Kurki, S., Peltonen, K., Latonen, L., Kiviharju, T. M., Ojala, P. M., Meek, D., et al. (2004). Nucleolar protein NPM interacts with HDM2 and protects tumor suppressor protein p53 from HDM2-mediated degradation. *Cancer Cell* 5, 465–475. doi: 10.1016/s1535-6108(04)00110-2

Kwon, I., Xiang, S., Kato, M., Wu, L., Theodoropoulos, P., Wang, T., et al. (2014). Poly-dipeptides encoded by the C9orf72 repeats bind nucleoli, impede RNA biogenesis, and kill cells. *Science* 345, 1139–1145. doi: 10.1126/science.1254917

Laiho, M., and Latonen, L. (2003). Cell cycle control, DNA damage checkpoints and cancer. *Ann. Med.* 35, 391–397. doi: 10.1080/07853890310014605

Latonen, L. (2011). Nucleolar aggresomes as counterparts of cytoplasmic aggresomes in proteotoxic stress. Proteasome inhibitors induce nuclear ribonucleoprotein inclusions that accumulate several key factors

of neurodegenerative diseases and cancer. *Bioessays* 33, 386–395. doi: 10.1002/bies.201100008

Latonen, L., Kurki, S., Pitkänen, K., and Laiho, M. (2003). p53 and MDM2 are regulated by PI-3-kinases on multiple levels under stress induced by UV radiation and proteasome dysfunction. *Cell. Signal.* 15, 95–102. doi: 10.1016/s0898-6568(02)00044-x

Latonen, L., Moore, H. M., Bai, B., Jäämaa, S., and Laiho, M. (2011). Proteasome inhibitors induce nucleolar aggregation of proteasome target proteins and polyadenylated RNA by altering ubiquitin availability. *Oncogene* 30, 790–805. doi: 10.1038/onc.2010.469

Lee, K. H., Zhang, P., Kim, H. J., Mitrea, D. M., Sarkar, M., Freibaum, B. D., et al. (2016). C9orf72 dipeptide repeats impair the assembly, dynamics, and function of membrane-less organelles. *Cell* 167:774–788.e17. doi: 10.1016/j.cell.2016.10.002

Lehman, N. L. (2009). The ubiquitin proteasome system in neuropathology. *Acta Neuropathol.* 118, 329–347. doi: 10.1007/s00401-009-0560-x

Leung, A. K., and Lamond, A. I. (2003). The dynamics of the nucleolus. *Crit. Rev. Eukaryot. Gene Expr.* 13, 39–54.

Levy, C. B., Stumbo, A. C., Ano Bom, A. P., Portari, E. A., Cordeiro, Y., Silva, J. L., et al. (2011). Co-localization of mutant p53 and amyloid-like protein aggregates in breast tumors. *Int. J. Biochem. Cell Biol.* 43, 60–64. doi: 10.1016/j.biocel.2010.10.017

Lin, Y., Mori, E., Kato, M., Xiang, S., Wu, L., Kwon, I., et al. (2016). Toxic PR poly-dipeptides encoded by the C9orf72 repeat expansion target LC domain polymers. *Cell* 167:789–802.e12. doi: 10.1016/j.cell.2016.10.003

Lindström, M. S., and Latonen, L. (2013). "The nucleolus as a stress response organelle," in *Proteins of the Nucleolus. Regulation, Translocation and Biomedical Functions*, eds D. H. O'Day and A. Catalano (Berlin: Springer), 251–273. doi: 10.1007/978-94-007-5818-6_11

Lohrum, M. A., Ludwig, R. L., Kubbutat, M. H., Hanlon, M., and Vousden, K. H. (2003). Regulation of HDM2 activity by the ribosomal protein L11. *Cancer Cell* 3, 577–587. doi: 10.1016/s1535-6108(03)00134-x

Louvet, E., Junéra, H. R., Le Panse, S., and Hernandez-Verdun, D. (2005). Dynamics and compartmentation of the nucleolar processing machinery. *Exp. Cell Res.* 304, 457–470. doi: 10.1016/j.yexcr.2004.11.018

Louvet, E., Yoshida, A., Kumeta, M., and Takeyasu, K. (2014). Probing the stiffness of isolated nucleoli by atomic force microscopy. *Histochem. Cell Biol.* 141, 365–381. doi: 10.1007/s00418-013-1167-9

Lyons, S. M., and Anderson, P. (2016). RNA-seeded functional amyloids balance growth and survival. *Dev. Cell* 39, 131–132. doi: 10.1016/j.devcel.2016.10.005

Maghames, C. M., Lobato-Gil, S., Perrin, A., Trauchessec, H., Rodriguez, M. S., Urbach, S., et al. (2018). NEDDylation promotes nuclear protein aggregation and protects the ubiquitin proteasome system upon proteotoxic stress. *Nat. Commun.* 9:4376. doi: 10.1038/s41467-018-06365-0

Mangan, H., Gailín, M. Ó., and McStay, B. (2017). Integrating the genomic architecture of human nucleolar organizer regions with the biophysical properties of nucleoli. *FEBS J.* 284, 3977–3985. doi: 10.1111/febs.14108

Martin, C., Chen, S., Maya-Mendoza, A., Lovric, J., Sims, P. F., and Jackson, D. A. (2009). Lamin B1 maintains the functional plasticity of nucleoli. *J. Cell Sci.* 122, 1551–1562. doi: 10.1242/jcs.046284

Matsumoto, A., Sakamoto, C., Matsumori, H., Katahira, J., Yasuda, Y., Yoshidome, K., et al. (2016). Loss of the integral nuclear envelope protein SUN1 induces alteration of nucleoli. *Nucleus* 7, 68–83. doi: 10.1080/19491034.2016.1149664

Mattsson, K., Pokrovskaja, K., Kiss, C., Klein, G., and Szekely, L. (2001). Proteins associated with the promyelocytic leukemia gene product (PML)-containing nuclear body move to the nucleolus upon inhibition of proteasome-dependent protein degradation. *Proc. Natl. Acad. Sci. U.S.A.* 98, 1012–1017. doi: 10.1073/pnas.031566998

Mayer, C., and Grummt, I. (2005). Cellular stress and nucleolar function. *Cell Cycle* 4, 1036–1038. doi: 10.4161/cc.4.8.1925

Mayer, C., Schmitz, K. M., Li, J., Grummt, I., and Santoro, R. (2006). Intergenic transcripts regulate the epigenetic state of rRNA genes. *Mol. Cell* 22, 351–361. doi: 10.1016/j.molcel.2006.03.028

McStay, B. (2016). Nucleolar organizer regions: genomic 'dark matter' requiring illumination. *Genes Dev.* 30, 1598–1610. doi: 10.1101/gad.283838.116

Mekhail, K., Gunaratnam, L., Bonicalzi, M. E., and Lee, S. (2004a). HIF activation by pH-dependent nucleolar sequestration of VHL. *Nat. Cell Biol.* 6, 642–647. doi: 10.1038/ncb1144

Mekhail, K., Khacho, M., Gunaratnam, L., and Lee, S. (2004b). Oxygen sensing by H+: implications for HIF and hypoxic cell memory. *Cell Cycle* 3, 1027–1029.

Mekhail, K., Khacho, M., Carrigan, A., Hache, R. R., Gunaratnam, L., and Lee, S. (2005). Regulation of ubiquitin ligase dynamics by the nucleolus. *J. Cell Biol.* 170, 733–744. doi: 10.1083/jcb.200506030

Mekhail, K., Rivero-Lopez, L., Al-Masri, A., Brandon, C., Khacho, M., and Lee, S. (2007). Identification of a common subnuclear localization signal. *Mol. Biol. Cell* 18, 3966–3977. doi: 10.1091/mbc.e07-03-0295

Mekhail, K., Rivero-Lopez, L., Khacho, M., and Lee, S. (2006). Restriction of rRNA synthesis by VHL maintains energy equilibrium under hypoxia. *Cell Cycle* 5, 2401–2413. doi: 10.4161/cc.5.20.3387

Mitrea, D. M., Cika, J. A., Stanley, C. B., Nourse, A., Onuchic, P. L., Banerjee, P. R., et al. (2018). Self-interaction of NPM1 modulates multiple mechanisms of liquid-liquid phase separation. *Nat. Commun.* 9:842. doi: 10.1038/s41467-018-03255-3

Moore, H. M., Bai, B., Boisvert, F. M., Latonen, L., Rantanen, V., Simpson, J. C., et al. (2011). Quantitative proteomics and dynamic imaging of the nucleolus reveal distinct responses to UV and ionizing radiation. *Mol. Cell. Proteomics* 10:M111.009241. doi: 10.1074/mcp.M111.009241

Muller, P. A., and Vousden, K. H. (2013). p53 mutations in cancer. *Nat. Cell Biol.* 15, 2–8.

Narcís, J. O., Tapia, O., Tarabal, O., Piedrafita, L., Calderó, J., Berciano, M. T., et al. (2018). Accumulation of poly(A) RNA in nuclear granules enriched in Sam68 in motor neurons from the SMNΔ7 mouse model of SMA. *Sci. Rep.* 8:9646. doi: 10.1038/s41598-018-27821-3

Palanca, A., Casafont, I., Berciano, M. T., and Lafarga, M. (2014). Reactive nucleolar and Cajal body responses to proteasome inhibition in sensory ganglion neurons. *Biochim. Biophys. Acta* 1842, 848–859. doi: 10.1016/j.bbadis.2013.11.016

Puvion-Dutilleul, F., Mazan, S., Nicoloso, M., Pichard, E., Bachellerie, J. P., and Puvion, E. (1992). Alterations of nucleolar ultrastructure and ribosome biogenesis by actinomycin D. Implications for *U3* snRNP function. *Eur. J. Cell Biol.* 58, 149–162.

Rangel, L. P., Ferretti, G. D. S., Costa, C. L., Andrade, S. M. M. V., Carvalho, R. S., Costa, D. C. F., et al. (2019). p53 reactivation with induction of massive apoptosis-1 (PRIMA-1) inhibits amyloid aggregation of mutant p53 in cancer cells. *J. Biol. Chem.* 294, 3670–3682. doi: 10.1074/jbc.RA118.004671

Rökaeus, N., Klein, G., Wiman, K. G., Szekely, L., and Mattsson, K. (2007). PRIMA-1(MET) induces nucleolar accumulation of mutant p53 and PML nuclear body-associated proteins. *Oncogene* 26, 982–992. doi: 10.1038/sj.onc.1209858

Ruggero, D., and Pandolfi, P. P. (2003). Does the ribosome translate cancer? *Nat. Rev. Cancer* 3, 179–192. doi: 10.1038/nrc1015

Russo, D., Ottaggio, L., Penna, I., Foggetti, G., Fronza, G., Inga, A., et al. (2010). PRIMA-1 cytotoxicity correlates with nucleolar localization and degradation of mutant p53 in breast cancer cells. *Biochem. Biophys. Res. Commun.* 402, 345–350. doi: 10.1016/j.bbrc.2010.10.031

Salmina, K., Huna, A., Inashkina, I., Belyayev, A., Krigerts, J., Pastova, L., et al. (2017). Nucleolar aggresomes mediate release of pericentric heterochromatin and nuclear destruction of genotoxically treated cancer cells. *Nucleus* 8, 205–221. doi: 10.1080/19491034.2017.1279775

Santoro, R., Schmitz, K. M., Sandoval, J., and Grummt, I. (2010). Intergenic transcripts originating from a subclass of ribosomal DNA repeats silence ribosomal RNA genes in trans. *EMBO Rep.* 11, 52–58. doi: 10.1038/embor.2009.254

Savic, N., Bär, D., Leone, S., Frommel, S. C., Weber, F. A., Vollenweider, E., et al. (2014). lncRNA maturation to initiate heterochromatin formation in the nucleolus is required for exit from pluripotency in ESCs. *Cell Stem Cell.* 15, 720–734. doi: 10.1016/j.stem.2014.10.005

Sawyer, I. A., Sturgill, D., and Dundr, M. (2018). Membraneless nuclear organelles and the search for phases within phases. *Wiley Interdiscip Rev. RNA* 25:e1514. doi: 10.1002/wrna.1514

Sen Gupta, A., and Sengupta, K. (2017). Lamin B2 modulates nucleolar morphology, dynamics, and function. *Mol. Cell. Biol.* 37:e274-17. doi: 10.1128/MCB.00274-17

Shin, Y., and Brangwynne, C. P. (2017). Liquid phase condensation in cell physiology and disease. *Science* 357:eaaf4382. doi: 10.1126/science.aaf4382

Shou, W., Seol, J. H., Shevchenko, A., Baskerville, C., Moazed, D., Chen, Z. W., et al. (1999). Exit from mitosis is triggered by Tem1-dependent release of the

protein phosphatase Cdc14 from nucleolar RENT complex. *Cell* 97, 233–244. doi: 10.1016/s0092-8674(00)80733-3

Silva, J. L., De Moura Gallo, C. V., Costa, D. C., and Rangel, L. P. (2014). Prion-like aggregation of mutant p53 in cancer. *Trends Biochem. Sci.* 39, 260–267. doi: 10.1016/j.tibs.2014.04.001

Sirri, V., Urcuqui-Inchima, S., Roussel, P., and Hernandez-Verdun, D. (2008). Nucleolus: the fascinating nuclear body. *Histochem. Cell Biol.* 129, 13–31. doi: 10.1007/s00418-007-0359-6

Soragni, A., Janzen, D. M., Johnson, L. M., Lindgren, A. G., Thai-Quynh Nguyen, A., Tiourin, E., et al. (2016). A designed inhibitor of p53 aggregation rescues p53 tumor suppression in ovarian carcinomas. *Cancer Cell* 29, 90–103. doi: 10.1016/j.ccell.2015.12.002

Souquere, S., Weil, D., and Pierron, G. (2015). Comparative ultrastructure of CRM1-Nucleolar bodies (CNoBs), Intranucleolar bodies (INBs) and hybrid PML/p62 bodies uncovers new facets of nuclear body dynamic and diversity. *Nucleus* 6, 326–338. doi: 10.1080/19491034.2015.1082695

Tapia, O., Narcís, J. O., Riancho, J., Tarabal, O., Piedrafita, L., Calderó, J., et al. (2017). Cellular bases of the RNA metabolism dysfunction in motor neurons of a murine model of spinal muscular atrophy: role of Cajal bodies and the nucleolus. *Neurobiol. Dis.* 108, 83–99. doi: 10.1016/j.nbd.2017.08.004

Thiry, M., and Lafontaine, D. L. (2005). Birth of a nucleolus: the evolution of nucleolar compartments. *Trends Cell Biol.* 15, 194–199. doi: 10.1016/j.tcb.2005.02.007

Trettel, F., Rigamonti, D., Hilditch-Maguire, P., Wheeler, V. C., Sharp, A. H., Persichetti, F., et al. (2000). Dominant phenotypes produced by the HD mutation in STHdh(Q111) striatal cells. *Hum. Mol. Genet.* 9, 2799–2809. doi: 10.1093/hmg/9.19.2799

Van Treeck, B., and Parker, R. (2018). Emerging roles for intermolecular RNA-RNA interactions in RNP assemblies. *Cell* 174, 791–802. doi: 10.1016/j.cell.2018.07.023

Van Treeck, B., Protter, D. S. W., Matheny, T., Khong, A., Link, C. D., and Parker, R. (2018). RNA self-assembly contributes to stress granule formation and defining the stress granule transcriptome. *Proc. Natl. Acad. Sci. U.S.A.* 115, 2734–2739. doi: 10.1073/pnas.1800038115

Vilotti, S., Biagioli, M., Foti, R., Dal Ferro, M., Lavina, Z. S., Collavin, L., et al. (2012). The PML nuclear bodies-associated protein TTRAP regulates ribosome biogenesis in nucleolar cavities upon proteasome inhibition. *Cell Death Differ.* 19, 488–500. doi: 10.1038/cdd.2011.118

Visintin, R., Hwang, E. S., and Amon, A. (1999). Cfi1 prevents premature exit from mitosis by anchoring Cdc14 phosphatase in the nucleolus. *Nature* 398, 818–823. doi: 10.1038/19775

Wang, J., Choi, J. M., Holehouse, A. S., Lee, H. O., Zhang, X., Jahnel, M., et al. (2018). A molecular grammar governing the driving forces for phase separation of prion-like RNA binding proteins. *Cell* 174:688–699.e16. doi: 10.1016/j.cell.2018.06.006

Wang, M., Tao, X., Jacob, M. D., Bennett, C. A., Ho, J. J. D., Gonzalgo, M. L., et al. (2018). Stress-induced low complexity RNA activates physiological amyloidogenesis. *Cell Rep.* 24, 1713–1721.e4. doi: 10.1016/j.celrep.2018.07.040

Weber, J. D., Taylor, L. J., Roussel, M. F., Sherr, C. J., and Bar-Sagi, D. (1999). Nucleolar Arf sequesters Mdm2 and activates p53. *Nat. Cell Biol.* 1, 20–26. doi: 10.1038/8991

Woerner, A. C., Frottin, F., Hornburg, D., Feng, L. R., Meissner, F., Patra, M., et al. (2016). Cytoplasmic protein aggregates interfere with nucleocytoplasmic transport of protein and RNA. *Science* 351, 173–176. doi: 10.1126/science.aad2033

Wong, J. M., Kusdra, L., and Collins, K. (2002). Subnuclear shuttling of human telomerase induced by transformation and DNA damage. *Nat. Cell Biol.* 4, 731–736. doi: 10.1038/ncb846

Woodruff, J. B., Hyman, A. A., and Boke, E. (2018). Organization and function of non-dynamic biomolecular condensates. *Trends Biochem. Sci.* 43, 81–94. doi: 10.1016/j.tibs.2017.11.005

Xing, Y. H., and Chen, L. L. (2018). Processing and roles of snoRNA-ended long noncoding RNAs. *Crit Rev Biochem Mol Biol.* 25, 1–11. doi: 10.1080/10409238.2018.1508411

Xing, Y. H., Yao, R. W., Zhang, Y., Guo, C. J., Jiang, S., Xu, G., et al. (2017). SLERT regulates DDX21 rings associated with Pol I transcription. *Cell* 169:664–678.e16. doi: 10.1016/j.cell.2017.04.011

Xirodimas, D., Saville, M. K., Edling, C., Lane, D. P., and Laín, S. (2001). Different effects of p14ARF on the levels of ubiquitinated p53 and Mdm2 *in vivo*. *Oncogene* 20, 4972–4983. doi: 10.1038/sj.onc.1204656

Xu, J., Reumers, J., Couceiro, J. R., De Smet, F., Gallardo, R., Rudyak, S., et al. (2011). Gain of function of mutant p53 by coaggregation with multiple tumor suppressors. *Nat. Chem. Biol.* 7, 285–295. doi: 10.1038/nchembio.546

Zhang, Y., and Lu, H. (2009). Signaling to p53: ribosomal proteins find their way. *Cancer Cell* 16, 369–377. doi: 10.1016/j.ccr.2009.09.024

Zhou, X., Chen, X., Wang, Y., Feng, X., and Guang, S. (2017). A new layer of rRNA regulation by small interference RNAs and the nuclear RNAi pathway. *RNA Biol.* 14, 1492–1498. doi: 10.1080/15476286.2017.1341034

Conflict of Interest Statement: The author declares that the research was conducted in the absence of any commercial or financial relationships that could be construed as a potential conflict of interest.

frontiers in Cellular Neuroscience

REVIEW
published: 30 April 2019
doi: 10.3389/fncel.2019.00156

Emerging Role of the Nucleolar Stress Response in Autophagy

*Astrid S. Pfister**

Institute of Biochemistry and Molecular Biology, Faculty of Medicine, Ulm University, Ulm, Germany

Autophagy represents a conserved self-digestion program, which allows regulated degradation of cellular material. Autophagy is activated by cellular stress, serum starvation and nutrient deprivation. Several autophagic pathways have been uncovered, which either non-selectively or selectively target the cellular cargo for lysosomal degradation. Autophagy engages the coordinated action of various key regulators involved in the steps of autophagosome formation, cargo targeting and lysosomal fusion. While non-selective (macro)autophagy is required for removal of bulk material or recycling of nutrients, selective autophagy mediates specific targeting of damaged organelles or protein aggregates. By proper action of the autophagic machinery, cellular homeostasis is maintained. In contrast, failure of this fundamental process is accompanied by severe pathophysiological conditions. Hallmarks of neuropathological disorders are for instance accumulated, mis-folded protein aggregates and damaged mitochondria. The nucleolus has been recognized as central hub in the cellular stress response. It represents a sub-nuclear organelle essential for ribosome biogenesis and also functions as stress sensor by mediating cell cycle arrest or apoptosis. Thus, proper nucleolar function is mandatory for cell growth and survival. Here, I highlight the emerging role of nucleolar factors in the regulation of autophagy. Moreover, I discuss the nucleolar stress response as a novel signaling pathway in the context of autophagy, health and disease.

Keywords: ribosome biogenesis, rRNA processing, nucleoli, nucleolar stress, autophagy, neuron, mitochondria, aggregates

OPEN ACCESS

Edited by:
Kerry Lee Tucker,
University of New England,
United States

Reviewed by:
Cláudia Pereira,
University of Coimbra, Portugal
Grzegorz Kreiner,
Polish Academy of Sciences, Poland

***Correspondence:**
Astrid S. Pfister
astrid.pfister@uni-ulm.de

Specialty section:
This article was submitted to Cellular Neurophysiology, a section of the journal Frontiers in Cellular Neuroscience

Received: *21 December 2018*
Accepted: *08 April 2019*
Published: *30 April 2019*

Citation:
Pfister AS (2019) Emerging Role of the Nucleolar Stress Response in Autophagy. Front. Cell. Neurosci. 13:156. doi: 10.3389/fncel.2019.00156

INTRODUCTION

Various high quality reviews are available on principles of ribosome biogenesis, nucleolar stress, apoptosis and autophagy, respectively. Given their essential role, it is well accepted that a mis-regulation of each is tightly linked to pathogenic conditions (Levine and Kroemer, 2008; Boulon et al., 2010; Freed et al., 2010; Ghavami et al., 2014; Schneider and Cuervo, 2014). In this review, the emerging connection of nucleolar stress to autophagic processes serves as a basis to discuss novel concepts and cure of diseases connected to nucleolar stress.

The Nucleolus as a Stress Sensor

The Nucleolus: Place for Ribosome Biogenesis

Nucleoli represent membrane-free, sub-nuclear compartments, where transcription and processing of rRNA takes place. Nucleoli can be considered as an assembly platform. They host several hundreds of essential rRNA binding and processing factors, which are involved in the highly complex process of ribosome biogenesis. Nucleoli form around repetitive rDNA clusters in a dynamic and cell cycle-dependent manner during G1 phase (Potmesil and Goldfeder, 1977; Mangan et al., 2017).

The rDNA clusters are transcribed into their respective large precursor rRNA by RNA polymerase I (RNA pol I); RNA polymerases II and III are as well essential for ribosome biogenesis, by driving the expression of ribosomal proteins (RNA pol II) and 5S rRNA (RNA pol III) (Eichler and Craig, 1994; Fatica and Tollervey, 2002). The complex mechanism of pre-rRNA processing involves the action of a multitude of ribosome biogenesis factors. These are assembled in pre-ribosomal complexes involved in cleavage and chemical modification of the maturating transcript (Fatica and Tollervey, 2002; Granneman and Baserga, 2004; Mullineux and Lafontaine, 2012).

The nucleolar size correlates with the rRNA transcription, cell growth and the metabolic rate of a cell (Boulon et al., 2010). Importantly, nucleolar size and function is changed during aging (Tiku et al., 2016; Buchwalter and Hetzer, 2017; Zlotorynski, 2017). Thus, the nucleolus emerges as critical regulator of cellular aging (Tiku and Antebi, 2018).

Large amounts of ribosomes are especially needed in highly proliferating cells, such as during embryonic development or cancer (Montanaro et al., 2008). Therefore, a lack of functional ribosomes impairs cellular growth and survival and is incompatible with life.

The Nucleolar Stress Response

Nucleoli are highly dynamic structures, closely connected to growth and survival (Mangan et al., 2017). The nucleolus is being recognized as a key hub in the cellular stress response by sensing and reacting to various stimuli.

Perturbation of the nucleolar structure and/or function ultimately impairs ribosome biogenesis and triggers the so-called nucleolar stress response (Boulon et al., 2010). A key mechanism involves the release of ribosomal proteins (RPs) from the nucleoli into the nucleoplasm. As a consequence of nucleoplasmic RP accumulation, the E3-ubiquitin ligase MDM2 is inhibited (Dai et al., 2004). MDM2 keeps the levels of the tumor suppressor protein p53 low by earmarking p53 for proteasomal degradation. Upon nucleolar stress, RPs are released and inhibit MDM2, which results in p53 accumulation. Finally, stabilized p53 induces cell cycle arrest and/or apoptosis (Pestov et al., 2001; Rubbi and Milner, 2003; Yuan et al., 2005; Fumagalli et al., 2012). The nucleolar stress response is further connected to the induction of senescence and DNA damage, by commonly engaging the classical p53 pathway (Rubbi and Milner, 2003; Lindstrom et al., 2018). A simplified model of the classical p53 nucleolar stress response is given in **Figure 1**.

More recently, novel pathways have been added to the increasing list, which demonstrate that nucleolar stress can also be propagated in the absence of functional p53 (Holmberg Olausson et al., 2012; James et al., 2014; Lindstrom et al., 2018).

In summary, nucleolar integrity reflects a general prerequisite for normal cellular function. Given that many tumor types are characterized by inactivation of p53, p53-independent pathways open novel avenues toward more customized anti-cancer therapies (Burger and Eick, 2013).

Autophagy Pathways

Macroautophagy

(Macro)autophagy is essential for cellular homeostasis by mediating destruction and recycling of bulk cytoplasmic material, defective organelles or proteins via lysosomal degradation (Mizushima, 2007; Marx, 2015). A mis-regulation of autophagy is tightly linked to the formation of diverse pathological conditions (Levine and Kroemer, 2008; Jiang and Mizushima, 2014; Schneider and Cuervo, 2014).

Autophagy can be induced by various cellular stresses, such as lack of nutrients, low energy or oxidative stress. As an upstream signaling pathway the conserved mTOR pathway plays an influential role in the regulation of autophagy (see section "mTOR Signaling Couples Autophagy and Ribosome Biogenesis") (Pattingre et al., 2008).

A central structure implicated in the process of (macro)autophagy is the double-membranous autophagosome, which mediates cellular cargo sequestration. Autophagy-related proteins (ATGs) govern autophagosome formation at different levels. Beclin1, the mammalian homologue of yeast Atg6, is mandatory for the initial steps of autophagosome formation (Pattingre et al., 2008). Originally, Beclin1 has been identified as an interaction partner of the anti-apoptotic factor Bcl-2 (B cell lymphoma 2) (Liang et al., 1998). Beclin1 is part of phosphoinoside 3 kinase (PI3K) complexes and functions in diverse membrane trafficking processes (Levine et al., 2015). Furthermore, Beclin1 interacts with kinases, de-/ubiquitinating enzymes and multiple other factors, among them p53 (Levine et al., 2015). Certain ATGs are necessary for the engulfment of cargo destined for lysosomal degradation in the autolysosome. Members of the Atg8 protein family are directly conjugated to the autophagosomal membrane by phosphaditylinositol lipidation. Hence, Atg8/LC3 (light chain 3) represents a key marker of autophagosomes. Atg8/LC3s are essential for autophagosome maturation and cargo sequestration. They can be sub-divided into LC3 and GABARAP proteins and fulfill critical tasks (Nguyen et al., 2016).

Note that intracellular Atg8/LC3-positive autophagosome accumulation is central for autophagy flux induction as well as inhibition. Opposing mechanisms result in the accumulation of autophagosomes, thereby requiring careful interpretation of experimental results. An increased rate of autophagosome formation (increase of autophagic flux), as well as decreased autophagosome clearance in the lysosome (impaired autophagic flux), resembles autophagosome accumulation under basal conditions. Thus, care has to be taken when interpreting results on "active" or "inhibited" autophagy. Meanwhile, several excellent reviews are available, which help to unravel these

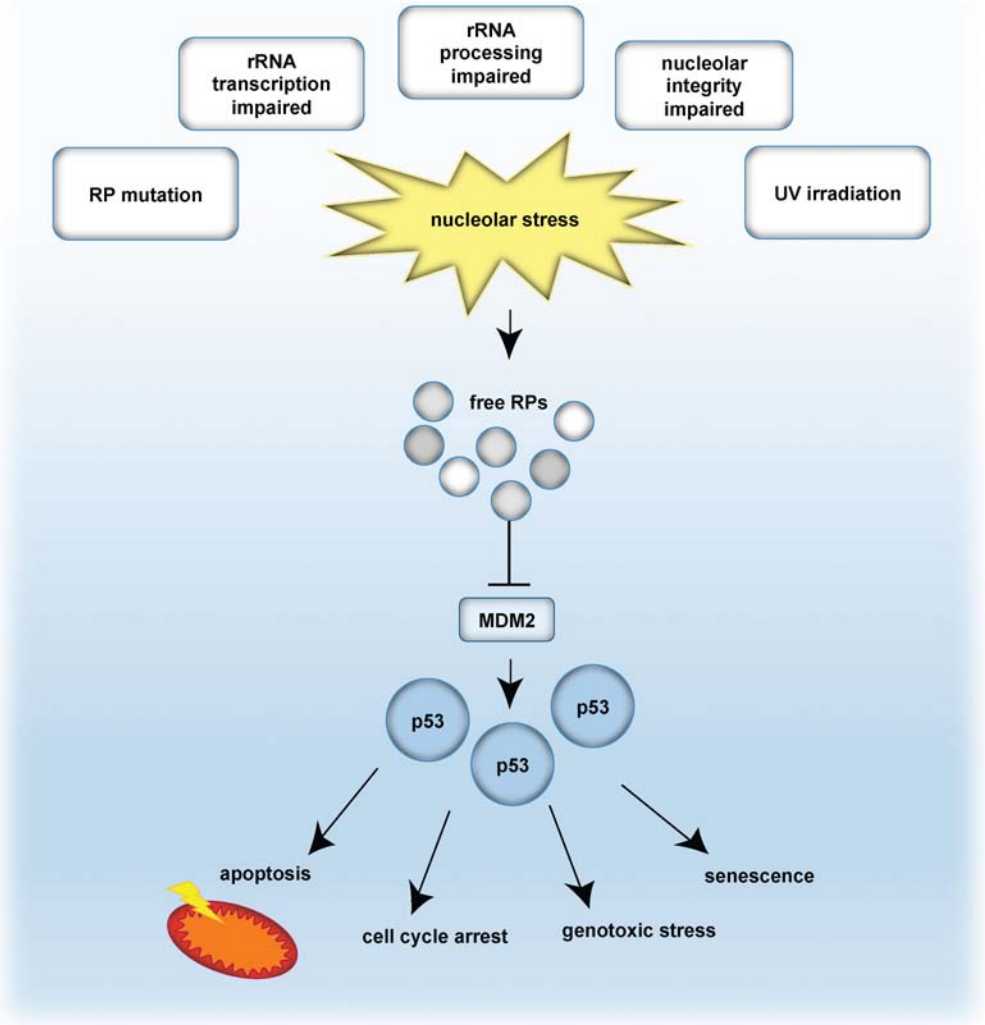

FIGURE 1 | The classical p53-dependent nucleolar stress response pathway. Nucleolar stress is caused by e.g., mutation of ribosomal proteins (RP), impaired transcription of rDNA into rRNA, abrogated rRNA processing, disrupted nucleolar integrity as well as by genotoxic stressors, such as UV irradiation. As a consequence, RPs are released and bind and inhibit the E3-ubiquitin ligase MDM2. In turn, p53 is no longer degraded in the proteasome and is stabilized. Given the p53 accumulation, p53-mediated effects are propagated, such as cell cycle arrest, senescence, apoptosis or genotoxic stress. Note that also p53-independent routes exist, which are not indicated in this scheme.

issues (Mizushima and Yoshimori, 2007; Mizushima et al., 2010; Klionsky, 2011; Gottlieb et al., 2015; Klionsky et al., 2016). So-called autophagic flux studies have become detrimental for understanding mechanisms of autophagy. Experts agree on combining various independent methods to allow solid data interpretation (Klionsky et al., 2016).

In general, autophagy is noticed as a protective mechanism by lowering the cellular stress.

Apoptosis and autophagy are both stimulated by similar stressors. However, they can be seen as opposing signaling events. Whereas autophagy acts in an anti-apoptotic manner and precedes apoptosis (Boya et al., 2005), apoptosis induction can block autophagy for instance by removing pro-autophagy proteins by caspases. However, this can even generate pro-apoptotic fragments of ATG autophagy regulators thereby triggering a fast forward response (Marino et al., 2014). Therefore, obviously a tight crosstalk exists, which goes into both directions, depending on the context. As a proof of principle, low sub-lethal levels of stress favor autophagy induction as a protective mechanism, whereas sustained stress beyond a certain threshold induces apoptosis. For instance, over-activation of autophagy can be a pro-death signal for autophagic cell death, and autophagy inducers can trigger apoptosis (Marino et al., 2014). Likewise, many stimuli that activate apoptosis can also stimulate autophagy. Extrinsic stress factors include chemotherapeutics, ionizing irradiation, lack of growth factors or nutrients. Intrinsically, p53 (see below), oncogenes (e.g., Myc), BH3-only proteins (Bcl-2 homology3) or serine/threonine kinases (such as JNK or AKT/PKB) are involved in the regulation of autophagy/apoptosis pathways

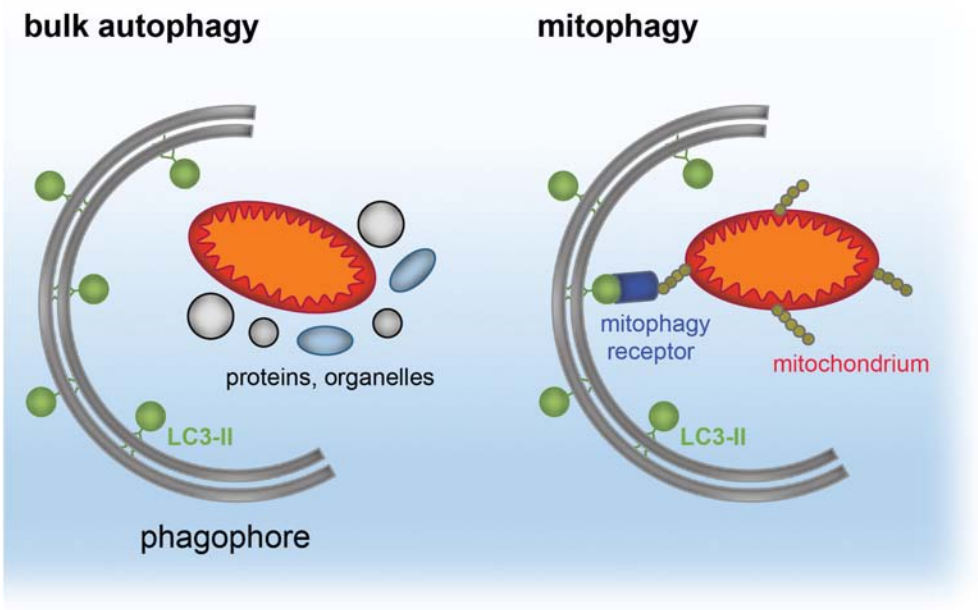

FIGURE 2 | Simplified model of cargo targeted by bulk autophagy or mitophagy. The phagophore forms around bulk material, such as proteins and organelles during bulk (macro)autophagy. The phagophore is a double-membranous structure, which forms around the cargo and gives rise to the autophagosome. In contrast, mitophagy reflects selective recruitment of ubiquitinated (yellow) mitochondria (red/orange) by the mitophagy receptors (blue) to LC3-II (green) located at the phagophore.

(Marino et al., 2014). For instance, the pro-apoptotic Beclin1 and anti-apoptotic Bcl-2 are commonly affected. Both interact with each other and thereby regulate the balance between autophagy or apoptosis. Also, mitochondrial integrity, caspase and ATG activation, mTOR signaling and multiple others are implicated (Marino et al., 2014).

Collectively, a mis-regulation of autophagy in either direction is connected to numerous pathophysiological conditions, and the same holds true for apoptosis (Maiuri et al., 2007; Jiang and Mizushima, 2014; Marino et al., 2014).

Selective Autophagy

Specific cellular cargo can be selectively targeted by autophagy (Kirkin et al., 2009). The pathways have been named according to their type of cargo, for instance mitophagy for specialized autophagy of mitochondria (Ding and Yin, 2012; Hamacher-Brady and Brady, 2016; Khaminets et al., 2016), nucleophagy for removal of the nucleus (Park et al., 2009; Mijaljica and Devenish, 2013), ribophagy for ribosomes (Beau et al., 2008; Kraft and Peter, 2008; Frankel et al., 2017), and aggrephagy for protein aggregates (Yamamoto and Simonsen, 2011).

Mitophagy is fundamental for the mitochondrial homeostasis and a mis-regulation of mitophagy is clearly implicated in the development of neurodegeneration (see section "Distinct Neurodevelopmental Pathologies, Common Concepts – A Short Overview"). The key players of mitophagy, Parkin and PINK1 [tumor suppressor phosphatase and tensin homolog (PTEN)-induced putative kinase 1], are mutated in patients with Parkinson's disease (Pickrell and Youle, 2015). Parkin functions as an E3-ubiquitin ligase, which is recruited to impaired mitochondria (Narendra et al., 2008). Parkin is required for ligation of ubiquitin marks to defective mitochondrial cargo (Ding and Yin, 2012; Harper et al., 2018). Parkin depends on the proper function of PINK1 (Vives-Bauza et al., 2010), an ubiquitin kinase located at the mitochondrial outer membrane (MOM) (Chin et al., 2010).

Mitophagy and apoptosis are both characterized by similar upstream events (Mukhopadhyay et al., 2014). Induction of mitophagy, for instance, is accompanied by activation of Bcl-2-associated X protein (BAX). This induces MOM perforation (MOMP), depolarization and release of cytochrome c from the mitochondrial intermembrane space (IMS) into the cytosol. As a consequence, PINK1 becomes stabilized at depolarized mitochondria and Parkin is subsequently translocated from the cytosol into the MOM (Vives-Bauza et al., 2010). By concerted action of both, mitochondria become decorated by ubiquitin marks (Lazarou et al., 2015) and can then be recognized by autophagy/mitophagy receptors such as the ubiquitin adaptor protein p62/sequestosome (Lamark et al., 2009; Geisler et al., 2010). In fact, autophagosome formation is mediated by different key mitophagy receptors such as optineurin and NPD52, which promote the recruitment of the autophagy initiating kinase ULK1 (Wong and Holzbaur, 2014; Heo et al., 2015; Lazarou et al., 2015). Nguyen et al. (2016) found that the GABARAP subfamily is essential for mitophagy. Meanwhile, the number of novel players involved in the complex process of selective autophagy is constantly expanding. Note that accumulation of damaged mitochondria, which are eliminated by mitophagy to a certain

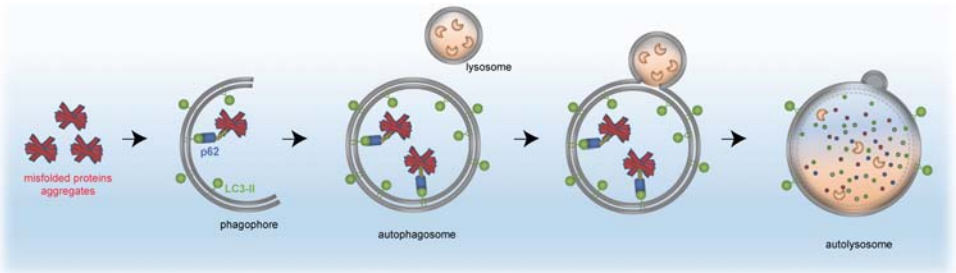

FIGURE 3 | Removal of protein aggregates by selective autophagy. Aggregated proteins (red) are bound by the autophagy receptor p62 (blue), which itself has interaction domains for autophagosomal LC3 (green, lipidated LC3-II) and ubiquitin (yellow). The cargo is engulfed by the mature autophagosome and subsequently fuses with the lysosome to form the autolysosome, in which the cellular material is degraded by acidic hydrolases (orange).

point, sets the threshold for apoptosis as a point of no return (Marino et al., 2014).

The autophagy receptor p62/sequestosome contains (i) interaction domains for ubiquitin, but at the same time also a LIR (LC3 interacting region) domain capable of binding to (ii) LC3, which itself is a key component of autophagosomal membranes. As a result, p62 recruits autophagosomal membranes to its selective, autophagosomal cargo (Lamark et al., 2009; Knaevelsrud and Simonsen, 2010).

The same principle of autophagy receptor (e.g., p62)/ubiquitin/LC3 cargo sequestration accounts also for removal of mis-folded protein aggregates, by a selective process termed aggrephagy (Lamark et al., 2009; Knaevelsrud and Simonsen, 2010; Yamamoto and Simonsen, 2011; Lamark and Johansen, 2012). Aggrephagy is also central to neurodegeneration (see section "Distinct Neurodevelopmental Pathologies, Common Concepts – A Short Overview"). A schematic for aggrephagy, bulk autophagy and mitophagy is depicted in **Figures 2**, **3**.

mTOR Signaling Couples Autophagy and Ribosome Biogenesis

The mammalian target of rapamycin (mTOR) pathway couples the intake of to nutrients, growth factors, energy and stress to the regulation of cell metabolism, growth, survival and autophagy (Pattingre et al., 2008). Deregulation is linked to various diseases and cancer formation.

Mammalian target of rapamycin signaling is recognized as essential pathway for proper neuronal development, neuronal survival and morphogenesis. Consequently, changes in mTOR signaling have been correlated with a spectrum of neuropathologies, such as epilepsy, intellectual disability, autism, brain injury, brain tumor formation and neurodegeneration (Crino, 2016; Switon et al., 2017). Likewise, mTOR inhibitors such as the bacterial macrolide rapamycin and its analogs are growingly used as therapeutic drugs and tested in clinical trials for effects in diverse neuropathological conditions (Laplante and Sabatini, 2009; Crino, 2016).

Mammalian target of rapamycin is a conserved serine-threonine kinase, which belongs to the phosphoinoside 3 kinase (PI3K) family. It assembles two large protein complexes, mTORC1 and mTORC2. The mTORC1 complex is considered as rapamycin sensitive complex (Pattingre et al., 2008). Rapamycin binds to FKBP12 and mTOR, thereby inhibiting mTORC1. mTORC1 signaling affects cell growth, metabolism and autophagy: Upon favorable conditions, mTOR is activated to allow cell growth by anabolic processes, such as rRNA biogenesis and protein translation. Upon nutrient deprivation and lack of growth factors, mTOR signaling is inhibited and cell growth is suppressed, whereas catabolic processes such as autophagy are induced to allow cell survival under unfavorable conditions. mTORC1 controls autophagy by regulating ULK1, ATG13 and FIP200, as well as by a reported rapamycin-insensitive mechanism (Laplante and Sabatini, 2009).

mTORC1 also regulates mitochondrial metabolism and biogenesis: mTORC1 inhibition impairs the MOM potential, reduces oxygen consumption and ATP levels. mTORC1 inhibition further decreases mitochondrial DNA levels and hampers mitochondrial biogenesis by affecting the transcriptional activity of the nuclear factor PGC1α (PPARγ co-activator 1) (Cunningham et al., 2007; Laplante and Sabatini, 2009).

Also p53 can regulate mTOR: DNA damage-induced p53 stabilization activates AMPK, which is a sensor of energy status and in turn results in mTORC1 inhibition. p53 also negatively controls mTORC1 by increasing *PTEN* expression, which functions as mTORC1 inhibitor. Inhibition of mTOR signaling diminishes nucleolar size and function and promotes longevity in different model organisms (Tiku and Antebi, 2018). However, the precise mechanisms regulating the crosstalk between ribosome biogenesis and autophagy remain to be determined.

A simplified model of mTORC1 signaling and the role of p53 is given in **Figure 4**.

NUCLEOLAR STRESS AND AUTOPHAGY: A TIGHT REGULATION BETWEEN HEALTH AND DISEASE

Defective ribosome biogenesis on the one hand and impaired autophagy on the other hand are largely contributing to several diseases. In the following, an overview is provided on common

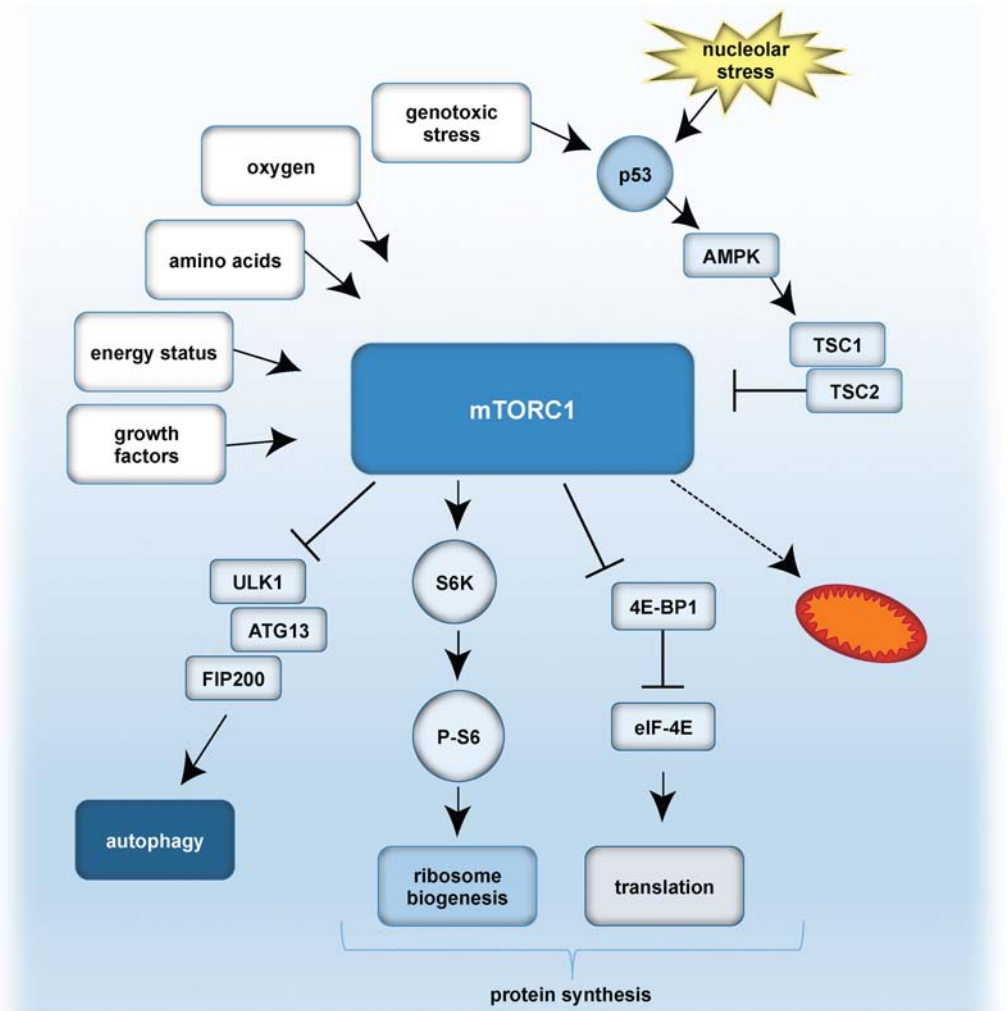

FIGURE 4 | A simplified model of mTOR signaling, and effect of nucleolar stress on p53. Growth factors, energy status, amino acid availability, oxygen levels and genotoxic stress can result in mTORC1 activation. p53 is stabilized either by genotoxic stress and/or nucleolar stress. p53 inhibits mTORC1 by activation of AMPK and TSC1/TSC2 (Tuberous sclerosis proteins 1 and 2). mTORC1 further activates autophagy by inhibitory effects on the ULK1 complex, composed of ULK1, ATG13 and FIP200. mTORC1 promotes protein synthesis by (i) S6K activation, which stimulates phosphorylation of S6 and thereby ribosome biogenesis, as well as by (ii) inhibitory effects on 4E-BP1 and eIF-4E. As a consequence, translation is activated. Furthermore, mTORC1 influences mitochondrial biogenesis and metabolism.

concepts of three key classes of diseases, classically or recently connected to nucleolar stress and autophagy with specific focus on neurodegeneration, cancer and ribosomopathies. For a more detailed overview see for instance (Parlato and Kreiner, 2013; Ghavami et al., 2014; Danilova and Gazda, 2015; Woods et al., 2015; Hetman and Slomnicki, 2019).

Distinct Neurodevelopmental Pathologies, Common Concepts – A Short Overview

The nervous system is vulnerable to intrinsic and extrinsic factors, which can give rise to distinct neurodevelopmental pathologies such as microcephaly, psychiatric disorders, autism, intellectual disability, epilepsy and neurodegeneration (please, be referred to review Hetman and Slomnicki, 2019). Causes include, for instance, gene mutations, infections or neurotoxins. As common concepts, gene expression, quality control mechanisms, cell proliferation, differentiation and apoptosis are mis-regulated. Apoptosis might give rise to microcephaly by eliminating, e.g., neuronal stem cells or post-mitotic neuronal cells (Hetman and Slomnicki, 2019). Likewise Zika virus infection, as an extrinsic factor for neurodevelopmental disorders, is tightly coupled to microcephaly. It has recently been demonstrated that it decreases mTOR signaling and over-activates autophagy (Liang et al., 2016). At the same time, ribosome biogenesis defects are emerging (reviewed in Hetman and Slomnicki, 2019).

Given the striking role of the nucleolus in coordinating mentioned neuropathological routes, deregulation of ribosome biogenesis rises as a potent upstream mechanism. In addition, also autophagy is activated in this context.

Neurodegeneration and Aging

Aging represents a general risk factor for the formation of neurodegenerative diseases and consequently, neurodegeneration accumulates within our society. Despite the rapid advances made in medicine, not all negative aspects of aging can simultaneously be addressed. Along these lines, increasing the society's age has to go together with improving anti-aging therapies. Our scientific knowledge on distinct neurodegenerative diseases has uncovered several common mechanisms, among them loss of neurons (Parlato and Kreiner, 2013; Parlato and Liss, 2014) and a prominent contribution of aggregate accumulation, induction of apoptosis and a mis-regulation of autophagy (Yamamoto and Simonsen, 2011; Ghavami et al., 2014). More recently, nucleolar stress has been connected to the induction of various types of neurodegenerative diseases, like Alzheimer's, Parkinson's, and Huntington's Disease (see below) (Hetman and Pietrzak, 2012). In line, aging functions as susceptibility factor for neurodegeneration. It is characterized by a loss of rDNA and is accompanied by reduction of nucleolar size and a decline in rRNA processing (Garcia Moreno et al., 1997; Hetman and Pietrzak, 2012; Parlato and Kreiner, 2013). Therefore, the nucleolus is tightly connected to lifespan regulation (Tiku and Antebi, 2018).

As both routes of apoptosis and autophagy are interwoven and not yet fully understood, mechanistic research is essential as a basis for development of therapeutic approaches. As a mandatory goal, novel drugs have to be tested for specificity and efficacy.

Neurodegeneration – Underlying Concepts

In protein mis-folding diseases, also known as proteopathies, proteins loose their normal structure and/or function. As a result, mis-folded proteins accumulate and cause a toxic intracellular environment. Normally, proper cellular homeostasis is maintained by several machinery: the ubiquitin-proteasome system (UPS) degrades proteins, whereas autophagy is capable of removing proteins and whole organelles by the lysosome. Hence, both routes are essential for a healthy cell and both have been implicated in the development of neurodegenerative diseases (Levine and Kroemer, 2008; Ghavami et al., 2014). Note that increased apoptosis induction plays a crucial role in eliminating these damaged cells. In addition, chronic inflammation and oxidative stress are observed in neurodegenerative disorders.

Several neurodegenerative disorders, such as PD, AD, and HD are characterized by accumulation of mis-folded, ubiquitinated proteins, which damage the affected cell (Yamamoto and Simonsen, 2011). The accumulating proteins form inclusion bodies, which can differ between the distinct pathologies. The formation of inclusion bodies/aggresomes/amyloid structures represents a double-edged sword: aggregate formation is not only toxic, it can actually be considered as beneficial and neuroprotective mechanism by reducing the toxic nature of mis-folded ubiquitin-containing protein aggregates (Rubinsztein, 2006; Yang et al., 2007).

With increasing age the autophagic program looses efficiency, thereby increasing the likelihood of aggregate accumulation.

Neurons are highly sensitive to accumulation of protein aggregates and require proper autophagy mechanisms to keep the intracellular toxicity low. Supporting data demonstrating the significant implication of the autophagic machinery were, for instance, obtained in mice lacking ATG7 in the central nervous system. ATG-deficient mice, which fail to perform autophagy, display an accumulation of inclusion bodies followed by neuronal loss (Komatsu et al., 2006).

However, autophagy might have dual functions with respect to neurodegeneration: On the one hand functional autophagy is neuroprotective, by removing defective mitochondria via mitophagy. On the other hand pro-death autophagy is considered to induce neuronal cell death.

Massive inhibition of autophagy can trigger apoptosis, which is observed by loss of neurons in neurodegeneration. Interfering with autophagy regulators and blocking autophagy, results in accumulation of cargo-filled autophagosomes and lysosomes, again being toxic for the cell. As a consequence, lysosome-mediated cell death occurs (Kroemer and Jaattela, 2005). Impairment of mitophagy causes accumulation of defective mitochondria, which in turn induces reactive oxygen species (ROS) formation and mitochondrial apoptosis (Seo et al., 2010).

Induction of apoptosis by the chemotherapeutic agent staurosporine is accompanied by mitophagy and autophagy induction in dopaminergic cells. Additional block of autophagy by Bafilomycin or inhibition of mitophagy in PINK null mice sensitizes cells to staurosporine-induced apoptosis. Autophagy and mitophagy seems to be neuroprotective upon staurosporine-mediated apoptosis induction in dopaminergic neurons (Ha et al., 2014). However, with respect to loss of dopaminergic neurons, it is not fully resolved whether autophagy is beneficial or pathogenic.

Keeping mitochondria healthy is a prerequisite for counteracting neurodegenerative diseases. Concepts include for instance maintaining mitochondrial membrane integrity and functionality. Mitochondrial membrane permeabilization is tightly coupled to apoptosis induction (Kroemer et al., 2007). Also anti-oxidants and ROS scavenging appear as beneficial strategies. Inhibitors of apoptosis are used as therapeutic drugs to inhibit neuronal loss. Anti-apoptotic drugs prevent mitochondrial apoptosis by blocking release of cytochrome c from the mitochondria or activation of pro-apoptotic BAX (Westphal et al., 2014). Alternatively, the activity or abundance of anti-apoptotic factors can be elevated.

Alzheimer's Disease

Alzheimer's disease is the most common neurodegenerative disorder and has both sporadic and hereditary origin. Mostly, AD is diagnosed as sporadic form by the age of 65 years and represents the primary cause of dementia within the elderly generation (Seshadri et al., 1997; Ding et al., 2005).

Classically, prominent accumulation of defective mitochondria, increase of ROS, and apoptosis induction are found in patient's neurons. A decline in autophagy during aging further promotes the mitochondrial release of cytochrome c, which serves as pro-apoptotic stimulus.

Also decreased nucleolar volume has been detected in AD patients (Iacono et al., 2008; Pietrzak et al., 2011). Mechanistically, inhibition of rDNA transcription by rDNA

promoter methylation, reduced 28S/18S ratio, reduced tRNA abundance and increased rRNA oxidation has been linked to AD (Payao et al., 1998; da Silva et al., 2000; Ding et al., 2005; Pietrzak et al., 2011). In a similar manner, a decline of 28S rRNA was found in elderly healthy probes when compared to younger control groups (Payao et al., 1998; da Silva et al., 2000). The patient data suggest that impairment of ribosome biogenesis and protein synthesis is one of the earliest events observed in the pathogenesis of AD characterized by mild cognitive impairment (Ding et al., 2005).

Parkinson's Disease

Parkinson's disease is the second most common neurodegenerative disease after AD (Parlato and Liss, 2014). PD is characterized by loss of dopaminergic neurons in the brain stem. Patients display tremor, dementia and depression. Also in PD, most cases are sporadic. Typical risk factors are aging and exposure to (mitochondrial) toxins. A key feature of PD is deposition of Lewy bodies, which reflects deposition of α-Synuclein oligomers (Ghavami et al., 2014). These oligomers trigger mitochondrial damage. Hereditary forms of PD involve mutation of the key mitophagy regulators PINK and Parkin. Mutations of both result in impaired mitophagy. Given that α-Synuclein serves as a substrate of the E3-ubiquitin ligase Parkin, accumulation of α-Synuclein is also detected in a Parkin mutated background. Also ER stress is implicated in PD. However, mild ER stress is attributed to function rather in a neuroprotective manner by inducing pro-survival autophagy. PD is mimicked by treating neuronal cells with chemicals, such as MPP+ and rotenone, which trigger mitochondrial dysfunction and cell death (Nicklas et al., 1987).

More recently, disruption of nucleolar integrity has been observed in human post mortem samples of patients with PD (Rieker et al., 2011). In support of a nucleolar contribution, the ribosome biogenesis factor Nucleolin interacts with α-Synuclein. Consequently, damaged mitochondria, ROS, as well as autophagosomes accumulate and cause apoptosis (Rieker et al., 2011).

Disruption of nucleoli, cell cycle arrest and p53-mediated apoptosis is observed by depletion of the transcription initiation factor IA (TIF-1A), required for the recruitment of RNA pol I, in mouse embryonic fibroblasts (Yuan et al., 2005). Ablation of TIF-1A in DA neurons of mice results in Parkinsonism and progressive loss of DA neurons (Rieker et al., 2011) and likewise, reduced expression of *TIF-1A* is detected in PD patient samples (Evsyukov et al., 2017). Treatment with the neurotoxin MPTP worsens the effect of nucleolar stress. In this model, also p53 is stabilized and mTOR signaling decreased. Finally, ROS-mediated oxidative stress is induced and defects are detected in mitochondria, such as impaired mitochondrial transcription and COX (cytochrome c oxidase) activity (Rieker et al., 2011). Therefore nucleolar stress, by inhibiting mTOR signaling, can impair mitochondrial function, which represents a key hallmark of several neurodegenerative diseases.

To determine effects of specific PD mutations on nucleolar function irrespective of neuronal loss, pre-symptomatic, digenic PD models were analyzed. Mild overexpression of mutant human α-Synuclein in PINK1 null background (hA53T-SNCA/PINKKO) revealed differential nucleolar activity: On the one hand, reduced nucleolar activity and impaired nucleolar integrity was found in a subset of DA neurons, whereas others showed elevated nucleolar function, thereby suggesting possible compensatory mechanisms. In contrast, inactivation of PINK1 and DJ-1 showed no alterations, pointing to mutated α-Synuclein as the main contributor of nucleolar stress in the hA53T-SNCA/PINKKO model (Evsyukov et al., 2017).

Hemoglobin (Hb) is strongly expressed in dopaminergic neurons in the substantia nigra and is found in patient samples of AD and PD. Hb has recently been connected to mitochondrial function and apoptosis. Hb can form toxic aggregates in the nucleolus after stimulation with MPP+ and rotenone in a cellular model of PD. In turn, Hb overexpression impairs pre rRNA processing, induces nucleolar stress and sensitizes cells to apoptosis (Codrich et al., 2017). The authors further demonstrate decreased phosphorylation of the mTOR target 4E-BP1, decreased numbers of lysosomes in neurons and decreased levels of LC3-II following rotenone treatment, being indicative for inhibition of autophagy.

Huntington's Disease

Huntington's disease is caused by autosomal dominant mutation of the Huntingtin gene (*Htt*) and the onset of the disease is in average much earlier than AD and PD. Patients with HD display uncontrolled chorea movements and cognitive impairment (Ghavami et al., 2014). The onset of age also inversely correlates with the increasing number of repetitive Glutamine motifs present in mutated Huntingtin. Interestingly, capture of mutant Htt inside inclusion bodies was shown to be less toxic in comparison to accumulating free mutant Htt (Zuccato et al., 2010). Also in HD patients, apoptosis and mitochondrial damage is detected. Additionally, studies have demonstrated that rRNA transcription is affected in HD (Parlato and Kreiner, 2013). Triggering autophagy in mice models of HD can remove aggregates and increases their life span (Zheng et al., 2010).

Targeted disruption of nucleoli by conditional knockout of TIF-1A essential for the recruitment of RNA pol I in striatal neurons results in striatal degeneration and typical HD-like phenotypic alterations in mice (Kreiner et al., 2013). TIF-1A loss induces nucleolar disruption and nucleolar stress, which precedes neurodegeneration. Nucleophosmin (NPM) represents a multifunctional, nucleolar key factor involved in ribosome biogenesis, which fulfills a plethora of pro-survival processes (Colombo et al., 2011; Lindstrom, 2011). A down-regulation of NPM serves as readout for nucleolar stress induction and can be linked to neurodegeneration in several models of neurodegeneration (Marquez-Lona et al., 2012). In line, as a key marker for nucleolar stress (Colombo et al., 2002), NPM is reduced and p53 is stabilized in this model (Kreiner et al., 2013). As an early and p53-dependent pro-survival response, the p53 target PTEN (Stambolic et al., 2001) is induced in neurons. Given that the tumor suppressor PTEN counteracts the mTOR pathway, downstream targets of mTOR were analyzed for phosphorylation. It was found that p-S6 and p-4E-BP1 are reduced in the model. Inhibition of mTOR is connected to activation of autophagy and

the same holds true in the HD model (Kreiner et al., 2013). Thus, transient over-activation of autophagy seems to be induced as initial, neuroprotective mechanism in response to impaired ribosome biogenesis. However, after sustained nucleolar stress, apoptosis of striatal neurons is inevitable (Kreiner et al., 2013; Parlato and Liss, 2014).

Cockayne Syndrome

DNA damage and impaired rRNA transcription are connected to Cockayne Syndrome (CS), which is a rare, congenital, autosomal-recessive neurodegenerative disorder (Karikkineth et al., 2017; Hetman and Slomnicki, 2019). Patients are characterized by premature aging, dwarfism, microcephaly, and have an average life expectancy of 12 years. Commonly mutated genes are CSA (20% of cases) and CSB (80% of cases), which are both, besides their key role in nucleotide excision repair, also required for RNA pol I transcription (Lebedev et al., 2008; Koch et al., 2014). CSB was found to localize to mitochondria and bind to mtDNA (Aamann et al., 2010; Kamenisch et al., 2010). CSB-deficient cells show increased ROS production, increased mitochondrial content and accumulation of damaged mitochondria, in line with impaired mitophagy (Scheibye-Knudsen et al., 2012). Further, CSB promotes acetylation of α-tubulin (Majora et al., 2018), which is a modification involved in cargo transport along microtubules to facilitate autophagosome/autolysosome fusion and aggresome clearance (Xie et al., 2010; Li et al., 2011). CSB deficiency abrogates autophagy and results in increased number of dilated lysosomes with impaired function (Majora et al., 2018). In human CS cells, translational infidelity is observed, most likely due to accumulation of error-prone ribosomes as a consequence of impaired ribosome replacement. CS cells exhibit ER stress and an over-activated unfolded protein response, which can be counteracted by addition of pharmacological chaperones (Alupei et al., 2018).

Epilepsy – A Disease Related to Neurodegeneration

Epilepsy is characterized by recurrent seizures and represents a disease related to neurodegeneration. Abrogated morphogenesis and synaptic function is observed upon nucleolar stress and could be connected to epilepsy (reviewed in Hetman and Slomnicki, 2019). For example, pharmacologically induced short-term seizures in mice transiently affect RNA Pol I activity in hippocampi and result in decreased *de novo* synthesized 18S and 28S rRNAs. In contrast, long-term seizures were associated with increased ribosome biogenesis (Vashishta et al., 2018). Epilepsy is further tightly linked to mTOR hyper-stimulation and autophagy over-activation (Cao et al., 2009; Zeng et al., 2009). Strikingly, administration of the mTOR inhibitor rapamycin counteracts seizures and thus functions in an anti-epileptogenic manner (Zeng et al., 2009).

Rare, Pediatric Neurodegenerative Diseases – A Short Outlook

Also rare, pediatric neurodegenerative diseases are characterized by alterations in autophagy. As an example, the multisystemic Vici syndrome is neurologically characterized by microcephaly and cognitive impairment. Accumulation of ubiquitinated autophagic cargo, p62 and damaged mitochondria is observed, reminiscent of neurodegeneration (Ebrahimi-Fakhari et al., 2014). However, whether also ribosome biogenesis is also altered here, remains to be determined.

Cancer and Cancer Treatment

Key hallmarks of cancerous cells involve for instance mis-regulation of signaling pathways, rapid cell proliferation, accelerated tumor growth and inhibition of apoptosis (Hanahan and Weinberg, 2000, 2011). Large amounts of ribosomes are essential for cancerous cell growth and large nucleoli serve as prognostic marker in many tumor types (Montanaro et al., 2008; Penzo et al., 2019).

The nucleus arises as an essential target for cancer therapy (Woods et al., 2015; Pfister and Kuhl, 2018). Anti-tumor therapies utilize the high demand of cancer cells for the production of ribosomes by inhibiting RNA pol I. Inhibiting nucleolar structure/function and RNA pol I function has been characterized as beneficial in terms of triggering apoptotic cell death of cancer cells (Burger and Eick, 2013). Classical chemotherapeutics used in the clinics are for instance actinomycin D, 5-fluorouracil and metotrexat, which interfere with the nucleolar function (Boulon et al., 2010; Burger and Eick, 2013).

Novel drugs, which specifically impair rRNA transcription, are currently tested in clinical trials. The small molecule drug CX-5461 specifically inhibits transcription of RNA pol I and stabilizes p53, whereas RNA pol II is not affected. Also, translation and DNA replication is not impaired in human cancer cell lines (Drygin et al., 2011). The drug is further reported to impair proliferation in a p53-independent manner in cancer cell lines, whereas the effect on normal cell lines is minimal (Drygin et al., 2011).

Selective inhibition of RNA pol I by CX-5461 also robustly stimulates pro-death autophagy. Nucleolar stress and autophagy seem to be tightly coupled in distinct models and setups. Recently, CX-5461 was loaded on a nanoplatform to enrich for nucleolar accumulation of the drug in order to enhance the anti-cancer effect, without causing significant side effects. *In vivo* and *in vitro* assays confirm induction of pro-death autophagy in HeLa cells, as well anti-proliferative and anti-tumor effects (Duo et al., 2018).

Besides autophagy, CX-5461 induces also senescence in a p53-independent manner. In U2OS osteosarcoma cells, CX-5461 induces G2 arrest, but not apoptosis (Li et al., 2016). In response to CX-5461, p53 accumulates and *p21* is induced. In addition, increased levels of LC3-II are detected under basal conditions. Using TEM analysis, the authors noticed expanded vacuole-like structures filled with organelles, however, they report lack of clear identification of autophagosomal character. Knockdown of p53 by siRNA rescues p21 up-regulation and LC3-II accumulation and increases cell survival. The authors conclude that CX-5461 triggers p53-dependent autophagy. Autophagy occurs via the AMPK/mTOR pathway in U2OS cells, as evidenced by reduced p-mTOR and increased p-AMPK levels (Li et al., 2016). The p53 target p21 is shown to be up-regulated during autophagy and a p53-independent increase of p21 is reported in MNNG cells with mutant p53 (Li et al., 2016).

Taken together, autophagy induction as a response to nucleolar stress seems to be an initial surveillance mechanism in several models. However, also in terms of cancer, autophagy induction can have two modes of action: Autophagy induction is clearly beneficial for cells by preventing genotoxic stress and DNA damage. It removes cellular sources of ROS, such as defective mitochondria or proteins (Mrakovcic and Frohlich, 2018). In contrast, inhibition of autophagy represents an oncogenic event. At later stages over-activation of autophagy facilitates oncogenic drug-resistance. Autophagy inhibitors chloroquine and hydroxychloroquine have therefore been tested in clinical trials for cancer therapy (Yang et al., 2011; Marino et al., 2014).

Ribosomopathies

Impairment of ribosome biogenesis is connected to a diverse class of human diseases collectively termed ribosomopathies (Freed et al., 2010; Narla and Ebert, 2010; Danilova and Gazda, 2015; Yelick and Trainor, 2015). Patients exhibit either mutations and/or haploinsufficiency of RPs or ribosome biogenesis factors. Several players associated with ribosomopathies have been described (see also below). Classically, the nucleolar stress response and the tumor suppressor p53 are activated (Freed et al., 2010; James et al., 2014). Despite a common mechanism of interfering with ribosome biogenesis, the patient's phenotypes differ among the distinct syndromes. Intriguingly, though, some phenotypes are common and include defects of the craniofacial cartilage, anemia and increased cancer susceptibility. The elevated cancer risk appears paradoxical, given the great need of tumor cells for large amounts of ribosomes (Montanaro et al., 2008). Accordingly, pathways and mechanisms might well exist, which let both co-exist (Pfister and Kuhl, 2018). For example, specialized onco-ribosomes have recently been uncovered to increase the cellular fitness by mediating preferential translation of anti-apoptotic Bcl-2, as observed for the ribosome mutant RPL10-R98S in leukemia cells (Xue and Barna, 2012; Sulima et al., 2017; Kampen et al., 2018). However, the question on cause and consequence of ribosomopathy-induced cancer formation is still under debate.

Recently, examination of murine hepatocellular carcinoma and hepatoblastoma has revealed ribosomopathy-like features of nucleolar stress, such as deregulated expression of RPs and accumulation of unprocessed rRNA precursors. Despite the fact that p53 is stabilized, no growth inhibition occurs (Kulkarni et al., 2017). Therefore, compensating mechanisms might counteract apoptosis, involving up-regulation of anti-apoptotic Bcl-2, silencing of p19 ARF or cytosolic sequestration of p53. Those events would in turn inhibit the tumor suppressive mechanisms of cell cycle arrest and apoptosis in these cancers (Kulkarni et al., 2017).

Clearly, ribosome biogenesis is a highly energy-consuming process. An implication of autophagy comes in mind, which might compensate for the low levels of functional ribosomes observed in ribosomopathies. Many important questions arise. Is there a connection to bulk autophagy or selective autophagy of ribosomes (ribophagy) in ribosomopathy patients? Until now broad studies are lacking, which precisely address their implication in these issues. However, first data are collected, which indeed unravel involvement of autophagy in these processes (see section "Nucleolar Factors and Nucleolar Stress in the Regulation of Autophagy and *Vice Versa*").

An overview summarizing the emerging connection between nucleolar stress and autophagy in the diseases presented here is given in **Table 1**.

NUCLEOLAR FACTORS AND NUCLEOLAR STRESS IN THE REGULATION OF AUTOPHAGY AND *VICE VERSA*

Recently, inhibition of RNA pol I has been connected to autophagy, revealing that nucleolar stress functions upstream of autophagy. In the following, evidence is collected, which links the ribosome biogenesis machinery and the nucleolus to autophagy, and *vice versa*. As a common principle, different groups suggest implication of mTOR signaling in nucleolus-mediated autophagy (see below). Also here, p53-dependent and -independent pathways are being identified.

The p53 Family

Besides the classical role of p53 as guardian of the genome, by mediating cell cycle arrest and apoptosis, p53 has been reported

TABLE 1 | The role of nucleolar stress in mentioned diseases and effects on autophagy.

Condition/ Disease[1]	Effects related to nucleolar stress[1]	Effects related to autophagy[1]
Aging	Loss of rDNA rRNA processing impaired Nucleolar size reduced	Autophagy impaired
Alzheimer's Disease	rDNA transcription impaired Nucleolar volume decreased	Autophagy impaired Defective mitochondria
Parkinson's Disease	Nucleolar disruption Altered nucleolar function	mTOR pathway inhibition Autophagy altered Mitophagy impaired Defective mitochondria
Huntington's Disease	rDNA transcription impaired NPM reduced	mTOR pathway inhibition Autophagy transiently over-active Defective mitochondria
Cockayne syndrome	rDNA transcription impaired	Autophagy impaired Defective mitochondria
Epilepsy	RNA pol I altered	mTOR pathway activation Autophagy over-active
Ribosomopathies	rRNA processing impaired mutated RPs	mTOR over-activation Autophagy over-active ROS
Cancer	Need for ribosomes Large nucleoli Ribosomopathy-like	Autophagy conveys drug resistance Autophagy has dual roles
Zika virus infection	Nucleolar NPM displacement	mTOR pathway inhibition Autophagy over-active

[1] *Please, see text for references and details.*

to exert distinct roles in autophagy (Wang et al., 2014). This depends on its subcellular localization: nuclear, cytosolic or mitochondrial, respectively.

The effect of nuclear p53 as an inducer of autophagy mostly depends on its role as transcription factor. Nuclear p53 induces expression of ATGs thereby driving autophagy. In line, many promoters of autophagy related factors, such as ATGs or Parkin, are occupied by p53 (Zhang et al., 2011; Fullgrabe et al., 2016). Induction of pro-apoptotic target genes implicated in mTOR activation, such as *TCS2*, *AMPK*/*PTEN* and *Sestrin*, result in autophagy activation. The p53 target *DRAM* is directly involved in autophagosome formation. P53 further induces *BAX* and *Bcl-2* or *DAPK*, which in turn induce *Beclin1* (Mrakovcic and Frohlich, 2018). Moreover, the p53 family members p63 and p73 induce expression of the autophagy regulators *ATG5* and *ATG7*. Also E2F, an important co-regulator of p53, is involved in the transcriptional regulation of autophagy related genes (Polager and Ginsberg, 2009; Fullgrabe et al., 2016). Note that other p53 family members p63 and p73 can, in principal, compensate for a loss of p53 (Kenzelmann Broz et al., 2013; Fullgrabe et al., 2016). However, it remains to be determined, whether p53-independent pathways actually depend on the role of p63 and p73 or whether they are unrelated.

Cytosolic p53 counteracts autophagy by transcription-independent mechanisms. P53 inhibits AMPK and activates mTOR, p53 further interacts with Beclin and induces Beclin ubiquitination and degradation (Mrakovcic and Frohlich, 2018). Cytosolic p53 interacts with Parkin, which is the key regulator of mitophagy. It was reported that p53 counteracts Parkin recruitment to mitochondria, thereby impairing mitophagy (Hoshino et al., 2013).

Mitochondrial p53 has a plethora of functions: it triggers MOM permeabilization, ROS production, mitophagy and autophagy and is therefore implicated in neuropathological conditions (Marino et al., 2014; Wang et al., 2014).

mTOR Inhibition by Rapamycin

mTORC1 inhibition by rapamycin abrogates the nucleolar stress response induced by low, cytostatic doses of the chemotherapeutic actinomycin D (Goudarzi et al., 2014). As a result, p53 stabilization and p21 induction is impaired. The authors observe decreased interaction of RPL11 with MDM2 upon rapamycin and actinomycin D co-treatment and suggest a mechanism related to the classical RPL11-MDM2-p53-pathway. Also, they detected decreased RPL11 levels, as well as MDM2 stabilization, which might in part contribute to the rapamycin-mediated effects on p53. Interestingly, inhibition of mTOR by caffeine at physiologically relevant doses is capable of abrogating the actinomycin D-induced p53 response (Goudarzi et al., 2014). Thus, a complex network between mTOR inhibitors/autophagy, nucleolar stress and cancer treatment is established.

RNA pol I Inhibition and NPM

RNA pol I inhibition by actinomycin D or adriamycin is well known to trigger nucleolar disruption. Recently, the observation has been made that also autophagy can be induced with these drugs (Katagiri et al., 2015). The same holds true for knocking down the RNA pol I transcription factors TIF1A and POLR1A. Induction of autophagy has been monitored in flux experiments by counting LC3 punctae (being indicative for autophagosomal number) and determining levels of lipidated LC3-II (representing the autophagosome-bound form of LC3). At the same time the autophagy substrate p62/sequestosome is reduced, indicating increased turnover by autophagy. Autophagy induction can be rescued by treating cells with autophagy inhibitors or knocking down key autophagy regulators ATG5 and Beclin1. In contrast, nucleolar disruption is not rescued (Katagiri et al., 2015). Together, this finding places nucleolar disruption upstream of autophagy. As nucleolar stress is generally characterized by redistribution of nucleolar factors (such as NPM), or p53 stabilization, Katagiri et al. (2015) have determined, which accounts for the effects observed. They found that induction of autophagy by TIF1A knockdown is independent of p53, but depends on NPM. The induction of autophagy can be rescued by NPM knockdown, without reducing p53 levels. In contrast, neither the depletion of NPM affects starvation-induced autophagy; nor does nutrient deprivation have an impact on nucleolar integrity. This suggests that NPM might rather play a role in a specialized form of nucleolar stress-induced autophagy, than starvation-induced bulk autophagy.

The Nucleolar Factor – PICT-1

The nucleolar factor PICT-1/GLTSCR2 is considered a tumor suppressor, as it binds and stabilizes PTEN. In contrast, PICT-1 deletion is linked to cancer formation and functions as oncogenic regulator of the E3-ubiquitin ligase MDM2 by preventing nucleolar release of RPL11 (Sasaki et al., 2011; Suzuki et al., 2012). Consequently, p53 stabilization, G1 cell cycle arrest and apoptosis are observed, thereby counteracting tumor growth (Sasaki et al., 2011). Homozygous PICT1 deletion in mice is lethal and impairs survival of mouse ES cells. PICT-1 binds to rDNA and the RNA pol I transcription factor upstream binding factor-1 (UBF-1). It inhibits transcription of rRNA, which depends on its localization to nucleoli (Chen et al., 2016). With respect to autophagy, it has been shown that PICT-1 overexpression induces GFP-LC3 punctae and reduces p62 levels, and that it inhibits the AKT/mTOR/p70S6K pathway (Chen et al., 2016). As the autophagy inhibitor 3-MA (3-methyladenine) enhances cell death upon PICT-1 overexpression, the authors suggest induction of pro-death autophagy. Together, the authors conclude that PICT-1 overexpression triggers pro-death autophagy, without inducing the classical nucleolar stress response, such as p53 stabilization and nucleolar disruption (Chen et al., 2016).

The Ribosomopathy Factor – SBDS

Recent findings suggest that autophagy might be affected in patients with ribosomopathies. mTOR signaling regulates a variety of essential cellular processes, among them autophagy. In leukocytes derived from patients with the ribosomopathy syndrome Shwachman Bodian Diamond Syndrome (SBDS), a hyper-activation of mTOR phosphorylation is observed (Bezzerri et al., 2016). Also in intestinal epithelial cells autophagy

is over-activated. In this context, autophagy is independent of mTOR or p53 and is induced as a consequence of nucleolar/ribosomal stress (Bezzerri et al., 2016).

The Ribosomopathy Factor – RPS19

Disrupted ribosome biogenesis by knocking down RPS19 (ribosomal protein S19) is connected to the ribosomopathy syndrome Diamond Blackfan Anemia (DBA). RPS19 knockdown further affects autophagy in patient cells, and autophagy induction is also observed in red blood cells of zebrafish embryos (Heijnen et al., 2014).

RP-deficiency also recapitulates these effects in cells derived from SBDS. An increase in P-S6 as well as ROS is observed, whereas anti-oxidant treatment reverses p-S6, autophagy and p53 stabilization (Heijnen et al., 2014). Thus, the observed effects turn out to be ROS-dependent and suggest a contribution of oxidative stress in ribosomopathies.

The Ribosomopathy Factor – pwp2h

The zebrafish titania mutant (tti^{s450}) harbors a recessive, lethal mutation of the *pwp2h* gene encoding a factor of the small ribosomal subunit (Boglev et al., 2013). In this mutants reduced 18S rRNA, impaired ribosome biogenesis and p53 stabilization is observed. *pwp2h* is highly expressed in intestinal, epithelial cells, but also in the brain retinal pigmented epithelium, liver and pancreas, which are rapidly dividing tissues. Also here, defects in craniofacial formation, typical hallmarks of ribosomopathies, can be detected.

Intestinal epithelial cells of the mutant larvae display accumulation of autophagosomes. In autophagic flux experiments using the autophagy inhibitor chloroquine and activator rapamycin, increased accumulation of LC3-II is observed in the mutants, indicating autophagy induction (Boglev et al., 2013). Also p-RP-S6, reflecting mTORC1 activity, is increased. Inhibiting autophagy by morpholino-mediated knockdown of ATG5 triggers apoptosis of intestinal epithelial cells specifically in the mutants, whereas the wildtype is not affected. This suggests that autophagy induction counteracts apoptosis as survival mechanism in response to nucleolar stress. Also, no signs of apoptosis are detected in the mutants, ruling out toxic levels of autophagy activation. Interestingly, autophagy induction in the zebrafish mutants occurs in mTOR and p53-independent manner (Boglev et al., 2013). However, the molecular mechanisms and pathways affected remain elusive.

The *Drosophila* Nopp140

Nopp140 is in structure and function related to Treacle, representing an essential gene in the ribosomopathy syndrome Treacher Collins syndrome (TCS) (Valdez et al., 2004; Sakai and Trainor, 2009; Dai et al., 2016). Depletion of the nucleolar phosphoprotein Nopp140 in the imaginal wing disks of *Drosophila* results in nucleolar stress, loss of ribosomes and p53-independent apoptosis (James et al., 2013). Since there are no detectible levels of MDM2, NPM/B23 and ARF in *Drosophila*, the authors conclude that an alternative nucleolar stress response might exist. They consider JNK as an interesting link, which has earlier been shown to induce autophagy in response to oxidative stress and induce transcription of *ATG* genes (Wu et al., 2009; Zhou et al., 2015). In addition, oxidative stress induces accumulation of the autophagy marker GFP-LC3 and lysosomes in the intestinal epithelium, which is dependent on JNK signaling (Wu et al., 2009). As also in larval polyploidy midgut cells mCherry-ATG8a is accumulated after Nopp140 depletion, the authors conclude an accumulation of autophagosomes and a premature induction of autophagy regulated by loss of Nopp140 (James et al., 2013).

NAT10 and Glucose Deprivation Stress

NAT10 drives ribosome biogenesis by mediating acetylation of the RNA pol I transcription factor UBF-1 and facilitating processing of the 18S rRNA (Kong et al., 2011; Ito et al., 2014). Under normal conditions, NAT10 is auto-acetylates and promotes recruitment of PAF53 and RNA pol I to mediate rRNA biogenesis (Cai et al., 2017), whereas autophagy is inhibited (Liu et al., 2018).

The mechanisms, which link inhibition of rRNA biogenesis to induction of autophagy in response to energy stress were determined by Liu et al. (2018). They demonstrate that NAT10 binds and acetylates the autophagy regulator Che1 (AATF) in a p53-independent manner. As a consequence of acetylation, the transcriptional activation of target genes *Redd1* and *Deptor* is off. Thus, Che1 enhances autophagy by activating the transcription of *Redd1* and *Deptor*, two critical inhibitors of mTOR signaling (Desantis et al., 2015a).

Interestingly, Che-1 is also important for RNA pol II, the DNA damage response (DDR) and drives p53 expression. Upon DDR, Che1 increasingly interacts with p53 and drives the expression of genes implicated in cell cycle regulation, for instance *p21* (Desantis et al., 2015b).

Upon energy stress and glucose deprivation, Sirt1 deacetylates NAT10. ChIP analysis has demonstrated that deacetylated NAT10 does not bind to rDNA upon glucose deprivation and thus NAT10-mediated ribosome biogenesis is inhibited. Under this condition, the inhibition of Che1 is released (Liu et al., 2018).

In HCT116 cells, LC3-II levels are increased both in presence or absence of chloroquine, showing that NAT10 knockdown increases basal autophagic flux. Also, p62 is reduced upon NAT10 depletion. Strikingly, the effects observed are independent of p53, as demonstrated in HCT116 p53$^{-/-}$ cells. In rescue experiments with HCT116-NAT10-Cas9 knockout clones, overexpression of NAT10 reverses the effects observed on p62 and LC3-II, whereas acetylation mutants fail to do so (Liu et al., 2018). Glucose withdrawal triggers release of NAT10 from nucleoli. Treatment of cells with RNAseA also leads to a loss of NAT10 from nucleoli and impairs binding to UBF-1, suggesting that rRNA binding is essential for nucleolar accumulation of NAT10. In contrast, the acetylation status does not matter as determined by use of a NAT10 mutant.

Together, Sirt1 mediated deacetylation of NAT10 impairs rRNA biogenesis and results in release of NAT10 from nucleoli. Therefore, both regulate the switch between ribosome biogenesis and autophagy as a response to energy stress to maintain cellular survival.

The Autophagy Regulator LC3/Atg8 – Present in the Nucleolus

Besides its localization in the autophagosomal membranes and the cytosol, LC3 can rapidly shuttle into and out of the nucleus. Endogenous and overexpressed LC3 has been found to be associated with nucleoli. However, the authors point out a weak signal being indicative for a low degree of enrichment (Kraft et al., 2016). A triple arginine motif is essential for the nucleolar targeting of LC3. The arginine motif mediates protein-protein interaction and binding to RNAs, suggesting accumulation at nucleoli by interaction with rRNAs and/or nucleolar RNA binding proteins (Zhou et al., 1997; Behrends et al., 2010). Likewise, LC3 has been connected to interaction with the 60S ribosomal subunit (Kraft et al., 2016). In addition, a hydrophobic binding interface contributes to nucleolar localization. In contrast, the lipidation site of LC3 is dispensable for nucleolar targeting. Interestingly, several 40S RPs such as S27, S5, S18, and S20, have been identified as interaction partners of LC3 by MS analysis. The authors speculate that nucleolar LC3 might counteract p53 stabilization by preventing interaction of RPs with MDM2 (Kraft et al., 2016).

TP53INP2/DOR

TP53INP2/DOR (tumor protein p53 inducible protein nuclear protein 2) is a nuclear protein, which interacts with the LC3-related GABARAP, GABARAP-like2, as well as with LC3 via its N-terminus. TP53INP2/DOR also binds to VMP1, a transmembrane protein of autophagosomes. Upon starvation by rapamycin or EBSS incubation, TP53INP2-EGFP translocates from nuclei to the cytoplasm where it co-localizes with LC3 family proteins, indicating autophagosomal recruitment (Nowak et al., 2009). Knockdown of TP53INP2 in HeLa cells reduces rapamycin-induced accumulation of LC3-II, as well as the number of RFP-LC3 punctae per cell. Also, less Beclin1 is recruited to the autophagosomes upon knockdown of TP53INP2. The rapamycin-induced recruitment of TP53INP2 to autophagosomes is dependent of autophagy: it depends on ATG5, as demonstrated in ATG5$^{-/-}$ MEFs, and it is stimulated by rapamycin. Further, it depends on PI3K as revealed by inhibition by the PI3K inhibitor wortmannin (Nowak et al., 2009).

Huang and Liu (2015) determined the molecular mechanisms underlying recruitment of LC3 from the nucleus to the cytoplasm (Liu and Klionsky, 2015). By use of an NES mutant of TP53INP2/DOR, which cannot exit the nucleus, LC3 is captured in the nucleus under starvation. This data suggest that TP53INP2/DOR mediates export of nuclear LC3 during autophagy (Huang and Liu, 2015). Also, loss of Beclin1 and ATG14 inhibits the exit (Huang and Liu, 2015). Upon nutrient deprivation, SIRT1 deacetylates nuclear LC3 at K49 and K51. SIRT1 is activated by metabolic stress and functions as essential activator of autophagy by deacetylating its substrates, among them p53 and ATGs (Vaziri et al., 2001; Lee et al., 2008; Lapierre et al., 2015). This increases the interaction of TP53INP2/DOR with deacetylated LC3 and mediates cytosolic export of LC3. The authors show that LC3 derived from the nucleus is the primary source of membrane-bound LC3. As a consequence, LC3 is lipidated and autophagosome biogenesis is initiated. Therefore, TP53INP2/DOR has a key role as a scaffold for LC3, by mediating LC3 lipidation. SIRT1 is essential for deacetylation, which is required for the interaction with ATG7 (Huang and Liu, 2015).

The autophagy regulator TP53INP2/DOR has recently been found in nucleoli. TP53INP2/DOR-RFP co-localizes with Nucleophosmin-GFP and Fibrillarin in HeLa cells. Upon co-expression of a dominant negative NPM mutant, the double leucine mutant NPMdL, which cannot exit the nucleus (Maggi et al., 2008), TP53INP2/DOR is still able to perform nucleo-cytoplasmic shuttling. However, on longer term its localization to the nucleolus is impaired (Mauvezin et al., 2012). Localization of TP53INP2/DOR is mediated by a C-terminal nucleolar localization signal (NoLS) (Xu et al., 2016). ChIP analysis identified binding to rDNA, and a nucleolar exclusion of TP53INP2/DOR led to impaired rRNA synthesis. TP53INP2/DOR is capable of directly binding to the RNA pol I pre initiation complex.

In summary, TP53INP2/DOR has a dual function by mediating ribosome biogenesis in the nucleolus and regulating autophagy.

Drosophila – RPD3

Rpd3 represents a *Drosophila* homologue of histone deacetylase 1 (HDAC1). At early stages of starvation, Rpd3 accumulates in the nucleolus and co-localizes with the nucleolar factor Fibrillarin in *Drosophila*. Following starvation, 18S rRNA and Rpd3 mRNAs increases transiently. ChIP analysis has demonstrated that Rpd3 binds to the rDNA promoter. Rpd3 upregulates rRNA synthesis, whereas a Rpd3 knockdown reduces the number of polysomes during starvation (Nakajima et al., 2016). Also, knockdown flies die faster in response to starvation. In the knockdown flies, reduced levels of *Atg9* mRNA are detected, which is induced in response to starvation in controls, revealing decreased tolerance to starvation-mediated stress.

Drosophila – Nucleostemin-Like 2

In *Drosophila*, nucleostemin-like protein NS2, which is a homologue of human NGP1/GNL2, localizes to nucleoli. Loss of NS2 results in ribosomal stress and block of nucleolar release of 60S subunits as evidenced by increased GFP-RPL11 in nucleoli (Wang and DiMario, 2017). In polyploid midgut cells, mCherry-Atg8a positive autophagosomes are detected by immunofluorescence analysis, as well as autophagosomes containing mitochondria by TEM analysis. In contrast, in larval imaginal disks induction of apoptosis is observed (Wang and DiMario, 2017).

CLIP – Nucleophagy of Nucleolar Factors in Yeast

In budding yeast, nutrient deprivation and TORC inhibition triggers nucleophagy, the selective degradation of the nuclear compartment. In particular, nucleolar factors are degraded,

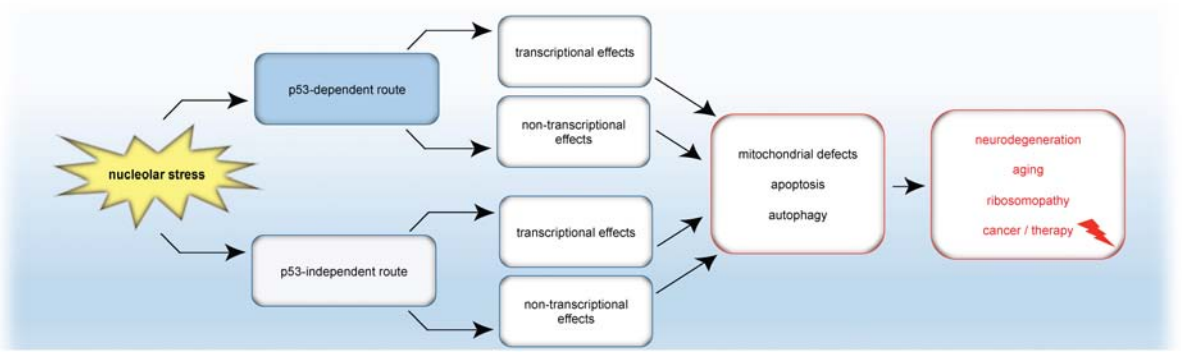

FIGURE 5 | Model: Nucleolar stress in apoptosis, autophagy and disease. Nucleolar stress triggers either the classical p53 response or p53-independent mechanisms. In turn, transcriptional programs and/or transcription-independent mechanisms are induced, which finally cause mitochondrial changes, autophagy or apoptosis. As a consequence of nucleolar stress, not only apoptosis but also autophagy is emerging as a tightly coupled stress response pathway for the formation or cure of pathological conditions.

whereas rDNA is excluded (Mostofa et al., 2018). The authors establish that autophagy induction by rapamycin triggers the redistribution of nucleolar proteins and rDNA, thereby separating rDNA from nucleophagy. CLIP and cohibin, which are essential for tethering rDNA to the inner nuclear membrane, are responsible for the repositioning of rDNA and nucleolar proteins in yeast. They are also required for the nucleophagic degradation of nucleolar factors. In contrast, rDNA is not degraded by macro-nucleophagy (Mostofa et al., 2018).

Thus, starvation-mediated autophagy, at least in yeast, removes specifically nucleolar factors. It seems likely that autophagy allows inhibition of the energy-consuming process of ribosome biogenesis by selectively removing the processing machinery.

A simplified model summarizing the emerging connection between nucleolar stress and autophagy presented in this review is given in **Figure 5**.

CLOSING REMARKS AND PERSPECTIVES

Despite the recent advances made in uncovering the relationship between nucleolar stress and autophagy, our understanding is far from being complete. A critical need to elucidate the underlying causes is apparent.

On a mechanistic level it seems likely that p53-dependent as well as -independent effects account for the induction of the autophagic nucleolar stress response.

It might well be that reduced ribosome biogenesis, by reducing protein synthesis, triggers autophagy as a general stress response. Nevertheless, extra ribosomal functions might as well coincide.

As precise underlying mechanisms are currently missing, many questions and possibilities rise: How are both signaling pathways integrated with each other? Which effects are cell type and context dependent? Under which conditions is autophagy either beneficial or a contributor to the pathology? Is there a p53 or compensatory p63/p73 autophagy response triggered in nucleolar stress? Does selective autophagy and other forms of autophagy such as micro-autophagy play a fundamental pathogenic role in other diseases connected to nucleolar stress?

The initial and common concepts of nucleolar stress and autophagy open novel avenues for investigating specific therapeutic approaches. Many autophagy inhibitors and activators might be contemplated as therapies for nucleolar-stress mediated diseases. They might well be combined with, e.g., RNA pol I inhibitors and tested for synergy to increase selectivity but simultaneously reduce toxicity for patients.

To get a deeper understanding of the underlying events, a challenge will be to elaborate state of the art autophagy methods on monitoring the autophagy flux in cellular models of diseases, patient tissues and blood samples (Jiang and Mizushima, 2014). Research on the autophagic transcriptome and spatio-temporal expression patterns of regulators of the autophagic machinery or nucleolar response will advance our knowledge on mechanisms coupling the nucleolar stress response to autophagy.

AUTHOR CONTRIBUTIONS

AP performed the literature research, conceptualization, and wrote the review.

FUNDING

AP lab is supported by Ulm University (Baustein 3.2, LSBN0101) and by Deutsche Krebshilfe (70112329).

ACKNOWLEDGMENTS

I would like to thank D. Dannheisig for initial help with the graphical illustrations. My apologies to all authors contributing, excellent work I could not cite owing space limitations.

REFERENCES

Aamann, M. D., Sorensen, M. M., Hvitby, C., Berquist, B. R., Muftuoglu, M., Tian, J., et al. (2010). Cockayne syndrome group B protein promotes mitochondrial DNA stability by supporting the DNA repair association with the mitochondrial membrane. *FASEB J.* 24, 2334–2346. doi: 10.1096/fj.09-147991

Alupei, M. C., Maity, P., Esser, P. R., Krikki, I., Tuorto, F., Parlato, R., et al. (2018). Loss of proteostasis is a pathomechanism in cockayne syndrome. *Cell Rep.* 23, 1612–1619. doi: 10.1016/j.celrep.2018.04.041

Beau, I., Esclatine, A., and Codogno, P. (2008). Lost to translation: when autophagy targets mature ribosomes. *Trends Cell Biol.* 18, 311–314. doi: 10.1016/j.tcb.2008.05.001

Behrends, C., Sowa, M. E., Gygi, S. P., and Harper, J. W. (2010). Network organization of the human autophagy system. *Nature* 466, 68–76. doi: 10.1038/nature09204

Bezzerri, V., Vella, A., Calcaterra, E., Finotti, A., Gasparello, J., Gambari, R., et al. (2016). New insights into the shwachman-diamond syndrome-related haematological disorder: hyper-activation of mTOR and STAT3 in leukocytes. *Sci. Rep.* 6:33165.

Boglev, Y., Badrock, A. P., Trotter, A. J., Du, Q., Richardson, E. J., Parslow, A. C., et al. (2013). Autophagy induction is a Tor- and Tp53-independent cell survival response in a zebrafish model of disrupted ribosome biogenesis. *PLoS Genet.* 9:e1003279. doi: 10.1371/journal.pgen.1003279

Boulon, S., Westman, B. J., Hutten, S., Boisvert, F. M., and Lamond, A. I. (2010). The nucleolus under stress. *Mol. Cell.* 40, 216–227. doi: 10.1016/j.molcel.2010.09.024

Boya, P., Gonzalez-Polo, R. A., Casares, N., Perfettini, J. L., Dessen, P., Larochette, N., et al. (2005). Inhibition of macroautophagy triggers apoptosis. *Mol. Cell. Biol.* 25, 1025–1040. doi: 10.1128/mcb.25.3.1025-1040.2005

Buchwalter, A., and Hetzer, M. W. (2017). Nucleolar expansion and elevated protein translation in premature aging. *Nat. Commun.* 8:328.

Burger, K., and Eick, D. (2013). Functional ribosome biogenesis is a prerequisite for p53 destabilization: impact of chemotherapy on nucleolar functions and RNA metabolism. *Biol. Chem.* 394, 1133–1143.

Cai, S., Liu, X., Zhang, C., Xing, B., and Du, X. (2017). Autoacetylation of NAT10 is critical for its function in rRNA transcription activation. *Biochem. Biophys. Res. Commun.* 483, 624–629. doi: 10.1016/j.bbrc.2016.12.092

Cao, R., Li, A., and Cho, H. Y. (2009). mTOR signaling in epileptogenesis: too much of a good thing? *J. Neurosci.* 29, 12372–12373. doi: 10.1523/jneurosci.3486-09.2009

Chen, H., Duo, Y., Hu, B., Wang, Z., Zhang, F., Tsai, H., et al. (2016). PICT-1 triggers a pro-death autophagy through inhibiting rRNA transcription and AKT/mTOR/p70S6K signaling pathway. *Oncotarget* 7, 78747–78763.

Chin, L. S., Olzmann, J. A., and Li, L. (2010). Parkin-mediated ubiquitin signalling in aggresome formation and autophagy. *Biochem. Soc. Trans.* 38, 144–149. doi: 10.1042/bst0380144

Codrich, M., Bertuzzi, M., Russo, R., Francescatto, M., Espinoza, S., Zentilin, L., et al. (2017). Neuronal hemoglobin affects dopaminergic cells' response to stress. *Cell Death Dis.* 8:e2538. doi: 10.1038/cddis.2016.458

Colombo, E., Alcalay, M., and Pelicci, P. G. (2011). Nucleophosmin and its complex network: a possible therapeutic target in hematological diseases. *Oncogene* 30, 2595–2609. doi: 10.1038/onc.2010.646

Colombo, E., Marine, J. C., Danovi, D., Falini, B., and Pelicci, P. G. (2002). Nucleophosmin regulates the stability and transcriptional activity of p53. *Nat. Cell Biol.* 4, 529–533. doi: 10.1038/ncb814

Crino, P. B. (2016). The mTOR signalling cascade: paving new roads to cure neurological disease. *Nat. Rev. Neurol.* 12, 379–392. doi: 10.1038/nrneurol.2016.81

Cunningham, J. T., Rodgers, J. T., Arlow, D. H., Vazquez, F., Mootha, V. K., and Puigserver, P. (2007). mTOR controls mitochondrial oxidative function through a YY1-PGC-1alpha transcriptional complex. *Nature* 450, 736–740. doi: 10.1038/nature06322

da Silva, A. M., Payao, S. L., Borsatto, B., Bertolucci, P. H., and Smith, M. A. (2000). Quantitative evaluation of the rRNA in Alzheimer's disease. *Mech. Ageing Dev.* 120, 57–64.

Dai, J., Si, J., Wang, M., Huang, L., Fang, B., Shi, J., et al. (2016). Tcof1-related molecular networks in treacher collins syndrome. *J. Craniofacial Surg.* 27, 1420–1426. doi: 10.1097/scs.0000000000002719

Dai, M. S., Zeng, S. X., Jin, Y., Sun, X. X., David, L., and Lu, H. (2004). Ribosomal protein L23 activates p53 by inhibiting MDM2 function in response to ribosomal perturbation but not to translation inhibition. *Mol. Cell. Biol.* 24, 7654–7668. doi: 10.1128/mcb.24.17.7654-7668.2004

Danilova, N., and Gazda, H. T. (2015). Ribosomopathies: how a common root can cause a tree of pathologies. *Dis. Models Mech.* 8, 1013–1026. doi: 10.1242/dmm.020529

Desantis, A., Bruno, T., Catena, V., De Nicola, F., Goeman, F., Iezzi, S., et al. (2015a). Che-1-induced inhibition of mTOR pathway enables stress-induced autophagy. *EMBO J.* 34, 1214–1230. doi: 10.15252/embj.201489920

Desantis, A., Bruno, T., Catena, V., De Nicola, F., Goeman, F., Iezzi, S., et al. (2015b). Che-1 modulates the decision between cell cycle arrest and apoptosis by its binding to p53. *Cell Death Dis.* 6:e1764. doi: 10.1038/cddis.2015.117

Ding, Q., Markesbery, W. R., Chen, Q., Li, F., and Keller, J. N. (2005). Ribosome dysfunction is an early event in Alzheimer's disease. *J. Neurosci.* 25, 9171–9175. doi: 10.1523/jneurosci.3040-05.2005

Ding, W. X., and Yin, X. M. (2012). Mitophagy: mechanisms, pathophysiological roles, and analysis. *Biol. Chem.* 393, 547–564.

Drygin, D., Lin, A., Bliesath, J., Ho, C. B., O'Brien, S. E., Proffitt, C., et al. (2011). Targeting RNA polymerase I with an oral small molecule CX-5461 inhibits ribosomal RNA synthesis and solid tumor growth. *Cancer Res.* 71, 1418–1430. doi: 10.1158/0008-5472.can-10-1728

Duo, Y., Yang, M., Du, Z., Feng, C., Xing, C., Wu, Y., et al. (2018). CX-5461-loaded nucleolus-targeting nanoplatform for cancer therapy through induction of pro-death autophagy. *Acta Biomater.* 79, 317–330. doi: 10.1016/j.actbio.2018.08.035

Ebrahimi-Fakhari, D., Wahlster, L., Hoffmann, G. F., and Kolker, S. (2014). Emerging role of autophagy in pediatric neurodegenerative and neurometabolic diseases. *Pediatr. Res.* 75, 217–226. doi: 10.1038/pr.2013.185

Eichler, D. C., and Craig, N. (1994). Processing of eukaryotic ribosomal RNA. *Prog. Nucleic Acid Res. Mol. Biol.* 49, 197–239. doi: 10.1016/s0079-6603(08)60051-3

Evsyukov, V., Domanskyi, A., Bierhoff, H., Gispert, S., Mustafa, R., Schlaudraff, F., et al. (2017). Genetic mutations linked to Parkinson's disease differentially control nucleolar activity in pre-symptomatic mouse models. *Dis. Models Mech.* 10, 633–643. doi: 10.1242/dmm.028092

Fatica, A., and Tollervey, D. (2002). Making ribosomes. *Curr. Opin. Cell Biol.* 14, 313–318. doi: 10.1016/s0955-0674(02)00336-8

Frankel, L. B., Lubas, M., and Lund, A. H. (2017). Emerging connections between RNA and autophagy. *Autophagy* 13, 3–23. doi: 10.1080/15548627.2016.1222992

Freed, E. F., Bleichert, F., Dutca, L. M., and Baserga, S. J. (2010). When ribosomes go bad: diseases of ribosome biogenesis. *Mol. Biosyst.* 6, 481–493.

Fullgrabe, J., Ghislat, G., Cho, D. H., and Rubinsztein, D. C. (2016). Transcriptional regulation of mammalian autophagy at a glance. *J. Cell Sci.* 129, 3059–3066. doi: 10.1242/jcs.188920

Fumagalli, S., Ivanenkov, V. V., Teng, T., and Thomas, G. (2012). Suprainduction of p53 by disruption of 40S and 60S ribosome biogenesis leads to the activation of a novel G2/M checkpoint. *Genes Dev.* 26, 1028–1040. doi: 10.1101/gad.189951.112

Garcia Moreno, L. M., Cimadevilla, J. M., Gonzalez Pardo, H., Zahonero, M. C., and Arias, J. L. (1997). NOR activity in hippocampal areas during the postnatal development and ageing. *Mech. Ageing Dev.* 97, 173–181. doi: 10.1016/s0047-6374(97)00054-7

Geisler, S., Holmstrom, K. M., Skujat, D., Fiesel, F. C., Rothfuss, O. C., Kahle, P. J., et al. (2010). PINK1/Parkin-mediated mitophagy is dependent on VDAC1 and p62/SQSTM1. *Nat. Cell Biol.* 12, 119–131. doi: 10.1038/ncb2012

Ghavami, S., Shojaei, S., Yeganeh, B., Ande, S. R., Jangamreddy, J. R., Mehrpour, M., et al. (2014). Autophagy and apoptosis dysfunction in neurodegenerative disorders. *Prog. Neurobiol.* 112, 24–49.

Gottlieb, R. A., Andres, A. M., Sin, J., and Taylor, D. P. (2015). Untangling autophagy measurements: all fluxed up. *Circ. Res.* 116, 504–514. doi: 10.1161/circresaha.116.303787

Goudarzi, K. M., Nister, M., and Lindstrom, M. S. (2014). mTOR inhibitors blunt the p53 response to nucleolar stress by regulating RPL11 and MDM2 levels. *Cancer Biol. Ther.* 15, 1499–1514. doi: 10.4161/15384047.2014.955743

Granneman, S., and Baserga, S. J. (2004). Ribosome biogenesis: of knobs and RNA processing. *Exp. Cell Res.* 296, 43–50. doi: 10.1016/j.yexcr.2004.03.016

Ha, J. Y., Kim, J. S., Kim, S. E., and Son, J. H. (2014). Simultaneous activation of mitophagy and autophagy by staurosporine protects against dopaminergic neuronal cell death. *Neurosci. Lett.* 561, 101–106. doi: 10.1016/j.neulet.2013.12.064

Hamacher-Brady, A., and Brady, N. R. (2016). Mitophagy programs: mechanisms and physiological implications of mitochondrial targeting by autophagy. *Cell. Mol. Life Sci.* 73, 775–795. doi: 10.1007/s00018-015-2087-8

Hanahan, D., and Weinberg, R. A. (2000). The hallmarks of cancer. *Cell* 100, 57–70.

Hanahan, D., and Weinberg, R. A. (2011). Hallmarks of cancer: the next generation. *Cell* 144, 646–674. doi: 10.1016/j.cell.2011.02.013

Harper, J. W., Ordureau, A., and Heo, J. M. (2018). Building and decoding ubiquitin chains for mitophagy. *Nat. Rev. Mol. Cell Biol.* 19, 93–108. doi: 10.1038/nrm.2017.129

Heijnen, H. F., van Wijk, R., Pereboom, T. C., Goos, Y. J., Seinen, C. W., van Oirschot, B. A., et al. (2014). Ribosomal protein mutations induce autophagy through S6 kinase inhibition of the insulin pathway. *PLoS Genet.* 10:e1004371. doi: 10.1371/journal.pgen.1004371

Heo, J. M., Ordureau, A., Paulo, J. A., Rinehart, J., and Harper, J. W. (2015). The PINK1-PARKIN mitochondrial ubiquitylation pathway drives a program of OPTN/NDP52 recruitment and TBK1 activation to promote mitophagy. *Mol. Cell.* 60, 7–20. doi: 10.1016/j.molcel.2015.08.016

Hetman, M., and Pietrzak, M. (2012). Emerging roles of the neuronal nucleolus. *Trends Neurosci.* 35, 305–314. doi: 10.1016/j.tins.2012.01.002

Hetman, M., and Slomnicki, L. P. (2019). Ribosomal biogenesis as an emerging target of neurodevelopmental pathologies. *J. Neurochem.* 148, 325–347. doi: 10.1111/jnc.14576

Holmberg Olausson, K., Nister, M., and Lindstrom, M. S. (2012). p53 -dependent and -independent nucleolar stress responses. *Cells* 1, 774–798. doi: 10.3390/cells1040774

Hoshino, A., Mita, Y., Okawa, Y., Ariyoshi, M., Iwai-Kanai, E., Ueyama, T., et al. (2013). Cytosolic p53 inhibits Parkin-mediated mitophagy and promotes mitochondrial dysfunction in the mouse heart. *Nat. Commun.* 4:2308.

Huang, R., and Liu, W. (2015). Identifying an essential role of nuclear LC3 for autophagy. *Autophagy* 11, 852–853. doi: 10.1080/15548627.2015.1038016

Iacono, D., O'Brien, R., Resnick, S. M., Zonderman, A. B., Pletnikova, O., Rudow, G., et al. (2008). Neuronal hypertrophy in asymptomatic Alzheimer disease. *J. Neuropathol. Exp. Neurol.* 67, 578–589. doi: 10.1097/nen.0b013e3181772794

Ito, S., Horikawa, S., Suzuki, T., Kawauchi, H., Tanaka, Y., Suzuki, T., et al. (2014). Human NAT10 is an ATP-dependent RNA acetyltransferase responsible for N4-acetylcytidine formation in 18 S ribosomal RNA (rRNA). *J. Biol. Chem.* 289, 35724–35730. doi: 10.1074/jbc.c114.602698

James, A., Cindass, R., Mayer, D., Terhoeve, S., Mumphrey, C., and DiMario, P. (2013). Nucleolar stress in *Drosophila melanogaster*: RNAi-mediated depletion of Nopp140. *Nucleus* 4, 123–133. doi: 10.4161/nucl.23944

James, A., Wang, Y., Raje, H., Rosby, R., and DiMario, P. (2014). Nucleolar stress with and without p53. *Nucleus* 5, 402–426. doi: 10.4161/nucl.32235

Jiang, P., and Mizushima, N. (2014). Autophagy and human diseases. *Cell Res.* 24, 69–79.

Kamenisch, Y., Fousteri, M., Knoch, J., von Thaler, A. K., Fehrenbacher, B., Kato, H., et al. (2010). Proteins of nucleotide and base excision repair pathways interact in mitochondria to protect from loss of subcutaneous fat, a hallmark of aging. *J. Exp. Med.* 207, 379–390. doi: 10.1084/jem.20091834

Kampen, K. R., Sulima, S. O., and Keersmaecker, K. (2018). Rise of the specialized onco-ribosomes. *Oncotarget* 9, 35205–35206.

Karikkineth, A. C., Scheibye-Knudsen, M., Fivenson, E., Croteau, D. L., and Bohr, V. A. (2017). Cockayne syndrome: clinical features, model systems and pathways. *Ageing Res. Rev.* 33, 3–17. doi: 10.1016/j.arr.2016.08.002

Katagiri, N., Kuroda, T., Kishimoto, H., Hayashi, Y., Kumazawa, T., and Kimura, K. (2015). The nucleolar protein nucleophosmin is essential for autophagy induced by inhibiting Pol I transcription. *Sci. Rep.* 5:8903.

Kenzelmann Broz, D., Spano Mello, S., Bieging, K. T., Jiang, D., Dusek, R. L., Brady, C. A., et al. (2013). Global genomic profiling reveals an extensive p53-regulated autophagy program contributing to key p53 responses. *Genes Dev.* 27, 1016–1031. doi: 10.1101/gad.212282.112

Khaminets, A., Behl, C., and Dikic, I. (2016). Ubiquitin-dependent and independent signals in selective autophagy. *Trends Cell Biol.* 26, 6–16. doi: 10.1016/j.tcb.2015.08.010

Kirkin, V., McEwan, D. G., Novak, I., and Dikic, I. (2009). A role for ubiquitin in selective autophagy. *Mol. Cell.* 34, 259–269. doi: 10.1016/j.molcel.2009.04.026

Klionsky, D. J. (2011). For the last time, it is GFP-Atg8, not Atg8-GFP (and the same goes for LC3). *Autophagy* 7, 1093–1094. doi: 10.4161/auto.7.10.15492

Klionsky, D. J., Abdelmohsen, K., Abe, A., Abedin, M. J., Abeliovich, H., Acevedo Arozena, A., et al. (2016). Guidelines for the use and interpretation of assays for monitoring autophagy (3rd edition). *Autophagy* 12, 1–222.

Knaevelsrud, H., and Simonsen, A. (2010). Fighting disease by selective autophagy of aggregate-prone proteins. *FEBS Lett.* 584, 2635–2645. doi: 10.1016/j.febslet.2010.04.041

Koch, S., Garcia Gonzalez, O., Assfalg, R., Schelling, A., Schafer, P., Scharffetter-Kochanek, K., et al. (2014). Cockayne syndrome protein A is a transcription factor of RNA polymerase I and stimulates ribosomal biogenesis and growth. *Cell Cycle* 13, 2029–2037. doi: 10.4161/cc.29018

Komatsu, M., Waguri, S., Chiba, T., Murata, S., Iwata, J., Tanida, I., et al. (2006). Loss of autophagy in the central nervous system causes neurodegeneration in mice. *Nature* 441, 880–884. doi: 10.1038/nature04723

Kong, R., Zhang, L., Hu, L., Peng, Q., Han, W., Du, X., et al. (2011). hALP, a novel transcriptional U three protein (t-UTP), activates RNA polymerase I transcription by binding and acetylating the upstream binding factor (UBF). *J. Biol. Chem.* 286, 7139–7148. doi: 10.1074/jbc.m110.173393

Kraft, C., and Peter, M. (2008). Is the Rsp5 ubiquitin ligase involved in the regulation of ribophagy? *Autophagy* 4, 838–840. doi: 10.4161/auto.6603

Kraft, L. J., Manral, P., Dowler, J., and Kenworthy, A. K. (2016). Nuclear LC3 associates with slowly diffusing complexes that survey the nucleolus. *Traffic* 17, 369–399. doi: 10.1111/tra.12372

Kreiner, G., Bierhoff, H., Armentano, M., Rodriguez-Parkitna, J., Sowodniok, K., Naranjo, J. R., et al. (2013). A neuroprotective phase precedes striatal degeneration upon nucleolar stress. *Cell Death. Diff.* 20, 1455–1464. doi: 10.1038/cdd.2013.66

Kroemer, G., Galluzzi, L., and Brenner, C. (2007). Mitochondrial membrane permeabilization in cell death. *Physiol. Rev.* 87, 99–163. doi: 10.1152/physrev.00013.2006

Kroemer, G., and Jaattela, M. (2005). Lysosomes and autophagy in cell death control. *Nat. Rev. Cancer* 5, 886–897. doi: 10.1038/nrc1738

Kulkarni, S., Dolezal, J. M., Wang, H., Jackson, L., Lu, J., Frodey, B. P., et al. (2017). Ribosomopathy-like properties of murine and human cancers. *PLoS One* 12:e0182705. doi: 10.1371/journal.pone.0182705

Lamark, T., and Johansen, T. (2012). Aggrephagy: selective disposal of protein aggregates by macroautophagy. *Int. J. Cell Biol.* 2012:736905.

Lamark, T., Kirkin, V., Dikic, I., and Johansen, T. (2009). NBR1 and p62 as cargo receptors for selective autophagy of ubiquitinated targets. *Cell Cycle* 8, 1986–1990. doi: 10.4161/cc.8.13.8892

Lapierre, L. R., Kumsta, C., Sandri, M., Ballabio, A., and Hansen, M. (2015). Transcriptional and epigenetic regulation of autophagy in aging. *Autophagy* 11, 867–880. doi: 10.1080/15548627.2015.1034410

Laplante, M., and Sabatini, D. M. (2009). mTOR signaling at a glance. *J. Cell Sci.* 122, 3589–3594. doi: 10.1242/jcs.051011

Lazarou, M., Sliter, D. A., Kane, L. A., Sarraf, S. A., Wang, C., Burman, J. L., et al. (2015). The ubiquitin kinase PINK1 recruits autophagy receptors to induce mitophagy. *Nature* 524, 309–314. doi: 10.1038/nature14893

Lebedev, A., Scharffetter-Kochanek, K., and Iben, S. (2008). Truncated Cockayne syndrome B protein represses elongation by RNA polymerase I. *J. Mol. Biol.* 382, 266–274. doi: 10.1016/j.jmb.2008.07.018

Lee, I. H., Cao, L., Mostoslavsky, R., Lombard, D. B., Liu, J., Bruns, N. E., et al. (2008). A role for the NAD-dependent deacetylase Sirt1 in the regulation of autophagy. *Proc. Natl. Acad. Sci. U.S.A.* 105, 3374–3379. doi: 10.1073/pnas.0712145105

Levine, B., and Kroemer, G. (2008). Autophagy in the pathogenesis of disease. *Cell* 132, 27–42. doi: 10.1016/j.cell.2007.12.018

Levine, B., Liu, R., Dong, X., and Zhong, Q. (2015). Beclin orthologs: integrative hubs of cell signaling, membrane trafficking, and physiology. *Trends Cell Biol.* 25, 533–544. doi: 10.1016/j.tcb.2015.05.004

Li, G., Jiang, H., Chang, M., Xie, H., and Hu, L. (2011). HDAC6 alpha-tubulin deacetylase: a potential therapeutic target in neurodegenerative diseases. *J. Neurol. Sci.* 304, 1–8. doi: 10.1016/j.jns.2011.02.017

Li, L., Li, Y., Zhao, J., Fan, S., Wang, L., and Li, X. (2016). CX-5461 induces autophagy and inhibits tumor growth via mammalian target of

rapamycin-related signaling pathways in osteosarcoma. *OncoTargets Ther.* 9, 5985–5997. doi: 10.2147/ott.s104513

Liang, Q., Luo, Z., Zeng, J., Chen, W., Foo, S. S., Lee, S. A., et al. (2016). Zika virus NS4A and NS4B proteins deregulate Akt-mTOR signaling in human fetal neural stem cells to inhibit neurogenesis and induce autophagy. *Cell Stem Cell* 19, 663–671. doi: 10.1016/j.stem.2016.07.019

Liang, X. H., Kleeman, L. K., Jiang, H. H., Gordon, G., Goldman, J. E., Berry, G., et al. (1998). Protection against fatal Sindbis virus encephalitis by beclin, a novel Bcl-2-interacting protein. *J. Virol.* 72, 8586–8596.

Lindstrom, M. S. (2011). NPM1/B23: a multifunctional chaperone in ribosome biogenesis and chromatin remodeling. *Biochem. Res. Int.* 2011:195209.

Lindstrom, M. S., Jurada, D., Bursac, S., Orsolic, I., Bartek, J., and Volarevic, S. (2018). Nucleolus as an emerging hub in maintenance of genome stability and cancer pathogenesis. *Oncogene* 37, 2351–2366. doi: 10.1038/s41388-017-0121-z

Liu, X., Cai, S., Zhang, C., Liu, Z., Luo, J., Xing, B., et al. (2018). Deacetylation of NAT10 by Sirt1 promotes the transition from rRNA biogenesis to autophagy upon energy stress. *Nucleic Acids Res.* 46, 9601–9616. doi: 10.1093/nar/gky777

Liu, X., and Klionsky, D. J. (2015). TP53INP2/DOR protein chaperones deacetylated nuclear LC3 to the cytoplasm to promote macroautophagy. *Autophagy* 11, 1441–1442. doi: 10.1080/15548627.2015.1074373

Maggi, L. B., Kuchenruether, M., Dadey, D. Y., Schwope, R. M., Grisendi, S., Townsend, R. R., et al. (2008). Nucleophosmin serves as a rate-limiting nuclear export chaperone for the Mammalian ribosome. *Mol. Cell. Biol.* 28, 7050–7065. doi: 10.1128/mcb.01548-07

Maiuri, M. C., Zalckvar, E., Kimchi, A., and Kroemer, G. (2007). Self-eating and self-killing: crosstalk between autophagy and apoptosis. *Nat. Rev. Mol. Cell Biol.* 8, 741–752. doi: 10.1038/nrm2239

Majora, M., Sondenheimer, K., Knechten, M., Uthe, I., Esser, C., Schiavi, A., et al. (2018). HDAC inhibition improves autophagic and lysosomal function to prevent loss of subcutaneous fat in a mouse model of Cockayne syndrome. *Sci. Transl. Med.* 10, eaam7510. doi: 10.1126/scitranslmed.aam7510

Mangan, H., Gailin, M. O., and McStay, B. (2017). Integrating the genomic architecture of human nucleolar organizer regions with the biophysical properties of nucleoli. *FEBS J.* 3977–3955.

Marino, G., Niso-Santano, M., Baehrecke, E. H., and Kroemer, G. (2014). Self-consumption: the interplay of autophagy and apoptosis. *Nat. Rev. Mol. Cell Biol.* 15, 81–94. doi: 10.1038/nrm3735

Marquez-Lona, E. M., Tan, Z., and Schreiber, S. S. (2012). Nucleolar stress characterized by downregulation of nucleophosmin: a novel cause of neuronal degeneration. *Biochem. Biophys. Res. Commun.* 417, 514–520. doi: 10.1016/j.bbrc.2011.11.152

Marx, V. (2015). Autophagy: eat thyself, sustain thyself. *Nat. Methods* 12, 1121–1125. doi: 10.1038/nmeth.3661

Mauvezin, C., Sancho, A., Ivanova, S., Palacin, M., and Zorzano, A. (2012). DOR undergoes nucleo-cytoplasmic shuttling, which involves passage through the nucleolus. *FEBS Lett.* 586, 3179–3186. doi: 10.1016/j.febslet.2012.06.032

Mijaljica, D., and Devenish, R. J. (2013). Nucleophagy at a glance. *J. Cell Sci.* 126, 4325–4330. doi: 10.1242/jcs.133090

Mizushima, N. (2007). Autophagy: process and function. *Genes Dev.* 21, 2861–2873. doi: 10.1101/gad.1599207

Mizushima, N., and Yoshimori, T. (2007). How to interpret LC3 immunoblotting. *Autophagy* 3, 542–545. doi: 10.4161/auto.4600

Mizushima, N., Yoshimori, T., and Levine, B. (2010). Methods in mammalian autophagy research. *Cell* 140, 313–326. doi: 10.1016/j.cell.2010.01.028

Montanaro, L., Trere, D., and Derenzini, M. (2008). Nucleolus, ribosomes, and cancer. *Am. J. Pathol.* 173, 301–310. doi: 10.2353/ajpath.2008.070752

Mostofa, M. G., Rahman, M. A., Koike, N., Yeasmin, A. M., Islam, N., Waliullah, T. M., et al. (2018). CLIP and cohibin separate rDNA from nucleolar proteins destined for degradation by nucleophagy. *J. Cell Biol.* 217, 2675–2690. doi: 10.1083/jcb.201706164

Mrakovcic, M., and Frohlich, L. F. (2018). p53-mediated molecular control of autophagy in tumor cells. *Biomolecules* 8, E14.

Mukhopadhyay, S., Panda, P. K., Sinha, N., Das, D. N., and Bhutia, S. K. (2014). Autophagy and apoptosis: where do they meet? *Apoptosis* 19, 555–566. doi: 10.1007/s10495-014-0967-2

Mullineux, S. T., and Lafontaine, D. L. (2012). Mapping the cleavage sites on mammalian pre-rRNAs: where do we stand? *Biochimie* 94, 1521–1532. doi: 10.1016/j.biochi.2012.02.001

Nakajima, E., Shimaji, K., Umegawachi, T., Tomida, S., Yoshida, H., Yoshimoto, N., et al. (2016). The histone deacetylase gene rpd3 is required for starvation stress resistance. *PLoS One* 11:e0167554. doi: 10.1371/journal.pone.0167554

Narendra, D., Tanaka, A., Suen, D. F., and Youle, R. J. (2008). Parkin is recruited selectively to impaired mitochondria and promotes their autophagy. *J. Cell Biol.* 183, 795–803. doi: 10.1083/jcb.200809125

Narla, A., and Ebert, B. L. (2010). Ribosomopathies: human disorders of ribosome dysfunction. *Blood* 115, 3196–3205. doi: 10.1182/blood-2009-10-178129

Nguyen, T. N., Padman, B. S., Usher, J., Oorschot, V., Ramm, G., and Lazarou, M. (2016). Atg8 family LC3/GABARAP proteins are crucial for autophagosome-lysosome fusion but not autophagosome formation during PINK1/Parkin mitophagy and starvation. *J. Cell Biol.* 215, 857–874. doi: 10.1083/jcb.201607039

Nicklas, W. J., Youngster, S. K., Kindt, M. V., and Heikkila, R. E. (1987). MPTP, MPP+ and mitochondrial function. *Life Sci.* 40, 721–729.

Nowak, J., Archange, C., Tardivel-Lacombe, J., Pontarotti, P., Pebusque, M. J., Vaccaro, M. I., et al. (2009). The TP53INP2 protein is required for autophagy in mammalian cells. *Mol. Biol. Cell* 20, 870–881. doi: 10.1091/mbc.e08-07-0671

Park, Y. E., Hayashi, Y. K., Bonne, G., Arimura, T., Noguchi, S., Nonaka, I., et al. (2009). Autophagic degradation of nuclear components in mammalian cells. *Autophagy* 5, 795–804. doi: 10.4161/auto.8901

Parlato, R., and Kreiner, G. (2013). Nucleolar activity in neurodegenerative diseases: a missing piece of the puzzle? *J. Mol. Med.* 91, 541–547. doi: 10.1007/s00109-012-0981-1

Parlato, R., and Liss, B. (2014). How Parkinson's disease meets nucleolar stress. *Biochim. Biophys. Acta* 1842, 791–797. doi: 10.1016/j.bbadis.2013.12.014

Pattingre, S., Espert, L., Biard-Piechaczyk, M., and Codogno, P. (2008). Regulation of macroautophagy by mTOR and Beclin 1 complexes. *Biochimie* 90, 313–323. doi: 10.1016/j.biochi.2007.08.014

Payao, S. L., Smith, M. A., Winter, L. M., and Bertolucci, P. H. (1998). Ribosomal RNA in Alzheimer's disease and aging. *Mech. Ageing Dev.* 105, 265–272.

Penzo, M., Montanaro, L., Trere, D., and Derenzini, M. (2019). The ribosome biogenesis-cancer connection. *Cells* 8:55. doi: 10.3390/cells8010055

Pestov, D. G., Strezoska, Z., and Lau, L. F. (2001). Evidence of p53-dependent cross-talk between ribosome biogenesis and the cell cycle: effects of nucleolar protein Bop1 on G(1)/S transition. *Mol. Cell. Biol.* 21, 4246–4255. doi: 10.1128/mcb.21.13.4246-4255.2001

Pfister, A. S., and Kuhl, M. (2018). Of Wnts and ribosomes. *Prog. Mol. Biol. Transl. Sci.* 153, 131–155. doi: 10.1016/bs.pmbts.2017.11.006

Pickrell, A. M., and Youle, R. J. (2015). The roles of PINK1, parkin, and mitochondrial fidelity in Parkinson's disease. *Neuron* 85, 257–273. doi: 10.1016/j.neuron.2014.12.007

Pietrzak, M., Rempala, G., Nelson, P. T., Zheng, J. J., and Hetman, M. (2011). Epigenetic silencing of nucleolar rRNA genes in Alzheimer's disease. *PLoS One* 6:e22585. doi: 10.1371/journal.pone.0022585

Polager, S., and Ginsberg, D. (2009). p53 and E2f: partners in life and death. *Nat. Rev. Cancer* 9, 738–748. doi: 10.1038/nrc2718

Potmesil, M., and Goldfeder, A. (1977). Identification and kinetics of G1 phase-confined cells in experimental mammary carcinomas. *Cancer Res.* 37, 857–864.

Rieker, C., Engblom, D., Kreiner, G., Domanskyi, A., Schober, A., Stotz, S., et al. (2011). Nucleolar disruption in dopaminergic neurons leads to oxidative damage and parkinsonism through repression of mammalian target of rapamycin signaling. *J. Neurosci.* 31, 453–460. doi: 10.1523/jneurosci.0590-10.2011

Rubbi, C. P., and Milner, J. (2003). Disruption of the nucleolus mediates stabilization of p53 in response to DNA damage and other stresses. *EMBO J.* 22, 6068–6077. doi: 10.1093/emboj/cdg579

Rubinsztein, D. C. (2006). The roles of intracellular protein-degradation pathways in neurodegeneration. *Nature* 443, 780–786. doi: 10.1038/nature05291

Sakai, D., and Trainor, P. A. (2009). Treacher Collins syndrome: unmasking the role of Tcof1/treacle. *Int. J. Biochem. Cell Biol.* 41, 1229–1232. doi: 10.1016/j.biocel.2008.10.026

Sasaki, M., Kawahara, K., Nishio, M., Mimori, K., Kogo, R., Hamada, K., et al. (2011). Regulation of the MDM2-P53 pathway and tumor growth by PICT1 via nucleolar RPL11. *Nat. Med.* 17, 944–951. doi: 10.1038/nm.2392

Scheibye-Knudsen, M., Ramamoorthy, M., Sykora, P., Maynard, S., Lin, P. C., Minor, R. K., et al. (2012). Cockayne syndrome group B protein prevents

the accumulation of damaged mitochondria by promoting mitochondrial autophagy. *J. Exp. Med.* 209, 855–869. doi: 10.1084/jem.20111721

Schneider, J. L., and Cuervo, A. M. (2014). Autophagy and human disease: emerging themes. *Curr. Opin. Genet. Dev.* 26, 16–23. doi: 10.1016/j.gde.2014.04.003

Seo, A. Y., Joseph, A. M., Dutta, D., Hwang, J. C., Aris, J. P., and Leeuwenburgh, C. (2010). New insights into the role of mitochondria in aging: mitochondrial dynamics and more. *J. Cell Sci.* 123, 2533–2542. doi: 10.1242/jcs.070490

Seshadri, S., Wolf, P. A., Beiser, A., Au, R., McNulty, K., White, R., et al. (1997). Lifetime risk of dementia and Alzheimer's disease. The impact of mortality on risk estimates in the Framingham Study. *Neurology* 49, 1498–1504.

Stambolic, V., MacPherson, D., Sas, D., Lin, Y., Snow, B., Jang, Y., et al. (2001). Regulation of PTEN transcription by p53. *Mol. Cell.* 8, 317–325. doi: 10.1016/s1097-2765(01)00323-9

Sulima, S. O., Hofman, I. J. F., De Keersmaecker, K., and Dinman, J. D. (2017). How ribosomes translate cancer. *Cancer Discov.* 7, 1069–1087. doi: 10.1158/2159-8290.cd-17-0550

Suzuki, A., Kogo, R., Kawahara, K., Sasaki, M., Nishio, M., Maehama, T., et al. (2012). A new PICTure of nucleolar stress. *Cancer Sci.* 103, 632–637. doi: 10.1111/j.1349-7006.2012.02219.x

Switon, K., Kotulska, K., Janusz-Kaminska, A., Zmorzynska, J., and Jaworski, J. (2017). Molecular neurobiology of mTOR. *Neuroscience* 341, 112–153.

Tiku, V., and Antebi, A. (2018). Nucleolar function in lifespan regulation. *Trends Cell Biol.* 28, 662–672. doi: 10.1016/j.tcb.2018.03.007

Tiku, V., Jain, C., Raz, Y., Nakamura, S., Heestand, B., Liu, W., et al. (2016). Small nucleoli are a cellular hallmark of longevity. *Nat. Commun.* 8:16083. doi: 10.1038/ncomms16083

Valdez, B. C., Henning, D., So, R. B., Dixon, J., and Dixon, M. J. (2004). The treacher Collins syndrome (TCOF1) gene product is involved in ribosomal DNA gene transcription by interacting with upstream binding factor. *Proc. Natl. Acad. Sci. U.S.A.* 101, 10709–10714. doi: 10.1073/pnas.0402492101

Vashishta, A., Slomnicki, L. P., Pietrzak, M., Smith, S. C., Kolikonda, M., Naik, S. P., et al. (2018). RNA polymerase 1 is transiently regulated by seizures and plays a role in a pharmacological kindling model of epilepsy. *Mol. Neurobiol.* 55, 8374–8387. doi: 10.1007/s12035-018-0989-9

Vaziri, H., Dessain, S. K., Ng Eaton, E., Imai, S. I., Frye, R. A., Pandita, T. K., et al. (2001). hSIR2(SIRT1) functions as an NAD-dependent p53 deacetylase. *Cell* 107, 149–159. doi: 10.1016/s0092-8674(01)00527-x

Vives-Bauza, C., Zhou, C., Huang, Y., Cui, M., de Vries, R. L., Kim, J., et al. (2010). PINK1-dependent recruitment of Parkin to mitochondria in mitophagy. *Proc. Natl. Acad. Sci. U.S.A.* 107, 378–383.

Wang, D. B., Kinoshita, C., Kinoshita, Y., and Morrison, R. S. (2014). p53 and mitochondrial function in neurons. *Biochim. Biophys. Acta* 1842, 1186–1197.

Wang, Y., and DiMario, P. (2017). Loss of Drosophila nucleostemin 2 (NS2) blocks nucleolar release of the 60S subunit leading to ribosome stress. *Chromosoma* 126, 375–388. doi: 10.1007/s00412-016-0597-2

Westphal, D., Kluck, R. M., and Dewson, G. (2014). Building blocks of the apoptotic pore: how Bax and Bak are activated and oligomerize during apoptosis. *Cell Death. Diff.* 21, 196–205. doi: 10.1038/cdd.2013.139

Wong, Y. C., and Holzbaur, E. L. (2014). Optineurin is an autophagy receptor for damaged mitochondria in parkin-mediated mitophagy that is disrupted by an ALS-linked mutation. *Proc. Natl. Acad. Sci. U.S.A.* 111, E4439–E4448.

Woods, S. J., Hannan, K. M., Pearson, R. B., and Hannan, R. D. (2015). The nucleolus as a fundamental regulator of the p53 response and a new target for cancer therapy. *Biochim. Biophys. Acta* 1849, 821–829. doi: 10.1016/j.bbagrm.2014.10.007

Wu, H., Wang, M. C., and Bohmann, D. (2009). JNK protects *Drosophila* from oxidative stress by trancriptionally activating autophagy. *Mech. Dev.* 126, 624–637. doi: 10.1016/j.mod.2009.06.1082

Xie, R., Nguyen, S., McKeehan, W. L., and Liu, L. (2010). Acetylated microtubules are required for fusion of autophagosomes with lysosomes. *BMC Cell Biol.* 11:89. doi: 10.1186/1471-2121-11-89

Xu, Y., Wan, W., Shou, X., Huang, R., You, Z., Shou, Y., et al. (2016). TP53INP2/DOR, a mediator of cell autophagy, promotes rDNA transcription via facilitating the assembly of the POLR1/RNA polymerase I preinitiation complex at rDNA promoters. *Autophagy* 12, 1118–1128. doi: 10.1080/15548627.2016.1175693

Xue, S., and Barna, M. (2012). Specialized ribosomes: a new frontier in gene regulation and organismal biology. *Nat. Rev. Mol. Cell Biol.* 13, 355–369. doi: 10.1038/nrm3359

Yamamoto, A., and Simonsen, A. (2011). The elimination of accumulated and aggregated proteins: a role for aggrephagy in neurodegeneration. *Neurobiol. Dis.* 43, 17–28. doi: 10.1016/j.nbd.2010.08.015

Yang, H., Zhong, X., Ballar, P., Luo, S., Shen, Y., Rubinsztein, D. C., et al. (2007). Ubiquitin ligase Hrd1 enhances the degradation and suppresses the toxicity of polyglutamine-expanded huntingtin. *Exp. Cell Res.* 313, 538–550. doi: 10.1016/j.yexcr.2006.10.031

Yang, Z. J., Chee, C. E., Huang, S., and Sinicrope, F. A. (2011). The role of autophagy in cancer: therapeutic implications. *Mol. Cancer Ther.* 10, 1533–1541. doi: 10.1158/1535-7163.mct-11-0047

Yelick, P. C., and Trainor, P. A. (2015). Ribosomopathies: global process, tissue specific defects. *Rare Dis.* 3:e1025185. doi: 10.1080/21675511.2015.1025185

Yuan, X., Zhou, Y., Casanova, E., Chai, M., Kiss, E., Grone, H. J., et al. (2005). Genetic inactivation of the transcription factor TIF-IA leads to nucleolar disruption, cell cycle arrest, and p53-mediated apoptosis. *Mol. Cell* 19, 77–87. doi: 10.1016/j.molcel.2005.05.023

Zeng, L. H., Rensing, N. R., and Wong, M. (2009). The mammalian target of rapamycin signaling pathway mediates epileptogenesis in a model of temporal lobe epilepsy. *J. Neurosci.* 29, 6964–6972. doi: 10.1523/jneurosci.0066-09.2009

Zhang, C., Lin, M., Wu, R., Wang, X., Yang, B., Levine, A. J., et al. (2011). Parkin, a p53 target gene, mediates the role of p53 in glucose metabolism and the Warburg effect. *Proc. Natl. Acad. Sci. U.S.A.* 108, 16259–16264. doi: 10.1073/pnas.1113884108

Zheng, S., Clabough, E. B., Sarkar, S., Futter, M., Rubinsztein, D. C., and Zeitlin, S. O. (2010). Deletion of the huntingtin polyglutamine stretch enhances neuronal autophagy and longevity in mice. *PLoS Genet.* 6:e1000838. doi: 10.1371/journal.pgen.1000838

Zhou, B., Boudreau, N., Coulber, C., Hammarback, J., and Rabinovitch, M. (1997). Microtubule-associated protein 1 light chain 3 is a fibronectin mRNA-binding protein linked to mRNA translation in lamb vascular smooth muscle cells. *J. Clin. Invest.* 100, 3070–3082. doi: 10.1172/jci119862

Zhou, Y. Y., Li, Y., Jiang, W. Q., and Zhou, L. F. (2015). MAPK/JNK signalling: a potential autophagy regulation pathway. *Biosci. Rep.* 35:e00199.

Zlotorynski, E. (2017). Ageing: live longer with small nucleoli. *Nat. Rev. Mol. Cell Biol.*18:651. doi: 10.1038/nrm.2017.100

Zuccato, C., Valenza, M., and Cattaneo, E. (2010). Molecular mechanisms and potential therapeutical targets in Huntington's disease. *Physiol. Rev.* 90, 905–981. doi: 10.1152/physrev.00041.2009

Conflict of Interest Statement: The author declares that the research was conducted in the absence of any commercial or financial relationships that could be construed as a potential conflict of interest.

frontiers in Cellular Neuroscience

MINI REVIEW
published: 14 May 2019
doi: 10.3389/fncel.2019.00218

Roles of Primary Cilia in the Developing Brain

*Sang Min Park[1], Hee Jin Jang[1] and Jeong Ho Lee[1,2]**

[1] Biomedical Science and Engineering Interdisciplinary Program, Korea Advanced Institute of Science and Technology, Daejeon, South Korea, [2] Graduate School of Medical Science and Engineering, Korea Advanced Institute of Science and Technology, Daejeon, South Korea

Essential to development, primary cilia are microtubule-based cellular organelles that protrude from the surface of cells. Acting as cellular antenna, primary cilia play central roles in transducing or regulating several signaling pathways, including Sonic hedgehog (Shh) and Wnt signaling. Defects in primary cilia contribute to a group of syndromic disorders known as "ciliopathies" and can adversely affect development of the brain and other essential organs, including the kidneys, eyes, and liver. The molecular mechanisms of how defective primary cilia contribute to neurological defects, however, remain poorly understood. In this mini review, we summarize recent advances in understanding of the interactions between primary cilia and signaling pathways essential to cellular homeostasis and brain development.

Keywords: primary cilia, Wnt, MTOR, autophagy, ciliopathy, FMCD

OPEN ACCESS

Edited by:
Rosanna Parlato,
University of Ulm, Germany

Reviewed by:
Elisabeth Traiffort,
Institut National de la Santé et de la Recherche Médicale (INSERM), France
Esther Stoeckli,
University of Zurich, Switzerland

***Correspondence:**
Jeong Ho Lee
jhlee4246@kaist.ac.kr

Specialty section:
This article was submitted to Cellular Neurophysiology, a section of the journal Frontiers in Cellular Neuroscience

Received: *16 January 2019*
Accepted: *30 April 2019*
Published: *14 May 2019*

Citation:
Park SM, Jang HJ and Lee JH (2019) Roles of Primary Cilia in the Developing Brain. Front. Cell. Neurosci. 13:218. doi: 10.3389/fncel.2019.00218

INTRODUCTION

Primary cilia are microtubule-based cellular organelles that aid in sensing and transducing environmental signals during development (Goetz and Anderson, 2010): primary cilia transduce or regulate several signaling pathways, including Sonic hedgehog (Shh) and Wnt signaling (Corbit et al., 2005; Rohatgi et al., 2007; Gerdes and Katsanis, 2008; Goetz et al., 2009). This antenna-like structure was first observed using electron microscopy at the lumen of kidney tubules in 1898 and has since been intensively studied (Zimmermann, 1898). Emanating from the apical surface of basal body, the axoneme structure of primary cilium comprises a radial array of nine microtubule doublets lacking a central pair (9+0 structure) (**Figure 1A**; Davenport and Yoder, 2005). At the base of primary cilium, protein entry and exit are regulated via a transition fiber that anchors the axoneme to the ciliary membrane, compartmentalizing this distinct organelle from the cytosol while remaining continuous with the plasma membrane (Gherman et al., 2006; Marshall, 2008; Reiter et al., 2012).

Leading to defective primary cilia, mutations in genes necessary for ciliogenesis and ciliary structure and function are known to cause a group of human genetic disorders described as "ciliopathies." To date, 187 mutated genes in 35 known ciliopathies and 241 ciliopathy-associated genes essential to ciliary structure and function that could potentially be causative for ciliopathies have been documented (Reiter and Leroux, 2017). These ciliopathies affect the body's essential organs, including the kidneys, eyes, brain, liver, and skeleton, during development and tend to share clinical phenotypes (Hildebrandt et al., 2011): for example, as primary cilia are critical to development of the central nervous system (CNS), many ciliopathies, such as Joubert syndrome (JBTS), Meckel syndrome (MKS), and orofaciodigital syndrome (OFD), commonly exhibit neurological defects of CNS malformation, intellectual disability, ataxia, and retina

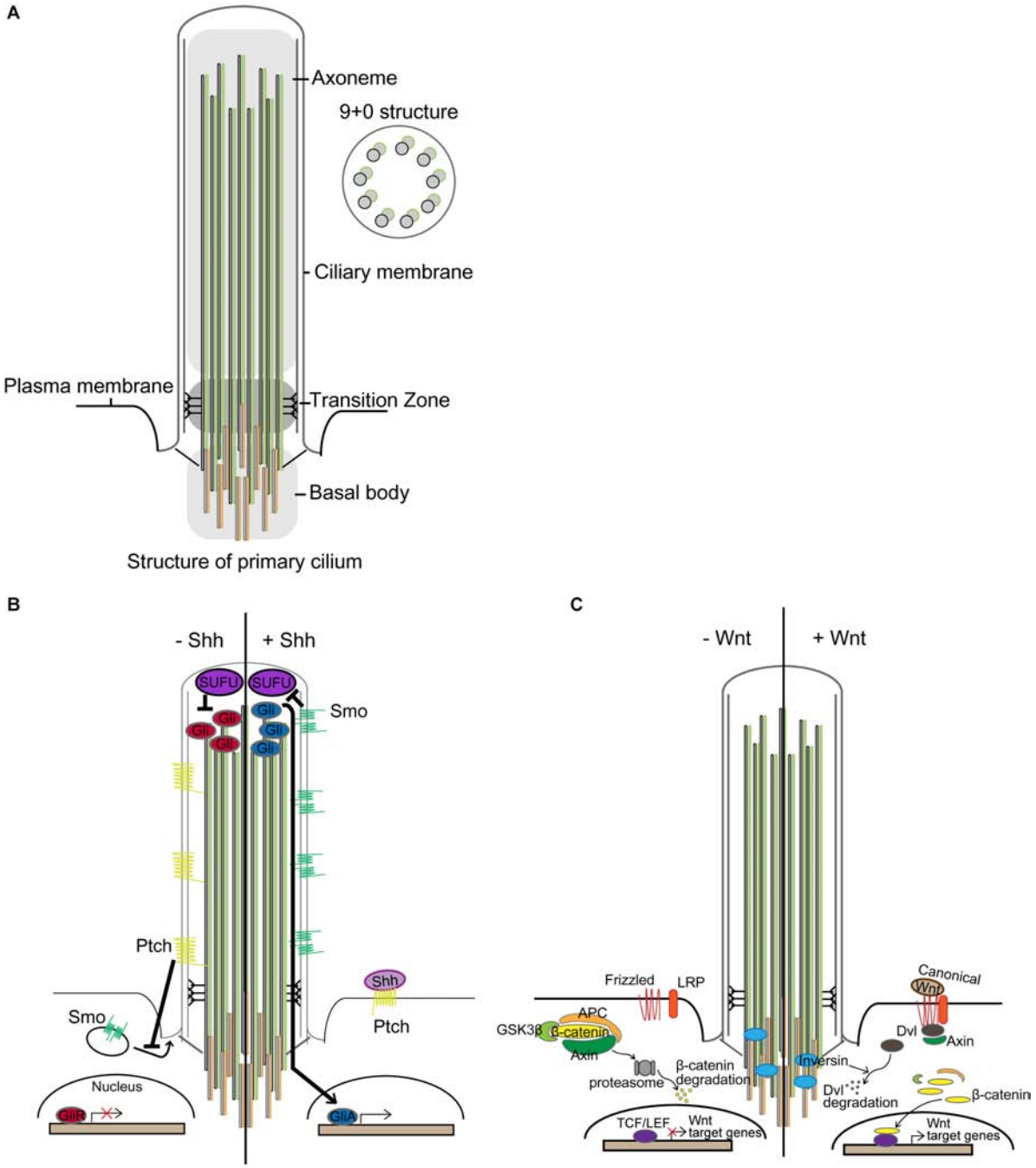

FIGURE 1 | Primary cilia and signal transduction. **(A)** Structure of primary cilium. Microtubules extend from the centriole constituting the basal body and form the axoneme. The surrounding membrane is called the ciliary membrane, distinct from other membranes. Unlike motile cilium with a 9+2 structure, primary cilium has a 9+0 structure. Only ciliary proteins are allowed to access the cilium, and the transition zone performs the filtering function. **(B)** In the absence of Shh, Patched (Ptch) inhibits the translocation of Smoothened (Smo), a membrane G protein-coupled receptor (GPCR)-like protein. Suppressor of Fused (SUFU) in the tip of the cilium represses Gli, causing Gli to be present in an inactive form. In the presence of Shh, Shh binds to Ptch, making it no longer able to suppress Smo. Smo, relieved from suppression, translocates into the cilium and represses SUFU. Gli is then converted to its active form and translocates from the cilium to the nucleus and transcribes target genes. **(C)** Primary cilia in Wnt signaling. In the absence of Wnt ligand, the β-catenin destruction complex, comprising glycogen synthase kinase 3β (GSK3β), adenomatous polyposis coli (APC), and Axin, phosphorylates β-catenin, leading to its proteasomal degradation, which occurs near the basal body. Wnt signaling is activated by binding extracellular Wnt ligand to the membrane-bounded receptor family, frizzled and low-density lipoprotein receptor-related protein (LRP). Then, the β-catenin destruction complex is destabilized by anchoring Axin to the plasma membrane through Dishevelled (Dvl), which leads to stabilization and nuclear localization of β-catenin for transcriptional activation of target genes under T-cell factor/lymphoid enhancer-binding factor (TCF/LEF) promoters (van Amerongen and Nusse, 2009). Inversin, for which ciliary localization has been reported, mediates proteasomal degradation of Dvl to regulate Wnt signaling.

dystrophy (Valente et al., 2014). Here, we summarize our recent understanding of the interactions between primary cilia and several signaling pathways essential for cellular homeostasis and for brain development.

SIGNALING PATHWAYS AND BIOLOGICAL PROCESSES MEDIATED BY PRIMARY CILIA

Shh Signaling

Sonic hedgehog signal transduction is accomplished through binding of Shh to the transmembrane receptor Patched (Ptch). In the absence of Shh, Ptch inhibits the ciliary localization of Smoothened (Smo), a membrane G protein-coupled receptor (GPCR)-like protein. When present, Shh binds to Ptch to alleviate the suppression of Smo, which, in turn, translocates to the primary cilium to repress Suppressor of Fused (SUFU) (Rohatgi et al., 2007; Tukachinsky et al., 2010; Sasai and Briscoe, 2012). This initiates the activation of Gli transcriptional factors (**Figure 1B**; Alcedo et al., 1996): Gli regulates the transcription of target genes that regulate the Shh signaling (e.g., Ptch1, Gli1), proliferation (e.g., cyclin D1, MYC), and apoptosis (e.g., Bcl-2) (Scales and de Sauvage, 2009). Shh, Ptch, Smo, and Gli are expressed in the developing and adult brain (Echelard et al., 1993; Ekker et al., 1995).

Sonic hedgehog signaling is critical to spatial patterning of the neuroepithelium, cellular identity in CNS, axonal guidance, wiring of the neural network, and neuronal activity. As Shh signaling-related proteins are located within primary cilium, Shh signaling is not properly achieved in mice with defective cilia, resulting in several defects in brain development such as defective neural patterning, cerebellar hypoplasia, and defective hippocampal neurogenesis (reviewed in Ferent and Traiffort, 2015). For example, mice with mutation in *Kinesin family member 3A (Kif3a)*, which is important for ciliogenesis, show reduced Gli1 expression, thereby leading to defects in hippocampal neurogenesis and formation of neural stem cells (Han et al., 2008). *Stumpy* mutant mice exhibit defective ciliogenesis leading to prenatal hydrocephalus and severe polycystic kidney disease. The *Stumpy* gene, located on mouse chromosome 7, encodes B9 protein domain 2 (B9D2), which is localized with basal bodies along ciliary axonemes and appears to play a role in ciliogenesis in association with intraflagellar transport proteins (IFTs) (Town et al., 2008). Conditional *Stumpy* mutant mice (driven by Nestin-Cre) have been found to show abrogated Shh signaling and Gli processing in the hippocampus (Breunig et al., 2008).

Wnt Signaling

Wnt signaling is another developmental signaling pathway mediated by primary cilia (**Figure 1C**; May-Simera and Kelley, 2012). Wnt signaling can be divided into (1) β-catenin dependent (canonical) and (2) β-catenin independent (non-canonical) signaling (reviewed in Berbari et al., 2009; Oh and Katsanis, 2013). Several studies have shown that perturbation of ciliary genes aberrantly activates canonical Wnt signaling and disrupts non-canonical Wnt signaling (Lin et al., 2003; Cano et al., 2004; Ross et al., 2005; Simons et al., 2005; Gerdes et al., 2007; Corbit et al., 2008). In particular, Inversin, which is localized in cilium, mediates the proteasomal degradation of Dishevelled (Dvl) to regulate both canonical and non-canonical Wnt signaling (Simons et al., 2005). Perturbations in several ciliopathy-related genes have been found to elicit de-regulated canonical Wnt signaling in fibroblasts and in the forebrain (Willaredt et al., 2008; Abdelhamed et al., 2013; Wheway et al., 2013). Also, ciliary ablation in adult-born dentate granule cells in the hippocampus has been shown to aberrantly activate canonical Wnt signaling, concomitant with severe defects in dendritic refinement and synapse formation (Kumamoto et al., 2012). Additionally, researchers have recently demonstrated that defective neuronal ciliogenesis caused by hyperactivating mutation in *MTOR* elicits abnormal activation of canonical Wnt signaling and inactivation of non-canonical Wnt signaling, resulting in defective neuronal migration due to disrupted neuronal polarization (Park et al., 2018). Notwithstanding, several studies have reported that ciliary dysfunction does not affect Wnt signaling, as evidenced by constant activity of Wnt signaling reporter and expression of Wnt target genes (Huang and Schier, 2009; Ocbina et al., 2009). Interestingly, however, deregulated canonical Wnt signaling via deletion of adenomatous polyposis coli (APC) was found to cause a loss of primary cilia in association with radial progenitor malformation in the neocortex (Nakagawa et al., 2017). In these regards, the interaction between primary cilia and Wnt signaling may be context-dependent, and more thorough studies will be necessary to elucidate it.

MTOR Signaling

MTOR is a serine/threonine kinase essential for protein translation, lipid synthesis, and autophagy, and plays an essential role in neural differentiation, neuronal migration, and synaptic formation, all of which are crucial to brain development. Disruption of MTOR signaling has been documented in numerous pathological conditions, including cancer, neurological disorder, and metabolic disorder (Lipton and Sahin, 2014; Saxton and Sabatini, 2017) Polycystic kidney disease (PKD) patients with inherited mutations in ciliary genes show deregulation of the MTOR signaling pathway (Shillingford et al., 2006; Wahl et al., 2006). In particular, *polycystin-1*, which is recurrently mutated in PKD, has been shown to inhibit MTOR through interaction with TSC2, a component of the TSC complex that inhibits MTOR (Shillingford et al., 2006). Studies have also identified that, by bending stimulus via fluid flow, primary cilia downregulate AMPK-MTOR signaling, which, in turn, induces autophagy to control cell size via LKB1 localized at primary cilia in the kidneys (Boehlke et al., 2010; Orhon et al., 2016). Recently, research has demonstrated that, during brain development, mice with defective cilia present abnormal increases in MTOR signaling, leading to enlarged apical domains of radial glial cells (RGCs) and subsequent dilatation of brain ventricles (Foerster et al., 2017). Conversely, in *TSC1*- or *TSC2*-null fibroblasts, TSC1 and TSC2 have been found to positively

regulate ciliogenesis without using the TSC-MTOR signaling axis (i.e., rapamycin-insensitive) (Hartman et al., 2009). Nevertheless, a recent independent study which also performed with *TSC1*- or *TSC2*-null fibroblasts reported different ciliary phenotypes marked by a longer ciliary length in *TSC1*-null cells and a shorter ciliary length in *TSC2*-null cells, and there was a discrepancy between the two cell types in that only the elongated ciliary phenotype in *TSC1*-null cells could be rescued by rapamycin treatment (Rosengren et al., 2018). In focal malformations of cortical developments (FMCDs), such as hemimegalencephaly (HME) and focal cortical dysplasia (FCD), which are highly associated with intractable epilepsy and autism-spectrum disorders, brain somatic activating mutations in *MTOR* eliciting blockage of autophagy have been described as disrupting neuronal ciliogenesis in brain tissues from FMCD patients (Wegiel et al., 2010; Lim and Crino, 2013; Park et al., 2018; **Figures 2A,B**). Given the complex reciprocal interaction between primary cilia and MTOR signaling, further mechanism studies are yet needed.

Autophagy

Autophagy is a cellular degradative process by which a cell gains nutrients to maintain homeostasis (Mizushima, 2007). Two independent studies have provided evidence of links between ciliogenesis and autophagy: In serum-nutrient conditions, basal autophagy degrades the ciliary protein IFT20, while OFD1 protein at centriolar satellites inhibits ciliogenesis. Upon serum-withdrawal, the centriolar satellite pool of OFD1 is degraded by inducible autophagy, while IFT20 initiates ciliary trafficking, leading to ciliogenesis (Pampliega et al., 2013; Tang et al., 2013). Cilia-mediated Shh signaling has been found to assemble several proteins needed for autophagy at the periciliary region, thus activating Shh signaling induces autophagy flux. Interestingly, one study described defects in serum-withdrawal-induced autophagy and biogenesis of autophagosome among Ift20- or Ift88-compromised cells (Pampliega et al., 2013). In line with this, others have found that treatment of Shh to cultured-hippocampal neurons upregulates several autophagy-related genes and enhances autophagy (Petralia et al., 2013).

Meanwhile, dysregulated ciliogenesis in relation to defective autophagy has been described in several diseases. Previous studies have reported suppressed autophagic flux in ciliary dysfunctional PKD mouse models and impairment of autophagosome formation in cells derived from PKD patients (Belibi et al., 2011; Zhu et al., 2017). Interestingly, Hürthle cells found in thyroid cancer were found to show defective ciliogenesis, and this defect in Hürthle cells eliciting high basal autophagic flux was restored by autophagy inhibition (Lee et al., 2016). Dysregulated ciliogenesis has also been reported in Huntington's disease (HD), for which defective autophagy has been well recognized (Keryer et al., 2011; Kaliszewski et al., 2015). Although *Huntingtin*, which is mutated in HD, is known to regulate autophagy, it also participates in trafficking pericentriolar material 1 (PCM1) to the centrosome. When *Huntingtin* is mutated, aberrant accumulation of PCM1 occurs, which, in turn, causes dysregulated ciliogenesis (Keryer et al., 2011; Rui et al., 2015). Further studies, however, are required to elucidate the direct interaction between ciliary abnormality and defective autophagy in HD. Finally, as stated in the previous section on MTOR signaling, defective autophagy and resultant disruption of ciliogenesis have been demonstrated in FMCDs (Park et al., 2018). Brain somatic activating mutations in *MTOR*, which are causative for FMCDs, block autophagy, resulting in defective neuronal ciliogenesis due to aberrant accumulation of OFD1 (**Figure 2C**; Park et al., 2018). Although defective autophagy has been implicated in many neurodevelopmental and neurodegenerative disorders, much more studies are needed to elucidate the pathophysiological role of primary cilia in these disorders (Levine and Kroemer, 2008; Lee et al., 2013; Marsh and Dragich, 2018).

DEVELOPMENTAL FUNCTIONS OF NEURONAL CILIA

Patterning and Morphogenesis of the Forebrain

One of the well-established developmental functions of primary cilia is to control forebrain patterning, which is severely defected in human ciliopathies (Vogel et al., 2012). Patterning in the neural tube of the CNS occurs through progressive subdivisions along the dorsal to ventral and the rostral to caudal axes (Dessaud et al., 2008). *Cobblestone* mice (*Ift88*$^{cbs/cbs}$), which show severe disorganization of the telencephalon, have been found to exhibit an ambiguous dorsal-ventral forebrain boundary and dorsal telencephalic-diencephalic boundary, concomitant with increased levels of full-length Gli3 (Willaredt et al., 2008). Meanwhile, mice lacking primary cilia as a result of mutation in the ciliopathy gene *Rpgrip1l* exhibited defective phenotypes associated with MKS and JBTS. In these mice, a mislocalized olfactory bulb-like structure and ambiguous dorsal-ventral patterning were observed, both of which were rescued upon introduction of constitutively active repressor form of Gli3 (Besse et al., 2011). Other mice with defective cilia through loss of *Ttc21b* (encoding retrograde Ift139) have also been shown to display defects in dorsal–ventral patterning and rostral–caudal patterning. Researchers have reported that *Ttc21b*-null mice exhibit normal anterograde transport that permits entry of Shh signaling components into cilium but partially defective retrograde transport. Overactivation of GLI2 and GLI3A in these mice could accounts for activation of Shh signaling and abnormal patterning, suggesting a periciliary role for retrograde IFT in GLI3 processing and GLI2 activity (Huangfu and Anderson, 2005; May et al., 2005; Tran et al., 2008; Stottmann et al., 2009). Crossing *Ttc21b*-null mice with mice heterozygous for a null allele of *Shh* to reduce levels of Shh ligand was found to partially rescue their defective phenotypes (Tran et al., 2008; Stottmann et al., 2009). This paradoxical effect of retrograde IFT mutants on Shh signaling (i.e., activation of Shh signaling) was well reviewed by Pal and Mukhopadhyay (2015) and Bangs and Anderson (2017). In line with the importance of primary cilia in cortical patterning, mice with mutant *Slb* (encoding anterograde Ift172) that possess very short axonemes with no visible microtubules

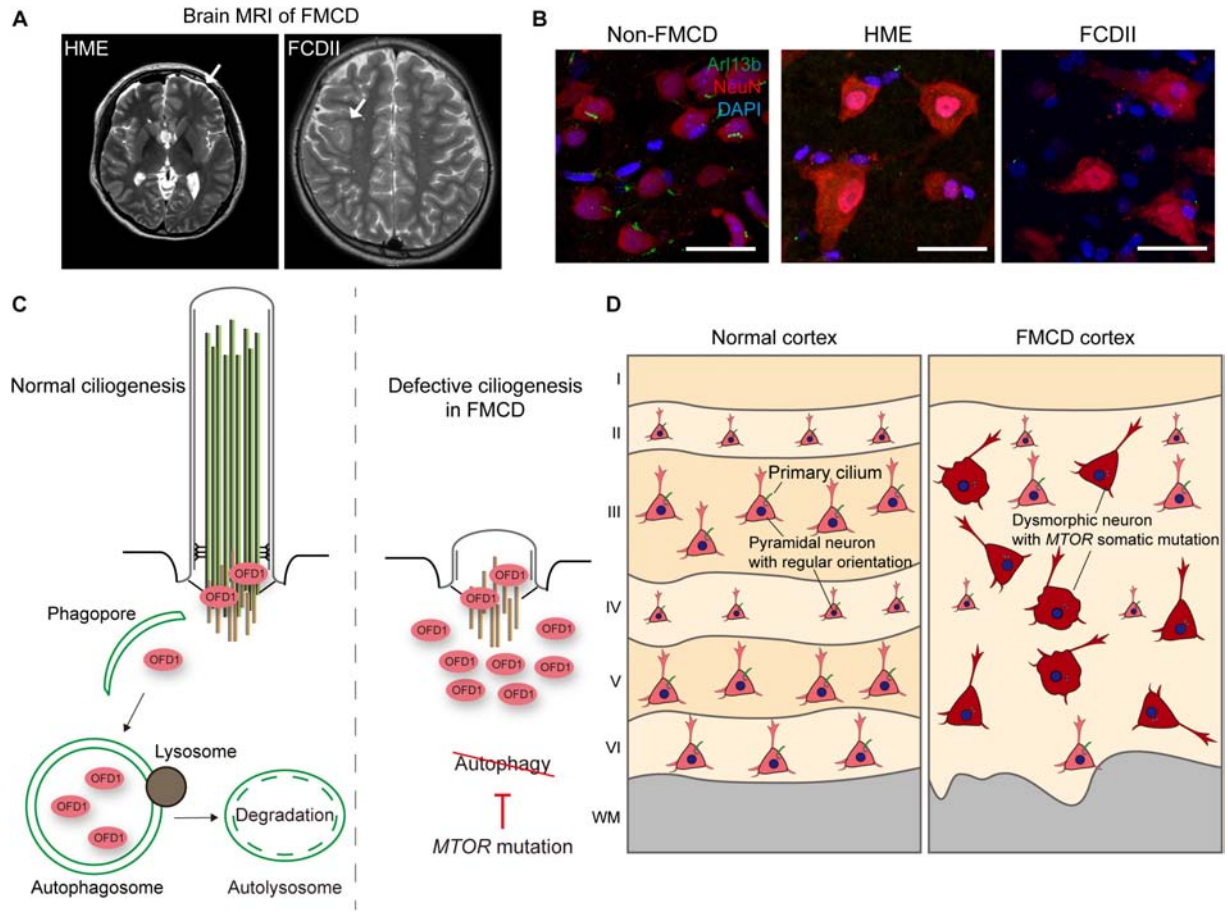

FIGURE 2 | Defective ciliogenesis due to brain somatic mutations in *MTOR* accounts for cortical dyslamination in FMCDs. **(A)** Representative brain MRIs of patients with FMCDs, including hemimegalencephaly (HME) and focal cortical dysplasia (FCD) type II. Arrows indicate the affected region of the brain. Adapted from Park et al. (2018), with permission. **(B)** Immunostaining for Arl13b, a marker for primary cilia, and NeuN, a marker for neurons, with DAPI co-staining in brain tissue from FMCD patients. While primary cilium normally forms at each neuron in brain tissue from non-FMCD, FMCD patients with brain somatic mutations in *MTOR* exhibit defective neuronal ciliogenesis. Scale bars, 30 μm. Adapted from Park et al. (2018), with permission. **(C)** Autophagic degradation of the centriolar satellite pool of OFD1 induces primary ciliogenesis. However, brain somatic activating mutation in *MTOR*, which blocks autophagy, disrupts ciliogenesis in brain tissues with FMCDs. **(D)** Cortical dyslamination with ciliary defective dysmorphic neurons in the cerebral cortex of a FMCD patient. Somatic activating mutations in *MTOR*, causative for FMCDs, disrupt neuronal ciliogenesis through blockage of autophagy, resulting in cortical dyslamination.

in their cilia have also been found to exhibit a global brain-patterning defect along the dorsal–ventral and rostral–caudal axes (Gorivodsky et al., 2009). Collectively, these studies suggest the importance of Gli3 processing, which could be mediated by primary cilia, in forebrain patterning.

The establishment of polarized radial glial scaffold formation during cortical development has been shown to be regulated by Arl13b, a small GTPase enriched in primary cilia (Higginbotham et al., 2013). *Arl13b* mutant mice ($Arl13b^{hnn/hnn}$), which display defective cilia, surprisingly exhibit dramatic inversion of the apicobasal polarity of the radial glial scaffold, which, in turn, changes the location of the progenitor zone to the outer part of the cortex. This defect is also observed when *Arl13b* is removed just before the formation of radial glia from neuroepithelial cells using Foxg1-driven Cre. However, *Arl13b* removal after establishment of the radial glial scaffold using Nestin- or GFAP-driven Cre has not been found to generate this intriguing phenotype, suggesting that the role of Arl13b in polarization is temporally restricted to the period during which the radial glial scaffold develops (Higginbotham et al., 2013). This reversed apicobasal polarity seen in *Arl13b* mutant mice has not been reported in mice deficient of other ciliary genes. In line with this temporally restricted role of a ciliary gene during development, a recent study performed conditional knockout (KO) of *Kif3a*, *Ift88*, and *Ttc21b* in a series of specific spatiotemporal domains. Intriguingly, the observed neurological defects, including forebrain expansion, cortical malformations, impaired olfactory bulb development, and ventriculomegaly, were significantly different across four different Cre transgenic alleles (Foxg1-Cre, Emx1-Cre, Wnt1-Cre, and AP2-Cre), indicating that the roles of cilia in cortical development are discretely spatiotemporal. For example, the deletion of *Ift88* at earlier stages of development, driven by Foxg1-Cre, was found to increase brain size; however, when

deleted at later stages, driven by Emx1-Cre, there were no significant differences in brain size (Snedeker et al., 2017). Taken together, these experimental studies of perturbations of primary cilia in mice support the crucial role of primary cilia in forebrain development, which, when disrupted, lead to severe morphological malformations in the brain.

Neuronal Migration

During brain cortical development, newly born neurons follow one of two main migratory routes to reach their final destination, known as radial and tangential migration (Hatten, 1999). The role of primary cilia in radially migrating pyramidal neurons remains unclear. In a previous study, cerebral cortical lamination was not apparently affected in *Arl13b*-conditional KO mice driven by Nex-Cre or in *Stumpy*-, *Kif3a*-, and *Ift88*-conditional KO mice driven by Nestin-Cre (Arellano et al., 2012; Higginbotham et al., 2012; Tong et al., 2014). However, a recent *in vivo* systemic study revealed that genes linked to ciliopathies affect cortical development, including neuronal radial migration, neural progenitor development, neuronal differentiation, and early neuronal connectivity (Guo et al., 2015). In this study, knockdown of 17 ciliopathy genes in the developing neocortex resulted in delayed neuronal radial migration in association with transient multipolar stage, multipolar-to-bipolar transition, and glial-guided radial migration (Guo et al., 2015). Meanwhile, others have suggested that the defective phenotypes seen in ciliary conditional KO mice driven by Nestin-Cre, the expression of which is broad and is also seen in non-RGCs at later developmental stages, may be partly attributable to non-cell-autonomous effects (Foerster et al., 2017; Chen et al., 2018). Accordingly, the cell-autonomous function of primary cilia in neural stem cells at the late developmental stage was investigated via acute knockdown of ciliary genes (*Kif3a* or *Ift88*) in the developing cortex, which resulted in defective neuronal differentiation and migration; this was accompanied by delays in neural stem cell cycle progression and failures in interkinetic nuclear migration (Chen et al., 2018). In FMCDs, the molecular mechanism of how somatic mutations in *MTOR* lead to focal cortical dyslamination appears to be related to defective neuronal ciliogenesis by *MTOR* mutation, which affects the multipolar to bipolar transition essential for neuronal radial migration (**Figures 2C,D**; Park et al., 2018).

Interneurons originating from the medial ganglionic eminence migrate along a tangential path in the cortical plate, either at the marginal zone or intermediate zone. These neurons change their orientation from a tangential to radial path to colonize the cortical plate and to differentiate into GABAergic neurons (Guo and Anton, 2014). Recent studies have demonstrated that disruption of primary cilia at interneurons affects the interneuronal migratory process, suggesting the importance of primary cilia in neuronal migration (Baudoin et al., 2012; Higginbotham et al., 2012). In a previous study, mice with conditional KO of *Arl13b* genes driven by Dlx5/6-Cre showed disruption of interneuron placement at *Arl13b*-deleted cortices caused by defects in interneuron migration and branching. However, when the *Arl13b* gene was disrupted in post-migratory interneurons driven by PV-Cre, there was no significant difference in the morphology of dendritic arbors during neuronal differentiation. Such defective interneuron migration may be a potential pathophysiological mechanism underlying neurological defects in JBTS with *Arl13b* mutations (Higginbotham et al., 2012). Meanwhile, a recent study showed that disruption of cilia in interneurons using Nkx2.1-Cre to ablate *Ift88* or *Kif3a* genes led to defective migration of interneurons, marked by an aberrant accumulation of interneurons at their first tangential path, not radial streams in the cortical plate, as well as abnormal positioning and density of interneurons in the postnatal cortex (Baudoin et al., 2012). Taken together, these studies emphasize that primary cilia in immature interneurons are crucial to interneuron migration in the developing cortex and the underlying mechanisms thereof (Baudoin et al., 2012). Nevertheless, the role of primary cilia in neuronal migration needs further study, especially in regards to which other cilia-mediated signaling pathways are involved. These future studies on neuronal migration should shed light on the pathophysiology of ciliopathies presenting with cognitive deficits, which may be attributable to defective neuronal migration and disrupted neural connectivity.

Cerebellum Development

Ataxia due to cerebellar malformation is one major symptom of ciliopathies, particularly JBTS. During development of the cerebellum, Purkinje cells secrete Shh, which regulates the proliferation of cerebellar neuronal precursor (Wechsler-Reya and Scott, 1999; Haldipur et al., 2012): Shh signaling mediated by primary cilia occurs in late embryonic stages of cerebellum development, during which Shh is required for expansion of the granule neuron precursor population, but not for the subsequent differentiation of these cells (Lewis et al., 2004). Primary cilia control cerebellar morphogenesis by promoting the expansion of the granule progenitor pool. Loss of either *Ift88* or *Kif3a* causes severe cerebellar hypoplasia and inhibits the expansion of the granule cell progenitor population. Although Ift88 and Kif3a are not required for the specification and differentiation of cerebellar cell types, they affect granular cell progenitor proliferation. Researches have shown that the expression of Gli1 at the external granule cell layer in *Kif3a* mutant mice is lower than that in controls (Chizhikov et al., 2007; Spassky et al., 2008). These studies demonstrate that ablation of primary cilia impairs Shh signaling, which regulates the development of the cerebellum, particularly expansion of cerebellar progenitors. This mechanism could explain the hypoplasia of the cerebellum and cerebellar ataxia seen in patients with ciliopathies such as JBTS.

Learning and Memory

Patients with ciliopathies commonly present with intellectual disability (ID) as a neurological deficit. Although there are not enough studies to explain the mechanism underlying ID as a result of defects in primary cilia, several studies have shown that depletion of primary cilia leads to hippocampal-dependent learning and memory deficits (Breunig et al., 2008; Han et al., 2008; Amador-Arjona et al., 2011). Hippocampal neurogenesis plays a role in fear conditioning, recognition, spatial memory, and pattern separation (Cameron and Glover, 2015). Also, Shh

signaling mediated by primary cilia controls the proliferation of neural progenitor cells (NPCs). As evidence thereof, Emx1-Cre-dependent *Shh*-conditional KO mice were found to show smaller dorsal telencephalons at E18.5 and decreased proliferation and increased apoptosis of neural stem cells (NSCs) and NPCs in the dorsal pallium (Komada et al., 2008). Meanwhile, Nestin-Cre- and hGFAP-Cre-dependent *Smo* KO mice exhibited smaller postnatal dentate gyruses and fewer proliferating cells than those in controls (Machold et al., 2003; Han et al., 2008). In *Kif3a* mutant and *Ift88* mutant mice, neuronal proliferation in the subgranular zone (SGZ) and subventricular zone (SVZ) was decreased, and Gli1 expression was abolished (Han et al., 2008; Tong et al., 2014; Gazea et al., 2016) These demonstrate that Shh signaling is involved in the proliferation and survival of NSCs and NPCs. Hypomorphic *Ift88*-mutant mice, in which *Ift88* mRNA and protein are reduced by 70–80%, showed disorganization of the midbrain dopominergic neuron (mDA) progenitors domain, and the number of mDA neurons was severly reduced (Gazea et al., 2016). Considering that primary cilia regulate neurogenesis by mediating Shh signaling, defects in learning and memory and ID might be caused by decreased neurogenesis due to aberrant Shh signaling. Expanding on the above research, additional studies are needed to determine how defective neuronal cilia lead to learning and memory impairment and ID.

CONCLUDING REMARKS

In this review, we briefly summarized the interaction between primary cilia and several signaling pathways, including Shh, Wnt, MTOR, and autophagy, all of which are essential to cellular homeostasis. Given that neurological disorders are typical symptoms of ciliopathies, the importance of primary cilia during brain development cannot be emphasized enough. At present, however, we are unable to fully understand the underlying mechanisms by which defective neuronal cilia contribute the pathogenesis of neurological defects in ciliopathies. Future studies of neuronal cilia in relation to signaling pathways may provide better understanding of the functions of neuronal cilia and may help to develop novel treatments for ciliopathies by targeting neuronal cilia-mediated signaling pathways. Compared with considerable studies on neuronal cilia, there is a lack of research on the role of primary cilia in glial cells, another major component of the brain. Glial cells, such astrocytes and oligodendrocytes, also possess a single primary cilium (Berbari et al., 2007; Bishop et al., 2007; Kasahara et al., 2014). Recently, studies reported defective ciliogenesis in glioblastoma (GBM), a high-grade astrocytic malignancy, and demonstrated the potential role of primary cilia on GBM progression (Moser et al., 2014; Hoang-Minh et al., 2016a,b; Loskutov et al., 2018). Further studies on the role of primary cilia in glial cells, as well as neurons, will advance our understanding of the role of primary cilia in brain development.

To help achieve a better understanding of human ciliopathies resulting from mutations in ciliary genes, CRISPR/Cas9 genome editing of identified mutations in human ciliopathies or 3D culture of brain organoids derived from pluripotent stem cells from ciliopathy patients can be used to generate more pathophysiologically relevant models for ciliopathy, thereby overcoming the gap between animal models and human subjects. Also, increasing studies on interactions between primary cilia and other signaling pathways may uncover a previously unknown role for cilia in the pathogenesis of human neurological diseases that are not considered classical ciliopathies, such as FMCD, brain cancer (medulloblastoma and GBM), and neurodegenerative diseases (Alzheimer's disease and HD) (Sotthibundhu et al., 2009; Keryer et al., 2011; Eguether and Hahne, 2018). Future studies of these disorders may help us to further the molecular basis of human diseases characterized by defects in primary cilia.

AUTHOR CONTRIBUTIONS

SP, HJ, and JL conceived the idea and wrote the manuscript.

FUNDING

This work was supported by grants from the Suh Kyungbae Foundation (to JL); Korean Health Technology R&D Project, Ministry of Health and Welfare, Republic of Korea (H15C3143 and H16C0415 to JL).

REFERENCES

Abdelhamed, Z. A., Wheway, G., Szymanska, K., Natarajan, S., Toomes, C., Inglehearn, C., et al. (2013). Variable expressivity of ciliopathy neurological phenotypes that encompass Meckel-Gruber syndrome and Joubert syndrome is caused by complex de-regulated ciliogenesis, Shh and Wnt signalling defects. *Hum. Mol. Genet.* 22, 1358–1372. doi: 10.1093/hmg/dds546

Alcedo, J., Ayzenzon, M., Von Ohlen, T., Noll, M., and Hooper, J. E. (1996). The *Drosophila* smoothened gene encodes a seven-pass membrane protein, a putative receptor for the hedgehog signal. *Cell* 86, 221–232. doi: 10.1016/s0092-8674(00)80094-x

Amador-Arjona, A., Elliott, J., Miller, A., Ginbey, A., Pazour, G. J., Enikolopov, G., et al. (2011). Primary cilia regulate proliferation of amplifying progenitors in adult hippocampus: implications for learning and memory. *J. Neurosci.* 31, 9933–9944. doi: 10.1523/jneurosci.1062-11.2011

Arellano, J. I., Guadiana, S. M., Breunig, J. J., Rakic, P., and Sarkisian, M. R. (2012). Development and distribution of neuronal cilia in mouse neocortex. *J. Compar. Neurol.* 520, 848–873. doi: 10.1002/cne.22793

Bangs, F., and Anderson, K. V. (2017). Primary cilia and mammalian hedgehog signaling. *Cold Spring Harb. Perspect. Biol.* 9:a028175. doi: 10.1101/cshperspect.a028175

Baudoin, J. P., Viou, L., Launay, P. S., Luccardini, C., Espeso Gil, S., Kiyasova, V., et al. (2012). Tangentially migrating neurons assemble a primary cilium that promotes their reorientation to the cortical plate. *Neuron* 76, 1108–1122. doi: 10.1016/j.neuron.2012.10.027

Belibi, F., Zafar, I., Ravichandran, K., Segvic, A. B., Jani, A., Ljubanovic, D. G., et al. (2011). Hypoxia-inducible factor-1alpha (HIF-1alpha) and autophagy in polycystic kidney disease (PKD). *Am. J. Physiol. Renal Physiol.* 300, F1235–F1243.

Berbari, N. F., Bishop, G. A., Askwith, C. C., Lewis, J. S., and Mykytyn, K. (2007). Hippocampal neurons possess primary cilia in culture. *J. Neurosci. Res.* 85, 1095–1100. doi: 10.1002/jnr.21209

Berbari, N. F., O'connor, A. K., Haycraft, C. J., and Yoder, B. K. (2009). The primary cilium as a complex signaling center. *Curr. Biol.* 19, R526–R535.

Besse, L., Neti, M., Anselme, I., Gerhardt, C., Ruther, U., Laclef, C., et al. (2011). Primary cilia control telencephalic patterning and morphogenesis via Gli3 proteolytic processing. *Development* 138, 2079–2088. doi: 10.1242/dev.059808

Bishop, G. A., Berbari, N. F., Lewis, J., and Mykytyn, K. (2007). Type III adenylyl cyclase localizes to primary cilia throughout the adult mouse brain. *J. Compar. Neurol.* 505, 562–571. doi: 10.1002/cne.21510

Boehlke, C., Kotsis, F., Patel, V., Braeg, S., Voelker, H., Bredt, S., et al. (2010). Primary cilia regulate mTORC1 activity and cell size through Lkb1. *Nat. Cell Biol.* 12, 1115–1122. doi: 10.1038/ncb2117

Breunig, J. J., Sarkisian, M. R., Arellano, J. I., Morozov, Y. M., Ayoub, A. E., Sojitra, S., et al. (2008). Primary cilia regulate hippocampal neurogenesis by mediating sonic hedgehog signaling. *Proc. Natl. Acad. Sci. U.S.A.* 105, 13127–13132. doi: 10.1073/pnas.0804558105

Cameron, H. A., and Glover, L. R. (2015). Adult neurogenesis: beyond learning and memory. *Annu. Rev. Psychol.* 66, 53–81. doi: 10.1146/annurev-psych-010814-015006

Cano, D. A., Murcia, N. S., Pazour, G. J., and Hebrok, M. (2004). Orpk mouse model of polycystic kidney disease reveals essential role of primary cilia in pancreatic tissue organization. *Development* 131, 3457–3467. doi: 10.1242/dev.01189

Chen, J. L., Chang, C. H., and Tsai, J. W. (2018). Gli2 rescues delays in brain development induced by Kif3a dysfunction. *Cereb. Cortex* 29, 751–764. doi: 10.1093/cercor/bhx356

Chizhikov, V. V., Davenport, J., Zhang, Q., Shih, E. K., Cabello, O. A., Fuchs, J. L., et al. (2007). Cilia proteins control cerebellar morphogenesis by promoting expansion of the granule progenitor pool. *J. Neurosci.* 27, 9780–9789. doi: 10.1523/jneurosci.5586-06.2007

Corbit, K. C., Aanstad, P., Singla, V., Norman, A. R., Stainier, D. Y., and Reiter, J. F. (2005). Vertebrate smoothened functions at the primary cilium. *Nature* 437, 1018–1021. doi: 10.1038/nature04117

Corbit, K. C., Shyer, A. E., Dowdle, W. E., Gaulden, J., Singla, V., Chen, M. H., et al. (2008). Kif3a constrains beta-catenin-dependent Wnt signalling through dual ciliary and non-ciliary mechanisms. *Nat. Cell Biol.* 10, 70–76. doi: 10.1038/ncb1670

Davenport, J. R., and Yoder, B. K. (2005). An incredible decade for the primary cilium: a look at a once-forgotten organelle. *Am. J. Physiol. Renal Physiol.* 289, F1159–F1169.

Dessaud, E., Mcmahon, A. P., and Briscoe, J. (2008). Pattern formation in the vertebrate neural tube: a sonic hedgehog morphogen-regulated transcriptional network. *Development* 135, 2489–2503. doi: 10.1242/dev.009324

Echelard, Y., Epstein, D. J., St-Jacques, B., Shen, L., Mohler, J., Mcmahon, J. A., et al. (1993). Sonic hedgehog, a member of a family of putative signaling molecules, is implicated in the regulation of CNS polarity. *Cell* 75, 1417–1430. doi: 10.1016/0092-8674(93)90627-3

Eguether, T., and Hahne, M. (2018). Mixed signals from the cell's antennae: primary cilia in cancer. *EMBO Rep.* 19:e46589. doi: 10.15252/embr.201846589

Ekker, S. C., Ungar, A. R., Greenstein, P., Von Kessler, D. P., Porter, J. A., Moon, R. T., et al. (1995). Patterning activities of vertebrate hedgehog proteins in the developing eye and brain. *Curr. Biol.* 5, 944–955. doi: 10.1016/s0960-9822(95)00185-0

Ferent, J., and Traiffort, E. (2015). Hedgehog: multiple paths for multiple roles in shaping the brain and spinal cord. *Neuroscientist* 21, 356–371. doi: 10.1177/1073858414531457

Foerster, P., Daclin, M., Asm, S., Faucourt, M., Boletta, A., Genovesio, A., et al. (2017). mTORC1 signaling and primary cilia are required for brain ventricle morphogenesis. *Development* 144, 201–210. doi: 10.1242/dev.138271

Gazea, M., Tasouri, E., Tolve, M., Bosch, V., Kabanova, A., Gojak, C., et al. (2016). Primary cilia are critical for Sonic hedgehog-mediated dopaminergic neurogenesis in the embryonic midbrain. *Dev. Biol.* 409, 55–71. doi: 10.1016/j.ydbio.2015.10.033

Gerdes, J. M., and Katsanis, N. (2008). Ciliary function and Wnt signal modulation. *Curr. Top. Dev. Biol.* 85, 175–195. doi: 10.1016/s0070-2153(08)00807-7

Gerdes, J. M., Liu, Y., Zaghloul, N. A., Leitch, C. C., Lawson, S. S., Kato, M., et al. (2007). Disruption of the basal body compromises proteasomal function and perturbs intracellular Wnt response. *Nat. Genet.* 39, 1350–1360. doi: 10.1038/ng.2007.12

Gherman, A., Davis, E. E., and Katsanis, N. (2006). The ciliary proteome database: an integrated community resource for the genetic and functional dissection of cilia. *Nat. Genet.* 38, 961–962. doi: 10.1038/ng0906-961

Goetz, S. C., and Anderson, K. V. (2010). The primary cilium: a signalling centre during vertebrate development. *Nat. Rev. Genet.* 11, 331–344. doi: 10.1038/nrg2774

Goetz, S. C., Ocbina, P. J., and Anderson, K. V. (2009). The primary cilium as a Hedgehog signal transduction machine. *Methods Cell Biol.* 94, 199–222. doi: 10.1016/s0091-679x(08)94010-3

Gorivodsky, M., Mukhopadhyay, M., Wilsch-Braeuninger, M., Phillips, M., Teufel, A., Kim, C., et al. (2009). Intraflagellar transport protein 172 is essential for primary cilia formation and plays a vital role in patterning the mammalian brain. *Dev. Biol.* 325, 24–32. doi: 10.1016/j.ydbio.2008.09.019

Guo, J., and Anton, E. S. (2014). Decision making during interneuron migration in the developing cerebral cortex. *Trends Cell Biol.* 24, 342–351. doi: 10.1016/j.tcb.2013.12.001

Guo, J., Higginbotham, H., Li, J., Nichols, J., Hirt, J., Ghukasyan, V., et al. (2015). Developmental disruptions underlying brain abnormalities in ciliopathies. *Nat. Commun.* 6:7857.

Haldipur, P., Bharti, U., Govindan, S., Sarkar, C., Iyengar, S., Gressens, P., et al. (2012). Expression of Sonic hedgehog during cell proliferation in the human cerebellum. *Stem Cells Dev.* 21, 1059–1068. doi: 10.1089/scd.2011.0206

Han, Y. G., Spassky, N., Romaguera-Ros, M., Garcia-Verdugo, J. M., Aguilar, A., Schneider-Maunoury, S., et al. (2008). Hedgehog signaling and primary cilia are required for the formation of adult neural stem cells. *Nat. Neurosci.* 11, 277–284. doi: 10.1038/nn2059

Hartman, T. R., Liu, D., Zilfou, J. T., Robb, V., Morrison, T., Watnick, T., et al. (2009). The tuberous sclerosis proteins regulate formation of the primary cilium via a rapamycin-insensitive and polycystin 1-independent pathway. *Hum. Mol. Genet.* 18, 151–163. doi: 10.1093/hmg/ddn325

Hatten, M. E. (1999). Central nervous system neuronal migration. *Annu. Rev. Neurosci.* 22, 511–539. doi: 10.1146/annurev.neuro.22.1.511

Higginbotham, H., Eom, T. Y., Mariani, L. E., Bachleda, A., Hirt, J., Gukassyan, V., et al. (2012). Arl13b in primary cilia regulates the migration and placement of interneurons in the developing cerebral cortex. *Dev. Cell* 23, 925–938. doi: 10.1016/j.devcel.2012.09.019

Higginbotham, H., Guo, J., Yokota, Y., Umberger, N. L., Su, C. Y., Li, J., et al. (2013). Arl13b-regulated cilia activities are essential for polarized radial glial scaffold formation. *Nat. Neurosci.* 16, 1000–1007. doi: 10.1038/nn.3451

Hildebrandt, F., Benzing, T., and Katsanis, N. (2011). Ciliopathies. *N. Engl. J. Med.* 364, 1533–1543.

Hoang-Minh, L. B., Deleyrolle, L. P., Nakamura, N. S., Parker, A. K., Martuscello, R. T., Reynolds, B. A., et al. (2016a). PCM1 depletion inhibits glioblastoma cell ciliogenesis and increases cell death and sensitivity to temozolomide. *Transl. Oncol.* 9, 392–402. doi: 10.1016/j.tranon.2016.08.006

Hoang-Minh, L. B., Deleyrolle, L. P., Siebzehnrubl, D., Ugartemendia, G., Futch, H., Griffith, B., et al. (2016b). Disruption of KIF3A in patient-derived glioblastoma cells: effects on ciliogenesis, hedgehog sensitivity, and tumorigenesis. *Oncotarget* 7, 7029–7043.

Huang, P., and Schier, A. F. (2009). Dampened Hedgehog signaling but normal Wnt signaling in zebrafish without cilia. *Development* 136, 3089–3098. doi: 10.1242/dev.041343

Huangfu, D., and Anderson, K. V. (2005). Cilia and Hedgehog responsiveness in the mouse. *Proc. Natl. Acad. Sci. U.S.A.* 102, 11325–11330. doi: 10.1073/pnas.0505328102

Kaliszewski, M., Knott, A. B., and Bossy-Wetzel, E. (2015). Primary cilia and autophagic dysfunction in Huntington's disease. *Cell Death Differ.* 22, 1413–1424. doi: 10.1038/cdd.2015.80

Kasahara, K., Miyoshi, K., Murakami, S., Miyazaki, I., and Asanuma, M. (2014). Visualization of astrocytic primary cilia in the mouse brain by immunofluorescent analysis using the cilia marker Arl13b. *Acta Med. Okayama* 68, 317–322.

Keryer, G., Pineda, J. R., Liot, G., Kim, J., Dietrich, P., Benstaali, C., et al. (2011). Ciliogenesis is regulated by a huntingtin-HAP1-PCM1 pathway and is altered in Huntington disease. *J. Clin. Invest.* 121, 4372–4382. doi: 10.1172/jci57552

Komada, M., Saitsu, H., Kinboshi, M., Miura, T., Shiota, K., and Ishibashi, M. (2008). Hedgehog signaling is involved in development of the neocortex. *Development* 135, 2717–2727. doi: 10.1242/dev.015891

Kumamoto, N., Gu, Y., Wang, J., Janoschka, S., Takemaru, K., Levine, J., et al. (2012). A role for primary cilia in glutamatergic synaptic integration of adult-born neurons. *Nat. Neurosci.* 15:S391.

Lee, J., Yi, S., Kang, Y. E., Chang, J. Y., Kim, J. T., Sul, H. J., et al. (2016). Defective ciliogenesis in thyroid hurthle cell tumors is associated with increased autophagy. *Oncotarget* 7, 79117–79130.

Lee, K. M., Hwang, S. K., and Lee, J. A. (2013). Neuronal autophagy and neurodevelopmental disorders. *Exp. Neurobiol.* 22, 133–142.

Levine, B., and Kroemer, G. (2008). Autophagy in the pathogenesis of disease. *Cell* 132, 27–42. doi: 10.1016/j.cell.2007.12.018

Lewis, P. M., Gritli-Linde, A., Smeyne, R., Kottmann, A., and Mcmahon, A. P. (2004). Sonic hedgehog signaling is required for expansion of granule neuron precursors and patterning of the mouse cerebellum. *Dev. Biol.* 270, 393–410. doi: 10.1016/j.ydbio.2004.03.007

Lim, K. C., and Crino, P. B. (2013). Focal malformations of cortical development: new vistas for molecular pathogenesis. *Neuroscience* 252, 262–276. doi: 10.1016/j.neuroscience.2013.07.037

Lin, F., Hiesberger, T., Cordes, K., Sinclair, A. M., Goldstein, L. S., Somlo, S., et al. (2003). Kidney-specific inactivation of the KIF3A subunit of kinesin-II inhibits renal ciliogenesis and produces polycystic kidney disease. *Proc. Natl. Acad. Sci. U.S.A.* 100, 5286–5291. doi: 10.1073/pnas.0836980100

Lipton, J. O., and Sahin, M. (2014). The neurology of mTOR. *Neuron* 84, 275–291.

Loskutov, Y. V., Griffin, C. L., Marinak, K. M., Bobko, A., Margaryan, N. V., Geldenhuys, W. J., et al. (2018). LPA signaling is regulated through the primary cilium: a novel target in glioblastoma. *Oncogene* 37, 1457–1471. doi: 10.1038/s41388-017-0049-3

Machold, R., Hayashi, S., Rutlin, M., Muzumdar, M. D., Nery, S., Corbin, J. G., et al. (2003). Sonic hedgehog is required for progenitor cell maintenance in telencephalic stem cell niches. *Neuron* 39, 937–950. doi: 10.1016/s0896-6273(03)00561-0

Marsh, D., and Dragich, J. M. (2018). Autophagy in mammalian neurodevelopment and implications for childhood neurological disorders. *Neurosci. Lett.* 697, 29–33. doi: 10.1016/j.neulet.2018.04.017

Marshall, W. F. (2008). Basal bodies platforms for building cilia. *Curr. Top. Dev. Biol.* 85, 1–22.

May, S. R., Ashique, A. M., Karlen, M., Wang, B., Shen, Y., Zarbalis, K., et al. (2005). Loss of the retrograde motor for IFT disrupts localization of Smo to cilia and prevents the expression of both activator and repressor functions of Gli. *Dev. Biol.* 287, 378–389. doi: 10.1016/j.ydbio.2005.08.050

May-Simera, H. L., and Kelley, M. W. (2012). Cilia, Wnt signaling, and the cytoskeleton. *Cilia* 1:7.

Mizushima, N. (2007). Autophagy: process and function. *Genes Dev.* 21, 2861–2873. doi: 10.1101/gad.1599207

Moser, J. J., Fritzler, M. J., and Rattner, J. B. (2014). Ultrastructural characterization of primary cilia in pathologically characterized human glioblastoma multiforme (GBM) tumors. *BMC Clin. Pathol.* 14:40. doi: 10.1186/1472-6890-14-40

Nakagawa, N., Li, J., Yabuno-Nakagawa, K., Eom, T. Y., Cowles, M., Mapp, T., et al. (2017). APC sets the Wnt tone necessary for cerebral cortical progenitor development. *Genes Dev.* 31, 1679–1692. doi: 10.1101/gad.302679.117

Ocbina, P. J., Tuson, M., and Anderson, K. V. (2009). Primary cilia are not required for normal canonical Wnt signaling in the mouse embryo. *PLoS One* 4:e6839. doi: 10.1371/journal.pone.0006839

Oh, E. C., and Katsanis, N. (2013). Context-dependent regulation of Wnt signaling through the primary cilium. *J. Am. Soc. Nephrol.* 24, 10–18. doi: 10.1681/asn.2012050526

Orhon, I., Dupont, N., Zaidan, M., Boitez, V., Burtin, M., Schmitt, A., et al. (2016). Primary-cilium-dependent autophagy controls epithelial cell volume in response to fluid flow. *Nat. Cell Biol.* 18, 657–667. doi: 10.1038/ncb3360

Pal, K., and Mukhopadhyay, S. (2015). Primary cilium and sonic hedgehog signaling during neural tube patterning: role of GPCRs and second messengers. *Dev. Neurobiol.* 75, 337–348. doi: 10.1002/dneu.22193

Pampliega, O., Orhon, I., Patel, B., Sridhar, S., Diaz-Carretero, A., Beau, I., et al. (2013). Functional interaction between autophagy and ciliogenesis. *Nature* 502, 194–200. doi: 10.1038/nature12639

Park, S. M., Lim, J. S., Ramakrishina, S., Kim, S. H., Kim, W. K., Lee, J., et al. (2018). Brain somatic mutations in MTOR disrupt neuronal ciliogenesis, leading to focal cortical dyslamination. *Neuron* 99:e87.

Petralia, R. S., Schwartz, C. M., Wang, Y. X., Kawamoto, E. M., Mattson, M. P., and Yao, P. J. (2013). Sonic hedgehog promotes autophagy in hippocampal neurons. *Biol. Open* 2, 499–504. doi: 10.1242/bio.20134275

Reiter, J. F., Blacque, O. E., and Leroux, M. R. (2012). The base of the cilium: roles for transition fibres and the transition zone in ciliary formation, maintenance and compartmentalization. *EMBO Rep.* 13, 608–618. doi: 10.1038/embor.2012.73

Reiter, J. F., and Leroux, M. R. (2017). Genes and molecular pathways underpinning ciliopathies. *Nat. Rev. Mol. Cell Biol.* 18, 533–547. doi: 10.1038/nrm.2017.60

Rohatgi, R., Milenkovic, L., and Scott, M. P. (2007). Patched1 regulates hedgehog signaling at the primary cilium. *Science* 317, 372–376. doi: 10.1126/science.1139740

Rosengren, T., Larsen, L. J., Pedersen, L. B., Christensen, S. T., and Moller, L. B. (2018). TSC1 and TSC2 regulate cilia length and canonical Hedgehog signaling via different mechanisms. *Cell. Mol. Life Sci.* 75, 2663–2680. doi: 10.1007/s00018-018-2761-8

Ross, A. J., May-Simera, H., Eichers, E. R., Kai, M., Hill, J., Jagger, D. J., et al. (2005). Disruption of bardet-biedl syndrome ciliary proteins perturbs planar cell polarity in vertebrates. *Nat. Genet.* 37, 1135–1140. doi: 10.1038/ng1644

Rui, Y. N., Xu, Z., Patel, B., Chen, Z., Chen, D., Tito, A., et al. (2015). Huntingtin functions as a scaffold for selective macroautophagy. *Nat. Cell Biol.* 17, 262–275. doi: 10.1038/ncb3101

Sasai, N., and Briscoe, J. (2012). Primary cilia and graded Sonic Hedgehog signaling. *Wiley Interdiscip. Rev. Dev. Biol.* 1, 753–772. doi: 10.1002/wdev.43

Saxton, R. A., and Sabatini, D. M. (2017). mTOR signaling in growth, metabolism, and disease. *Cell* 168, 960–976.

Scales, S. J., and de Sauvage, F. J. (2009). Mechanisms of hedgehog pathway activation in cancer and implications for therapy. *Trends Pharmacol. Sci.* 30, 303–312. doi: 10.1016/j.tips.2009.03.007

Shillingford, J. M., Murcia, N. S., Larson, C. H., Low, S. H., Hedgepeth, R., Brown, N., et al. (2006). The mTOR pathway is regulated by polycystin-1, and its inhibition reverses renal cystogenesis in polycystic kidney disease. *Proc. Natl. Acad. Sci. U.S.A.* 103, 5466–5471. doi: 10.1073/pnas.0509694103

Simons, M., Gloy, J., Ganner, A., Bullerkotte, A., Bashkurov, M., Kronig, C., et al. (2005). Inversin, the gene product mutated in nephronophthisis type II, functions as a molecular switch between Wnt signaling pathways. *Nat. Genet.* 37, 537–543. doi: 10.1038/ng1552

Snedeker, J., Schock, E. N., Struve, J. N., Chang, C. F., Cionni, M., Tran, P. V., et al. (2017). Unique spatiotemporal requirements for intraflagellar transport genes during forebrain development. *PLoS One* 12:e0173258. doi: 10.1371/journal.pone.0173258

Sotthibundhu, A., Li, Q. X., Thangnipon, W., and Coulson, E. J. (2009). Abeta(1-42) stimulates adult SVZ neurogenesis through the p75 neurotrophin receptor. *Neurobiol. Aging* 30, 1975–1985. doi: 10.1016/j.neurobiolaging.2008.02.004

Spassky, N., Han, Y. G., Aguilar, A., Strehl, L., Besse, L., Laclef, C., et al. (2008). Primary cilia are required for cerebellar development and Shh-dependent expansion of progenitor pool. *Dev. Biol.* 317, 246–259. doi: 10.1016/j.ydbio.2008.02.026

Stottmann, R. W., Tran, P. V., Turbe-Doan, A., and Beier, D. R. (2009). Ttc21b is required to restrict sonic hedgehog activity in the developing mouse forebrain. *Dev. Biol.* 335, 166–178. doi: 10.1016/j.ydbio.2009.08.023

Tang, Z., Lin, M. G., Stowe, T. R., Chen, S., Zhu, M., Stearns, T., et al. (2013). Autophagy promotes primary ciliogenesis by removing OFD1 from centriolar satellites. *Nature* 502, 254–257. doi: 10.1038/nature12606

Tong, C. K., Han, Y. G., Shah, J. K., Obernier, K., Guinto, C. D., and Alvarez-Buylla, A. (2014). Primary cilia are required in a unique subpopulation of neural progenitors. *Proc. Natl. Acad. Sci. U.S.A.* 111, 12438–12443. doi: 10.1073/pnas.1321425111

Town, T., Breunig, J. J., Sarkisian, M. R., Spilianakis, C., Ayoub, A. E., Liu, X., et al. (2008). The stumpy gene is required for mammalian ciliogenesis. *Proc. Natl. Acad. Sci. U.S.A.* 105, 2853–2858. doi: 10.1073/pnas.0712385105

Tran, P. V., Haycraft, C. J., Besschetnova, T. Y., Turbe-Doan, A., Stottmann, R. W., Herron, B. J., et al. (2008). THM1 negatively modulates mouse sonic hedgehog signal transduction and affects retrograde intraflagellar transport in cilia. *Nat. Genet.* 40, 403–410. doi: 10.1038/ng.105

Tukachinsky, H., Lopez, L. V., and Salic, A. (2010). A mechanism for vertebrate Hedgehog signaling: recruitment to cilia and dissociation of SuFu-Gli protein complexes. *J. Cell Biol.* 191, 415–428. doi: 10.1083/jcb.201004108

Valente, E. M., Rosti, R. O., Gibbs, E., and Gleeson, J. G. (2014). Primary cilia in neurodevelopmental disorders. *Nat. Rev. Neurol.* 10, 27–36. doi: 10.1038/nrneurol.2013.247

van Amerongen, R., and Nusse, R. (2009). Towards an integrated view of Wnt signaling in development. *Development* 136, 3205–3214. doi: 10.1242/dev.033910

Vogel, T. W., Carter, C. S., Abode-Iyamah, K., Zhang, Q., and Robinson, S. (2012). The role of primary cilia in the pathophysiology of neural tube defects. *Neurosurg. Focus* 33:E2.

Wahl, P. R., Serra, A. L., Le Hir, M., Molle, K. D., Hall, M. N., and Wuthrich, R. P. (2006). Inhibition of mTOR with sirolimus slows disease progression in Han:SPRD rats with autosomal dominant polycystic kidney disease (ADPKD). *Nephrol. Dial Transplant.* 21, 598–604. doi: 10.1093/ndt/gfi181

Wechsler-Reya, R. J., and Scott, M. P. (1999). Control of neuronal precursor proliferation in the cerebellum by Sonic Hedgehog. *Neuron* 22, 103–114. doi: 10.1016/s0896-6273(00)80682-0

Wegiel, J., Kuchna, I., Nowicki, K., Imaki, H., Wegiel, J., Marchi, E., et al. (2010). The neuropathology of autism: defects of neurogenesis and neuronal migration, and dysplastic changes. *Acta Neuropathol.* 119, 755–770. doi: 10.1007/s00401-010-0655-4

Wheway, G., Abdelhamed, Z., Natarajan, S., Toomes, C., Inglehearn, C., and Johnson, C. A. (2013). Aberrant Wnt signalling and cellular over-proliferation in a novel mouse model of Meckel-Gruber syndrome. *Dev. Biol.* 377, 55–66. doi: 10.1016/j.ydbio.2013.02.015

Willaredt, M. A., Hasenpusch-Theil, K., Gardner, H. A., Kitanovic, I., Hirschfeld-Warneken, V. C., Gojak, C. P., et al. (2008). A crucial role for primary cilia in cortical morphogenesis. *J. Neurosci.* 28, 12887–12900. doi: 10.1523/jneurosci.2084-08.2008

Zhu, P., Sieben, C. J., Xu, X., Harris, P. C., and Lin, X. (2017). Autophagy activators suppress cystogenesis in an autosomal dominant polycystic kidney disease model. *Hum. Mol. Genet.* 26, 158–172.

Zimmermann, K. W. (1898). Beiträge zur Kenntniss einiger Drüsen und Epithelien. *Archiv. Mikrosk. Anat.* 52, 552–706. doi: 10.1007/bf02975837

Conflict of Interest Statement: JL is a co-founder of SoVarGen, Inc. that develops new diagnostics and therapeutics for brain disorders.

The remaining authors declare that the research was conducted in the absence of any commercial or financial relationships that could be construed as a potential conflict of interest.

frontiers in Cellular Neuroscience

BRIEF RESEARCH REPORT
published: 24 May 2019
doi: 10.3389/fncel.2019.00226

Anomalies in Dopamine Transporter Expression and Primary Cilium Distribution in the Dorsal Striatum of a Mouse Model of Niemann-Pick C1 Disease

*Micaela Lucarelli[1,2], Chiara Di Pietro[3], Gina La Sala[3], Maria Teresa Fiorenza[1], Daniela Marazziti[3] and Sonia Canterini[1]**

[1] Division of Neuroscience, Department of Psychology, Center for Research in Neurobiology 'Daniel Bovet', Sapienza University of Rome, Rome, Italy, [2] PhD Program in Behavioral Neuroscience, Sapienza University of Rome, Rome, Italy, [3] Institute of Cell Biology and Neurobiology, Italian National Research Council, Rome, Italy

OPEN ACCESS

Edited by:
Rosanna Parlato,
Ulm University, Germany

Reviewed by:
Martin Witt,
Rostock University Hospital, Germany
Bronwyn Maree Kivell,
Victoria University of Wellington, New Zealand
Andreas Wree,
University of Rostock, Germany

***Correspondence:**
Sonia Canterini
sonia.canterini@uniroma1.it

Specialty section:
This article was submitted to Cellular Neurophysiology, a section of the journal Frontiers in Cellular Neuroscience

Received: 23 January 2019
Accepted: 06 May 2019
Published: 24 May 2019

Citation:
Lucarelli M, Di Pietro C, La Sala G, Fiorenza MT, Marazziti D and Canterini S (2019) Anomalies in Dopamine Transporter Expression and Primary Cilium Distribution in the Dorsal Striatum of a Mouse Model of Niemann-Pick C1 Disease. Front. Cell. Neurosci. 13:226. doi: 10.3389/fncel.2019.00226

The Niemann-Pick type C1 (NPC1) is a rare genetic disease characterized by the accumulation of endocytosed cholesterol and other lipids in the endosome/lysosome compartments. In the brain, the accumulation/mislocalization of unesterified cholesterol, gangliosides and sphingolipids is responsible for the appearance of neuropathological hallmarks, and progressive neurological decline in patients. The imbalance of unesterified cholesterol and other lipids, including GM2 and GM3 gangliosides, alters a number of signaling mechanisms impacting on the overall homeostasis of neurons. In particular, lipid depletion experiments have shown that lipid rafts regulate the cell surface expression of dopamine transporter (DAT) and modulate its activity. Dysregulated dopamine transporter's function results in imbalanced dopamine levels at synapses and severely affects dopamine-induced locomotor responses and dopamine receptor-mediated synaptic signaling. Recent studies begin to correlate dopaminergic stimulation with the length and function of the primary cilium, a non-motile organelle that coordinates numerous signaling pathways. In particular, the absence of dopaminergic D2 receptor stimulation induces the elongation of dorso-striatal neuron's primary cilia. This study has used a mouse model of the NPC1 disease to correlate cholesterol dyshomeostasis with dorso-striatal anomalies in terms of DAT expression and primary cilium (PC) length and morphology. We found that juvenile *Npc1*^{nmf164} mice display a reduction of dorso-striatal DAT expression, with associated alterations of PC number, length-frequency distribution, and tortuosity.

Keywords: Niemann-Pick C1, mouse model, striatum, primary cilium, dopamine

INTRODUCTION

Niemann-Pick type C1 (NPC1) is a rare lysosomal lipid storage disorder caused by mutations in the *NPC1* gene, whose protein mediates the egress of cholesterol from lysosomes/endosomes (Peake and Vance, 2010). NPC1 patients develop severe neurological-neurovisceral disorders, including cerebellar ataxia, dysarthria, dysphagia, seizures, and progressive dementia (Vanier, 2010, 2013).

Niemann-Pick type C1 cells display defective synthesis and mobilization of endocytosed cholesterol to the plasma membrane, which affects the functions of neurotransmitters, and their receptors (Fiorenza et al., 2013, 2018).

Dopamine transporter (DAT) regulates the spatio/temporal dynamics of dopamine (DA) neurotransmission by regulating the reuptake of extracellular DA into presynaptic terminals. DAT localization and function are directly regulated by cholesterol (Jones et al., 2012). For instance, cholesterol depletion studies have shown that lipid rafts regulate DAT cell-surface expression (Foster et al., 2008; Gabriel et al., 2013), and modulate its activity (Adkins et al., 2007). In addition, cholesterol has been shown to stabilize DAT conformation and DA binding (Hong and Amara, 2010). A number of G protein-coupled receptors including dopaminergic D2-receptors (D2R) are localized to the primary cilium (PC) of mammalian neurons and the lack of D2 dopaminergic input increases striatal PC length (Marley and von Zastrow, 2010; Miyoshi et al., 2014).

We have recently reported an impairment of Sonic hedgehog (Shh) signaling and PC density and length, in hippocampal neurons of *Npc1*$^{-/-}$ mice and fibroblasts of NPC1 patients (Canterini et al., 2017). PC is a non-motile organelle that plays critical roles in coordinating numerous neuronal/developmental signaling pathways. Alterations of PC morphology and localization are responsible for ciliopathies, disorders that manifest, like the NPC1 disease, a constellation of clinical features including ataxia, retinal degeneration, behavioral disturbance, and intellectual disability (Waters and Beales, 2011; Guo et al., 2015).

In this study we investigate DA signaling and reception in the striatum of mouse of the *Npc1*^{nmf164} strain, that bears a point mutation in the *Npc1* gene (D1005G), resulting in a milder, and late-onset form comparable to the most part of human cases (Maue et al., 2012). In this study, we show that juvenile *Npc1*^{nmf164} mice display a reduction of DAT expression and alteration of PC number and length-frequency distribution in the dorsal striatum.

Our findings identify early and subtle anomalies in striatal dopaminergic neurotransmission that might contribute to the subsequent appearance of NPC1 disease manifestations.

MATERIALS AND METHODS

Animals and Treatments

Homozygous *Npc1*^{nmf164} mice maintained on BALB/cJ background were derived from heterozygous matings. Genotypes were identified by PCR analysis of tail DNA (Palladino et al., 2015).

Animal experimental protocols and related procedures were approved by the Italian Ministry of Health-General Directorate of Animal Health (995/2016; D.Igs. 26/2014). All efforts were made to minimize animal suffering, according to European Directive 2010/63/EU.

Tissue Dissection

Brains of postnatal (PN) day 30 *Npc1*^{nmf164} mice and wild-type (*wt*) littermates (5 mice/genotype) (**Supplementary Table S1**) were collected on ice-cold PBS and cut along the mid-sagittal plane. For Western Blotting, punches of the dorsal striatum (DS) were obtained from coronal slices of one hemisphere using a steel needle (1.5 mm diameter) (Colelli et al., 2010; Campus et al., 2017). The other hemisphere was fixed overnight in 4% paraformaldehyde and cut on Leica-Vibratome (S1000, Leica), for immunohistochemistry (IHC).

Western Blot Analysis

Tissue punches of DS were processed for protein extraction and Western blot analysis as previously described (Di Pietro et al., 2017). Primary and secondary antibodies used are listed in **Supplementary Table S2**. Band intensity was normalized to α-tubulin signal. The average values were expressed in arbitrary units, as a ratio to *wt* mean values.

IHC of Primary Cilium Markers and Measurements

Double IHC staining on free-floating sections (30 μm) was performed as previously described (Canterini et al., 2012). Primary and secondary antibodies data are listed in **Supplementary Table S2**.

Only striatal PC "clearly" double-stained for γ-tubulin (basal-body) and ACIII (PC-shaft) were selected for morphological analysis using Neurolucida analysis system (MBF Bioscience, Williston, VT, United States), connected to Olympus BX53 microscope (100X/1.25 numerical aperture) with 40X/100X immersion objective lens. An average of 6 PC was measured from 10 random fields per mice (n = 318 PC/genotype).

Statistics

A Mann-Whitney U-test was used to determine the difference in protein levels (GraphPad Software, Inc). The D'Agostino & Pearson omnibus normality test was used to assess the distribution of values. Differences in PC distribution were determined by Chi-squared test, whereas PC lengths and related parameters were analyzed by non-parametric Mann-Withney U-test and Spearman's correlation analysis. P-values < 0.05 were considered significant.

RESULTS

Reduction of Striatal DAT Expression Without Alteration of D2R and TH Levels in *Npc1*^{nmf164} Mice

It is know the functional relation between DAT and TH expression in the striatum (Salvatore et al., 2016) and the physical association between D2R and DAT proteins at striatal presynaptic terminals (Lee et al., 2007). To examine whether the dysregulation of cholesterol homeostasis in *Npc1*-mutant mice affects dopaminergic signaling in DS, Western blot analysis for the mature form of DAT (mDAT), D2R, TH was performed on protein extracted from tissue punches of PN30 *Npc1*^{nmf164} mice, and *wt* littermates (**Figure 1A**). Only striatal mDAT levels were found significantly reduced in *Npc1*^{nmf164} mice compared to control littermates ($P < 0.01$; **Figure 1B**).

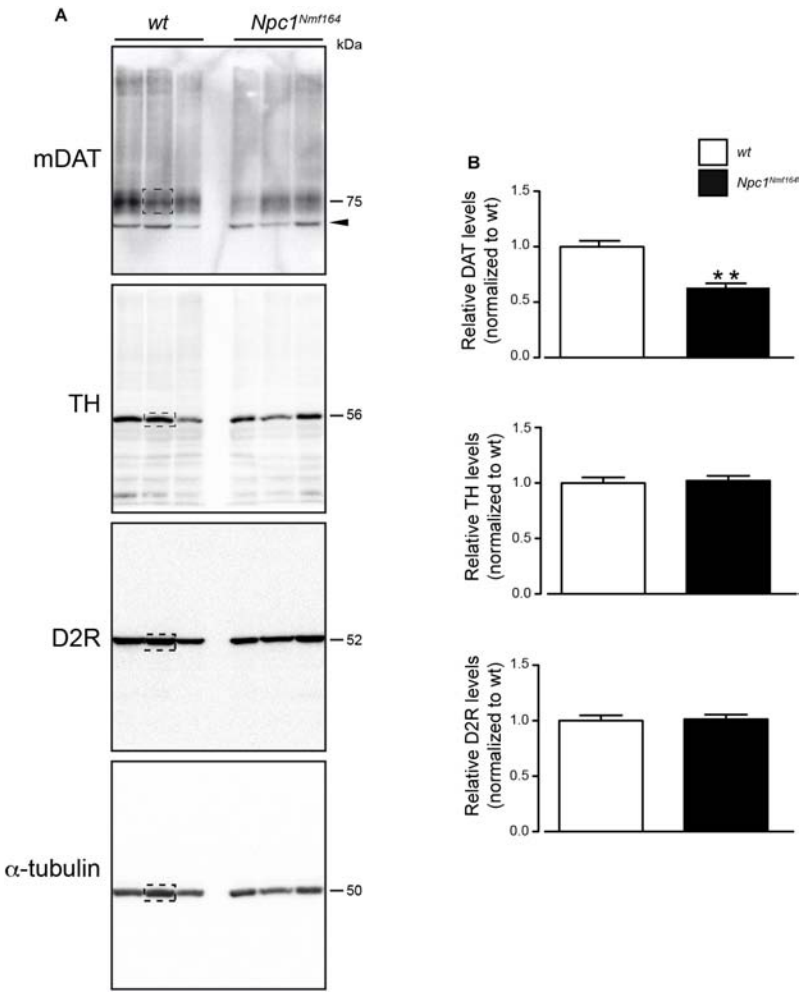

FIGURE 1 | *Npc1*^{nmf164} mice display reduction of striatal mDAT expression. **(A)** Western blot analysis of DAT, D2R, TH, and α-tubulin in representative dorsal striatum (DS) samples of *wt* or *Npc1*^{nmf164} juvenile littermate mice. Boxed areas highlight bands of interest. **(B)** Densitometric quantification of immunostained mDAT, D2R, and TH proteins in DS extracts prepared from juvenile *wt* or *Npc1*^{nmf164} littermate mice are shown as median ± SEM (n = 5 mice per group), $^{**}P < 0.01$, Mann-Withney *U*-test. Arrowhead indicates likely immature form of DAT.

3D Analysis of Striatal PC: Novel Measurement Method Displays Comparable Average Length of PC but a Different Length Frequency Distribution

Npc1^{nmf164} mice show a reduction of mDAT expression that is likely associated to increased dopaminergic stimulation, which controls PC length through the cAMP pathway (Neve et al., 2004; Ou et al., 2009). To study possible variations of PC morphology in striatal sections from *Npc1*^{nmf164} and *wt* mice, we performed a double IHC labeling with antibodies against γ-tubulin (as basal body marker) and ACIII (as neuronal ciliary shaft marker) (**Figure 2A**) coupled to the Neurolucida acquisition system. The latter allows the application to PC analysis of standard tools used for neuron tracing, as simultaneous and precise 3D measurements (±0.5 μm) of length, diameter, and tortuosity.

The experimental results revealed no significant difference between the two genotypes in the mean length of neuronal PC (**Figure 2B**), as well as in other parameters, including ciliary area, volume, tortuosity, and diameter (**Figure 2C**). In *Npc1*^{nmf164} mice, however, significant differences were observed in the number of ACIII-positive PC (P = 0.03) and distribution of PC lengths (P = 0.02), with an increment of PC with very short (2 μm), or very long length (17 μm and over), compared to control mice (**Figure 2D**).

Finally, Spearman's correlation analysis was used to investigate the relationships between three major PC morphological parameters: length, diameter, and tortuosity. The analysis between ACIII-positive PC length and tortuosity, defined as greater bends or kinks in the ciliary axoneme, surprisingly demonstrated a perfect Spearmann's correlation in *Npc1*^{nmf164} mice, in contrast to *wt* mice. In mutant mice, in fact, the tortuosity progressively rises with increasing length, whereas in

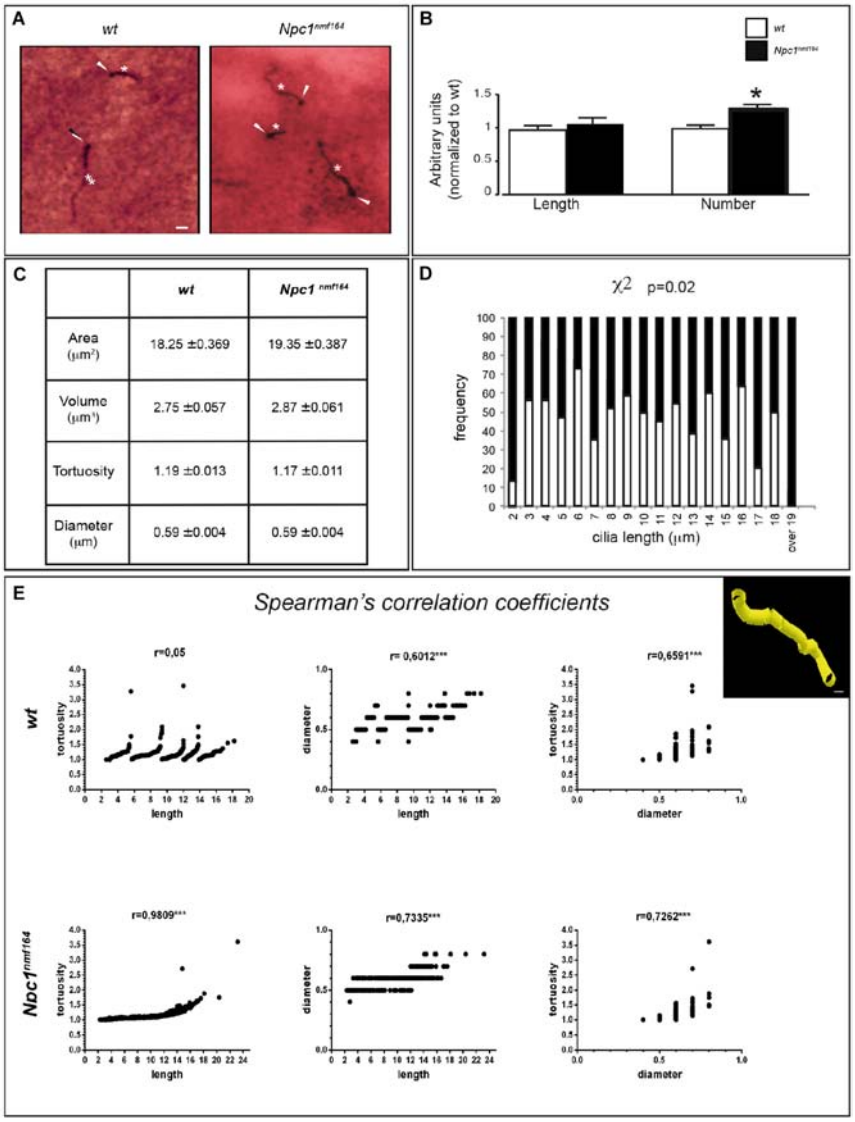

FIGURE 2 | *Npc1*^{nmf164} mice show an altered number and length distribution of striatal neuronal primary cilia. **(A)** Detection of primary cilia (PC) in the DS of PN30 *wt* and *Npc1*^{nmf164} mouse by double IHC with antibodies against γ-tubulin (basal body) and adenylyl cyclase III (ACIII, PC shaft) as indicated by arrowheads and asterisks, respectively. Scale bar: 5 μm. **(B)** Histograms represent (median ± SE) the quantification of PC length and number in *wt* (empty bars) and *Npc1*^{nmf164} (full bars) mice (n = 5 animals/genotype). Asterisks indicate statistically significant differences (*$P < 0.05$, Mann-Withney U-test and Student's t-tests). **(C)** Summary of ciliary morphological features and corresponding average values, indicated as median ± SE. No significant differences were found. **(D)** Histograms show the significant difference in the distributions of ACIII-positive ciliary length values in the dorsal striatum, between *wt* and *Npc1*^{nmf164} mice (P = 0.02). **(E)** Scatter plot and Spearman's correlation coefficients between three morphological features (ciliary length, tortuosity and diameter) for each genotype (***$P < 0.0005$). The upper right panel shows a representative 3D Neurolucida reconstruction of dorsal striatal PC. Scale bar: 1 μm.

wt mice a considerable tortuosity variability is observed both in long and short cilia. Concerning length-diameter and diameter-tortuosity relationships, similar positive Spearman coefficients were found in both *wt* and mutant samples (**Figure 2E**).

DISCUSSION

The prominent feature of the NPC1 disease is a distinctive progressive neurodegeneration, with cerebellum and Purkinje neurons being particularly vulnerable (Higashi et al., 1993; Nusca et al., 2014). Some clinical features, however, overlap between lysosomal storage disorders as NPC1 and Parkinson's disease, suggesting that the two disorders may be pathogenically linked (Storch et al., 2004; Deng et al., 2015).

To characterize the likely contribution of striatal component in the etiology of NPC1 disease, we analyzed the expression of effectors of DA signaling, including mDAT, D2R, and TH by Western Blot analysis of striatal samples from *Npc1*^{nmf164} mice at a juvenile, asymptomatic age in comparison to *wt* littermates.

The reduction of mDAT protein levels in PN30 *Npc1*^{nmf164} mice is in agreement with the marked symmetrical loss of striatal DAT, especially in the putamen, observed in NPC1 patients by DAT-scan analysis (Terbeek et al., 2017; Tomic, 2018).

The absence of D2R-mediated stimulation increases cAMP level, which in turn leads to neuronal PC elongation (Besschetnova et al., 2010; Miyoshi et al., 2014). It is also known that PC length and density exhibit brain region-specific changes (Sipos et al., 2018) and ciliary D1-receptor translocates to and from cilia in response to environmental cues (Domire et al., 2011). In addition, DAT, TH, and D2R proteins colocalize in nigrostriatal terminals and their expression levels are often affected in neurological/neurodegenerative disorders. The distribution of D1R and D2R varies along the rostro-caudal axis of the DS (Gangarossa et al., 2013), whereas DAT and D2R directly interact to facilitate the recruitment of DAT to the plasma membrane (Lee et al., 2007).

We have recently reported that there is a reduction of PC density and length in hippocampal neurons of *Npc1*$^{-/-}$ mice as well as in fibroblasts of NPC1 patients, with associated dysregulation of expression/subcellular localization of Shh pathway components (Canterini et al., 2017). As no previous information was available on *Npc1* deficiency-dependent morphological changes of striatal PC, we performed a 3D analysis of ciliary images for understanding structural determinants of normal and pathological PC function.

The remarkable length of PC of striatal neurons of either *wt* or *Npc1*^{nmf164} mice is in agreement with a previous study that reported the presence in the striatum of a large number of long ACIII-positive PC (Bishop et al., 2007). The absence of statistically significant differences between the two genotypes in the average values of ACIII-, γ tubulin-positive PC length, and related parameters indicates that the mild alteration of DAT expression that we found does not lead to a structural remodeling of dorsal striatal PC in mutant mice. However, a more detailed analysis showed that *Npc1*^{nmf164} mice display an increased number of ACIII-, γ-tubulin-positive PC and a different distribution of their lengths, together with increased tortuosity in a length-dependent manner, suggesting anomalies of ciliary functions.

The wider range of lengths and the positive correlation between length and tortuosity observed in *Npc1*^{nmf164} suggest that mutant cilia are "unstable." Such instability possibly reflects a mis-regulation of axonemal length. Mutant cilia could undergo excessive elongation and fragmentation that would explain the increment of either very short or very long PC, which is observed in mutant mice. Similar ciliary instability was reported in Kdm3a mutants (Yeyati et al., 2017).

The reason of regional difference of PC expression in NPC1 disease is still unclear. It could be attributable to multiple factors such as regional changes in dopaminergic signaling or projections, spatial regulation of Shh released from dendrites and axons of dopaminergic neurons or to differences in intracellular cAMP levels that positively regulate the length of PC through the modulation of protein kinase A activity.

In conclusion, our findings identify for the first time subtle changes occurring in the striatum of juvenile asymptomatic *Npc1*^{nmf164} mice that could contribute to NPC1 disease neurological manifestations. This is in agreement with: (i) our previous studies that demonstrated early developmental defects which occur postnatally in the cerebellum of *Npc1*-deficient mice and largely anticipate motor deficits, typically observed during adulthood (Nusca et al., 2014; Caporali et al., 2016); (ii) reported embryonic abnormalities in the metabolism of cholesterol in striatal neurons of *Npc1*-deficient mice (Henderson et al., 2000); (iii) DAT KO-mice display ataxic symptoms, tremors, dystonia and saccade-failure (Cyr et al., 2003), typical of related-dopamine-transporter-deficiency syndrome (Ng et al., 2014) and late-onset NPC1 disease (Vanier, 2010).

Although the anomalies in DAT expression and PC of Pn30 Npc1 mice we report in this study appear mild, we expect later stages of the disease to be landmarked by more robust alterations, with a decrement of DAT expression and PC length, as consequence of a progressive worsening of the perturbations of plasma membrane lipid content (Peake and Vance, 2010).

ETHICS STATEMENT

Animal experimental protocols and related procedures were approved by the Italian Ministry of Health-General Directorate of Animal Health (995/2016; D.Igs. 26/2014). All efforts were made to minimize animal suffering, according to European Directive 2010/63/EU.

AUTHOR CONTRIBUTIONS

ML performed IHC, image acquisition, and statistical data-analysis. CDP and GLS performed Western Blot and statistical data-analysis. MF contributed with advise and discussion. SC conceived the project. SC and DM directed the project, prepared the figures, and wrote the manuscript.

FUNDING

This study was supported by FFABR to SC and Ateneo La Sapienza (RM11615501ED6577) to MF.

ACKNOWLEDGMENTS

We are grateful to Raffaele Matteoni for critically reading the manuscript.

SUPPLEMENTARY MATERIAL

The Supplementary Material for this article can be found online at: https://www.frontiersin.org/articles/10.3389/fncel.2019.00226/full#supplementary-material

REFERENCES

Adkins, E. M., Samuvel, D. J., Fog, J. U., Eriksen, J., Jayanthi, L. D., Vaegter, C. B., et al. (2007). Membrane mobility and microdomain association of the dopamine transporter studied with fluorescence correlation spectroscopy and fluorescence recovery after photobleaching. *Biochemistry* 46, 10484–10497. doi: 10.1021/bi700429z

Besschetnova, T. Y., Kolpakova-Hart, E., Guan, Y., Zhou, J., Olsen, B. R., and Shah, J. V. (2010). Identification of signaling pathways regulating primary cilium length and flow-mediated adaptation. *Curr. Biol.* 20, 182–187. doi: 10.1016/j.cub.2009.11.072

Bishop, G. A., Berbari, N. F., Lewis, J., and Mykytyn, K. (2007). Type III adenylyl cyclase localizes to primary cilia throughout the adult mouse brain. *J. Comp. Neurol.* 505, 562–571. doi: 10.1002/cne.21510

Campus, P., Canterini, S., Orsini, C., Fiorenza, M. T., Puglisi-Allegra, S., and Cabib, S. (2017). Stress-induced reduction of dorsal striatal D2 dopamine receptors prevents retention of a newly acquired adaptive coping strategy. *Front. Pharmacol.* 8:621. doi: 10.3389/fphar.2017.00621

Canterini, S., Bosco, A., Carletti, V., Fuso, A., Curci, A., Mangia, F., et al. (2012). Subcellular TSC22D4 localization in cerebellum granule neurons of the mouse depends on development and differentiation. *Cerebellum* 11, 28–40. doi: 10.1007/s12311-010-0211-8

Canterini, S., Dragotto, J., Dardis, A., Zampieri, S., De Stefano, M. E., Mangia, F., et al. (2017). Shortened primary cilium length and dysregulated sonic hedgehog signaling in niemann-pick C1 disease. *Hum. Mol. Genet.* 26, 2277–2289. doi: 10.1093/hmg/ddx118

Caporali, P., Bruno, F., Palladino, G., Dragotto, J., Petrosini, L., Mangia, F., et al. (2016). Developmental delay in motor skill acquisition in niemann-pick C1 mice reveals abnormal cerebellar morphogenesis. *Acta Neuropath. Commun.* 4:94. doi: 10.1186/s40478-016-0370-z

Colelli, V., Fiorenza, M. T., Conversi, D., Orsini, C., and Cabib, S. (2010). Strain-specific proportion of the two isoforms of the dopamine D2 receptor in the mouse striatum: associated neural and behavioral phenotypes. *Genes Brain Behav.* 9, 703–711. doi: 10.1111/j.1601-183X.2010.00604.x

Cyr, M., Beaulieu, J. M., Laakso, A., Sotnikova, T. D., Yao, W. D., Bohn, L. M., et al. (2003). Sustained elevation of extracellular dopamine causes motor dysfunction and selective degeneration of striatal GABAergic neurons. *Proc. Natl. Acad. Sci. U.S.A.* 16, 11035–11040. doi: 10.1073/pnas.1831768100

Deng, H., Xiu, X., and Jankovic, J. (2015). Genetic convergence of Parkinson's disease and lysosomal storage disorders. *Mol. Neurobiol.* 51, 1554–1568. doi: 10.1007/s12035-014-8832-4

Di Pietro, C., Marazziti, D., La Sala, G., Abbaszadeh, Z., Golini, E., Matteoni, R., et al. (2017). Primary cilia in the murine cerebellum and in mutant models of medulloblastoma. *Cell. Mol. Neurobiol.* 37, 145–154. doi: 10.1007/s10571-016-0354-3

Domire, J. S., Green, J. A., Lee, K. G., Johnson, A. D., Askwith, C. C., and Mykytyn, K. (2011). Dopamine receptor 1 localizes to neuronal cilia in a dynamic process that requires the Bardet-Biedl syndrome proteins. *Cell. Mol. Life Sci.* 68, 2951–2960. doi: 10.1007/s00018-010-0603-4

Fiorenza, M. T., Dardis, A., Canterini, S., and Erickson, R. P. (2013). Cholesterol metabolism associated molecules in late onset Alzheimer's disease. *J. Biol. Regul. Homeost. Agents* 27, 23–35.

Fiorenza, M. T., Moro, E., and Erickson, R. P. (2018). The pathogenesis of lysosomal storage disorders: beyond the engorgement of lysosomes to abnormal development and neuroinflammation. *Hum. Mol. Genet.* 27, R119–R129. doi: 10.1093/hmg/ddy155

Foster, J. D., Adkins, S. D., Lever, J. R., and Vaughan, R. A. (2008). Phorbol ester induced trafficking-independent regulation and enhanced phosphorylation of the dopamine transporter associated with membrane rafts and cholesterol. *J. Neurochem.* 105, 1683–1699. doi: 10.1111/j.1471-4159.2008.05262

Gabriel, L. R., Wu, S., Kearney, P., Bellvé, K. D., Standley, C., Fogarty, K. E., et al. (2013). Dopamine transporter endocytic trafficking in striatal dopaminergic neurons: differential dependence on dynamin and the actin cytoskeleton. *J. Neurosci.* 33, 17836–17846. doi: 10.1523/JNEUROSCI.3284-13.2013

Gangarossa, G., Espallergues, J., de Kerchove d'Exaerde, A., El Mestikawy, S., Gerfen, C. R., Hervé, D., et al. (2013). Distribution and compartmental organization of GABAergic medium-sized spiny neurons in the mouse nucleus accumbens. *Front. Neural. Circ.* 7:22. doi: 10.3389/fncir.2013.00022

Guo, J., Higginbotham, H., Li, J., Nichols, J., Hirt, J., Ghukasyan, V., et al. (2015). Developmental disruptions underlying brain abnormalities in ciliopathies. *Nat. Commun.* 6, 7857–7870. doi: 10.1038/ncomms8857

Henderson, L. P., Lin, L., Prasad, A., Paul, C. A., Chang, T. Y., and Maue, R. A. (2000). Embryonic striatal neurons from niemann-pick type C mice exhibit defects in cholesterol metabolism and neurotrophin responsiveness. *J. Biol. Chem.* 275, 20179–20187. doi: 10.1074/jbc.M001793200

Higashi, Y., Murayama, S., Pentchev, P. G., and Suzuki, K. (1993). Cerebellar degeneration in the niemann-pick type C mouse. *Acta Neuropathol.* 85, 175–184.

Hong, W. C., and Amara, S. G. (2010). Membrane cholesterol modulates the outward facing conformation of the dopamine transporter and alters cocaine binding. *J. Biol. Chem.* 285, 32616–32626. doi: 10.1074/jbc.M110.150565

Jones, K. T., Zhen, J., and Reith, M. E. (2012). Importance of cholesterol in dopamine transporter function. *J. Neurochem.* 123, 700–715. doi: 10.1111/jnc.12007

Lee, F. J. S., Pei, L., Moszczynska, A., Vukusic, B., Fletcher, P. J., and Liu, F. (2007). Dopamine transporter cell surface localization facilitated by a direct interaction with the dopamine D2 receptor. *EMBO J.* 26, 2127–2136. doi: 10.1038/sj.emboj.7601656

Marley, A., and von Zastrow, M. (2010). DISC1 regulates primary cilia that display specific dopamine receptors. *PLoS One* 5:e10902. doi: 10.1371/journal.pone.0010902

Maue, R. A., Burgess, R. W., Wang, B., Wooley, C. M., Seburn, K. L., Vanier, M. T., et al. (2012). A novel mouse model of niemann-pick type C disease carrying a D1005G-Npc1 mutation comparable to commonly observed human mutations. *Hum. Mol. Genet.* 21, 730–750. doi: 10.1093/hmg/ddr505

Miyoshi, K., Kasahara, K., Murakami, S., Takeshima, M., Kumamoto, N., Sato, A., et al. (2014). Lack of dopaminergic inputs elongates the primary cilia of striatal neuron. *PLoS One* 9:e97918. doi: 10.1371/journal.pone.0097918

Neve, K. A., Seamans, J. K., and Trantham-Davidson, H. (2004). Dopamine receptor signaling. *J. Recept. Signal Transduct. Res.* 24, 165–205. doi: 10.1081/rrs-200029981

Ng, J., Zhen, J., Meyer, E., Erreger, K., Li, Y., Kakar, N., et al. (2014). Dopamine transporter deficiency syndrome: phenotypic spectrum from infancy to adulthood. *Brain* 137, 1107–1119. doi: 10.1093/brain/awu022

Nusca, S., Canterini, S., Palladino, G., Bruno, F., Mangia, F., Erickson, R. P., et al. (2014). A marked paucity of granule cells in the developing cerebellum of the Npc1(-/-) mouse is corrected by a single injection of hydroxypropyl-β-cyclodextrin. *Neurobiol. Dis.* 70, 117–126. doi: 10.1016/j.nbd.2014.06.012

Ou, Y., Ruan, Y., Cheng, M., Moser, J. J., Rattner, J. B., and van der Hoorn, F. A. (2009). Adenylate cyclase regulates elongation of mammalian primary cilia. *Exp. Cell Res.* 315, 2802–2817. doi: 10.1016/j.yexcr.2009.06.028

Palladino, G., Loizzo, S., Fortuna, A., Canterini, S., Palombi, F., Erickson, R. P., et al. (2015). Visual evoked potentials of Niemann-Pick type C1 mice reveal an impairment of the visual pathway that is rescued by 2-hydroxypropyl-ß-cyclodextrin. *Orphanet J. Rare Dis.* 10, 133–144. doi: 10.1186/s13023-015-0348-0

Peake, K. B., and Vance, J. E. (2010). Defective cholesterol trafficking in niemann-pick C-deficient cells. *FEBS Lett.* 584, 2731–2739. doi: 10.1016/j.febslet.2010.04.047

Salvatore, M. F., Calipari, E. S., and Jones, S. R. (2016). Regulation of tyrosine hydroxylase expression and phosphorylation in dopamine transporter-deficient mice. *ACS Chem. Neurosci.* 7, 941–951. doi: 10.1021/acschemneuro.6b00064

Sipos, É, Komoly, S., and Ács, P. (2018). Quantitative comparison of primary cilia marker expression and length in the mouse brain. *J. Mol. Neurosci.* 64, 1–13. doi: 10.1007/s12031-018-1036-z

Storch, A., Ludolph, A. C., and Schwarz, J. (2004). Dopamine transporter: involvement in selective dopaminergic neurotoxicity and degeneration. *J. Neural. Transm.* 11, 1267–1286. doi: 10.1007/s00702-004-0203-2

Terbeek, J., Latour, P., Van Laere, K., and Vandenberghe, W. (2017). Abnormal dopamine transporter imaging in adult-onset niemann-pick disease type

C. *Parkinsonism. Relat. Disord.* 36, 107–108. doi: 10.1016/j.parkreldis.2016.12.029

Tomic, S. (2018). Dopamine transport system imaging is pathologic in niemann-pick type C-case report. *Neurol. Sci.* 39, 1139–1140. doi: 10.1007/s10072-018-3269-6

Vanier, M. T. (2010). Niemann-pick disease type C. *Orphanet J. Rare Dis.* 5, 16–33. doi: 10.1186/1750-1172-5-16

Vanier, M. T. (2013). Niemann–pick diseases. *Handb. Clin. Neurol.* 113, 1717–1721. doi: 10.1016/B978-0-444-59565-2.00041-1

Waters, A. M., and Beales, P. L. (2011). Ciliopathies: an expanding disease spectrum. *Pediatr. Nephrol.* 26, 1039–1056. doi: 10.1007/s00467-010-1731-7

Yeyati, P. L., Schiller, R., Mali, G., Kasioulis, I., Kawamura, A., Adams, I. R., et al. (2017). KDM3A coordinates actin dynamics with intraflagellar transport to regulate cilia stability. *J. Cell Biol.* 216, 999–1013. doi: 10.1083/jcb.201607032

Conflict of Interest Statement: The authors declare that the research was conducted in the absence of any commercial or financial relationships that could be construed as a potential conflict of interest.

frontiers in Cellular Neuroscience

BRIEF RESEARCH REPORT
published: 20 December 2019
doi: 10.3389/fncel.2019.00565

Targeted Depletion of Primary Cilia in Dopaminoceptive Neurons in a Preclinical Mouse Model of Huntington's Disease

*Rasem Mustafa[1,2], Grzegorz Kreiner[3], Katarzyna Kamińska[4,5], Amelia-Elise J. Wood[6], Joachim Kirsch[2], Kerry L. Tucker[6] and Rosanna Parlato[1,2]**

[1]*Institute of Applied Physiology, University of Ulm, Ulm, Germany,* [2]*Institute of Anatomy and Cell Biology, Medical Cell Biology, University of Heidelberg, Heidelberg, Germany,* [3]*Department of Brain Biochemistry, Maj Institute of Pharmacology, Polish Academy of Sciences, Kraków, Poland,* [4]*Department of Pharmacology, Maj Institute of Pharmacology, Polish Academy of Sciences, Kraków, Poland,* [5]*Jagiellonian Center for Experimental Therapeutics, Jagiellonian University, Kraków, Poland,* [6]*Department of Biomedical Sciences, Center for Excellence in the Neurosciences, College of Osteopathic Medicine, University of New England, Biddeford, ME, United States*

Multiple pathomechanisms triggered by mutant Huntingtin (mHTT) underlie progressive degeneration of dopaminoceptive striatal neurons in Huntington's disease (HD). The primary cilium is a membrane compartment that functions as a hub for various pathways that are dysregulated in HD, for example, dopamine (DA) receptor transmission and the mechanistic target of rapamycin (mTOR) pathway. The roles of primary cilia (PC) for the maintenance of striatal neurons and in HD progression remain unknown. Here, we investigated PC defects in vulnerable striatal neurons in a progressive model of HD, the mHTT-expressing knock-in zQ175 mice. We found that PC length is affected in striatal but not in cortical neurons, in association with the accumulation of mHTT. To explore the role of PC, we generated conditional mutant mice lacking IFT88, a component of the anterograde intraflagellar transport-B complex lacking PC in dopaminoceptive neurons. This mutation preserved the expression of the dopamine 1 receptor (D1R), and the survival of striatal neurons, but resulted in a mild increase of DA metabolites in the striatum, suggesting an imbalance of ciliary DA receptor transmission. Conditional loss of PC in zQ175 mice did not trigger astrogliosis, however, mTOR signaling was more active and resulted in a more pronounced accumulation of nuclear inclusions containing mHTT. Further studies will be required of aged mice to determine the role of aberrant ciliary function in more advanced stages of HD.

Keywords: primary cilium, dopamine system, Huntington's disease, mTOR, p62

OPEN ACCESS

Edited by:
Thomas Fath, Macquarie University, Australia

Reviewed by:
Jiro Kasahara, Tokushima University, Japan
Erik B. Malarkey, Vertex Pharmaceuticals, United States

****Correspondence:***
Rosanna Parlato
rosanna.parlato@uni-ulm.de

Received: *10 July 2019*
Accepted: *05 December 2019*
Published: *20 December 2019*

Citation:
Mustafa R, Kreiner G, Kamińska K, Wood A-EJ, Kirsch J, Tucker KL and Parlato R (2019) Targeted Depletion of Primary Cilia in Dopaminoceptive Neurons in a Preclinical Mouse Model of Huntington's Disease. Front. Cell. Neurosci. 13:565. doi: 10.3389/fncel.2019.00565

Abbreviations: ACIII, adenylate cyclase III; AD, Alzheimer's disease; DA, dopamine; DAPI, 4′,6′-diamidino-2-pheylindol; DOPAC, 3,4-dihydroxyphenylacetic acid; D1R, dopaminoceptive D1-receptor; GFAP, glial fibrillary acidic protein; HD, Huntington's disease; HPLC-EC, High-performance liquid chromatography-electrochemical detection; 5-HT, 5-hydroxytryptamine; HVA, homovanillic acid; IF, immunofluorescence; IFT-B, intraflagellar transport B; IHC, immunohistochemistry; mHTT, mutant Huntingtin; MSNs, medium spiny neurons; mTOR, mechanistic target of rapamycin; NeuN, neuronal nuclei; NPC1, Niemann-Pick type C1; PC, primary cilia; PD, Parkinson's disease; PFA, paraformaldehyde; phospho-S6, phosphorylated ribosomal protein S6; p62/SQSTM1, p62/sequestosome 1; TH, tyrosine-hydroxylase.

INTRODUCTION

Huntington's disease (HD) is an autosomal dominant progressive neurodegenerative disorder caused by the toxic expansion of CAG trinucleotide repeats at the N-terminus of the Huntingtin gene. The mechanisms underlying selective vulnerability of dopaminoceptive medium spiny neurons (MSNs), resulting in impaired control of voluntary movement in HD, remain elusive (Ghosh and Tabrizi, 2018). The variability of disease onset and progression depends on the CAG number, and on genetic modifiers interacting with the Huntingtin mutation [Genetic Modifiers of Huntington's Disease (GeM-HD) Consortium (2015)]. Multiple signaling pathways and cellular functions are affected by mutant Huntingtin (mHTT), including protein aggregate degradation, which results in the accumulation of toxic proteins (Saudou and Humbert, 2016).

Primary cilia (PC) are single, non-motile microtubule-based organelles resembling a cellular antenna that represents a hub for receptors and components of numerous signaling pathways (Malicki and Johnson, 2017). Lack of HTT results in reduced and aberrant PC growth, and increased mHTT results in increased ciliogenesis (Keryer et al., 2011). Notably, longer PC have been observed in immortalized cellular models of HD in culture, and ependymal cilia in the lateral ventricles are disorganized in a mouse model of HD and in HD human post-mortem brains (Keryer et al., 2011). Another study showed that photoreceptor cilia pathology accounts for their degeneration in the retina of R6/2 transgenic mice overexpressing exon 1 of the human mHTT (Karam et al., 2015). It has been previously proposed that PC altered structure might affect the function of signaling pathways whose components are localized in the PC (Maiuri et al., 2013; Kaliszewski et al., 2015).

Interestingly, increased PC length results in the induction of autophagy by inhibition of the mechanistic target of rapamycin (mTOR) kinase activity (Kaliszewski et al., 2015), and components essential for ciliogenesis are degraded by autophagy (Pampliega et al., 2013; Tang et al., 2013). Because autophagy is altered in HD (Ravikumar et al., 2004), as well as dopamine (DA)-mediated signaling (Chen et al., 2013), it is possible that HD pathophysiology depends, at least in part, on defective cilia. These previous studies investigated neither PC dysfunction in the most vulnerable striatal neurons, nor the impact of defective PC on HD pathogenesis in the striatum. A deeper understanding of the role of PC in mHTT-dependent neurotoxicity might help to identify new determinants modifying HD progression.

To this end, we monitored neuron- and stage-specific changes of PC structure in a full-length progressive mouse model of HD, called zQ175 (Menalled et al., 2012; Carty et al., 2015). This knock-in model carries a chimeric human/mouse *HTT* exon 1 containing expanded CAG repeats within the murine *htt* gene and recapitulates several hallmarks of HD pathology (Menalled et al., 2012; Farrar et al., 2014; Carty et al., 2015; Ma et al., 2015). Moreover, we generated a new genetic mouse model of defective ciliary function in striatal neurons, as a tool to investigate the specific impact of PC loss on striatal neuron maintenance and on HD neuropathological hallmarks.

MATERIALS AND METHODS

Mice

To generate a mutant mouse in which the *Ift88* gene is conditionally ablated by the Cre-LoxP system in MSNs, we employed the B6.FVB/N-Tg(D1RCre)Gsc (D1R:Cre) transgene, which expresses the Cre recombinase under the control of the dopamine 1 receptor (D1R) promoter (Lemberger et al., 2007). The D1R:Cre mice were crossed to $Ift88^{tm1.1Bky}$ mice carrying the *Ift88* floxed allele ($Ift88^{flox/flox}$; Haycraft et al., 2007) to generate $Ift88^{flox/flox}$; D1R:Cre mice ($Ift88^{D1RCre}$; here abbreviated *Ift88* cKO mice) that lack PC in MSNs. $Htt^{tmtm1Mfc}$/190tChdi (zQ175 knock-in) mice were received courtesy of the CHDI Foundation from the Jackson Laboratory. The analysis of the genotype was performed by PCR of tail snips as previously described (Levine et al., 1999). For the experiments reported here, male and female mice were used and wild-type and mutant littermates were analyzed. The zQ175 knock-in mice carry ca. 190 CAG repeats in a chimeric human/mouse exon 1 of the murine huntingtin gene (Menalled et al., 2012). The zQ175 mutation was kept in heterozygosity, to limit toxicity and mimic a genetic situation more relevant for the disease, as it is autosomal dominant (Menalled et al., 2012). These mutant mice were born at the expected Mendelian ratio; they showed normal lifespan and no gross abnormalities (monitored until 1-year-old).

For genotyping of D1R:Cre and floxed *Ift88* alleles by PCR the following primer pairs was used: forward-primer/Cre (5′-GGA AAT GGT TTC CCG CAG AAC-3′) and reverse-primer/Cre (5′-ACG GAA ATC CAT CGC TCG ACC-3′), BY919 (5′-GGTCCTAACAAGTAAGCCCAGTGTT-3′) and BY598 (5′-GCCTCCTGTTTCTTGACAACAGTG-3′), respectively. For the zQ175 we used forward-primer/Neo: 5′-GAT CGG CCA TTG AAC AAG ATG– 3′ and reverse-primer/Neo: 5′-AGA GCA GCC GAT TGT CTG TTG– 3′.

Brain Dissection and Tissue Preparation

For histological analysis, brains were either transcardially perfused or post-fixed in 4% paraformaldehyde (PFA; pH 7.2) overnight at 4°C. After washing in PBS (pH 7.2) the brains were cryoprotected by incubating them in 10%, 20%, and 30% sucrose for 3 days at 4°C. The brains were embedded in a coronal orientation (Tissue freezing medium, Leica), frozen by a mixture of liquid nitrogen and dry ice, and stored at −80°C until sectioning (Leica CM3050S cryostat). For the analysis of adult brains, we have used coronal sections from striatum collected serially on Superfrost Ultraplus glass slides (12 μm) and free-floating striatum (30 μm). We analyzed the striatum in the region comprised between Bregma +1.18 mm and −0.34 mm based on the adult mouse brain Atlas (Franklin, 2008). For immunofluorescence on paraffin sections, one brain hemisphere was fixed in 4% PFA in PBS, pH 7.2 overnight at 4°C and paraffin-embedded.

Immunofluorescence

Immunofluorescence (IF) on cryosections was performed according to established protocols (Gazea et al., 2016). Cryosections (12 μm) were pre-incubated with 5% normal pig

serum in PBS for 30 min at room temperature before overnight incubation at 4°C with the primary antibodies appropriately diluted in the blocking solution. After washing in PBS the sections were incubated with the secondary antibodies (diluted in 5% pig serum in PBS) for 30 min at room temperature. After further washes in PBS the sections were stained for 10 min with 4′,6′-diamidino-2-pheylindol (DAPI, Thermoscientific) diluted in PBS.

Free-floating cryosections (30 μm) were treated in a similar way; however, PBST (0.2% Triton X-100 in PBS) was used for washing steps and blocking solution. After staining the sections were placed on glass slides. Paraffin sections (7 μm) containing the striatum comprised between Bregma +0.14 mm and −0.98 mm were incubated with primary antibodies overnight at 4°C. Visualization of antigen-bound primary antibodies was carried out following antigen retrieval (HK086-9K, Biogenex). The following primary antibodies were used: EM48 (1:100, MAB5374, Millipore), NeuN (1:100, MAB377, Millipore), adenylate cyclase III (ACIII; 1:500, SC588, Santa Cruz Biotechnology, Dallas, TX, USA), TH (1:500, AB1542, Millipore), D1R (1:500, D2944, Sigma), glial fibrillary acidic protein (GFAP; 1:300, G-3893, Sigma), phospho-S6 (S235/236; 91B2; 1:100, 4857S, Cell Signaling), p62/SQSTM1 (1:100, P0067, Sigma). Incubation with the appropriate secondary antibodies marked with the fluorophores Alexa 594 or Alexa 488 (1:100, Thermoscientific) was followed by DAPI staining.

Confocal Microscopy Imaging and Image Analysis

Images were acquired by a Leica SP8 confocal and a Leica LASX software. For PC number and length quantification, we used a 63× oil-immersion objective maximal intensity projection z-stacked images (1 μm interval). To determine the number of striatal NeuN positive neurons showing PC stained by ACIII antibody eight non-consecutive free-floating cryosections per mouse were analyzed (one every fourth section, each 30 μm thick) in control and mutant mice. Either the number or the length of PC per microscopic field at 63× magnification was counted. In general, about 80 cells per mouse were measured by the ImageJ software after tracing the ACIII signal in line with established protocols (Miyoshi et al., 2014; Parker et al., 2016). For semi-quantitative analysis of D1R and TH immunoreactivity, and of GFAP and phosphoS6 positive cells, we used a 20× oil-immersion objective for single planes. For p62 positive cells, we used a 63× and for the EM48 a 100× oil-immersion objective. To determine D1R and TH immunoreactivity the optical fiber density was measured in cryosections (12 μm) at different ages by ImageJ software. The quantification was performed in eight coronal serial sections per mouse on 8-bit images (grayscale). To measure the mean optical intensity the "Mean Gray Value" was determined. The respective immunoreactivity was measured by subtracting the mean gray value of the respective background from the mean gray value of dorsal striatum. The measurements were limited to the drawn region of interest and the same area was selected in all sections (0.05 mm^2). The number of GFAP, pS6 and p62 and EM48 positive cells per microscopic field was counted in at least four independent paraffin sections per mouse in the dorsolateral striatal region. The EM48 signal area is calculated in μm^2. We used the Quick LUT view to avoid the acquisition of images with under- and over-saturated pixels. The quantification and counting were performed blind to genotype and age.

HPLC Analysis of Dopamine Content

The tissue levels of DA, 3,4-dihydroxyphenylacetic acid (DOPAC), homovanillic acid (HVA) and 3-methoxytyramine (3-MT), were measured using high-performance liquid chromatography with electrochemical detection (HPLC-EC). The concentrations of endogenous DA and its metabolites (DOPAC, HVA) were measured using HPLC-EC, according to a previously described method (Sikora et al., 2016). Briefly, the striatum was isolated by the adult mouse brain matrix (coronal slices, World Precision Instruments) in the 2 mm region comprised between Bregma +1.42 mm and −0.58 mm. After weighing the tissue samples were deep-frozen in dry ice and stored at −80°C until further use. Prior to analysis, the samples were homogenized in ice-cold 0.1 M $HClO_4$ and were centrifuged at 10,000 *g* for 10 min at 4°C. The supernatant (5 μl) was injected into the HPLC system. The chromatography system consisted of an LC-4C amperometric detector with a cross-flow detector cell (BAS, IN, USA), an Ultimate 3000 pump (Thermoscientific, USA) and a Hypersil Gold analytical column (3 μm, 100 × 3 mm, Thermoscientific, USA). The mobile phase consisted of 0.1 M KH_2PO_4, 0.5 mM Na_2EDTA, 80 mg/L sodium 1-octane sulfonate, and a 4% methanol, adjusted to pH 3.8 with an 85% H_3PO_4. The flow rate was 1 ml/min. The potential of a 3-mm glassy carbon electrode was set at 0.7 V with a sensitivity of 5 nA/V. The temperature of the column was maintained at 30°C. The Chromax 2007 program (Pol-Lab, Warszawa, Poland) was used for data collection and analysis. The external standard consisted of noradrenaline (NA), DA, 5-hydroxytryptamine (serotonin; 5-HT) and 5-hydroxy indole acetic acid (5-HIAA; SIGMA) at a concentration of 50 ng/ml.

Statistical Analysis

All data are expressed as mean ± SEM. Two-tailed unpaired Student's *t*-test was used for single comparisons. Multiple comparisons were performed either by one-way ANOVA or by two-way ANOVA with *post hoc* analyses as indicated in the figure legends (GraphPad Prism Software Inc.).

RESULTS

Altered Primary Cilia Length in the Striatum but Not in Cortex of zQ175 Mice

By IF and confocal analysis of brain sections, we observed the presence of sporadic mHTT inclusions at 4 months in the striatum. From 8 months mHTT accumulated mostly in the striatum but also in the cortex, in agreement with previous results (Carty et al., 2015; **Figures 1A–F**). To test the hypothesis that altered PC impacts HD neuropathology, we first investigated PC alterations in the heterozygous zQ175 knock-in model of HD. We measured the stage-specific alterations of PC length in both

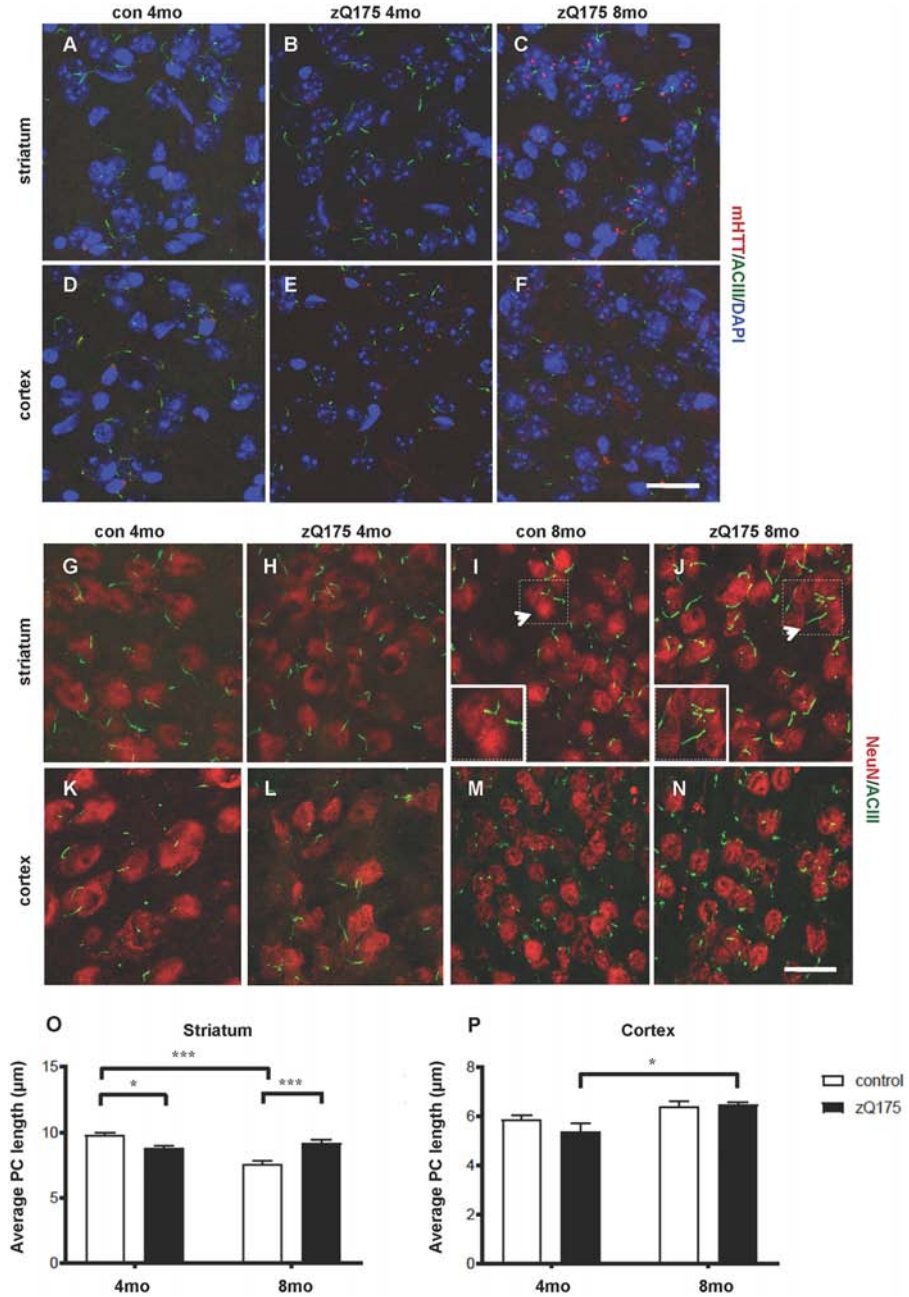

FIGURE 1 | Context-specific changes in primary cilia (PC) length in the zQ175 Huntington's disease (HD) mouse model are concomitant with mutant Huntingtin (mHTT) accumulation. **(A–F)** Representative confocal images of mHTT identified by the EM48 antibody (red) and of PC by adenylate cyclase III (ACIII), as a marker of PC (green) on cryosections from control and zQ175 mice in the dorsolateral striatum and cortex. Nuclei are visualized by 4′,6′-diamidino-2-pheylindol (DAPI) staining (blue). Scale bar: 25 μm. **(G–N)** Representative confocal images of immunofluorescent stainings on cryosections by NeuN, as a neuronal marker (red), ACIII (green), in the striatum **(G,J)** and cortex **(K,N)** to identify PC that protrudes from NeuN labeled neurons. Scale bars: 25 μm **(G–J, M,N)**, 12 μm **(K,L)**, 8 μm (insets, **I** and **J**). Arrows point to the area in the inset. **(O,P)** Diagrams showing the analysis of PC average length in striatal and cortical neurons at 4 and 8 months in control and zQ175 mice; $N = 3$, 5 control, and $N = 4$, 4 zQ175. Values represent means ± SEM. $^{*}p < 0.05$, $^{***}p < 0.0005$, two-way ANOVA followed by Tukey's *post hoc* test for multiple comparisons.

striatum and cortex at 4 and 8 months in control and zQ175 mice, focusing on cells labeled by the neuronal nuclei marker NeuN (**Figures 1G–P**). PC were identified by ACIII, a major PC marker in many regions of the adult mouse brain (Bishop et al., 2007). We found that PC in dorsolateral striatum of zQ175 mice were shorter than their littermate controls at 4 months, while they were longer than respective controls at 8 months (**Figure 1O**). Notably, PC length in the striatum of controls, decreased between

4 and 8 months, but this age-dependent decrease did not occur in the zQ175 mice (**Figure 1O**). Next, we analyzed the cell-specificity of this phenotype by measuring the average PC length in cortical cells (**Figures 1K–N**). Interestingly, cortical cells of zQ175 mice did not show changes in PC length at any of the considered stages (**Figure 1P**).

Hence, mHTT accumulation either directly or indirectly affects PC length in a stage- and region-specific fashion, suggesting that altered PC function might contribute to striatal vulnerability in HD.

Conditional Ablation of the Ift88 Gene in Dopaminoceptive Neurons Leads to a Mild Increase of Dopamine Metabolite Levels in the Striatum

To investigate the effects of PC loss on HD neuropathology, we first generated inducible mutant mice conditionally lacking *Ift88*, a gene encoding a microtubular component essential for the formation of the PC (Haycraft et al., 2007). These mice are characterized by the expression of Cre recombinase under the control of dopaminoceptive D1-receptor (D1R; Lemberger et al., 2007; **Figures 2A–D**). The conditional ablation of the *Ift88* gene resulted in D1R:Cre;*Ift88*$^{flox/flox}$ (abbreviated as Ift88 cKO) mice lacking PC in most of the striatal neurons stained for neuronal nuclei (NeuN; **Figure 2E**). The *Ift88* cKO mice did not show any gross abnormalities. We monitored changes in body weight (g) over time and we found evidence of increased weight in the Ift88 cKO at 1 year (eight male control, 34.4 ± 6.1 vs. six male mutants, 44.9 ± 4.9; $p = 0.004$ two-tailed Student's *t*-test). This conditional model enabled us to mimic a condition of loss of PC in dopaminoceptive neurons to identify their context-specific function. Next, we analyzed D1R expression as a read-out of the survival of positive neurons in control and Ift88 cKO at different ages (1, 3, 6, and 12 months; **Figures 2F–H**). To investigate the impact of PC loss on neuronal survival, we analyzed the immunoreactivity of D1R in dorsolateral striatum at different ages in control and *Ift88* cKO mice by IF and semi-quantitative analysis of D1R mean signal intensity upon confocal imaging (**Figure 2H**). This analysis showed no significant differences in D1R immunoreactivity at any of the considered ages in control and *Ift88* cKO mutant mice, if at all a tendency to higher D1R immunoreactivity, suggesting that PC is not required for survival of D1R MSNs under basal conditions.

To further characterize the phenotype of the *Ift88* cKO, we investigated dopaminergic input to dopaminoceptive striatal neurons (**Figure 3**). To this end, we focused on young (1 month) and older (1 year) mice. We measured tyrosine-hydroxylase (TH) immunoreactivity by IF (**Figures 3A,B**). Interestingly, TH immunoreactivity increased in the mutant at 1 year (**Figure 3C**). Next, we asked whether the loss of PC in D1R neurons affects DA content in the striatum (**Figures 3D–G**). High performance liquid chromatography followed by electrochemical detection (HPLC-EC) showed that 1-year-old *Ift88* cKO mutant mice are characterized both by a tendency to increased levels of total DA content in the striatum as well as by a mild but significant increase of the two most important DA metabolites DOPAC, and HVA (**Figures 3D–F**).

These observations indicate subtle PC-dependent crosstalk between PC-depleted dopaminoceptive neurons and dopaminergic neurons to cope with a potentially altered dopaminergic neurotransmission.

Loss of PC in the zQ175 HD Mice Results in mTOR Activation and in Larger mHTT Nuclear Inclusions

To study the impact of PC loss on HD neuropathology, we generated zQ175 heterozygous mice lacking PC in striatal but not in cortical neurons in an *Ift88* cKO background (double mutants, dm; **Supplementary Figure S1**). To establish whether PC loss is toxic in combination with the zQ175 mutation and whether the combination of these mutations results in a more severe HD phenotype, we analyzed control, *Ift88* cKO, zQ175, and dm at 8 months (**Supplementary Figure S2** and **Figure 4**). We found no significant difference in the number of GFAP positive cells, as a marker of astrogliosis, associated with neurodegeneration, suggesting that there is no induction of massive degeneration at least until this stage (**Supplementary Figures S2A–D,I**). To monitor the clearance of protein aggregates, we quantified changes in the number of sequestosome 1 (SQSTM1/p62) protein immunopositive cells in the dorsolateral striatum by IF in the four experimental groups above (**Supplementary Figures S2E–H,J**). p62 is a cargo-binding protein associated with proteotoxic stress (Johansen and Lamark, 2011). As shown in **Supplementary Figures S2G,H**, the localization of p62 in the zQ175 and in the dm mice was intra-nuclear rather than cytoplasmic, as in controls and *Ift88* cKO, however, the number of p62 positive cells was comparable between all groups. Next, we investigated mTOR kinase activity by IF based on the levels of one of its targets, phosphorylated ribosomal protein S6 (phospho-S6, pS6; **Figures 4A–E**). Interestingly, zQ175 and dm mice showed a higher number of pS6 positive cells in comparison to controls, and this was significantly higher in the dm in comparison to the zQ175 (**Figure 4E**), suggesting that PC loss in the zQ175 mice promotes mTOR activation. Moreover, we analyzed mHTT nuclear inclusions that are absent in controls and Ift88 cKO, and visible in the zQ175 and dm (**Figures 4F–I**). At the age examined (8 months), the number of mHTT positive cells was similar in the zQ175 and dm mice (**Figure 4J**). The area of the mHTT signal in the dm is ca. Thirty percent larger in comparison to the zQ175 mice, indicating that PC limit mHTT accumulation in this model (**Figure 4K**).

DISCUSSION

In the present study, we addressed the following three questions: (1) whether PC is specifically altered in different neuronal types and HD stages; (2) what are the consequences of PC disruption in striatal neurons for their survival; and (3) to what extent these contribute to HD neuropathology in a neuronal population vulnerable in HD such as the striatum. We showed

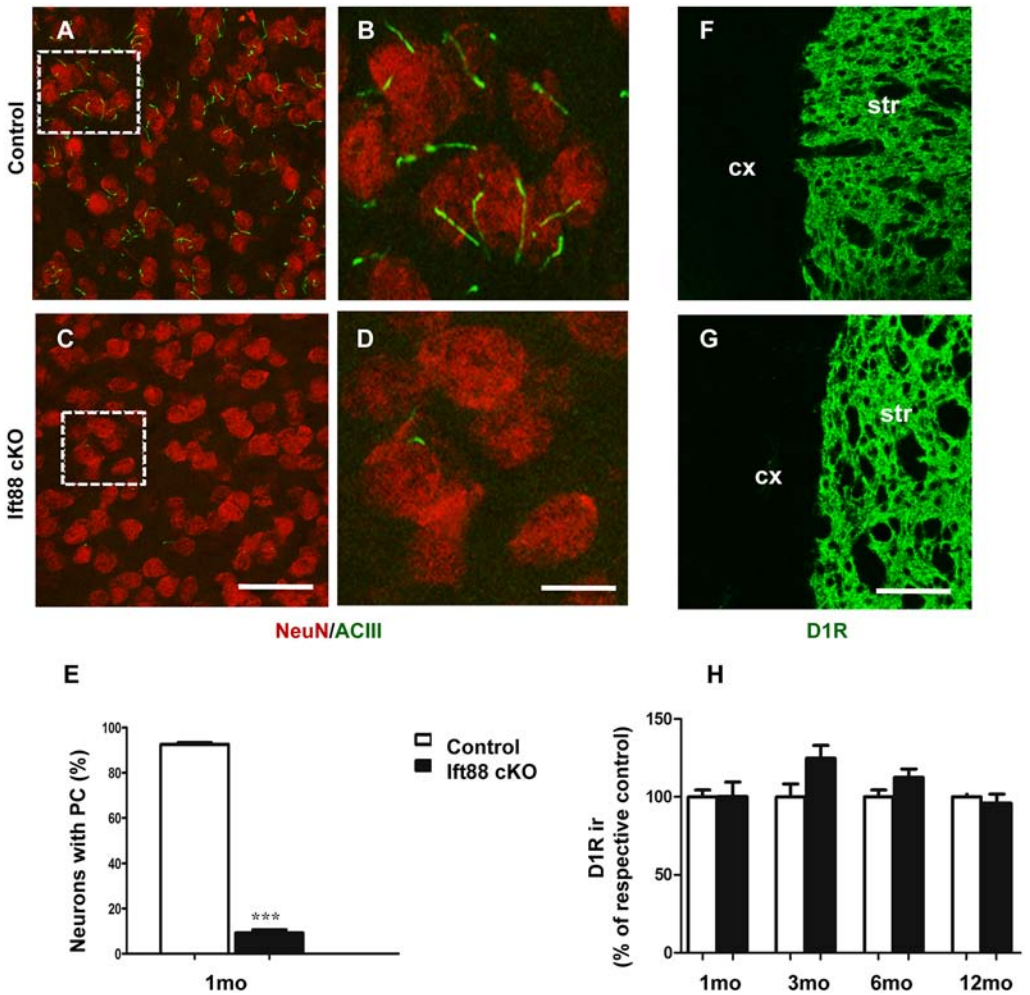

FIGURE 2 | PC is dispensable for the maintenance of dopaminoceptive D1-receptor (D1R) expression in the striatum. **(A–D)** Representative images of immunofluorescent stainings showing PC stained with ACIII (green) and NeuN (red) in control and Ift88 cKO mice at 1 month. **(E)** Diagram shows the percentage of NeuN positive cells showing ACIII staining in control and Ift88 cKO at 1 month ($N = 3$). Error bars represent SEM, $^{***}p < 0.001$ based on two-tailed unpaired Student's *t*-test. Scale bars represent 30 μm in **(A,C)** and 12 μm in **(B,D)**. **(F,G)** Examples of D1R immunostaining (green) on cryosections showing dorsolateral striatum in control and Ift88 cKO at 6 months; str, striatum; cx, cortex. **(H)** Diagram showing semi-quantitative analysis of D1R immunoreactivity (ir) in dorsolateral striatum at different ages; $N = 3$–5 controls, $N = 3$–5 Ift88 cKO. Values represent means ± SEM. Scale bar in **(F,G)**: 100 μm. No significant differences with respective controls by unpaired Student's *t*-test.

that PC length is affected in the striatum in association with mHTT accumulation. PC disruption in MSN does not affect neuronal survival. Subtle compensatory mechanisms might be activated by dopaminergic neurons in response to PC loss on dopaminoceptive neurons; however, a detailed characterization awaits future experiments. PC disruption in striatal neurons of an HD mouse model results in increased mTOR activation and larger mHTT nuclear inclusions, suggesting that PC is required in a pathological context.

Changes in PC length have been reported in previous animal and cellular models expressing mHTT; however, this is the first study focusing on PC pathology in the striatal neurons that are pathologically affected in HD and addressing the impact of loss of PC in a progressive mouse model of HD. Here, we identified changes in PC length that are concomitant with mHTT accumulation: PC length is altered in striatal but not in cortical neurons in the zQ175 mice. Previous work has indicated that HTT is important for the transport of proteins required for ciliogenesis (Keryer et al., 2011). Ciliogenesis is a tightly regulated process, and it is crucial for its proper function that PC is produced in the right size and time (Avasthi and Marshall, 2012). Given the time- and cell-specific impact of mHTT on PC, it will be important to better understand how differences in mHTT state differentially modulate PC maintenance.

Interestingly, various HD models show altered levels of DA and its metabolites (Smith et al., 2014; Koch and Raymond, 2019), and lack of dopaminergic inputs results in longer PC in the striatum (Miyoshi et al., 2014). Hence changes of DA input in the zQ175 mice might alter PC length. Because DA receptors are located in the PC membrane

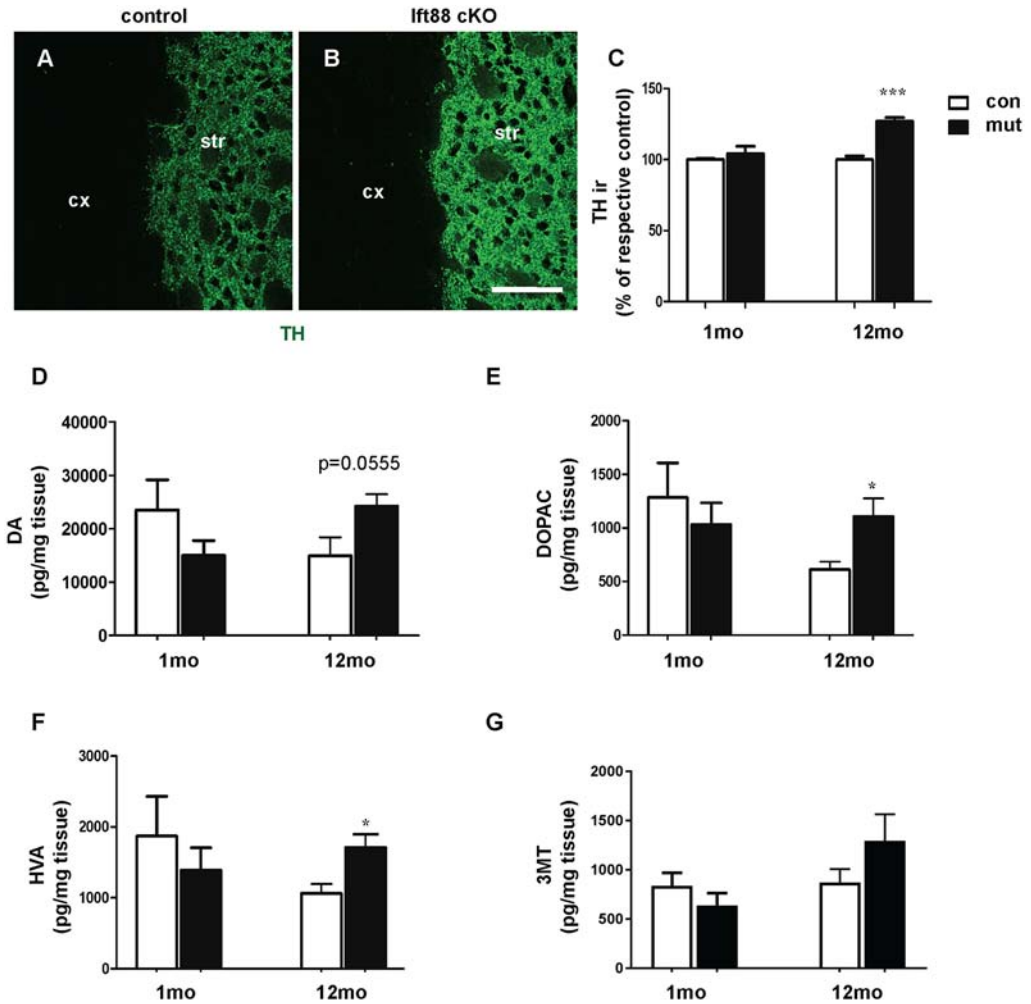

FIGURE 3 | Loss of striatal PC results in a mild increase of dopamine (DA) metabolites in the striatum. **(A,B)** Examples of tyrosine-hydroxylase (TH) immunofluorescence (IF), as a marker for dopaminergic projections, in cryosections from the dorsolateral striatum of control and Ift88 cKO mice (1-year-old). Scale bar: 100 μm. **(C)** Semi-quantitative analysis of TH immunoreactivity (ir) at 1 and 12 months; $N = 5$ per group. **(D–G)** Levels of DA and its major metabolites [3,4-dihydroxyphenylacetic acid (DOPAC), homovanillic acid (HVA), 3-methoxytyramine (3-MT)] in the striatum by HPLC-EC; $N = 5$ per group. Values represent means ± SEM. $^{*}p < 0.05$, $^{***}p < 0.001$ by unpaired Student's *t*-test with respective controls.

(Marley and von Zastrow, 2010; Domire et al., 2011; Leaf and Von Zastrow, 2015), it will be important to investigate striatal synaptic transmission, and motor and psychiatric phenotypes in the HD mice lacking PC. Future studies should address the behavioral implications of the mild increase in DA metabolite levels and increased TH expression in the striatum. These studies might help to understand the impact of current DA-based symptomatic HD treatments on PC physiology and homeostasis.

The generation of tools enabling targeting of PC function independently of changes in their structural integrity might be necessary to define subtle regulatory functions. The *Ift88* cKO approach, in which both PC function and structure are affected, does not allow us to dissect out the specific role of PC signaling from PC structure, however, it does allow us to identify cell-autonomous effects as well as non-cell autonomous responses to ciliary impairment. In aged homozygous zQ175 mice mTOR activity increases (Abd-Elrahman and Ferguson, 2019). We found in the zQ175 and in the dm mice increased phospho-S6 positive cells. Hence, another possible mechanism to explain changes in PC length might be linked to a block of autophagy by mTOR activation (Pampliega et al., 2013). Together, it will be important to analyze older zQ175 and dm mice. Conditional ablation of Ift88 in neural progenitors by the Nestin-Cre transgenic line revealed a significant increase in mTOR pathway activity and phospho-S6 ribosomal protein levels, resulting in hydrocephaly at late embryonic stages (Foerster et al., 2017). In the D1R-Cre driven conditional Ift88 knock-out, phospho-S6 does not increase in comparison to controls. These results indicate the cell-type, developmental stage and age-specific function of PC alterations, and support the need to further address this question in a mature and aging brain.

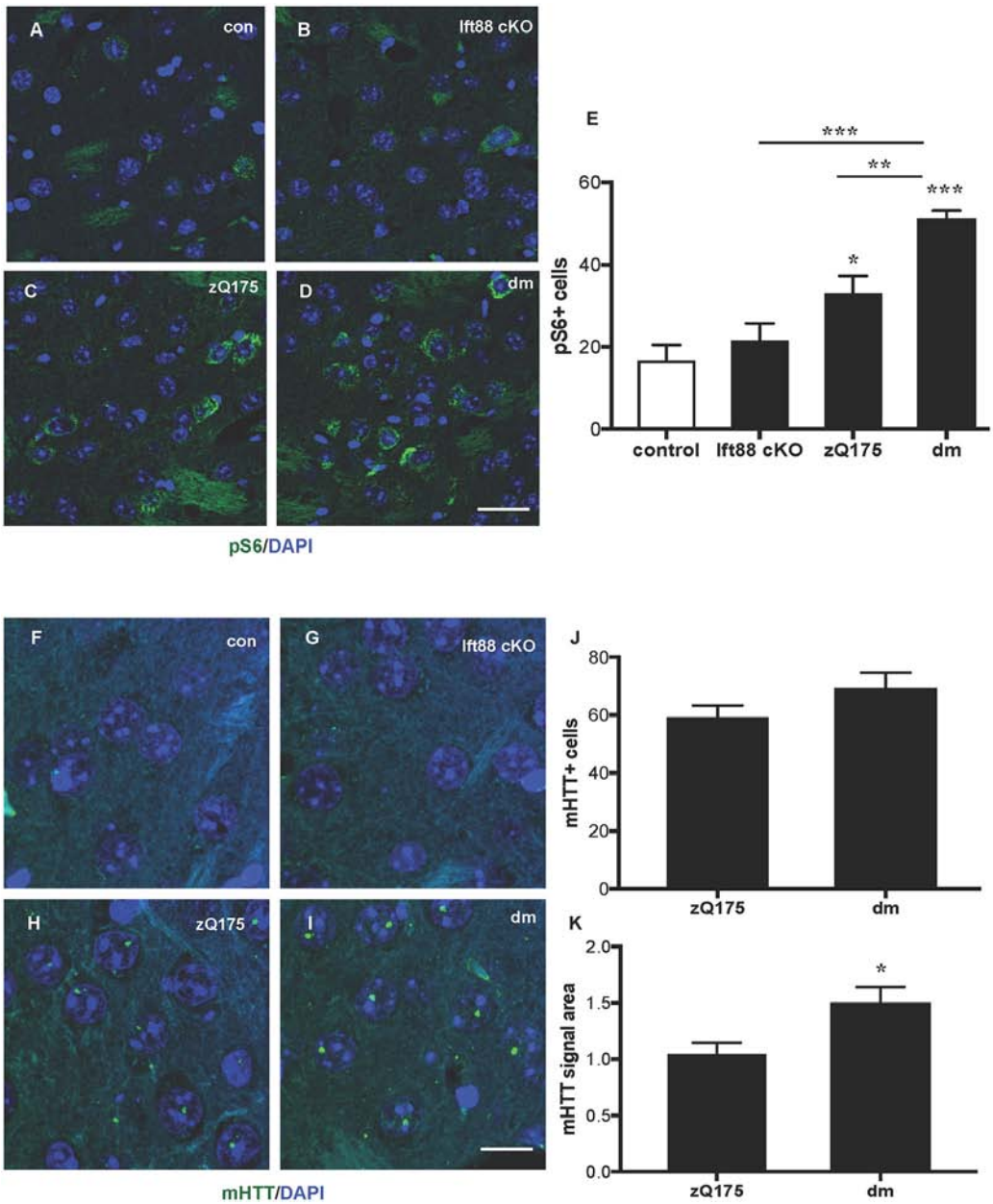

FIGURE 4 | Impact of PC loss in medium spiny neurons (MSNs) of zQ175 HD mice on the mechanistic target of rapamycin (mTOR) pathway and mHTT nuclear inclusions. **(A–D)** Representative confocal images of phopsho-S6 (pS6) IF (green) and DAPI staining (blue) on paraffin sections showing dorsolateral striatum in control, Ift88 cKO, zQ175, and dm at 8 months. Scale bar: 25 μm. **(E)** Quantification of the pS6 positive cells expressed as mean values of the number of counted cells per microscopic field. Control vs. zQ175 $^{*}p < 0.05$; control vs. dm $^{***}p < 0.0001$ Ift88 cKO vs. dm $^{***}p < 0.001$, zQ175 vs. dm $^{**}p < 0.01$ by one-way ANOVA followed by Dunnett's *post hoc* test for multiple comparisons. Values represent means ± SEM. pS6: control ($N = 5$), Ift88 cKO ($N = 5$), zQ175 ($N = 6$) and dm ($N = 5$) mice. **(F–I)** Representative confocal images of mHTT immunostaining (green) by EM48 antibody and DAPI (blue) on paraffin sections from dorsolateral striatum in control, Ift88 cKO, zQ175, and dm at 8 months. Scale bar: 10 μm. **(J,K)** Quantification of the EM48 positive cells expressed as a percentage of DAPI positive cells and of the mean EM48 signal area (in μm^2) per microscopic field. Values represent means ± SEM. $^{*}p < 0.05$ ($p = 0.019$) based on two-tailed unpaired Student's *t*-test; zQ175 ($N = 8$) and dm ($N = 6$) mice.

Diseases primarily caused by ciliary dysfunctions are commonly referred to as ciliopathies. As of yet, we cannot ascribe HD among the primary ciliopathies, nevertheless, PC structure and function are altered in association with a more severe phenotype. Notably, the role of PC in neuronal homeostasis, and in the control of the cellular stress response signaling cascades is emerging in other neurodegenerative disorders. PC pathology has been described for example in Alzheimer's disease (AD), in Parkinson's disease (PD) and in spinocerebellar ataxias, another polyglutamine disease, although distinct mechanisms are

probably involved (Steger et al., 2017; Bowie et al., 2018; Dhekne et al., 2018; Vorobyeva and Saunders, 2018). Interestingly, PC were elongated in the hippocampus of the APP/PS1 mouse models of AD compared with wild-type mice, and serotonin 5-HT6 receptors playing a critical role in AD development regulate the morphology and function of neuronal PC (Hu et al., 2017). Moreover, in mouse models of PD expressing mutant LRRK2 R1441C, PC was affected in cholinergic neurons while the overall ciliation of neurons in the striatum was not significantly different from wild type (Steger et al., 2017; Dhekne et al., 2018). Nevertheless, defective ciliogenesis in striatal cholinergic neurons might impair a protective mechanism involving non-cell autonomous Sonic hedgehog between cholinergic and dopaminergic neurons (Gonzalez-Reyes et al., 2012). The Spinocerebellar ataxia type 11-associated mutation of the serine/threonine kinase Tau tubulin kinase 2 dominantly interferes with ciliogenesis and cilium stability (Bowie et al., 2018). Shortened primary cilium length and dysregulated Sonic hedgehog signaling were also reported in Niemann-Pick type C1 (NPC1) disease, a neurodegenerative lysosomal storage disorder caused by mutations in the NPC1 gene (Canterini et al., 2017).

In summary, although we obtained similar mean PC length as previously reported for striatum and cortex in mice (Sipos et al., 2018), a systematic quantitative comparison of PC marker expression and length in various neurodegenerative disease models and in human tissues will benefit from the use of automatized segmentation approaches (Vorobyeva and Saunders, 2018), and high content automated image acquisition. These future studies will be important to determine in other disease models which cells and tissues display the cilia defects and at what stages, and try to understand when, whether and how those changes lead to specific neuronal loss in the brain.

DATA AVAILABILITY STATEMENT

All datasets generated for this study are included in the article/**Supplementary Material**.

ETHICS STATEMENT

Procedures involving animal care were approved by the Committee on Animal Care and Use (Regierungspräsidium Karlsruhe, Germany) in accordance with the local Animal Welfare Act and the European Communities Council Directives (2010/63/EU and 2012/707/EU; Ref. number: G-252/17).

AUTHOR CONTRIBUTIONS

RM, GK, KK, and RP: data acquisition. RM, GK, JK, A-EW, KT, and RP: data analysis and interpretation. RP: study concept and design, drafting of the manuscript. All authors revised the submitted manuscript.

FUNDING

This work was supported by the European Huntington's Disease Network (EHDN) seed-fund project 0907, by the "Deutsche Forschungsgemeinschaft" (DFG): DFG PA 1529/2-1 to RP, by start-up funds from the Center for Excellence in the Neurosciences at the University of New England (KT), and by the 2017/25/B/NZ7/02406 (Opus13) grant from the National Science Center and statutory funds of the Institute of Pharmacology (PAS) to GK and KK.

ACKNOWLEDGMENTS

We acknowledge the CHDI Foundation for providing the zQ175 mice used to establish the colony.

SUPPLEMENTARY MATERIAL

The Supplementary Material for this article can be found online at: https://www.frontiersin.org/articles/10.3389/fncel.2019.00565/full#supplementary-material.

REFERENCES

Abd-Elrahman, K. S., and Ferguson, S. S. G. (2019). Modulation of mTOR and CREB pathways following mGluR5 blockade contribute to improved Huntington's pathology in zQ175 mice. *Mol. Brain* 12:35. doi: 10.1186/s13041-019-0456-1

Avasthi, P., and Marshall, W. F. (2012). Stages of ciliogenesis and regulation of ciliary length. *Differentiation* 83, S30–S42. doi: 10.1016/j.diff.2011.11.015

Bishop, G. A., Berbari, N. F., Lewis, J., and Mykytyn, K. (2007). Type III adenylyl cyclase localizes to primary cilia throughout the adult mouse brain. *J. Comp. Neurol.* 505, 562–571. doi: 10.1002/cne.21510

Bowie, E., Norris, R., Anderson, K. V., and Goetz, S. C. (2018). Spinocerebellar ataxia type 11-associated alleles of Ttbk2 dominantly interfere with ciliogenesis and cilium stability. *PLoS Genet.* 14:e1007844. doi: 10.1371/journal.pgen.1007844

Canterini, S., Dragotto, J., Dardis, A., Zampieri, S., De Stefano, M. E., Mangia, F., et al. (2017). Shortened primary cilium length and dysregulated Sonic hedgehog signaling in Niemann-Pick C1 disease. *Hum. Mol. Genet.* 26, 2277–2289. doi: 10.1093/hmg/ddx118

Carty, N., Berson, N., Tillack, K., Thiede, C., Scholz, D., Kottig, K., et al. (2015). Characterization of HTT inclusion size, location, and timing in the zQ175 mouse model of Huntington's disease: an *in vivo* high-content imaging study. *PLoS One* 10:e0123527. doi: 10.1371/journal.pone.0123527

Chen, J. Y., Wang, E. A., Cepeda, C., and Levine, M. S. (2013). Dopamine imbalance in Huntington's disease: a mechanism for the lack of behavioral flexibility. *Front. Neurosci.* 7:114. doi: 10.3389/fnins.2013.00114

Dhekne, H. S., Yanatori, I., Gomez, R. C., Tonelli, F., Diez, F., Schüle, B., et al. (2018). A pathway for Parkinson's disease LRRK2 kinase to block primary cilia and Sonic hedgehog signaling in the brain. *Elife* 7:e40202. doi: 10.7554/eLife.40202

Domire, J. S., Green, J. A., Lee, K. G., Johnson, A. D., Askwith, C. C., and Mykytyn, K. (2011). Dopamine receptor 1 localizes to neuronal cilia in a dynamic process that requires the Bardet-Biedl syndrome proteins. *Cell. Mol. Life Sci.* 68, 2951–2960. doi: 10.1007/s00018-010-0603-4

Farrar, A. M., Murphy, C. A., Paterson, N. E., Oakeshott, S., He, D., Alosio, W., et al. (2014). Cognitive deficits in transgenic and knock-in HTT mice parallel those in Huntington's disease. *J. Huntingtons Dis.* 3, 145–158. doi: 10.3233/jhd-130061

Foerster, P., Daclin, M., Asm, S., Faucourt, M., Boletta, A., Genovesio, A., et al. (2017). mTORC1 signaling and primary cilia are required for brain ventricle morphogenesis. *Development* 144, 201–210. doi: 10.1242/dev.138271

Franklin, P. (2008). *The Mouse Brain in Stereotaxic Coordinates*. San Diego, CA: Elsevier.

Gazea, M., Tasouri, E., Tolve, M., Bosch, V., Kabanova, A., Gojak, C., et al. (2016). Primary cilia are critical for Sonic hedgehog-mediated dopaminergic neurogenesis in the embryonic midbrain. *Dev. Biol.* 409, 55–71. doi: 10.1016/j.ydbio.2015.10.033

Genetic Modifiers of Huntington's Disease (GeM-HD) Consortium. (2015). Identification of genetic factors that modify clinical onset of Huntington's disease. *Cell* 162, 516–526. doi: 10.1016/j.cell.2015.07.003

Ghosh, R., and Tabrizi, S. J. (2018). Clinical features of Huntington's disease. *Adv. Exp. Med. Biol.* 1049, 1–28. doi: 10.1007/978-3-319-71779-1_1

Gonzalez-Reyes, L. E., Verbitsky, M., Blesa, J., Jackson-Lewis, V., Paredes, D., Tillack, K., et al. (2012). Sonic hedgehog maintains cellular and neurochemical homeostasis in the adult nigrostriatal circuit. *Neuron* 75, 306–319. doi: 10.1016/j.neuron.2012.05.018

Haycraft, C. J., Zhang, Q., Song, B., Jackson, W. S., Detloff, P. J., Serra, R., et al. (2007). Intraflagellar transport is essential for endochondral bone formation. *Development* 134, 307–316. doi: 10.1242/dev.02732

Hu, L., Wang, B., and Zhang, Y. (2017). Serotonin 5-HT6 receptors affect cognition in a mouse model of Alzheimer's disease by regulating cilia function. *Alzheimers Res. Ther.* 9:76. doi: 10.1186/s13195-017-0304-4

Johansen, T., and Lamark, T. (2011). Selective autophagy mediated by autophagic adapter proteins. *Autophagy* 7, 279–296. doi: 10.4161/auto.7.3.14487

Kaliszewski, M., Knott, A. B., and Bossy-Wetzel, E. (2015). Primary cilia and autophagic dysfunction in Huntington's disease. *Cell Death Differ.* 22, 1413–1424. doi: 10.1038/cdd.2015.80

Karam, A., Tebbe, L., Weber, C., Messaddeq, N., Morle, L., Kessler, P., et al. (2015). A novel function of Huntingtin in the cilium and retinal ciliopathy in Huntington's disease mice. *Neurobiol. Dis.* 80, 15–28. doi: 10.1016/j.nbd.2015.05.008

Keryer, G., Pineda, J. R., Liot, G., Kim, J., Dietrich, P., Benstaali, C., et al. (2011). Ciliogenesis is regulated by a huntingtin-HAP1-PCM1 pathway and is altered in Huntington disease. *J. Clin. Invest.* 121, 4372–4382. doi: 10.1172/jci57552

Koch, E. T., and Raymond, L. A. (2019). Dysfunctional striatal dopamine signaling in Huntington's disease. *J. Neurosci. Res.* 97, 1636–1654. doi: 10.1002/jnr.24495

Leaf, A., and Von Zastrow, M. (2015). Dopamine receptors reveal an essential role of IFT-B, KIF17, and Rab23 in delivering specific receptors to primary cilia. *Elife* 4:e06996. doi: 10.7554/eLife.06996

Lemberger, T., Parlato, R., Dassesse, D., Westphal, M., Casanova, E., Turiault, M., et al. (2007). Expression of Cre recombinase in dopaminoceptive neurons. *BMC Neurosci.* 8:4. doi: 10.1186/1471-2202-8-4

Levine, M. S., Klapstein, G. J., Koppel, A., Gruen, E., Cepeda, C., Vargas, M. E., et al. (1999). Enhanced sensitivity to N-methyl-D-aspartate receptor activation in transgenic and knockin mouse models of Huntington's disease. *J. Neurosci. Res.* 58, 515–532. doi: 10.1002/(sici)1097-4547(19991115)58:4<515::aid-jnr5>3.3.co;2-6

Ma, Q., Yang, J., Li, T., Milner, T. A., and Hempstead, B. L. (2015). Selective reduction of striatal mature BDNF without induction of proBDNF in the zQ175 mouse model of Huntington's disease. *Neurobiol. Dis.* 82, 466–477. doi: 10.1016/j.nbd.2015.08.008

Maiuri, T., Woloshansky, T., Xia, J., and Truant, R. (2013). The huntingtin N17 domain is a multifunctional CRM1 and Ran-dependent nuclear and cilial export signal. *Hum. Mol. Genet.* 22, 1383–1394. doi: 10.1093/hmg/dds554

Malicki, J. J., and Johnson, C. A. (2017). The cilium: cellular antenna and central processing unit. *Trends Cell Biol.* 27, 126–140. doi: 10.1016/j.tcb.2016.08.002

Marley, A., and von Zastrow, M. (2010). DISC1 regulates primary cilia that display specific dopamine receptors. *PLoS One* 5:e10902. doi: 10.1371/journal.pone.0010902

Menalled, L. B., Kudwa, A. E., Miller, S., Fitzpatrick, J., Watson-Johnson, J., Keating, N., et al. (2012). Comprehensive behavioral and molecular characterization of a new knock-in mouse model of Huntington's disease: zQ175. *PLoS One* 7:e49838. doi: 10.1371/journal.pone.0049838

Miyoshi, K., Kasahara, K., Murakami, S., Takeshima, M., Kumamoto, N., Sato, A., et al. (2014). Lack of dopaminergic inputs elongates the primary cilia of striatal neurons. *PLoS One* 9:e97918. doi: 10.1371/journal.pone.0097918

Pampliega, O., Orhon, I., Patel, B., Sridhar, S., Diaz-Carretero, A., Beau, I., et al. (2013). Functional interaction between autophagy and ciliogenesis. *Nature* 502, 194–200. doi: 10.1038/nature12639

Parker, A. K., Le, M. M., Smith, T. S., Hoang-Minh, L. B., Atkinson, E. W., Ugartemendia, G., et al. (2016). Neonatal seizures induced by pentylenetetrazol or kainic acid disrupt primary cilia growth on developing mouse cortical neurons. *Exp. Neurol.* 282, 119–127. doi: 10.1016/j.expneurol.2016.05.015

Ravikumar, B., Vacher, C., Berger, Z., Davies, J. E., Luo, S., Oroz, L. G., et al. (2004). Inhibition of mTOR induces autophagy and reduces toxicity of polyglutamine expansions in fly and mouse models of Huntington disease. *Nat. Genet.* 36, 585–595. doi: 10.1038/ng1362

Saudou, F., and Humbert, S. (2016). The biology of huntingtin. *Neuron* 89, 910–926. doi: 10.1016/j.neuron.2016.02.003

Sikora, M., Tokarski, K., Bobula, B., Zajdel, J., Jastrębska, K., Cieślak, P. E., et al. (2016). NMDA receptors on dopaminoceptive neurons are essential for drug-induced conditioned place preference. *eNeuro* 3:ENEURO.0084-15.2016. doi: 10.1523/eneuro.0084-15.2016

Sipos, É., Komoly, S., and Ács, P. (2018). Quantitative comparison of primary cilia marker expression and length in the mouse brain. *J. Mol. Neurosci.* 64, 397–409. doi: 10.1007/s12031-018-1036-z

Smith, G. A., Rocha, E. M., McLean, J. R., Hayes, M. A., Izen, S. C., Isacson, O., et al. (2014). Progressive axonal transport and synaptic protein changes correlate with behavioral and neuropathological abnormalities in the heterozygous Q175 KI mouse model of Huntington's disease. *Hum. Mol. Genet.* 23, 4510–4527. doi: 10.1093/hmg/ddu166

Steger, M., Diez, F., Dhekne, H. S., Lis, P., Nirujogi, R. S., Karayel, O., et al. (2017). Systematic proteomic analysis of LRRK2-mediated Rab GTPase phosphorylation establishes a connection to ciliogenesis. *Elife* 6:e31012. doi: 10.7554/eLife.31012

Tang, Z., Lin, M. G., Stowe, T. R., Chen, S., Zhu, M., Stearns, T., et al. (2013). Autophagy promotes primary ciliogenesis by removing OFD1 from centriolar satellites. *Nature* 502, 254–257. doi: 10.1038/nature12606

Vorobyeva, A. G., and Saunders, A. J. (2018). Amyloid-β interrupts canonical Sonic hedgehog signaling by distorting primary cilia structure. *Cilia* 7:5. doi: 10.1186/s13630-018-0059-y

Conflict of Interest: The authors declare that the research was conducted in the absence of any commercial or financial relationships that could be construed as a potential conflict of interest.

Advantages of publishing in Frontiers

OPEN ACCESS
Articles are free to read for greatest visibility and readership

FAST PUBLICATION
Around 90 days from submission to decision

HIGH QUALITY PEER-REVIEW
Rigorous, collaborative, and constructive peer-review

TRANSPARENT PEER-REVIEW
Editors and reviewers acknowledged by name on published articles

Frontiers
Avenue du Tribunal-Fédéral 34
1005 Lausanne | Switzerland

Visit us: www.frontiersin.org
Contact us: info@frontiersin.org | +41 21 510 17 00

REPRODUCIBILITY OF RESEARCH
Support open data and methods to enhance research reproducibility

DIGITAL PUBLISHING
Articles designed for optimal readership across devices

FOLLOW US
@frontiersin

IMPACT METRICS
Advanced article metrics track visibility across digital media

EXTENSIVE PROMOTION
Marketing and promotion of impactful research

LOOP RESEARCH NETWORK
Our network increases your article's readership